

**THE STREAMLINED SITE ASSESSMENT METHODOLOGY:
A NEW APPROACH FOR WIND ENERGY SITE ASSESSMENT**

A Dissertation Presented

by

MATTHEW A. LACKNER

Submitted to the Graduate School of the
University of Massachusetts Amherst in partial fulfillment
of the requirements for the degree of

DOCTOR OF PHILOSOPHY

February 2008

Mechanical Engineering

UMI Number: 3315476

INFORMATION TO USERS

The quality of this reproduction is dependent upon the quality of the copy submitted. Broken or indistinct print, colored or poor quality illustrations and photographs, print bleed-through, substandard margins, and improper alignment can adversely affect reproduction.

In the unlikely event that the author did not send a complete manuscript and there are missing pages, these will be noted. Also, if unauthorized copyright material had to be removed, a note will indicate the deletion.



UMI Microform 3315476
Copyright 2008 by ProQuest LLC
All rights reserved. This microform edition is protected against
unauthorized copying under Title 17, United States Code.

ProQuest LLC
789 East Eisenhower Parkway
P.O. Box 1346
Ann Arbor, MI 48106-1346

© Copyright by Matthew A. Lackner 2008

All Rights Reserved

**THE STREAMLINED SITE ASSESSMENT METHODOLOGY:
A NEW APPROACH FOR WIND ENERGY SITE ASSESSMENT**

A Dissertation Presented

by

MATTHEW A. LACKNER

Approved as to style and content by:

James F. Manwell, Co-Chair

Jon G. McGowan, Co-Chair

Andreas Muschinski, Member

Mario Rotea, Department Head
Mechanical and Industrial Engineering

ACKNOWLEDGMENTS

I would like to thank my Co-Chairs, Jim Manwell and Jon McGowan, for giving me an opportunity at the RERL. Their guidance and wisdom were invaluable to me, and I am extremely grateful for all of their contributions to both my dissertation work and my future career.

I want to especially thank Tony Rogers for his remarkable and outstanding advising during my time at UMass. Without his deep knowledge and incredible commitment, my experience and accomplishments would have been greatly diminished. I am deeply indebted to him.

Thanks to Chris and Melissa Elkinton, who read my work along the way, and all of the other graduate students who let me bounce ideas off of them, and made my experience more joyful than a graduate student ever expects to be.

I am so thankful to my wife, Julie, for dealing with the distance between us during my time in Amherst, supporting me throughout, and especially compensating for my outrageous forgetfulness. I literally would have lost my way without you.

Finally, thanks to the Massachusetts Technology Collaborative for funding this research.

ABSTRACT

THE STREAMLINED SITE ASSESSMENT METHODOLOGY: A NEW APPROACH FOR WIND ENERGY SITE ASSESSMENT

FEBRUARY 2008

MATTHEW A. LACKNER, B.S.E., PRINCETON UNIVERSITY

M.S., MASSACHUSETTS INSTITUTE OF TECHNOLOGY

Ph.D., UNIVERSITY OF MASSACHUSETTS AMHERST

Directed by: Professor James F. Manwell

This research develops superior approaches to the traditional site assessment process, as well as novel strategies that offer a distinct advantage over the traditional process. Two major contributions are presented: new analysis approaches for site assessment, and new technical approaches to wind resource monitoring.

Two new analysis approaches for wind energy site assessment are developed. The first is a method for site assessment uncertainty analysis. Analytical expressions for the sensitivity factors of the Weibull parameters are developed, which yield exact values for any combination of wind resource, power curve, and energy losses. This enables better determination of the uncertainty in the annual energy production estimate. The second approach is a decision making strategy to determine whether or not to stop measuring the wind resource at any point in the process. In contrast, in the standard approach, the wind resource is almost always measured for a full year, which can be inefficient in many

cases. The results show that this approach is just as accurate as measuring for a year, but saves significant time and money.

Two new technical approaches for measuring the wind resource are developed. The first measures multiple sites in a year using one ground-based device, which is brought back and forth between sites, resulting in two discontinuous measured data sets, each distributed over the year. The accuracy and uncertainty of the predictions of the wind resource are equivalent to those using a full year of measured data. The second new technical approach can improve shear extrapolation. It relies on short-term data from a ground-based device at a site where a met tower is installed for a year. The short-term data are used to correct the year-long shear parameter. The results show substantial improvements in the accuracy and uncertainty of shear predictions.

These new analysis approaches and technical monitoring strategies are unified into a comprehensive “Streamlined Site Assessment Methodology.” It provides a flexible, unified approach for executing the site assessment process in which the specific priorities and constraints of the project dictate the resulting approach. This methodology can drastically alter and improve site assessment.

TABLE OF CONTENTS

ACKNOWLEDGMENTS	iv
ABSTRACT.....	v
LIST OF FIGURES	xiii
CHAPTER	
I. INTRODUCTION	1
1.0 Traditional Wind Energy Site Assessment	2
1.1 The Traditional Wind Energy Site Assessment Process.....	3
1.2 Notable Features and Drawbacks of Traditional Wind Energy Site Assessment.....	10
2.0 Overview of Dissertation	12
2.1 Site Assessment and Uncertainty – Chapter III	14
2.2 Objective Decision Making in Site Assessment – Chapter IV	14
2.3 The Round Robin Site Assessment Strategy – Chapter V	15
2.4 The Short-Term Shear Measurement Strategy – Chapter VI.....	16
2.5 Wind Energy Economic Analysis – Chapter VII.....	16
2.6 Streamlined Site Assessment Methodology – Chapter VIII	18
II. BACKGROUND	20
1.0 Meteorological Towers and Wind Resource Measurement.....	20
1.1 Meteorological Towers	20
1.2 Wind Resource Measurement: Cup Anemometers and Wind Vanes	22
2.0 Ground-Based Wind Speed Measurement Devices	24
2.1 Sonic Detection and Ranging (SODAR)	24
2.1.1 Basic Operation of a SODAR	24
2.1.2 Potential Drawbacks on SODAR.....	25
2.1.3 SODAR and Wind Resource Assessment.....	26
2.2 Light Detection and Ranging (LIDAR)	29
2.2.1 Basic Operation of a LIDAR	29
2.2.2 Commercial LIDAR Systems	30

2.2.3	LIDAR and Wind Resource Assessment.....	30
3.0	Wind Turbine Power Curves	32
4.0	The Weibull Distribution	33
4.1	Weibull Parameter Estimation	35
4.2	Energy Production Estimates using the Weibull Distribution	35
4.3	Justification of the use of the Weibull Distribution	36
5.0	Measure-Correlate-Predict.....	37
5.1	A Review of MCP Models.....	39
5.2	The Variance Ratio MCP Method	40
5.3	Uncertainty in MCP Predictions	41
5.4	MCP Parameters Selection	42
6.0	Wind Shear Modeling and Extrapolation	43
6.1	Wind Shear in Site Assessment	43
6.2	Wind Shear Modeling.....	44
III.	SITE ASSESSMENT AND UNCERTAINTY	47
1.0	Introduction.....	47
1.1	Chapter Overview	49
2.0	Review of Error Sources and Measurement Uncertainty Analysis	49
2.1	Random Error Uncertainty.....	50
2.2	Bias and Unknown Bias Uncertainty	51
2.3	Combination of Uncertainties	53
3.0	The Wind Resource and Uncertainty	57
3.1	Wind Speed Measurement Uncertainty	58
3.2	Long-term Resource Estimation Uncertainty	79
3.3	Wind Resource Variability Uncertainty.....	83
3.4	Site Assessment Uncertainty.....	86
3.5	Summary of Wind Resource Uncertainties.....	93
3.6	Estimation of the Wind Resource and the Wind Resource Uncertainty ...	94
3.6.1	Estimation of $U_{LT_HUB}^-$, c_{LT_HUB} , and k_{LT_HUB}	94
3.6.2	Estimation of δk	95
3.6.3	Estimation of δU and δc	96

3.7	Example Calculation of δU , δc , and δk	100
3.8	Summary of Wind Resource Uncertainty	102
4.0	Wind Turbine Power Production and Uncertainty.....	103
4.1	Power Curve and Power Production Uncertainty Sources	103
4.1.1	Wind Turbine Specimen Variation Uncertainty	104
4.1.2	Power Curve Uncertainty.....	105
4.1.3	Air Density Uncertainty	109
4.2	Air Density Normalization.....	110
4.3	Summary of Power Curve and Power Production Uncertainties.....	113
4.4	Combination of Power Curve and Power Production Uncertainty	113
4.5	Example Calculation of δP	113
5.0	Energy Production Losses and Uncertainty	114
5.1	Justification for Normally Distributed Energy Loss Factors	114
5.2	Availability Losses and Uncertainty	118
5.3	Fouling Losses and Uncertainty.....	121
5.4	Array Losses and Uncertainty.....	123
5.5	Combination of Energy Losses and Uncertainties.....	125
5.6	Example Calculation of ELF and δELF	125
6.0	Combining Uncertainty – The Capacity Factor Uncertainty	126
6.1	Method for Estimating the Capacity Factor.....	128
6.2	Method for Estimating Capacity Factor Uncertainty.....	130
6.3	Summary of Method for Estimating CF and δCF	132
6.4	Example calculation of CF and δCF	134
6.5	Discussion of the Example Calculation	136
6.5.1	The Calculation of CF	136
6.5.2	The Calculation of δCF	137
6.5.3	The Sensitivity Factor $SF_{CF,c}$	138
6.5.4	The Sensitivity Factor $SF_{CF,k}$	141
6.5.5	The Weibull Shape Factor, k	142
7.0	Conclusions.....	143
IV.	OBJECTIVE DECISION MAKING IN SITE ASSESSMENT	146
1.0	Introduction.....	146
2.0	Motivation.....	147

3.0	Objective Decision Making Framework.....	148
3.1	Example Decision Tree.....	150
4.0	Data Analysis.....	154
4.1	Data Sets Used.....	155
4.2	Measure-Correlate-Predict.....	156
4.3	Energy Production Estimate.....	159
4.4	Economic Evaluation.....	160
4.4.1	Cash Flow Example.....	161
4.4.2	Economic Assumptions.....	162
4.5	Decision Model Parameters.....	165
4.6	Decision Space Example.....	167
4.7	Data Set Analysis Procedure.....	168
5.0	Results.....	170
6.0	Conclusions and Recommendations.....	174
V.	THE ROUND ROBIN SITE ASSESSMENT STRATEGY.....	180
1.0	Introduction.....	180
2.0	Data Sets Used.....	182
3.0	Data Analysis.....	184
3.1	Primary Analysis Parameters.....	187
3.2	Data Analysis Procedure.....	188
4.0	Results and Discussion.....	190
4.1	Prediction of the Mean Wind Speed.....	191
4.1.1	Accuracy of the Prediction of the Mean Wind Speed.....	191
4.1.2	Uncertainty of the Prediction of the Mean Wind Speed.....	193
4.1.3	Summary of Mean Wind Speed Predictions.....	198
4.2	Prediction of k	199
4.2.1	Accuracy of the Prediction of k	199
4.2.2	Uncertainty of the Prediction of k	201
4.2.3	Summary of Mean Wind Speed Predictions.....	203
5.0	Conclusions and Recommendations.....	204

5.1	Choice of the Round Robin Measurement Period	204
5.2	Choice of the Measured Data Length	205
5.3	Comparing Methods with Equal Measured Data Length	206
5.4	Comparing Methods to 1 Year of Measured Data	206
5.5	Recommendation for Implementing the Round Robin Site Assessment Method	207
VI.	THE SHORT-TERM SHEAR MEASUREMENT STRATEGY	209
1.0	Introduction	209
1.1	Background of Shear Modeling for Wind Energy Applications	209
1.2	Wind Resource Measurement Approaches	210
2.0	Scope and Objectives	210
2.1	Wind Shear Modeling	211
2.2	Selected Data Sets	212
2.3	Motivation for Improved Wind Shear Extrapolation Methods	214
2.4	Objectives	217
3.0	Data Analysis	218
3.1	Primary Analysis Parameters	218
3.2	Choice of Wind Shear Model	220
3.3	Scenario 1 Analysis	221
3.4	Scenario 2 Analysis	225
4.0	Results and Discussion	226
4.1	Scenario 1 Results	227
4.1.1	Scenario 1 Individual Site Predictions	232
4.2	Scenario 2 Results	235
5.0	Conclusions	242
6.0	Recommendations	244
VII.	WIND ENERGY ECONOMIC ANALYSIS	247
1.0	The Wind Energy Financial Calculator	248
1.1	Independent Power Producer	249
1.1.1	IPP Example	251

1.2	Investor Owned Utility	254
1.3	Government Owned Utility.....	255
1.4	WEFC Features.....	256
2.0	Alternative Wind Energy Evaluation Methods.....	264
2.1	External Cost Analysis.....	265
2.2	Advanced Finance Analysis.....	267
2.2.1	Capital Asset Pricing Model	267
2.2.2	Mean Variance Portfolio Theory	270
2.2.3	Advanced Finance Analysis Summary	271
2.3	Energy Balance Analysis	272
2.4	Alternative Wind Energy Evaluation Methods Conclusions	274
3.0	Conclusions.....	275
VIII.	THE STREAMLINED SITE ASSESSMENT METHODOLOGY	277
1.0	SSAM Description.....	277
1.1	The Ground-Based Device Site Assessment Option	278
1.2	The Met Tower Site Assessment Option	281
1.3	Uncertainty and Economic Analysis.....	283
1.4	SSAM Approach Summary	284
2.0	SSAM Software	284
2.1	SSAM Main Window	285
2.2	Configuration and Strategy Window	286
2.3	Wind Resource Evaluation Window.....	289
2.4	Energy Production and Uncertainty Window	290
2.5	Economic Analysis Window.....	292
2.6	Important SSAM Features	294
3.0	SSAM Conclusions.....	295
IX.	CONCLUSIONS.....	296
1.0	Summary	296
2.0	Recommendations.....	300
	REFERENCES	302

LIST OF FIGURES

Figure	Page
1 – Flow Chart of the Traditional Wind Energy Site Assessment Process.....	9
2 – Flow Chart of SSAM	19
3 – 50 m Met Tower Schematic / Raising of a 50 m Met Tower	21
4 – NRG Anemometer, Wind Vane / Booms, Sensors on a Met Tower	23
5 – ART VT-1 SODAR	26
6 – QinetiQ ZephIR LIDAR	30
7 – GE 1.5 MW Power Curve.....	33
8 – Example Weibull Distributions.....	34
9 – Reference/Target Site Data / Variance Ratio Fit to Concurrent Data.....	39
10 – Example of Rectangular and Normal Distribution	55
11 – Angular Response Graph of Risø Anemometer.....	65
12 - Angular Response Graph of NRG Maximum 40 Anemometer	70
13 – Effect of Data Removal	78
14 – Example Power Curve with Error Bars	106
15 – Power Curves for Different Density Sites	112
16 – Wind Farm Availability Data.....	116
17 – Distribution of Lifetime Availability Data	117
18 – Flow Chart of the Site Assessment Process.....	127
19 – GE 1.5 MW Power Curve.....	135
20 – Capacity Factor for Various Values of c and k	137
21 – Sensitivity Factor for c	139

22 – Various Weibull Distributions and Power Curve	140
23 – Sensitivity Factor for k	142
24 – Sample Decision Tree	151
25 – Mean Wind Speed Uncertainty	158
26 – Cash Flow Example	162
27 – NPV of building and DSCR as a function of Capacity Factor	164
28 – Decision Space for Example	168
29 – Correct Decision Percentage for Each Site	172
30 – Average Measurement Length for Each Site	173
31 – Average NPV Saved for Each Site	174
32 – Effect of Uncertainty on Decision Space.....	177
33 – Example of Measurements at Two Sites.....	185
34 – Accuracy of the Mean Wind Speed Predictions	192
35 – Uncertainty of the Mean Wind Speed Predictions.....	194
36 – Effect of the Round Robin Measurement Period.....	196
37 –Number of Trips in the Round Robin Site Assessment Method.....	197
38 – Accuracy of the Predictions of k	200
39 – Uncertainty of the Predictions of k	202
40 – Monthly Power Law Exponent	219
41 - z_0 versus U_2/U_1	221
42 – Accuracy of the Predictions, Scenario 1	228
43 - Average Shear Correction Factor, $N_{seg} = 1$, Scenario 1	230
44 – Uncertainty of the Predictions, Scenario 1	231

45 – Mean Wind Speed Predictions for Isabella, Scenario 1	233
46 – Mean Wind Speed Predictions for Glenmore, Scenario 1	234
47 – Accuracy of the Predictions, Scenario 2	236
48 – Uncertainty of the Predictions, Scenario 2	237
49 – Mean Wind Speed Predictions for Isabella, Scenario 2.....	240
50 – Mean Wind Speed Predictions for Glenmore, Scenario 2	241
51 – Cash Flow Example	253
52 – WEFC Main Window	257
53 – WEFC General Inputs Sub-Window	258
54 – WEFC Capital Costs and Expenses Sub-Window.....	259
55 – WEFC Financing and Taxes Sub-Window.....	260
56 – WEFC Economic Assumptions and Constraints Sub-Window	261
57 – WEFC IPP Results Sub-Window.....	262
58 – WEFC Sensitivity Plot.....	263
59 – Energy Return on Investment (EROI) for Various Energy Sources.....	274
60 – SSAM Flow Chart	278
61 – SSAM Main Window	286
62 – Configuration and Strategy Window for Met Tower.....	287
63 - Configuration and Strategy Window for Ground-Based Device.....	288
64 – Wind Resource Evaluation Window.....	290
65 – Energy Production and Uncertainty Window	291
66 – Economic Analysis Window.....	293
67 – SSAM Economic Results.....	294

CHAPTER I

INTRODUCTION

Wind energy site assessment evaluates the potential for a given site to produce energy from wind turbines. When wind energy development is under consideration, a site assessment is usually undertaken. Specifically, wind energy site assessment is the process of evaluating the wind resource at a potential wind turbine or wind farm location, estimating the energy production from a wind turbine or turbines, and then determining the economic viability of the project. The wind resource at a site directly affects the amount of energy that a wind turbine can extract, and therefore the success of the venture. The wind resource is primarily quantified by the mean wind speed at the site, although the turbulence intensity, the probability distribution of the wind speed, and the prevailing wind direction are also important factors. Once the wind resource is determined at a site, the expected annual energy production (*AEP*) of a selected wind turbine or turbines is calculated. This calculation combines the expected wind resource with the power curve of the wind turbine(s) and the expected energy losses in order to estimate how much energy the wind turbine(s) will actually produce at the site. Finally, the estimate of the energy production and the relevant economic parameters of the project are combined to determine the potential profitability or economic success of a wind energy development at the site.

This research presents an improved, innovative, and comprehensive approach to wind energy site assessment, dubbed the “Streamlined Site Assessment Methodology” (SSAM). SSAM encompasses both superior approaches to the traditional site assessment process, as well as novel site assessment strategies that offer a distinct advantage over the

traditional process. The results of this research can lead to a drastically different and improved approach to wind energy site assessment.

1.0 Traditional Wind Energy Site Assessment

Wind energy development is typically initiated by a private company, government body, or utility that is interested in producing wind energy in a particular region. The process generally begins with a “preliminary area identification,” which entails identifying a relatively large area where wind energy development is viable [1]. A wind atlas, such as the “Wind Energy Resource Atlas of the United States” [2], or wind maps can be used for this purpose.

Next, a specific site or sites within the preliminary area is selected for consideration for wind energy development. Ideally, these sites are selected based on topography and other factors that would suggest a successful project, although often zoning and community support dictate the actual locations. Regardless, these sites are then evaluated for their potential to produce wind energy by measuring the wind resource. The process of assessing the potential for a specific site to produce energy from wind turbines is the site assessment process. The “Wind Resource Assessment Handbook” [1] provides a detailed description of many aspects of the site assessment process, especially a method of evaluating the wind resource at a site.

The assessment of a specific site for wind energy development is the focus of this research. The larger strategic questions of regional development are not considered here. Rather, this research focuses on the process that follows the selection of a site.

1.1 The Traditional Wind Energy Site Assessment Process

Traditional wind energy site assessment is a well defined, established process whereby the wind resource at a site is evaluated, and the energy production and economic success of a wind energy development at the site are estimated. There is a general consensus as to how this process is performed. The Wind Resource Assessment Handbook, Wind Energy – The Facts (Volume 1, Chapter 2) [3], consulting firms [4], and state guidebooks on site assessment [5], all endorse a similar site assessment methodology. The steps that make up the site assessment process are:

1. Wind Resource Evaluation
 - a. Measurement of the Wind Resource
 - b. Estimation of the Long-Term Wind Resource
 - c. Extrapolation of the Wind Resource to the Turbine Hub Height and Location
2. Wind Turbine Selection and Power Curve Adjustment
3. Energy Loss Estimation
4. Energy Production and Uncertainty Estimation
5. Economic Evaluation

The steps are now described in detail.

1. Wind Resource Evaluation – Wind resource evaluation is the first major step in the wind energy site assessment process. It consists of using measured wind speed data to estimate the long-term hub height wind resource at the location of each turbine in the wind farm. The wind resource is usually characterized by the

mean wind speed and the Weibull parameters. Because the wind resource varies from year to year, an estimate of the long-term characteristics is critical to accurately estimate the energy production over the lifetime of the turbine [6],[7]. Also, wind turbine power output depends on the wind speed at the hub height and location of each turbine, among other factors. The result is that an estimate of the hub height and location wind resource is necessary for accurate estimations of *AEP*. Furthermore, when multiple wind turbines are installed at a site or when the met tower and the turbine are in different locations, the wind resource must be estimated at the location of each turbine, since terrain effects can alter the wind resource across a site [7],[8]. Wind resource evaluation is therefore comprised of three steps: wind resource measurement, long-term resource estimation, and hub height and location resource estimation.

- a. Measurement of the Wind Resource - In the traditional site assessment process, the wind resource at a site is measured using one or several meteorological towers (met towers). When a large wind farm sited over a large area is under consideration, multiple met towers may be necessary to assess the wind resource, especially if the terrain is complex [8]. Met towers are equipped with wind speed and direction sensors (usually cup anemometers and wind vanes) positioned at two or more heights on the tower. These sensors record the wind speed and direction, which are then reported as 10-minute or 1-hour averages. These time series of data are the measured wind resource data. A more detailed description of met towers is provided in Chapter II, Section 1.0.

A met tower is located at the site for at least a year. This is the recommendation of the Wind Resource Assessment Handbook [1], and it is the standard practice in almost all site assessment [3],[4],[5]. The wind resource at a site tends to have pronounced seasonal variations, and so one year of data is needed to capture these seasonal effects. Greater than a year of data allows for the capture of inter-annual variations in the wind resource as well, although rarely is the wind resource evaluated for more than two years.

- b. Estimation of the Long-Term Wind Resource - While wind resource measurement usually lasts for one year, the measured resource during this particular year may not be representative of the actual long-term resource at the site, due to inter-annual variations [6],[7],[9],[10],[11]. The long-term resource is characterized by the mean wind speed and wind speed distribution that exists at a site over a very long period of time, when these inter-annual variations are averaged out. Typically, twenty years is assumed to be a long enough time period to characterize the long-term wind resource. Since a twenty year measurement campaign is far too long for practical purposes, the long-term resource must be estimated from the measured data. The measured data, along with long-term data from a nearby site (the “reference site”), are generally used in a process called Measure-Correlate-Predict (MCP) to estimate the long-term wind resource at a site. A detailed description of the MCP process is provided in Chapter II, Section 5.0.

- c. Extrapolation of the Wind Resource to the Turbine Hub Height and Location - Met towers are generally between 40 m and 60 m tall, and so wind speed measurements usually take place at heights significantly lower than the hub height of a modern wind turbine. Because wind speeds tend to increase with height, a wind shear model is used to extrapolate the estimated long-term wind resource to the hub height [12]. The wind shear model is created using the measured wind speed data. A detailed description of wind shear is provided in Chapter II, Section 6.0.

Furthermore, the met tower measurement location is often not the same as the eventual turbine location, or multiple turbines are installed when only a single met tower is used to measure the wind resource. In these cases, the terrain can cause the wind resource to differ between the met tower locations and the eventual turbine location(s). Flow modeling is typically used to adjust the wind resource according to the varying terrain at a site, and to aid in the placement of the wind turbines [8]. Flow models are often referred to as “Wind Energy Design Tools” [3].

2. Wind Turbine Selection and Power Curve Adjustment – Once the wind resource is evaluated at a site, producing an estimate of the long-term hub height wind resource, a wind turbine is selected for the site. The type of wind turbine selected depends on the wind resource at the site, the goals of the developer, the capacity of the local grid, and many other factors. While maximizing energy production is one goal, issues such as durability are also important, especially at turbulent sites. A wind turbine is primarily characterized by its power curve, which defines the

wind turbine power output as a function of the incoming hub height wind speed. Wind turbine power curves are often adjusted for the specific site where the turbine is installed, as the air density, turbulence intensity, and wind shear can affect the power curve of the turbine. Furthermore, the wind resource may also affect the cost of the wind turbine at the site, as windier and more turbulent sites generally require more expensive turbines [13]. More details on power curves are provided in Chapter II, Section 3.0.

3. Energy Loss Estimation – A variety of factors can contribute to lost energy production from a wind turbine. These factors include losses due to maintenance and repair, blade icing and fouling, array losses from other wind turbines (where upstream turbines reduce the energy available to downstream turbines), and more. These factors are highly site dependent, and their overall effect is to reduce the actual energy production at the site to a value less than the ideal energy production.
4. Energy Production and Uncertainty Estimation – The estimated long-term hub height wind resource, the wind turbine power curve, and the energy losses are then combined to estimate the annual energy production (*AEP*) at the site. This is an estimate of the average *AEP* over the lifetime of the turbines, since the long-term wind resource is used in the calculation. The uncertainty of the *AEP* is important to estimate as well. The wind resource, power curve, and energy losses are all uncertain, and when they are combined to estimate the *AEP*, their respective uncertainties contribute to an overall *AEP* uncertainty. This uncertainty is critical in estimating the risk associated with the potential venture.

5. Economic Evaluation – Finally, an economic analysis of the project is performed, which combines the expected *AEP* with the relevant economic parameters of the project, such as the financing, taxes, subsidies, and expenses. The *AEP* is usually the most critical factor contributing to the economic success of a project. The typical economic metrics for evaluating a project include the levelized cost of energy, the internal rate of return, and the net present value. The uncertainty in the site assessment process is also a critical component to the economic evaluation of the project. The estimated *AEP* is an uncertain quantity, and so the risk of the project must be accounted for as well. This is often accomplished by requiring that when the 10th percentile value of *AEP* is used in the economic evaluation, the minimum debt service coverage ratio is at least one [14]. The issue of risk is described in more detail in later Chapters.

The previous steps summarize the traditional method for wind energy site assessment that is used most frequently today. The flow chart in Figure 1 shows a graphical representation of this process. The yellow boxes represent processes or calculations, and the blue parallelograms represent sources of data.

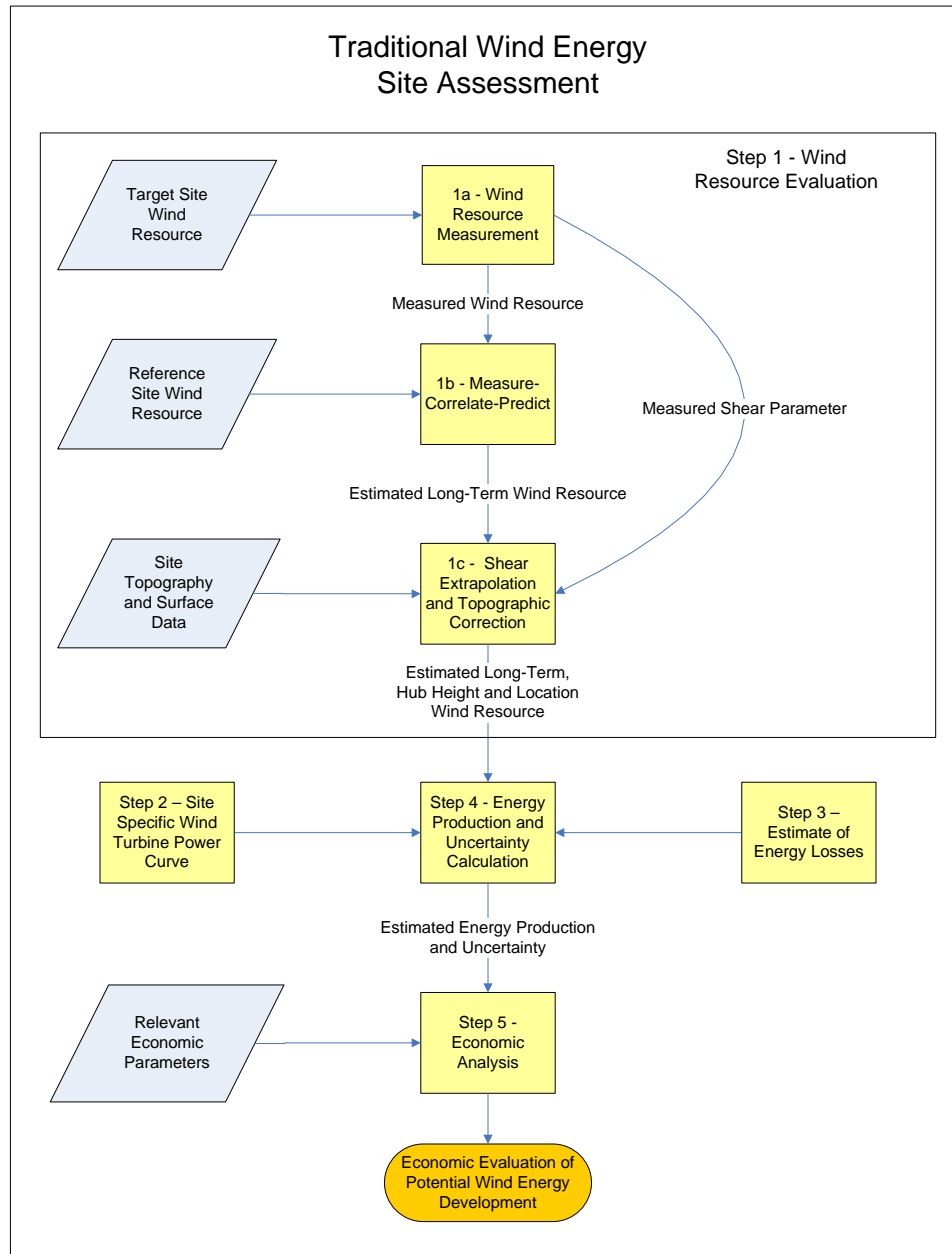


Figure 1 – Flow Chart of the Traditional Wind Energy Site Assessment Process

It should be noted that there are many alternatives to this process described above, and that permutations or fundamental changes to the process are certainly possible. For example, the long-term wind resource can be estimated solely based on wind maps, atlases, or nearby reference sites, completely eliminating the actual measurement step.

On the other hand, the method for estimating the wind resource is well established, and a significant deviation from this process is unlikely when hiring a professional to perform a site assessment. Moreover, the ability to secure a loan for a wind energy development is closely tied to the perceived risk associated with the estimate of the energy production and economic success of the project [14],[15]. The result is that the traditional site assessment process provides a fair representation of the standard process carried out in the wind energy industry today, and so it is used as a baseline for comparison when alternatives to the process are discussed in later Chapters.

1.2 Notable Features and Drawbacks of Traditional Wind Energy Site Assessment

The traditional site assessment process outlined above is widely accepted in the wind energy industry. There are two important characteristics of the site assessment process outlined above that are especially relevant to this research: the length of the wind resource measurement campaign, and the height of the wind resource measurement. Both characteristics partially result from the use of a met tower for the evaluation of the wind resource.

Wind resource measurement campaigns are almost always at least one year long in the traditional site assessment process. The practice of measuring the wind resource for at least one year is uniformly recommended in reputable manuals of site assessment [1],[3],[5]. This practice is accepted primarily because of seasonal variations in the wind resource. The wind speed at a site often varies substantially over the course of the year. In the northeast United States, the winter months tend to have the highest wind speeds, and the summer months the lowest. A full year of measurement is therefore needed to capture the seasonal variations at a site. Moreover, the installation of a met tower

requires a crew of several people at least a full day to both raise and lower the met tower. Because of the difficulty of installation, it is unlikely that a met tower would be deployed for less than one year.

In addition, most met towers are approximately 40 m to 60 m tall, and so they measure the wind resource at heights significantly lower than the hub heights of modern wind turbines. Towers of this height (including labor and sensors) cost on the order of \$20,000-30,000 [3]. Taller towers, with heights of 80 m and greater, are significantly more expensive (\$100,000 or more), and are potentially much more difficult to permit and install. The result is that the use of a standard met tower for site assessment necessitates a shear extrapolation model to estimate the hub height wind resource.

While the length of the wind speed measurement and the necessity for shear extrapolation are accepted characteristics of the site assessment process, these features are potentially significant drawbacks of the process as well. Along with the potentially lengthy permitting and construction phase of a wind energy project, the measurement of the wind resource at a site adds at least another year to the overall process of wind energy development. The uncertain nature of subsidies and turbine availability encourages rapid development of wind energy projects, which is potentially in direct conflict with the lengthy wind resource measurement time. Also, developers, consulting firms, or government sponsored wind energy assessment programs often have multiple candidate sites for site assessment, and so there is a strong motivation for quick measurement campaigns.

Shear extrapolation, which is necessitated by the measurement heights of met towers, is a highly uncertain process, and shear profiles are extremely site dependent [16].

Furthermore, without hub height measurements of the wind resource there is no way to know a priori if the shear model that is employed is appropriate. The result is that the use of shear extrapolation introduces a great deal of uncertainty into the estimate of the wind resource at the turbine hub height [17].

Thus, while the traditional site assessment process is well established, there are undesirable characteristics inherent in this process, which at least partially result from using a met tower for the evaluation of the wind resource.

2.0 Overview of Dissertation

This dissertation seeks to both improve the traditional site assessment process, and to offer alternative strategies for wind resource measurement that can be utilized to address the inherent drawbacks in traditional site assessment. The results and methods presented are applicable to wind energy consultants and developers, as well as government sponsored site assessment programs. The overall goal is to present a comprehensive strategy for site assessment, in which the specific priorities of a project dictate the particular approach taken in the site assessment [18].

Some of the strategies presented rely on the use of a ground-based device, such as SODAR or LIDAR, for the evaluation of the wind resource. Portable towers (“jack-up” towers), which are shorter than standard 50 m met towers, may also be used in some instances. Ground-based devices are described in more detail in Chapter II, Section 2.0. Ground-based devices are portable and capable of measuring at the hub height of modern wind turbines. These qualities are leveraged in several of the strategies that are developed, and enable potentially more efficient, accurate, and precise methods for conducting wind energy site assessment. Finally, it should be explicitly stated that these

new strategies for measuring the wind resource assume that reliable and accurate measurements are possible using these devices.

The contributions of this dissertation fall into three major categories:

1. New analysis approaches for wind energy site assessment are presented in this dissertation, which offer improved methods for analyzing components of wind energy site assessment. Specifically, this research develops new approaches to uncertainty analysis and decision making in wind energy site assessment. These approaches can lead to better estimates of uncertainty in the site assessment process, and more rapid, efficient, and affordable site assessment campaigns.
2. New technical approaches for monitoring the wind resource are described. This research proposes alternative methods for measuring the wind resource at a site. Specifically, two technical approaches are presented, with the capability of either drastically improving the efficiency, or significantly reducing the uncertainty of site assessment.
3. A unified framework for approaching site assessment is developed, and software tools are created in order to execute this approach. This methodology integrates the new analysis methods and technical approaches, along with economic analysis methods, into a coherent approach to wind energy site assessment. This methodology can then be implemented in a functional software tool.

The dissertation is organized into six major categories, each its own Chapter, along with Background and Conclusion Chapters. A brief overview of the content in each Chapter, except for the Background and Conclusion Chapters, is now presented.

2.1 Site Assessment and Uncertainty – Chapter III

Chapter III presents an in-depth analysis of the traditional site assessment process, with a focus on uncertainty analysis, as well as a new approach to handling uncertainty in the site assessment process. Each of the steps in the site assessment process, outlined above in Section 1.1, is reviewed, and a comprehensive listing of the uncertainty in each step is compiled. A detailed description of methods to estimate the wind resource and the energy production at a site is presented, as well as mathematically rigorous methods for handling uncertainty in the process. Furthermore, the uncertainty analysis techniques developed in Chapter III are generally applicable to all site assessment strategies, including the new technical approaches for measuring the wind resource presented in Chapters V - VI.

2.2 Objective Decision Making in Site Assessment – Chapter IV

While a full year of measured wind data may be desirable for site assessment, MCP can be applied to any length of measured data to estimate the long-term wind resource, including shorter measurement lengths on the order of weeks or months. Because of the lengthy installation process, however, it is unlikely that a met tower would be removed from a site in less than a year, regardless of the wind resource. The portability of ground-based devices eliminates this constraint on the measurement length, allowing for shorter wind resource measurement campaigns.

The research in Chapter IV describes the development of a new analysis approach: an objective decision making approach to wind energy site assessment. At any point in the site assessment process, one can choose between stopping measurement and building a wind farm, stopping measurement and not building a wind farm, and continuing

measurement. A decision making framework is developed, in which the three options are evaluated and compared after some period of data is measured, and the “best” of the three choices is determined. A recursive dynamic program is used to evaluate the option to continue measurement.

This method is especially well suited for an entity that has planned multiple site assessments. Furthermore, the objective decision making method can be used in concert with the round robin site assessment method (described next). These strategies are potentially complimentary, and allow for a great deal of flexibility and efficiency in deciding when and how long site assessment should occur at various sites. This strategy can be used with met towers as well, although ground-based devices are primarily considered because of their portability.

2.3 The Round Robin Site Assessment Strategy – Chapter V

The “round robin site assessment strategy” is a new technical approach to wind resource measurement. The premise of the round robin strategy is to measure the wind resource at multiple sites in a single year using a single portable ground-based device, but to discontinuously distribute the measurement time at each site over the whole year, so that the total measurement period is comprised of smaller segments of measured data. This measured data set is then utilized in the MCP process to predict the long-term wind resource at the site. The round robin site assessment method aims to increase the number of sites assessed in a single year, without the sacrifice in accuracy and precision of the MCP predictions that usually accompanies shorter measurement periods.

The round robin site assessment method also addresses the two drawbacks of the traditional site assessment process. By using a portable ground-based device to measure

the wind resource at multiple sites in a single year, the average wind resource measurement time per site is decreased substantially. Furthermore, the ground-based devices measure the wind resource at the hub height of a wind turbine, and therefore obviate the need for shear extrapolation. This method is especially well suited for an entity that has planned multiple site assessments, such as a state institution conducting a state-wide site assessment program.

2.4 The Short-Term Shear Measurement Strategy – Chapter VI

The “short-term shear measurement” is another new technical approach to wind resource measurement. This strategy relies on augmenting the one year of met tower measurements in the traditional site assessment process with short-term measurements from a ground-based device. The goal is to improve the accuracy of shear extrapolation from met tower data without the need to deploy a ground-based device at a site for a long period of time.

This strategy is complimentary to the traditional site assessment process, not substitutive. It is used in the traditional site assessment process to help mitigate the measurement height limitations of met towers. The short-term shear measurement strategy is extremely useful when multiple concurrent site assessments are in progress, each using a met tower, and only a limited number of ground-based devices (e.g., one) are available.

2.5 Wind Energy Economic Analysis – Chapter VII

Once the wind resource at a site is evaluated, and an estimate of the energy production is made, an economic analysis of the site is undertaken to determine the

viability of a wind energy development. Wind energy economic analysis can take on a variety of forms, from simple to very complex. Chapter VII presents two components of wind energy economics.

First, Chapter VII describes the development of a wind energy financial calculator, which is a general tool for analyzing wind energy finances. The calculator utilizes cash flow methods for determining the relevant economic results of wind energy projects, and provides a useful means for analyzing proposed wind energy developments. While there is no “correct” method for analyzing the economics of a wind farm (e.g., payback methods, levelized cost method, EPRI-TAG, etc), the cash flow method is similar to what a business or utility would actually do in evaluating a potential development. Furthermore, a cash flow method analysis is not particularly easy to implement, at least in relation to other methods, and so it lends itself well to programs that can perform the iterations automatically. The calculator has a graphical user interface (GUI) for easy use, and it is created as an executable program so it can be utilized on any computer.

Second, new and alternative methods for assessing and valuing wind energy, especially in its relation to other energy sources, are presented. These particular methods are by no means exhaustive; instead this review is meant to highlight a few particular areas in which alternative methods of analysis provide insight or different perspectives on the merit of wind energy from an economic perspective.

The material in Chapter VII is not original research; rather it presents the development of a tool based on established methods of economic analysis, and a consolidation of a variety of material focused on alternative means of evaluating energy production.

2.6 Streamlined Site Assessment Methodology – Chapter VIII

The research and tools developed in Chapters III – VII encompass a variety of strategies and methods for conducting the site assessment process. Some approaches are complimentary, while others are mutually exclusive. These strategies and methods are components of an integrated approach to site assessment: the streamlined site assessment methodology (SSAM). The flow chart in Figure 2 depicts this methodology; yellow boxes indicate processes or analyses, and the green diamonds indicate decision points.

The traditional site assessment process is a potential path in the SSAM process. It would entail choosing to install a met tower at the first decision point in Figure 2, choosing not to utilize a ground-based device at the second decision point, and choosing not to utilize the objective decision making approach at the third decision point.

Another notable feature of the SSAM process is that the uncertainty analysis developed in Chapter III is universally applicable, as it is employed for all the potential site assessment strategies. This is also the case for the economic analysis methods described in Chapter VII. Finally, Figure 2 emphasizes that the round robin strategy and the objective decision making strategy are complimentary and can be used in parallel.

The SSAM approach is implemented into a software program to allow its application to wind energy site assessment. Chapter VIII describes the development of the SSAM software. The software effectively implements the various strategies and analyses in the SSAM approach, allowing for an extremely useful and flexible tool for conducting site assessment. The software provides a convenient unification of this research.

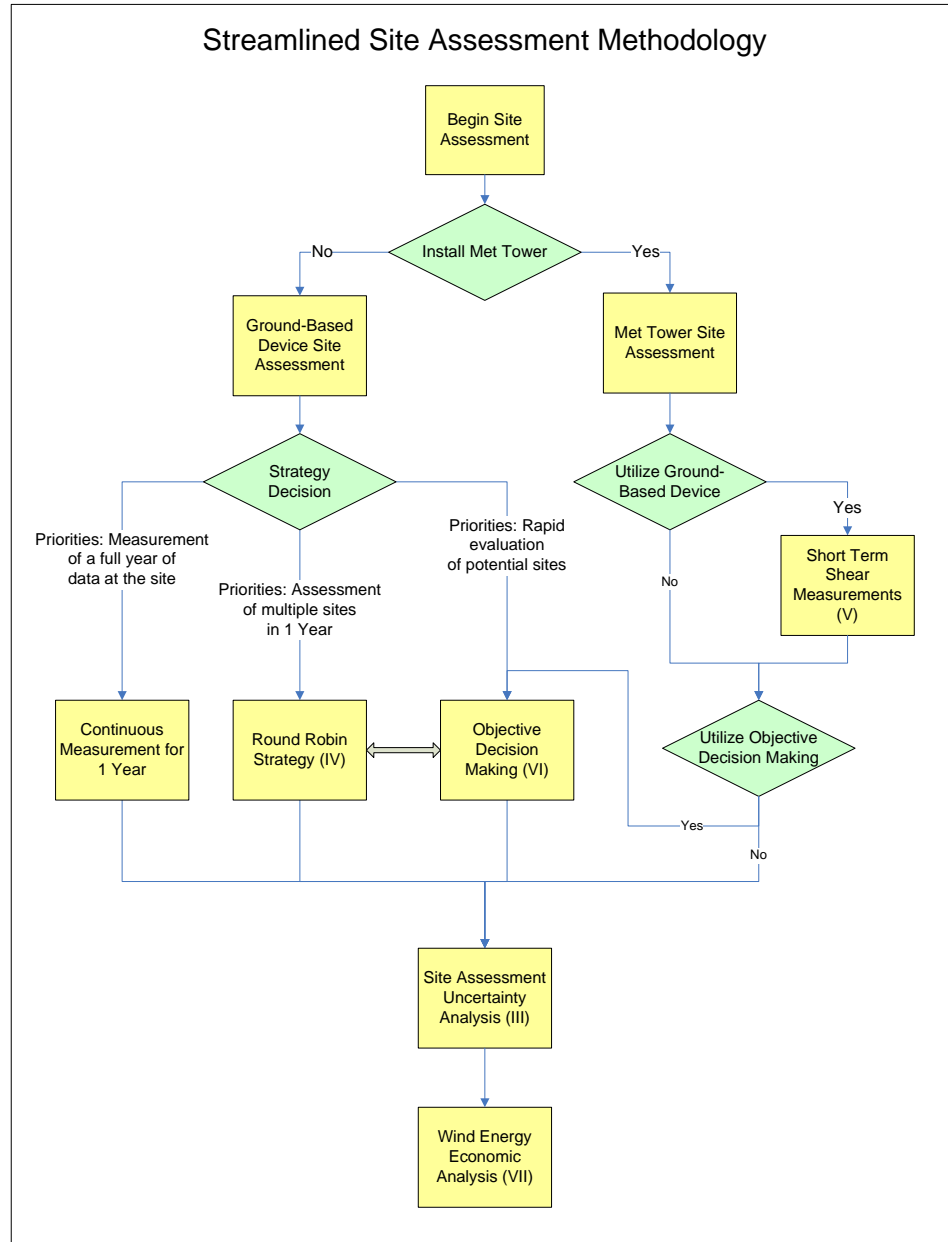


Figure 2 – Flow Chart of SSAM

CHAPTER II

BACKGROUND

This Chapter provides background information on a number of subjects relevant to this research. Each Section is meant to provide basic background knowledge, information, and assumptions for later use in the research, but not an exhaustive review of the topic.

1.0 Meteorological Towers and Wind Resource Measurement

The traditional site assessment process, described in Chapter I, Section 1.1, relies on the use of met towers and wind speed and direction sensors in order to evaluate the wind resource at a site. The most common wind speed and direction sensors are cup anemometers and wind vanes. This Section presents some basic background information on this process.

1.1 Meteorological Towers

Met towers are the most common means of assessing the wind resource at a location that is under consideration for wind energy development. Most met towers used in wind resource assessment are tall tubular steel towers, between 40 m and 60 m tall, with diameters of approximately 15-20 cm (6-8 in). These towers are secured via sets of guy wires, which connect from the tower at several heights to sets of anchors on the ground. The left diagram in Figure 3 shows a schematic of a 50 m NRG met tower [19]. Met towers of this type cost approximately \$10,000-20,000 [20]. Lattice towers are also sometimes used to mount wind monitoring equipment.

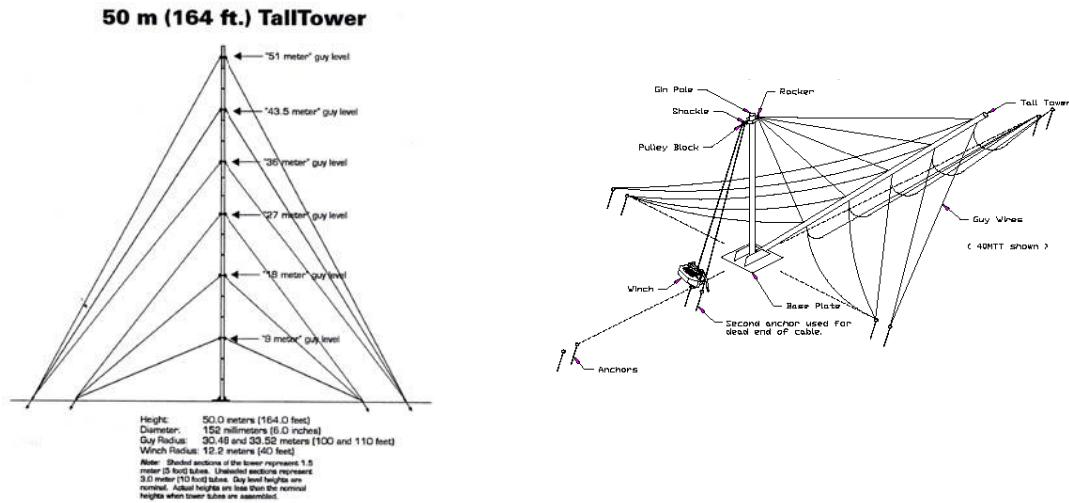


Figure 3 – 50 m Met Tower Schematic / Raising of a 50 m Met Tower

The installation of a met tower is an involved process, and requires a multi-person crew and at least a full day to complete. A common means of raising or lowering a met tower is with a “gin pole,” which is a smaller tubular tower, connected to the met tower, and raised or lowered using a winch. A schematic of this process is shown on the right side of Figure 3 [19]. Guy wires on the sides of the met tower are used to align the tower as it is raised or lowered. Finally, guy wires in four directions are used to stabilize the met tower once it is vertical.

Met towers usually must be approved and permitted by the town in which they are located [1]. Because met towers are temporary structures, this process can be quite easy to complete. However, local opposition can sometimes make the permitting of a met tower much more difficult. Other considerations when installing a met tower include leasing fees, liability, insurance, and the surrounding terrain [1].

1.2 Wind Resource Measurement: Cup Anemometers and Wind Vanes

The wind speed and direction are generally measured using anemometers for the wind speed, and wind vanes for the direction. These sensors are usually positioned at two or three heights on the tower, with two anemometers and one vane at each height. The redundant anemometers help combat tower shadow, which occurs when the wake of the tower affects the measurement of an anemometer. At each height, booms are attached to the tower extending horizontally. These booms are generally 2-3 m (6-9 ft) in length, and the wind monitoring sensors are secured to the end of the booms. By positioning the sensors away from the tower, the effects of the tower wake are reduced. A picture of booms extending off of an installed met tower is shown on the right in Figure 4. The sensors usually produce data that give the average wind speed and wind direction over 10-minute intervals. These data are recorded and stored by a logger box at the bottom of the tower, which is connected to the sensors via sensor cables.

The most common type of anemometer used for wind energy site assessment is the cup anemometer [21]. A popular three-cup anemometer made by NRG Systems, the Maximum 40 anemometer, is shown on the left in Figure 4 [20]. This anemometer costs approximately \$150 [20]. The performance of a cup anemometer is determined by a variety of factors, including its size and weight, bearing friction, and cup design [21],[22]. The accuracy of a cup anemometer is generally assumed to be approximately 0.1 m/s (1-2% of the mean wind speed), based on wind tunnel tests [23],[24],[25],[26]. The accuracy of wind speed measurements is discussed in great detail in Chapter III. The wind direction is usually measured using a wind vane. An NRG wind vane is also shown on the left in Figure 4 [20].



Figure 4 – NRG Anemometer, Wind Vane / Booms, Sensors on a Met Tower

Cup anemometers are often characterized by their distance constant. The distance constant indicates how rapidly the anemometer responds to changes in the wind speed. Formally, the distance constant is equal to the length of fluid flow past the anemometer required to cause it to respond to 63.2% of a step change in speed [21]. Anemometers with small distance constants respond rapidly to changes in the wind speed. Most cup anemometers used for wind resource assessment, such as the Maximum 40, have distance constants less than 5 m. In general, cup anemometers with small distance constants can be classified as “point measurements” of the wind speed, and so they measure the instantaneous wind speed at a given point in space and a given time.

The overall cost of a wind monitoring campaign using a met tower, anemometers, and wind vanes is approximately \$20,000-30,000, although it could vary depending on the price of labor [3].

2.0 Ground-Based Wind Speed Measurement Devices

LIDAR and SODAR are relatively new ground-based devices that can be used for wind resource assessment. Both devices are portable and capable of measuring the wind resource at wind turbine hub heights, as well as multiple heights simultaneously. Furthermore, in the new technical approaches for wind resource measurement described in Chapter V-VI, it is assumed that these devices are capable of producing unbiased estimates of the mean wind speed, equivalent to that which would be measured using a cup anemometer on a met tower. These devices are now described in greater detail.

2.1 Sonic Detection and Ranging (SODAR)

SODAR systems are ground-based wind speed measurement devices that utilize sound waves to measure the wind speed. While SODARs were first developed in the 1960's and 1970's for this purpose, it is only recently, with the advent of very high turbine hub heights, that SODARs have begun to be utilized for wind resource assessment [27]. This Section describes the basic operation of a SODAR, as well as some of its drawbacks, and its potential role in wind resource assessment.

2.1.1 Basic Operation of a SODAR

The motion of the atmosphere is inherently turbulent, with both thermally and mechanically induced eddies. The majority of SODARs today operate by emitting acoustic pulses at certain frequencies, which reflect off of the turbulent eddies in the atmosphere. The energy in the pulses is scattered, and a portion of this energy is returned to a receiving antenna, at some shifted frequency [28]. Most SODARs are monostatic, and so the receiving antenna and the transmitting antenna are located in the same place

[27]. The shift in the frequency of the pulse is called the Doppler shift, which can be used to calculate the movement of the turbulent eddy from which the pulse is reflected.

By emitting pulses in multiple axes (a multi-axes SODAR), a SODAR can determine the movement of the atmosphere in multiple directions, and so the wind speed and direction can be determined [27]. Furthermore, the vertical profile of the atmospheric movements can be determined by measuring the returned signal as a function of time. The length of the delay in receiving the signal is related to the height at which the signal is reflected. SODARs are typically capable of measuring to heights of a few hundred meters. The result is that a SODAR can be used to determine the wind speed and direction profile as a function of height.

2.1.2 Potential Drawbacks on SODAR

While potentially extremely useful for wind resource assessment, SODARs do suffer from some drawbacks. First, SODARs generally do not operate when it is raining, and so they cannot measure data during these periods. Second, SODARs are susceptible to noise contamination. Background noise near the frequency of the emitted pulse can contaminate the signal, especially data from higher heights [27]. Third, and most importantly, ground clutter can severely affect the SODAR operation. The emitted signal can reflect off of obstacles near the SODAR, such as trees or buildings. This reflected signal has zero frequency shift, and so appears to have zero velocity. The result is that ground clutter causes the wind speed measurement to be biased low. In general, it is much more effective to position a SODAR in an open area. Lastly, SODARs emit acoustic pulses, and the noise from their operation can be bothersome to surrounding residents, and preclude their deployment in certain areas.

2.1.3 SODAR and Wind Resource Assessment

SODAR systems are potentially extremely useful devices for wind resource assessment [29]. The most obvious advantage is their ability to measure both at multiple heights, and at much higher heights than a met tower. The result is that the hub height wind speed and the wind speed profile across the rotor face of a wind turbine can be measured using a SODAR. SODARs are also much more easily installed than a met tower, requiring only a single person and a few hours of installation time. A picture of an ART VT-1 SODAR is shown in Figure 5 [28]. A SODAR of this type costs approximately \$40,000.



Figure 5 – ART VT-1 SODAR

As stated above, SODARs have some drawbacks. Ground clutter is the most severe potential drawback of a SODAR, as it is capable of reducing the estimate of the mean wind speed by 20% or more [30]. When the SODAR is positioned in a very open area, such as a large field or prairie, ground clutter effects are negligible. However, if the SODAR is used in an area with nearby trees or buildings, ground clutter effects can be

very important. Rogers et al. investigate the mitigation of ground clutter effects in SODAR, with substantial success [30]. Data processing techniques for filtering out corrupted data are developed, with the resulting SODAR measurements being much closer to nearby anemometry measurements. Overall, along with growing experience in SODAR positioning and site selection, it appears that ground clutter effects can be greatly reduced using these processing methods.

Because anemometers are the industry standard method for measuring the wind resource for wind energy applications, the utility and functioning of a SODAR is often assessed by comparing it to a cup anemometer. One consideration when using SODARs for wind resource assessment is that they are volume-averaging devices, in contrast to anemometers, which are point measurement devices. Small scale turbulence within the SODAR measurement volume is averaged out in SODAR measurements. In contrast, a fast responding anemometer, with a distance constant less than 5 m, is affected by these small scale variations. Thus, SODAR and anemometers measure fundamentally different instantaneous wind speeds. This issue is mitigated when the data are averaged over a 10-minute period of time, which is standard. The effects of local turbulence on the anemometer are likely to be averaged out over this period of time, and so the average of the SODAR and the anemometer measurements are likely to be much closer together.

On the other hand, anemometers and SODARs often calculate the wind speed differently. Anemometers calculate the instantaneous scalar wind speed, and then these values are averaged over a 10-minute period to yield the average scalar wind speed. SODARs typically calculate the average Cartesian components of the wind speed, and

then compute the vector average wind speed. The scalar wind speed is typically 1-2% higher than the vector wind speed [28].

In general, it is important that unbiased estimates of the wind resource that would be obtained using a cup anemometer can be determined using a SODAR. Because SODARs and anemometers measure the wind speed in a fundamentally different manner, their measured values are not necessarily equivalent. It is therefore not necessarily proper to utilize SODAR data in lieu of anemometer data. For example, the power output of a wind turbine, defined by its power curve (see Chapter II, Section 3.0) is referenced to the wind speed measured using a cup anemometer [13]. If a SODAR is used to measure the wind resource at a site, the estimated mean wind speed using the SODAR must closely match the mean wind speed that would be measured using an anemometer, in order to accurately estimate the annual energy production at that site. Target site SODAR data could be used in the MCP process along with reference site anemometry data as well (see Chapter II, Section 5.0). In this case, a correlation is created between concurrent SODAR and anemometer data, implying that they are measuring equivalent wind speeds.

Overall, it is imperative that SODAR data used in site assessment approximate, as closely as possible, the wind speed that an anemometer would measure. The results of Rogers et al. indicate that data processing can be used to remove the effects of ground clutter, yielding a very good agreement between SODAR data and nearby anemometer data [30]. Careful calibration of a SODAR with a met tower is also recommended [29]. The effects of the different averaging methods can be corrected for as well. In general, it is assumed in this research that reliable SODAR measurements are possible, with some

reasonable uncertainty, which provide an unbiased approximation of the wind speed that would be measured using anemometers.

2.2 Light Detection and Ranging (LIDAR)

LIDAR systems are ground-based wind speed measurement devices that utilize electromagnetic radiation to measure the wind speed. They operate in a similar fashion to SODARs in that they use the Doppler shift to calculate the wind speed and direction. The use of LIDARs for wind resource assessment is an extremely recent development, as commercial systems have only become available in the last two years [31]. This Section describes the basic operation of a LIDAR and its potential role in wind resource assessment.

2.2.1 Basic Operation of a LIDAR

A LIDAR operates by emitting a beam of light upwards into the atmosphere. The radiation interacts with natural aerosols in the air, and some of the energy is reflected back to the LIDAR. The Doppler shift of the reflected light is then used to determine the speed and direction of the wind. In order to measure horizontal wind speeds, the beam from the LIDAR must be tilted off the vertical by some angle. Many LIDARs sweep the beam in a circle about the vertical axis, which allows for the horizontal wind speeds to be determined. The vertical profile of the wind speeds can be determined as well using a LIDAR, and so they can be used to measure the wind speed at multiple heights up to a few hundred meters [32].

2.2.2 Commercial LIDAR Systems

Currently, there are very few commercially available LIDAR systems for wind energy applications. The most developed seems to be the QinetiQ Ltd. ZephIR, which is a commercially available product [33]. This instrument is a 1.55 μm continuous wave (CW) coherent LIDAR that has a laser output power of 1-Watt with a measurement range from 10-150 m [32]. A picture of the ZephIR is shown in Figure 6. These devices cost on the order of \$150,000.



Figure 6 – QinetiQ ZephIR LIDAR

2.2.3 LIDAR and Wind Resource Assessment

LIDAR systems, like SODARs, are potentially extremely useful devices for wind energy site assessment, as they are portable and capable of measuring at the hub height of a wind turbine. While LIDAR systems are similar to SODARs, there are some important

differences. The most important difference for wind energy site assessment is that LIDARs are not affected by ground clutter. Whereas ground clutter can cause low biasing in SODAR systems, this is not an issue for LIDAR, and so the potential for grossly inaccurate wind speed measurements is reduced. Like SODAR, LIDAR is a volume averaging device, as opposed to cup anemometers which are point measurements.

The performance of LIDARs for wind resource assessment appears to be very promising. While there is not a great deal of experience with the use of LIDARs, preliminary evaluations of the ZephIR LIDAR show a high level of performance. The evaluations of the ZephIR from three separate institutions compare the LIDAR wind speed measurements to cup anemometer wind speed measurements from a met tower, and the results indicate very high correlation coefficients (~ 0.99) between the measurements, with average errors less than 1% [31],[33],[34]. Overall, the evaluations indicate that a LIDAR system has the potential to be utilized for wind resource assessment in lieu of cup anemometry.

It is important that unbiased estimates of the wind resource that would be obtained using a cup anemometer can be determined using a LIDAR. This is the case for SODAR as well. Energy production estimates and MCP predictions using LIDAR data are only valid if the wind speed data from the LIDAR is a close approximation to the wind speed that a cup anemometer would have measured at the location. The results from the evaluations of the ZephIR indicate that the LIDAR can provide a very close approximation to cup anemometer measurements. In general, it is assumed in this research that reliable LIDAR measurements are possible, with some reasonable

uncertainty, which provide an unbiased approximation of the wind speed that would be measured using anemometers.

3.0 Wind Turbine Power Curves

The performance of a wind turbine is often characterized by its power curve. The power curve indicates the instantaneous power output of the turbine as a function of the wind speed at the hub height of the turbine. The power curve is a simplification of wind turbine performance, as the instantaneous air density, turbulence, and wind shear also affect the power output, along with the hub height wind speed [35]. Often, power performance testing is necessary at a wind energy development site in order to adjust the power curve for the specific site [36]. Nonetheless, power curves are an extremely useful characterization of wind turbine performance, and so they are used often in this research.

Most modern wind turbines are variable speed, pitch controlled turbines, and so they operate near their optimal tip speed ratio a portion of the time when the wind speed is above the cut-in value and below the rated value, and at constant power for wind speeds greater than the rated value and less than the cut-out value. The result is a nearly cubic increase in the wind turbine power as the wind speed increases to the rated value, depending on the speed range, at which point it produces the constant rated power. A power curve from a GE 1.5 MW turbine is shown in Figure 7. This power curve is a good generalization of modern power curves.

In general, all analyses in this research assumes that the wind turbine is a variable speed, pitch controlled turbine, with a power curve qualitatively similar to the GE 1.5 MW power curve shown in Figure 7. The wind turbine power curve is generally labeled $P_w(U)$.

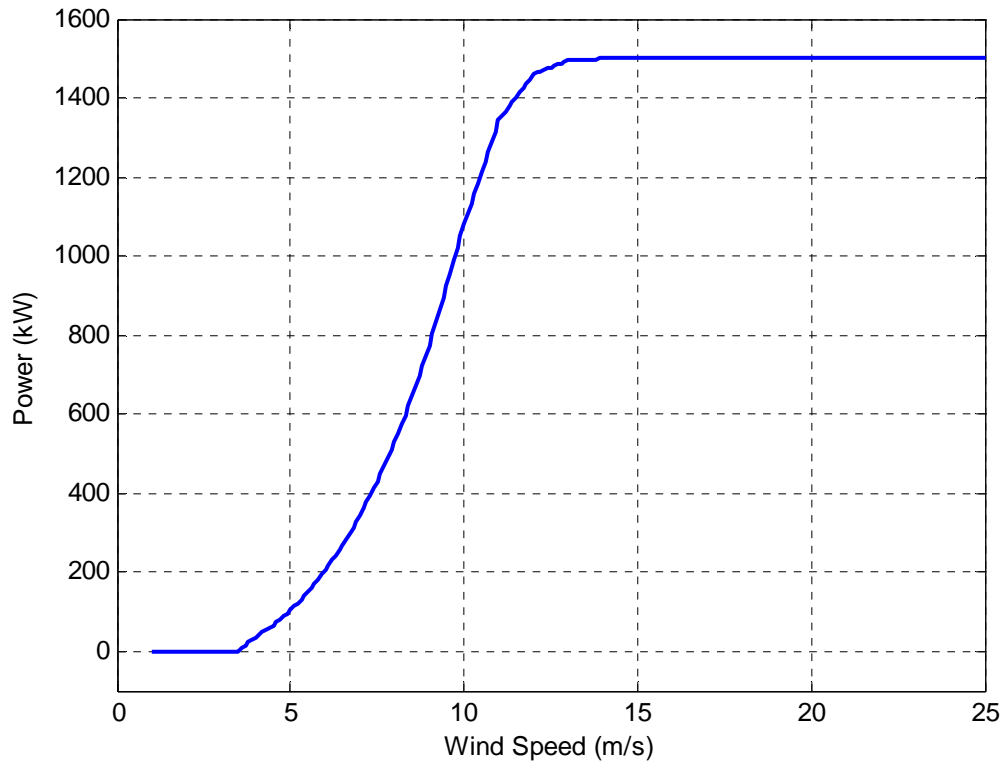


Figure 7 – GE 1.5 MW Power Curve

4.0 The Weibull Distribution

The Weibull distribution is used extensively in this research to model wind speed distributions. The Weibull distribution is commonly used for this purpose, and relies on two parameters: the scale factor c (c is sometimes referred to as A) and the shape factor k . The Weibull probability density function, where U is the wind speed, is given in Eq. 1, and a plot of the Weibull probability density function for $c=8$ m/s and $k=2$ is shown on the left in Figure 8.

$$p(U) = \left(\frac{k}{c}\right) \left(\frac{U}{c}\right)^{k-1} \exp\left[-\left(\frac{U}{c}\right)^k\right] \quad \text{Eq. 1}$$

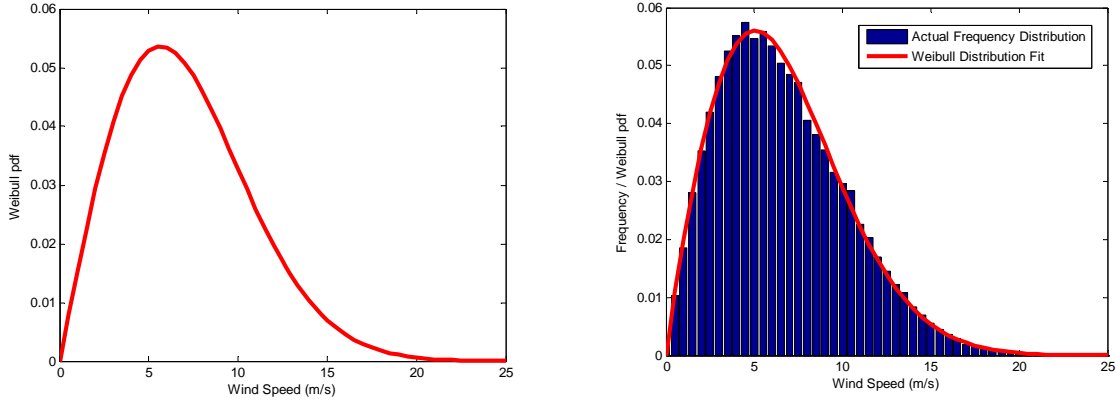


Figure 8 – Example Weibull Distributions

Often the Weibull distribution provides a good approximation of the actual wind speed distribution at a site, although this is not always the case. Shown in Figure 8 on the right is an example of a Weibull distribution fit to actual wind speed frequency distribution data. For this example, the Weibull distribution provides a good fit to the wind speed frequency distribution.

A statistical model approximation to the wind speed distribution, as opposed to simply using the measured time series or the frequency distribution of the measured data, is useful for several reasons. First, a statistical model allows for the shape of the distribution of the wind resource, and therefore the potential to produce energy from a wind turbine at the site, to be quantified by the parameters of the model. In the case of the Weibull distribution, the shape of the distribution of the wind resource is easily summarized by the values of c and k . Second, a statistical model is extremely useful for handling uncertainty both in wind resource assessment and in the *AEP* estimation. The

use of the Weibull distribution for uncertainty analysis in site assessment is explored in detail in Chapter III. On the other hand, a statistical model approximation can introduce error into the process, especially when the model does not provide a good fit to the data.

4.1 Weibull Parameter Estimation

There are several methods for estimating the Weibull parameters from a wind speed time series. These methods include: empirical methods, method of moments, maximum likelihood estimates, least square linear regression, and chi-squared methods. In general, an empirical method is used in this research, due to its simplicity. The empirical method is shown in Eq. 2, where σ_U is the standard deviation of the wind speed data, \bar{U} is the mean wind speed, and Γ is the gamma function [21].

$$\begin{aligned} k &= \left(\sigma_U / \bar{U} \right)^{-1.086} \\ c &= \bar{U} / \Gamma(1 + 1/k) \end{aligned} \quad \text{Eq. 2}$$

4.2 Energy Production Estimates using the Weibull Distribution

The Weibull distribution can be used to estimate the energy production of a wind turbine. The average power output of the turbine can be found by integrating the product of the wind speed distribution, $p(U)$, and the power curve, $P_w(U)$, over all values of wind speed, U , and then multiplying by the energy losses, ELF . AEP is simply the average power multiplied by the number of hours in a year, 8760. This is shown in Eq. 3.

$$\begin{aligned} AEP &= 8760 \cdot ELF \int_0^{\infty} P_w(U) p(U) dU \\ &= 8760 \cdot ELF \int_0^{\infty} P_w(U) \left(\frac{k}{c} \right) \left(\frac{U}{c} \right)^{k-1} \exp \left[- \left(\frac{U}{c} \right)^k \right] dU \end{aligned} \quad \text{Eq. 3}$$

The capacity factor is often used as a measure of the energy production, in lieu of *AEP*. The capacity factor is a non-dimensional number, equal to the average power divided by the rated power of the wind turbine, P_R . The equation for the capacity factor, CF , is shown in Eq. 4.

$$CF = \frac{ELF}{P_R} \int_0^{\infty} P_w(U) p(U) dU = \frac{ELF}{P_R} \int_0^{\infty} P_w(U) \left(\frac{k}{c}\right) \left(\frac{U}{c}\right)^{k-1} \exp\left[-\left(\frac{U}{c}\right)^k\right] dU \quad \text{Eq. 4}$$

4.3 Justification of the use of the Weibull Distribution

A statistical model approximation such as the Weibull distribution, while convenient, can introduce error into the calculation of the energy production, especially when the model does not provide a good fit to the data. An investigation to assess the validity of a statistical model approximation to the wind speed distribution is now described:

1. 30 different sites, with at least 3 years of data, are selected.
2. For each site, the mean wind speed and the Weibull parameters are calculated.
3. The actual frequency distribution is also determined, using 0.5 m/s bins.
4. The energy production for a GE 1.5 MW wind turbine is calculated, using the actual wind speed frequency distribution, as well as the Rayleigh and Weibull approximations to the wind speed distribution. The Rayleigh distribution is simply the special case of the Weibull distribution with $k=2$, and is also commonly used to model the wind speed distribution. The energy production when using the Weibull or Rayleigh distribution is calculated using Eq. 3.

The results are calculated by comparing the energy production estimates for the two statistical models to the estimate using the actual frequency distribution. The actual

frequency distribution is considered the “true” value. In general, these results are dependent on the bin width used to summarize the frequency distribution, and the method used to sum over the bins. The important results are:

- On average, using the Weibull distribution causes a 0.5% overestimation of the energy production, compared to using the actual frequency distribution. The error in the estimate has an approximately 1% standard deviation.
- The Rayleigh distribution overestimates the energy production by 3% on average, with a standard deviation of 7%.

Clearly the Weibull distribution is the superior statistical model compared to the Rayleigh, as the error and the variability in the estimates are much lower. Overall, it appears that the use of the Weibull distribution to represent the wind speed distribution and calculate the energy production from a wind turbine is justifiable.

5.0 Measure-Correlate-Predict

Wind speeds at a site vary with respect to a number of time scales, including diurnal variations, seasonal variations, and inter-annual variations. Whenever the wind resource is measured at a site, variations at time scales longer than the measurement length can cause the measured data to be unrepresentative of the actual long-term wind resource at the site. In the case of inter-annual variations, twenty years of measured data are often considered sufficient to capture the true long-term wind resource, and therefore average out the inter-annual variations [9],[11]. Since one of the primary goals of wind energy site assessment is to estimate the long-term wind resource at a site, it is critical to account

for these variations at longer time scales. On the other hand, measuring the wind resource for twenty years is not realistic.

Measure-Correlate-Predict (MCP) is a frequently used method for estimating the long-term wind resource at a “target site” that is being assessed for wind energy development [37]. MCP utilizes a nearby site, called the “reference site,” with a multi-year data set, as well as data concurrent with the target site. The steps involved in the general MCP process are:

1. Measure the wind speed at the target site. This is the “measure” step.
2. Obtain wind speed data from a nearby reference site, and find the concurrent data between the target site and the reference site.
3. Create a functional relationship between the concurrent data sets, which yields the target site wind speed (and possibly other conditions) as a function of the reference site wind speed (and possibly other conditions). This is the “correlate” step.
4. Apply this functional relationship to the full reference data set to estimate the long-term wind resource at the target site. This is the “predict” step.

The actual implementation of the MCP process can be visualized using Figure 9. The plot on the left shows wind speed data from two nearby sites [38]. The upper time series is the reference site, with approximately seven years of data, and the lower time series is the target site, with one year of data.

The concurrent data for the two sites, which are the one year of overlapping data in 2004, can then be displayed in a scatter plot, shown on the right. This plot shows the

target site data on the y-axis and the reference site data on the x-axis. Also shown in the plot is a linear fit to the data (more details on MCP models is provided later), which is one type of MCP correlation method that can be used. This model can then be applied to the seven years of reference site data, yielding a prediction of the long-term wind resource at the target site.

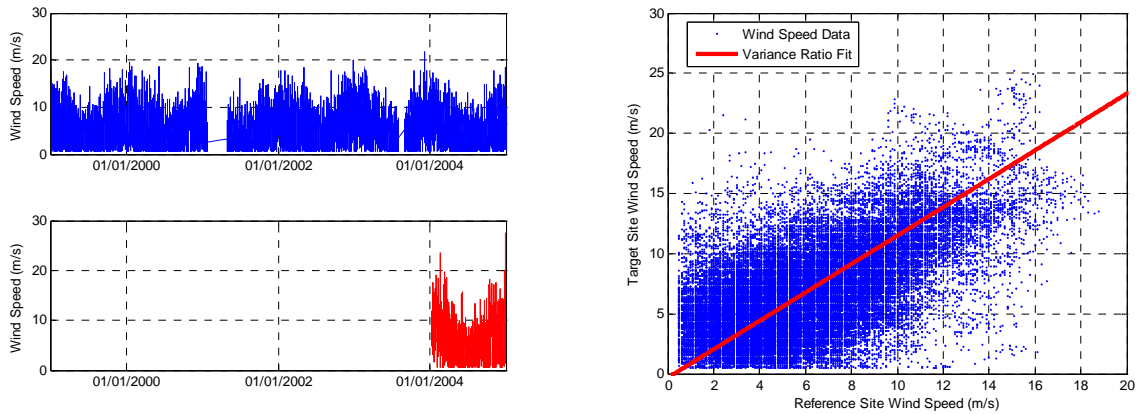


Figure 9 – Reference/Target Site Data / Variance Ratio Fit to Concurrent Data

The utility of MCP lies in the utilization of reference site data sets with much longer data lengths than the measured target site data. The long-term reference site data provide information about variations in the wind resource at time scales longer than the length of the target site data. A simple way to look at MCP, if one year of target site data is measured, is that it indicates if that particular year at the target site is a windy year or not. MCP is not restricted to a full year of target site data, however. Any length of target site data can be used in the MCP process.

5.1 A Review of MCP Models

The actual functional correlation in MCP, relating the reference site wind speed to the target site wind speed, can take on a variety of forms [37],[39]. Many models bin the

data by direction, and so model parameters are calculated and applied for each direction bin. These direction bins can be simple bins of equal size, such as eight direction sectors of 45 degrees each, or more complex binning methods can be used, such as dynamic sectoring [40] or matrix methods [41].

The types of models used in MCP include linear models [42],[43], non-linear models [40],[44], models that utilize temperature data [45], artificial neural networks [46],[47], Markov chain models [48], joint probability models [49], and more [50].

Rogers et al. [37] and Anderson et al. [39] provide detailed reviews of a variety of MCP methods, as well as a comparison of the performance of several methods. Anderson et al. point out that the more complex non-linear and neural network models do not perform substantially better than the simple 2-parameter linear models. Rogers et al. also develop a linear model, the “Variance Ratio” method, which performed well compared to three other models. This model is discussed next.

5.2 The Variance Ratio MCP Method

The Variance Ratio method is used exclusively in this research, for several reasons. First, linear models are simple to implement. Second, more complex non-linear and neural network models have not been shown to provide substantially better predictions. Finally, in one comparison to other linear models, the Variance Ratio method performs the best [37]. Overall, the Variance Ratio method appears to provide an appealing combination of performance and simplicity.

The Variance Ratio method is a linear model, and the parameters in the model are set to ensure that the variance of the predicted target site data is equal to the variance of the actual target site data. The formulation of the Variance Ratio method is shown in Eq. 5,

where μ_y and μ_x are the respective means of the concurrent target site and reference site data, and σ_y and σ_x are the respective standard deviations of the concurrent target site and reference site data. The long-term reference site wind speed data are denoted by x , and the predicted target site wind speed data are y' . An example fit to concurrent data is provided in Figure 9. In that example, $A = 1.18$ and $B = -0.34$.

$$\begin{aligned} y' &= Ax + B \\ A &= \sigma_y / \sigma_x \\ B &= \mu_y - A\mu_x \end{aligned} \tag{Eq. 5}$$

5.3 Uncertainty in MCP Predictions

MCP is an effective method for estimating the long-term wind resource at a site from short-term measured data [51]. To be truly useful in wind energy applications, the uncertainty of the MCP predictions must be estimated as well [52]. For a linear regression model, Derrick develops an approach for estimating the uncertainty of the MCP prediction [51]. However, as shown by Rogers et al., this approach significantly underestimates the actual uncertainty of the predictions [52]. This is because the wind data relationship between two sites is serially correlated, and so linear regression theory cannot be used to estimate the uncertainty associated with the MCP prediction.

An alternative approach to estimating the uncertainty is proposed by Rogers et al. that uses a jackknife estimate of variance [52]. This method determines the variability of the prediction by dropping out segments of the concurrent data set. The results of the investigation indicate that the jackknife estimate of uncertainty provides a significant improvement over linear regression theory in estimating the uncertainty associated with the MCP procedure, although there is still some underestimation of the uncertainty on

average. The jackknife estimate of variance is used often in this research to estimate the uncertainty of MCP predictions.

5.4 MCP Parameters Selection

There are a variety of parameters that can be adjusted when implementing the Variance Ratio MCP method. These parameters can affect the performance of the MCP predictions, so it is important to state their values for consistency and clarity. This Section briefly describes three important MCP parameters, and the values that are used in all later analyses. A rigorous justification for the choice of these parameters is not provided. Instead, the parameters are chosen to be certain values because they appeared to be “good enough.” The parameters are:

- The number of direction sectors. This parameter determines the number of bins that the target site and reference site data are grouped into by direction for MCP. The use of direction sectors is meant to account for varying relationships between the target and reference site as a function of direction. Eight or twelve direction sectors are common [51],[53]. This research uses one direction sector, as the accuracy and precision of the MCP predictions are often fairly insensitive to the number of direction sectors. Using a single direction sector is also useful when a small amount of target site data are available, as binning the data by direction can result in a very small amount of data length in some bins.
- The cutoff wind speed. This parameter determines the minimum target site or reference site wind speed for a data point to be used in the correlation step of MCP. That is, wind speed values less than a certain cutoff value are not used to calculate the fit to the concurrent data (e.g. the fit in Figure 9). This parameter is

utilized because there can be much more variability in the relationship between the two sites at low wind speeds, and this variability does not necessarily indicate any actual relationship between the sites [53]. All later analyses in this research use a cutoff wind speed of 2 m/s. The accuracy and precision of MCP predictions is slightly better for this value compared to 1 m/s or 3 m/s, although the difference is small.

- **Seasonal MCP Parameters.** Because the wind resource has pronounced seasonal variations, calculating MCP parameters for each season (or each month) may offer a means of incorporating these seasonal variations into the MCP algorithm. While this approach holds promise, it is not utilized in this research.

6.0 Wind Shear Modeling and Extrapolation

In the boundary layer of the earth, the wind speed tends to increase with height. This phenomenon is referred to as wind shear, and shear extrapolation is the process of estimating the wind speed at a higher height using measured data at a lower height. Wind shear extrapolation is an extremely important component of wind energy site assessment.

6.1 Wind Shear in Site Assessment

There are many approaches to dealing with wind shear in the site assessment process. Commonly, measured wind speed data from the met tower is used to calculate a shear parameter, and then a shear model is applied in order to estimate the wind resource at the turbine hub height. Another approach utilizes numerical flow models and the local topography and roughness to estimate the wind resource at higher heights. Regardless of the approach, these processes can introduce a great deal of uncertainty into the hub height

estimate, and consequently wind shear modeling and extrapolation is a critical step in the site assessment process.

Because wind speeds typically increase with height, there is a strong incentive to increase turbine hub heights in order to capture more energy from the wind. Wind turbine hub heights are increasing steadily, with heights as high as 100 m or higher built or planned [12]. The increased energy production often outweighs the increased tower cost, making taller wind turbines economically advantageous [54].

As the turbine hub heights increase, but met tower heights remain relatively constant, shear extrapolation becomes an extremely important component of the site assessment process. Accurate methods for shear extrapolation are needed to minimize the errors in the prediction of the hub height wind resource. However, as wind turbine hub heights and met tower measurement heights become separated by larger and larger distances, shear extrapolation becomes more uncertain [17].

6.2 Wind Shear Modeling

There are many approaches to shear extrapolation. In one method, standard values for the shear parameters (either the surface roughness length or the power law exponent) for a given type of terrain can be used. These “rules of thumb” values are based on experience and empirical data. The “ $1/7^{\text{th}}$ ” power law rule, for example, is often used in flat terrain. Elkinton et al., however, show that these rules of thumb values are often inadequate in predicting the wind resource at hub height, leading to large errors [16].

In a second approach, the shear parameter can be estimated if there are measured data from the met tower at two heights. In this case, the measured data are used to calculate the shear parameter at the site, which is then used to estimate the hub height wind

resource. Once again, this method can result in significant errors in the estimation of the hub height wind resource [16].

Lastly, numerical flow models can be used to estimate the wind resource at higher heights [8]. These models account for the local topography and roughness, and along with the measured data at one or several locations, estimate the wind resource at other locations and higher heights.

The power law and the log law are the two most commonly used models for approximating the wind shear at a site. The power law is shown in Eq. 6 and the log law is shown in Eq. 7 [21]. The relevant wind shear coefficient, either α or z_0 , can be calculated when the wind speed is measured at two heights.

$$\frac{U(z)}{U(z_r)} = \left(\frac{z}{z_r} \right)^\alpha \quad \text{Eq. 6}$$

- $U(z)$ is the wind speed at height z .
- $U(z_r)$ is the reference wind speed at the reference height z_r .
- α is the power law exponent.

$$\frac{U(z)}{U(z_r)} = \ln \left(\frac{z}{z_r} \right) / \ln \left(\frac{z_r}{z_0} \right) \quad \text{Eq. 7}$$

- $U(z)$ is the wind speed at height z .
- $U(z_r)$ is the reference wind speed at the reference height z_r .
- z_0 is the surface roughness length.

Elkinton et al. show that the power law and log law models perform equivalently in shear extrapolation predictions [16]. There are also more complex wind shear models that can be used. Some of these models incorporate the vertical temperature gradient at

the site to determine the atmospheric stability, yielding a more accurate shear model. Numerical models that incorporate the surrounding topography and surface roughness can also be used. These complex models are outside the scope of this research. In this research, the power law is primarily utilized.

CHAPTER III

SITE ASSESSMENT AND UNCERTAINTY

1.0 Introduction

The traditional wind energy site assessment process is described in detail in Chapter I, Section 1.1. While this description focuses primarily on the process of estimating the long-term wind resource and the energy production from a wind farm, another critical but sometimes overlooked component of this process is determining the uncertainty of these estimates. This Chapter focuses on uncertainty in the site assessment process.

Wind resource assessment is an uncertain process, and a large number of factors ranging from wind speed measurement errors to the inherent physical variations in the wind contribute to this uncertainty. Overall, these various individual sources of error must all be accounted for in order to provide an estimate of the total uncertainty of the estimated wind resource. Furthermore, power curves and energy loss terms are uncertain as well. When the wind resource, the power curve, and the energy losses are combined to estimate the annual energy production (*AEP*), the uncertainties from all the factors contribute to an overall *AEP* uncertainty. This uncertainty is critical in estimating the risk associated with the potential venture, and the ability to secure a loan for a wind energy development is closely tied to the perceived risk [14].

This Chapter considers the site assessment process in which meteorological towers (met towers) equipped with cup anemometry and vanes are the primary method for evaluating the wind resource, which is the most common method in the United States [55]. Alternative methods for site assessment are not considered in this Chapter. On the

other hand, many of the techniques developed in the Chapter can be modified and utilized to estimate the uncertainty when using alternative monitoring approaches, like those discussed in Chapters V-VI.

This Chapter has three goals. First, it seeks to identify a comprehensive set of the potential sources of error and the associated uncertainties inherent in wind resource assessment and energy production estimation. When possible, the uncertainties are quantified, or ranges of values are given. Second, it presents a method for estimating the long-term wind resource and then the *AEP* at a site, using the measured wind resource, the wind turbine(s) power curve(s), and the expected energy losses. Finally, methods for combining the individual uncertainty estimates into a final estimate of the overall uncertainty of the *AEP* are presented. This uncertainty depends on the respective uncertainties of the wind resource, the wind turbine power curve, and the expected energy losses, and combining all of the uncertainty sources is a complex process.

This Chapter utilizes the Weibull distribution as an approximation of the wind speed probability distribution, which is also described in Chapter II, Section 4.0. A statistical model is extremely useful for handling uncertainty both in wind resource assessment and in *AEP* estimation. Many of the statistical techniques presented in this Chapter rely on the ability to express the wind speed distribution in a functional form. By using a Weibull distribution to represent the wind speed distribution, the uncertainty in the wind resource can be expressed as uncertainty in the values of c and k . On the other hand, it is often easier to conceptualize and estimate uncertainty in the mean wind speed rather than in c . Thus, the uncertainty in the mean wind speed and k are determined first, and then the uncertainty in c is calculated from these values.

1.1 Chapter Overview

As stated above, the *AEP* estimate depends on the wind resource, the wind turbines' power curve, and the expected energy losses. These three factors and their respective uncertainty must be determined in order to estimate both the *AEP* and the uncertainty of the *AEP*.

This Chapter is organized as follows:

- Section 2 reviews error types and uncertainty analysis.
- Section 3 presents the process of estimating the long-term wind resource and the factors that contribute to uncertainty in evaluating the wind resource. For each of these factors, the contribution to the uncertainty in both the mean wind speed and k is estimated.
- Section 4 discusses the factors that contribute to uncertainty in the power curve and power production of a wind turbine.
- Section 5 describes the energy loss factors and their uncertainty.
- Section 6 provides a means of combining the wind resource, the power curve, and the energy loss factors into a final estimation of the *AEP* of a wind turbine or wind farm, and combining their respective uncertainties into an estimate of the overall *AEP* uncertainty.

2.0 Review of Error Sources and Measurement Uncertainty Analysis

Before discussing the details of wind resource uncertainty, it is important to review the basics of error types and uncertainty analysis. The error analysis concepts presented in this Section are used throughout the rest of the Chapter. All measurements, no matter

how carefully done, are subject to errors, which results in a measured value differing from the true value. The amount by which they differ (the size of the error) is unknown, and so all measurements are subject to some uncertainty. In this Chapter, the term “uncertainty” is used as a general measure of the size of the error. The error in a measurement is comprised of two components: the random error and the systematic error [56]. Each of these components is now discussed.

2.1 Random Error Uncertainty

Random error is produced by variability in the quantity being measured or the measurement procedure. For example, when measuring the duration of an event using a stopwatch, random error may arise when multiple measurements are made. The reaction time of the stopwatch operator may vary, causing each measurement to differ. The standard deviation of the measurements is a measure of the uncertainty of a single measurement due to random error. These errors are often assumed to have normal distributions about the true value. If the measurements have a normal distribution, then approximately 68% of the measurements are within one standard deviation of the mean, and approximately 95% are within two standard deviations of the mean.

Often, the mean of the measurements is the quantity of interest. The uncertainty of the mean of the measurements is not equal to the standard deviation of the measurements. Rather, using the central limit theorem, the uncertainty of the mean of the measurements, $\delta\bar{x}$, is equal to the standard deviation of the measurements, σ_x , divided by the square root of the number of measurements, N , assuming the measurements are independent. This relation is shown in Eq. 8.

$$\delta\bar{x} = \sigma_x / \sqrt{N} \quad \text{Eq. 8}$$

The uncertainty in the estimate of the mean decreases as the number of measurements increases. Furthermore, this uncertainty is normally distributed for a large N , even if the distribution of the measurements is not normal. Sources of random error are categorized as Type A uncertainty. In summary:

- Random error is due to variability in measurements, and can be identified from the measured data.
- The uncertainty is characterized by the standard deviation of the measurements.

The uncertainty in the mean of the measurements decreases with the number of measurements made. This uncertainty is labeled Type A.

2.2 Bias and Unknown Bias Uncertainty

Systematic errors, or biases, are constant over a set of identical measurements. These errors are often due to an error in a calibration constant. An example of a systematic error is a stopwatch that runs slowly. Any measure of the duration of an event with that stopwatch results in a value that is smaller than the true value. Systematic errors cannot be revealed by repeated measurements because they are constant over the set of measurements (assuming the same instruments are used, e.g., the same stopwatch).

Whenever a measurement is performed, effort should be made to identify the systematic errors, and to either remove the source of the errors or to adjust the measurements by the value of the bias. For example, if one knew that the stopwatch ran slowly by a certain amount, all measurements could be scaled to correct for this known bias. This scaled value is then the estimate of the true value of the measurement. Once the bias is accounted for by scaling the measurements, the uncertainty is expressed as a

value around the scaled value. An estimate of the bias of an instrument often requires comparison to an unbiased (generally more precise) instrument or comparison to measurements from multiple instruments. In this Chapter, for every source of error, the probable bias is estimated. A positive bias is used when a quantity is known to be overestimated and a negative bias when the quantity is known to be underestimated.

The issue is complicated when the bias in a measurement is unknown. Again using the stopwatch example, if one does not know how slowly or quickly a stopwatch is running, this produces additional uncertainty in the measurement. However, the bias, while unknown, is constant across every measurement, and so it does not behave like random error, which varies with each measurement and so can be calculated from the measured data. The uncertainty due to unknown systematic errors is typically estimated based on experience [57]. Furthermore, uncertainty due to unknown bias does not necessarily have to be characterized by a normal distribution, and therefore measured by the standard deviation.

The issue is resolved as follows. While any particular instrument can be subject to an unknown bias, the bias of a collection of all of those instruments is assumed to be normally distributed with a mean value of zero. For example, the mean bias of all the stopwatches from a certain model is assumed to be zero, and variability in the bias of the instruments is assumed to be normally distributed about zero. When one randomly selects a stopwatch from the set of all stopwatches, the uncertainty due to an unknown bias is equal to the standard deviation of the biases of the set of stopwatches. Thus, there is a random component to the unknown bias, even if it is constant for a single instrument. Therefore, the unknown bias uncertainty is characterized by a normal distribution, and so

the standard deviation is the measurement of the uncertainty. The standard deviation of the unknown bias can be measured if multiple instruments are used simultaneously. However, when only a single instrument is used, then the uncertainty has to be approximated. This uncertainty is approximated often in this Chapter, as it is generally not feasible to have multiple instruments taking simultaneous measurements. The uncertainty due to unknown bias is categorized as Type B uncertainty (in statistical literature, the Type A and Type B uncertainties would be called components of variance). In summary:

- In any measurement, effort should be made to identify and eliminate systematic errors.
- Systematic errors cannot be identified from the data.
- Unknown bias is inevitable, and no comprehensive theory exists for dealing with uncertainty due to unknown bias.
- This Chapter characterizes all uncertainty due to unknown bias using a normal distribution. This uncertainty is labeled Type B.

2.3 Combination of Uncertainties

This Chapter assumes that all Type A and Type B uncertainties are independent and normally distributed. These are similar assumptions to those recommended in the IEC 61400-12 standards and by Frandsen et al. [13],[57],[58]. Unless otherwise stated, uncertainties are characterized by the fractional standard uncertainty. The fractional standard uncertainty is a percentage uncertainty, and is calculated as the uncertainty of the measurement of a parameter divided by the absolute value of the expected value of the parameter. In contrast, the absolute standard uncertainty of a quantity is simply the

uncertainty of the measurement of the parameter and so it has units. Throughout this Chapter, a superscript ^{*} is used to denote absolute uncertainties. Fractional uncertainties do not have a ^{*} superscript.

In some cases, specific sources of Type B uncertainty are more easily characterized by an uncertainty limit. That is, the estimated distribution is rectangular, with a probability of one that the measurement occurs in some range, $\pm R$. In these cases, the standard uncertainty, δx , is equal to R divided by the square root of three, shown in Eq. 9 [13].

$$\delta x = R / \sqrt{3} \quad \text{Eq. 9}$$

An example is shown in Figure 10. In this example, a rectangular distribution, with a mean value of one and a range of two, is plotted. R is therefore equal to one, and so the standard uncertainty is equal to one divided by the square root of three, which is 0.577. A normal distribution with this standard deviation and a mean of one is also plotted in Figure 10.

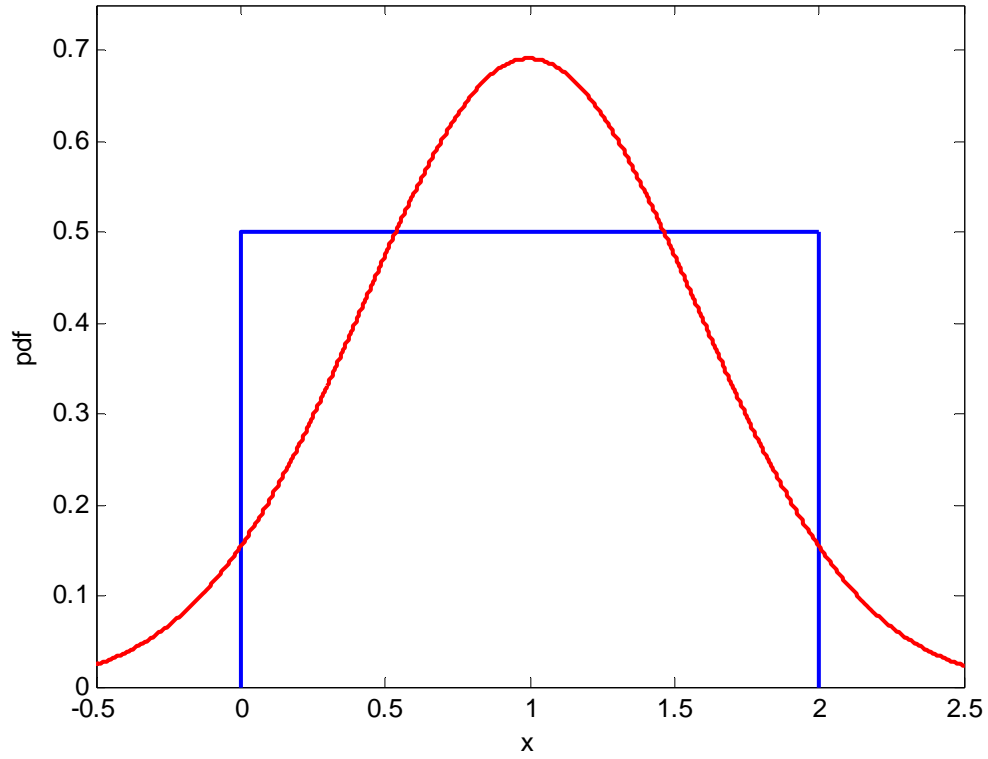


Figure 10 – Example of Rectangular and Normal Distribution

Once all of the uncertainty sources are identified and estimated, they can be combined to determine a total uncertainty. When multiple uncertain quantities are used to calculate some parameter, the uncertainties in the component quantities combine to yield a total uncertainty in the parameter. For a parameter f , that is a function of several variables, $f=f(x_1, \dots, x_n)$, the uncertainties of the variables, δx_1^* , ..., δx_n^* , are combined to yield an overall uncertainty, δf^* . δf^* is calculated using Eq. 10, as long as the uncertainties are independent [56]. All uncertainties in Eq. 10 are absolute uncertainties, and so they can have units.

$$\delta f = \sqrt{\left(\frac{\partial f}{\partial x_1} \delta x_1\right)^2 + \dots + \left(\frac{\partial f}{\partial x_n} \delta x_n\right)^2} \quad \text{Eq. 10}$$

Eq. 10 can be non-dimensionalized so that the uncertainties are expressed as fractional uncertainties. The non-dimensional form of Eq. 10 is shown in Eq. 11. In Eq. 11, δf and $\delta x_1, \dots, \delta x_n$ are now fractional uncertainties. The partial derivatives and the fractions, which multiply the fractional uncertainties, are referred to as “sensitivity factors,” since they measure how sensitive changes in f are to changes in the variables. For example, if f has a linear dependence on a variable, then the sensitivity factor is one for that variable. For a quadratic dependence, the sensitivity factor is two. The sensitivity factors may be positive or negative in order to indicate if a change in the individual variable causes an increase or a decrease in f . The sign is not particularly important though, since the terms are then squared. The sensitivity factors are also non-dimensional. If all of the sensitivity factors are equal to one, then Eq. 11 reduces to a simple root-sum-square technique (RSS).

$$\delta f = \sqrt{\left(\frac{\partial f}{\partial x_1} \frac{x_1}{f} \delta x_1\right)^2 + \dots + \left(\frac{\partial f}{\partial x_n} \frac{x_n}{f} \delta x_n\right)^2} \quad \text{Eq. 11}$$

In this Chapter, Type A and Type B uncertainties can be combined together using Eq. 11 as long as they are each expressed using the standard deviation as a measure of uncertainty. It must be emphasized that there is no definitive method for combining Type A errors and Type B errors. Both Taylor and Frandsen suggest this method as the best available option, assuming that the individual uncertainty sources are independent [56],[57]. Also, because the total uncertainty is the sum of multiple independent individual sources of uncertainty, by the central limit theorem, the distribution of the total uncertainty tends toward a normal distribution, regardless of the distribution of the

individual sources of uncertainty. In this Chapter, all sources of uncertainty are assumed to be normally distributed, so the distribution of the total uncertainty is also normal.

3.0 The Wind Resource and Uncertainty

Wind resource assessment is the first major step in the wind energy site assessment process. It consists of using measured wind speed data to estimate the long-term hub height wind resource at each turbine location. This process is briefly described in Chapter I, Section 1.0. The “Wind Resource Assessment Handbook” provides a detailed description of many aspects of the site assessment process, especially a method for measuring the wind resource at a site [1]. Because the wind resource varies from year to year, an estimate of the long-term value is critical to accurately estimate energy production [6],[7]. Also, wind turbine power output depends on the wind speed at the turbine hub height and location. The result is that an estimate of the hub height wind resource is necessary for accurate estimations of *AEP*. Furthermore, when multiple wind turbines are installed at a site or when the met tower and the turbine are in different locations, the wind resource must be estimated at the location of each turbine [7],[8].

When the Weibull distribution is used to characterize the wind resource, the goal of wind resource assessment is to estimate the long-term hub height values of the Weibull parameters, c_{LT_HUB} and k_{LT_HUB} at each turbine location. The values of these parameters can then be used in the estimate of *AEP*.

In general, wind resource evaluation is a time consuming process, subject to a great deal of uncertainty. This Section describes the four categories of uncertainty sources that arise in evaluating the wind resource. There are a total of fourteen individual component uncertainty sources identified in this Chapter that contribute to the wind resource

uncertainty, encompassed by the four categories of uncertainty. For each of the fourteen potential sources of error discussed in this Section, the contribution to the uncertainty in both the mean wind speed (and therefore c) and k is given, as well as the value for any known bias. After the discussion of each uncertainty, a table is given to summarize the results. Next, a method is presented for estimating c_{LT_HUB} and k_{LT_HUB} from measured wind speed data. This process for estimating the wind resource informs the process for estimating the wind resource uncertainty. Finally, a method for estimating the wind resource uncertainty is presented. The method uses the error analysis techniques outlined in Section 2.0. Specifically, sensitivity factors are calculated for the various categories of uncertainty. Because the Weibull distribution is used to characterize the wind resource, the wind resource uncertainty can be expressed as uncertainty in the values of c and k .

The causes of uncertainty that arise in wind resource assessment can be subdivided into four categories. These four categories are labeled with subscripts “ M ”, “ LT ”, “ V ”, and “ SA ”.

- I. Wind Speed Measurement Uncertainty (M).
- II. Long-term Resource Estimation Uncertainty (LT).
- III. Wind Resource Variability Uncertainty (V).
- IV. Site Assessment Uncertainty (SA).

3.1 Wind Speed Measurement Uncertainty

Uncertainty arises when measuring the actual wind speed at a site. The wind speed at a site is usually measured by taking 10-minute averages (sometimes 1-hour averages) of the wind speed, sampled at approximately 1 Hz. Wind data at a site are then presented as a time series of these 10-minute averages [1]. The 10-minute averaged wind speeds are

labeled U_M in this Chapter. The measured mean wind speed at a site is the mean of all the values of the measured wind speed. Likewise, the measured wind speed can be used to estimate the Weibull parameters. The measured mean wind speed and Weibull parameters are labeled U, \bar{U}_M, c_M , and k_M , respectively.

Several factors can contribute to errors in the measurement of the wind speed, and therefore in determination of U, \bar{U}_M, c_M , and k_M . They are labeled $\delta U_1, \delta U_2, \delta U_3, \delta U_4, \delta U_5, \delta U_6, \delta U_7$ and $\delta k_1, \delta k_2, \delta k_3, \delta k_4, \delta k_5, \delta k_6, \delta k_7$. They are:

1. Anemometer Uncertainty I (Calibration Uncertainty).
2. Anemometer Uncertainty II (Dynamic Overspeeding).
3. Anemometer Uncertainty III (Vertical Flow Effects).
4. Anemometer Uncertainty IV (Vertical Turbulence Effects).
5. Tower Effects.
6. Boom Effects.
7. Data Reduction Accuracy.

1. Anemometer Uncertainty I (Calibration Uncertainty) – While anemometers are the preferred means of measuring wind speed, they also have the potential for measurement error. The uncertainty due to this measurement error arises from variations between anemometers of a given model, and is referred to as a “calibration uncertainty.” While a general transfer function may exist for a particular model of anemometer, this transfer function may not exactly represent a specific anemometer, and therefore unknown bias may be present. Alternatively, if a specific anemometer is calibrated in a wind tunnel, measurement errors in the calibration process can again lead to an inaccurate

transfer function, and so unknown bias is once again present. Thus, this is a Type B uncertainty, since it is due to an unknown bias.

One of the most common anemometers used in the wind industry in the U.S. is the NRG Maximum 40 anemometer. This is also the anemometer used by the Renewable Energy Research Laboratory (RERL). Lockhart and Bailey investigate the accuracy of the Maximum 40 anemometer. They conclude that: “The #40 is accurate to within 0.1 m/s for the wind speed range 5 m/s to 25 m/s” [24]. This uncertainty therefore ranges between 0.4% and 2% depending on the wind speed. Likewise, the Risø P2546 model anemometer has an approximate uncertainty of 0.1 m/s [26]. Finally, the Thies First Class 4.3350.10.000 has an uncertainty of approximately 1% [25]. Overall, a reasonable estimate of the uncertainty of $U, {}^-_M$ due to anemometer calibration uncertainty is 1.5%, because this is an approximate average of the conservative values for the three anemometer models. This recommended value clearly depends on the type of anemometer used, and the wind resource at a site.

Uncertainties in the anemometer readings can also lead to uncertainties in k_M . In this particular case, an uncertainty of 0% for k_M is used since small uncertainties in an individual measurement of the wind speed should have a negligible effect on the shape of the wind speed distribution.

δU_1	δk_1	Bias U_1	Bias k_1
1.5%	0%	0%	0%

2. Anemometer Uncertainty II (Longitudinal Dynamic Overspeeding) - Overspeeding is a well-known source of error in cup anemometers, as their inherent physical design causes them to speed up more rapidly than they slow down, thereby

causing an overestimation of the wind speed. This overestimation does not come into play in laminar flow with very slow changes in the wind speed. Rather, overspeeding is caused by turbulent wind, where the wind speed changes rapidly. Thus, overspeeding is inextricably linked to turbulence in the wind. Perhaps unsurprisingly, overspeeding is therefore a function of the turbulence intensity (as well as other factors). The turbulence intensity is equal to the standard deviation of the wind speed measurements over a certain period, divided by the mean wind speed over that period, as shown in Eq. 12.

$$TI = \sigma / \bar{U} \quad \text{Eq. 12}$$

Turbulence intensity is a non-dimensional term that quantifies the degree of turbulence in the wind during a certain time period. Turbulence intensity can also be broken down into Cartesian components, so one can measure the longitudinal, lateral, and vertical turbulence intensity (the longitudinal direction is horizontal and in the direction of the mean wind speed whereas the lateral direction is perpendicular to the vertical and longitudinal directions), which are equal to the standard deviation of the wind speed component in the respective directions, divided by the overall mean wind speed. Overspeeding is traditionally defined as the effect due to the longitudinal turbulence – that is, turbulence in the direction of the mean wind speed.

It must be noted that the effects of turbulence on the measurements of cup anemometers is an extremely complicated phenomena, and it is still not fully understood [35],[36]. The discussion of overspeeding and turbulence effects presented here is by no means exhaustive. Instead, it is meant to provide some basic background information, to make the reader aware of the issue of turbulence effects, and to provide some guidance on approximating uncertainty and bias due to these effects. For more detailed

information on the physics and effects of turbulence on the measurements of cup anemometers, the reader is referred to the work of Kristensen [59],[60], and Papadopoulos et al. [61].

In the extensive work of Kristensen on this issue, he identifies four sources of error due to turbulence in the wind [60]. However, for the purposes of site assessment using cup anemometry, only two error sources are relevant [61]. These are longitudinal overspeeding and vertical turbulence effects, also called the u -bias (δ_u) and the w -bias (δ_w). Longitudinal overspeeding is what is commonly thought of as overspeeding. That is, overspeeding is generally considered to consist of just the effect of fluctuations in the direction of mean wind speed. However, the vertical component of turbulence can also cause error in the anemometer readings as well, sometimes much larger than the effect of overspeeding. Longitudinal overspeeding is discussed now, and the effects of vertical turbulence are discussed in a later source of uncertainty (Anemometer Uncertainty IV).

Kristensen shows that the error due to longitudinal overspeeding, δ_u , is proportional to the square of the longitudinal turbulence intensity [60]. Therefore, at sites with higher longitudinal turbulence intensity, the error due to overspeeding is larger. The longitudinal overspeeding is also proportional to the distance constant of the anemometer. The distance constant is a property of a cup anemometer that determines how rapidly it responds to changes in the wind speed. Cup anemometers with small distance constants respond to wind speed changes more rapidly than those with large distance constants, and so the smaller the distance constant, the lower the error due to longitudinal overspeeding. Typically, modern cup anemometers have distance constants less than 5 m to ensure that they have an acceptably rapid response to wind speed changes. Finally, longitudinal

overspeeding always produces a positive bias, so that the measured wind speed is larger than the true wind speed.

In general, overspeeding for modern cup anemometers with small distance constants is a fairly small effect. Several sources indicate that it is on the order of a few tenths of a percent, and almost certainly less than 1% [60],[61],[62]. This value depends on the turbulence at the site as well as the distance constant of the anemometer. Because the likely range for the overspeeding bias is between 0% and 1%, a 0.5% bias can be assumed. The standard uncertainty can be estimated using Eq. 9 since the overspeeding uncertainty is estimated as a maximum range. Since the range is 0.5%, the standard uncertainty is 0.3%. Overspeeding is unlikely to affect the shape of the wind speed distribution, so δk_2 can be assumed to be 0%.

δU_2	δk_2	Bias U_2	Bias k_2
0.3%	0%	0.5%	0%

3. Anemometer Uncertainty III (Vertical Flow Effects) - When the power curve of a wind turbine is calculated, the IEC standards require that the measured wind speed is the horizontal component (lateral and longitudinal, but not vertical) of the wind velocity vector. The standards state that: “The wind speed to be measured is defined as the average magnitude of the horizontal component of the instantaneous wind velocity vector, including only the longitudinal and lateral, but not the vertical, turbulence components” [13]. Therefore, when the wind speed is measured during site assessment, the goal should likewise be to measure the horizontal component of the wind speed. In this way, the measured wind speed and the wind speed measured during power curve

calibration are defined consistently, and so a power curve of a particular turbine accurately predicts the power output for a given measured wind resource.

In practice, the vertical component of the wind speed vector can affect the measurement of an anemometer. Different anemometers have different angular response characteristics, so they respond differently to flow that is not purely horizontal. At some sites, the terrain causes a consistent flow inclination that can affect the measured wind speed of an anemometer.

Currently, only three models of anemometer are approved by the IEC and MEASNET for power curve calculation – the Risø P2546A, Thies First Class 4.3350.10.000, and a Vector A100 model anemometer. In fact, the Thies anemometer has undergone a recent redesign specifically to address this point and make it less sensitive to vertical flow [25]. These three anemometers are approved in part because they are fairly insensitive to vertical flow, and so the wind speed measurement approximates the horizontal wind speed (i.e., they have 2D characteristics). Angular response graphs are often given for specific anemometers to indicate their sensitivity to vertical flow. Angular response curves plot the ratio of the measured wind speed to the full 3D wind speed as a function of tilt angle. An ideal 2D anemometer that only measures the horizontal wind speed has an angular response graph in which the measured wind speed decreases as the cosine of the flow inclination angle. That is, for a given flow inclination angle, α , the measured wind speed is equal to the actual 3D wind speed multiplied by the cosine of α . An example angular response curve is given in Figure 11, which shows the angular response characteristics of the Risø anemometer [26]. This ideal cosine response is also shown in Figure 11. Angular response curves are often available from the anemometer

manufacturer. Extensive testing is done to determine the angular response curves of anemometers [22],[35].

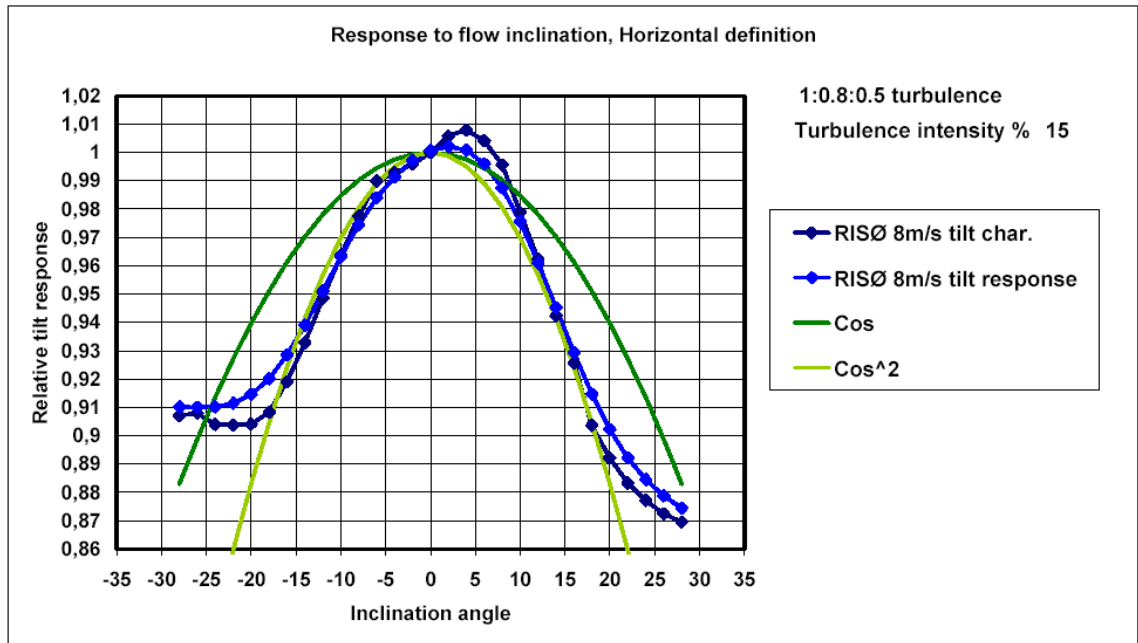


Figure 11 – Angular Response Graph of Risø Anemometer

In reality, no anemometer perfectly measures the horizontal wind speed. Figure 11 indicates that the Risø anemometer angular response curve is actually very closely approximated by a cosine-squared curve, and not a cosine curve. However, for reasonable tilt angles between -10 degrees and 10 degrees, the Risø anemometer provides a good approximation of the horizontal wind speed. Overall, while no anemometer has a perfect cosine angular response curve, the three IEC-approved anemometers provide good approximations of the horizontal wind speed, especially for small tilt angles.

Preferably, one of these three IEC approved anemometers should be used during site assessment. In this case, the measured wind speed at the site is consistent with the measured wind speed during power curve calculation. Regardless of what type of

anemometer is used, the flow inclination at the site should be considered. When the site is fairly flat, there is unlikely to be a consistent flow inclination greater than a few degrees. At flat sites, the minor flow inclination is likely difficult to measure as well. In this case, the error between the measured wind speed and the horizontal wind speed is small. Based on the angular response curves of a few commonly used anemometers, for flat sites with mean flow inclinations less than approximately 3-5 degrees, the error due to inclined flow is probably less than 1%. Thus, no matter what type of anemometer is used, a 0.5% uncertainty (using Eq. 9) due to the potential for minor inclined flow should be assumed. When the flow inclination is significant at a site (e.g., at a very hilly location), then the measured wind speed needs to be corrected using the angular response curve of the anemometer. This correction process is outside of the scope of this Chapter. However, Papadopoulos et al. provide one such method [61]. Their paper should be consulted whenever a site assessment is taking place at a location with a significant flow inclination.

For completeness, it is worth noting that wind turbines also have angular response characteristics. Pedersen explores the angular response and turbulence sensitivity of wind turbines [35]. He notes that wind turbine power decreases proportionally to the cosine-squared of the tilt angle. That is, the power output of a wind turbine does not obey the ideal cosine dependence, but instead it is proportional to the cosine-squared of the tilt angle. As stated previously, the three IEC approved anemometers have angular response characteristics that more closely obey a cosine-squared relationship, for tilt angles of +/- 20 degrees. The wind speed measured by the anemometers decreases approximately as the cosine-squared of the tilt angle, just as the power scales for wind

turbines. However, at small tilt angles, the difference between the actual angular response and the ideal response is negligible. For a tilt angle of 5 degrees, the difference is 0.4%, and for 10 degrees it is 1.5%. Thus, while the three IEC approved anemometers do not have exactly ideal angular response characteristics, they are extremely close for modest tilt angles. Furthermore, their angular response characteristics are similar to the angular response characteristics of wind turbines, and so even at large tilt angles, the power production is affected the same amount as the wind speed measurement.

To summarize:

- In flat terrain, a 0.5% uncertainty should be assumed for all anemometers due to the potential for small values of flow inclination.
- When large flow inclination exists at a site, a method proposed by Papadopoulos can be used to correct the measured wind speed values using the angular response curves.
- The shape of the wind speed distribution is unlikely to be affected by this issue, and so a 0% uncertainty for k_M can be assumed due to this uncertainty in wind speed measurements.

In Flat Terrain

δU_3	δk_3	Bias U_3	Bias k_3
0.5%	0%	0%	0%

4. Anemometer Uncertainty IV (Vertical Turbulence Effects) – Even at sites with no flow inclination, turbulence in the vertical direction can cause an overestimation of the mean wind speed. This effect is similar to overspeeding in that it is due to turbulence, and it is referred to as the w -bias. Like overspeeding, vertical turbulence effects depend on the physical characteristics of the cup anemometer. In the case of overspeeding, this

characteristic is the distance constant; in the case of vertical turbulence effects, the angular response curve is the relevant parameter. These effects are explored in detail by Kristensen and Papadopoulos et al. [60],[61]. However, the vertical turbulence effects can produce either positive or negative biases, which is not the case for overspeeding.

At flat sites, the turbulent nature of the wind causes turbulence in the vertical direction. This turbulence can be quantified by the vertical turbulence intensity. Vertical turbulence at a site can cause errors in the wind speed measured by a cup anemometer. The error is the difference between the measured wind speed and the actual horizontal wind speed, which is what one is trying to measure. This is the w -bias identified by Kristensen [60]. This error due to vertical turbulence is proportional to the square of the vertical turbulence intensity (similar to overspeeding errors). Furthermore, the magnitude of the error depends on the angular response curve of the anemometer. Not surprisingly, anemometers like the IEC-approved anemometers, with 2D angular response characteristics, have smaller errors due to vertical turbulence than anemometers that do not closely approximate the horizontal wind speed [61].

The effect of vertical turbulence is identified experimentally by Albers et al. [63],[64],[65]. They note that two anemometers of different designs, identically calibrated in a wind turbine with only horizontal flow, can easily read 2% different even in flat terrain. The source of this discrepancy is traced to sensitivity to vertical turbulence intensity. When the vertical turbulence intensity is high, certain anemometers measure noticeably higher wind speeds than other anemometers. In other words, different anemometers have different values of the w -bias, which causes them to provide different measured wind speeds when vertical turbulence is present. This observation is confirmed

by the work of Curvers and van der Werff [66]. The authors point out that if a site is assessed with a fast reading anemometer (i.e. one that is highly susceptible to the w -bias), then the annual energy production is significantly overestimated, leading to unfounded optimism in a potential site. This point is emphasized by Kline and Young [67].

Overall, anemometers have widely varying angular response characteristics. Theoretically, according to the work of Kristensen, those with 2D characteristics have smaller errors due to vertical turbulence than those with 3D characteristics. Albers et al. identify these discrepancies experimentally, and the work of Papadopoulos et al. confirms that they are in fact due to the w -bias. Thus, the magnitude of the w -bias depends on the type of anemometer that is being used. While no general rule can be stated for all site assessments using a cup anemometer, a few recommendations can be made:

- For the IEC-approved anemometers, with 2D angular response characteristics, the work of Albers et al. and Papadopoulos et al. indicates that these anemometers generally provide a close approximation to the horizontal wind speed [61],[64]. Therefore the w -bias is very low, and can be assumed to be 0%. However, there is some variation in the w -bias around 0%, so a 1% uncertainty in the mean wind speed should be used. This value is chosen to approximate the variation in the experimentally obtained results from Albers et al. and Papadopoulos et al.
- The NRG Maximum 40 anemometer has 3D angular response characteristics [35]. An ideal 3D anemometer would have a perfectly flat angular response curve, indicating that for any tilt angle the measured wind speed equals the true 3D wind speed. The angular response curve for the NRG Maximum 40, shown in Figure 12, is not a flat line like an ideal 3D anemometer, but on average it measures the

full 3D scalar wind speed for tilt angles between -20 degrees and 20 degrees. In fact, the angular response characteristics are similar to the older Thies models.

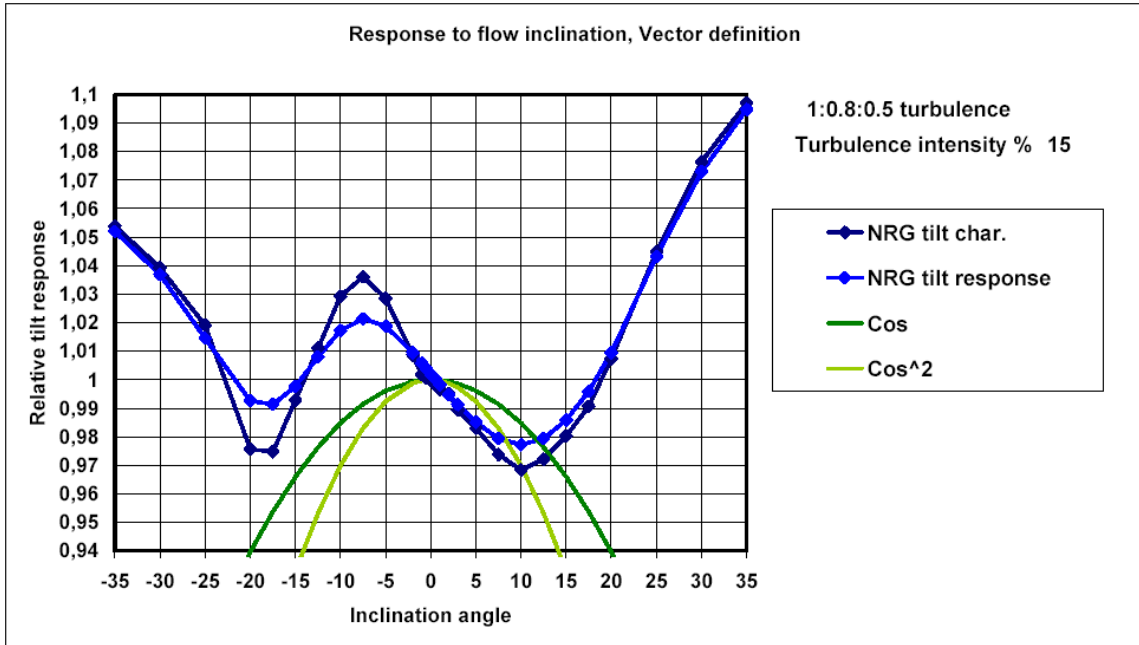


Figure 12 - Angular Response Graph of NRG Maximum 40 Anemometer

- In flat terrain, Albers et al. find that the older Thies model, which has similar angular response characteristics to the Maximum 40 anemometer, overestimates the mean wind speed compared to the Risø model, which closely approximates the 2D horizontal wind speed, by approximately 2% (a 2% w -bias). It is important to emphasize however, that this experiment is carried out in flat terrain, at high measuring heights (~ 80 m), and so there is almost no flow inclination and turbulence levels are low. Thus, 2% overestimation of the mean wind speed is a minimum value, and so a slightly larger value should be used in general. If one is assessing the wind resource in flat terrain using a Maximum 40 anemometer, or a similar 3D anemometer, then a 3% bias for U_M^- should be assumed, and a 2% uncertainty. This uncertainty is calculated using Eq. 9 (the uncertainty equals the

3% range divided by the square root of three). It is worth noting that since the uncertainties estimated here are standard uncertainties, there is actually a finite probability that the value of a quantity is outside the range defined by the uncertainty. In this way, using a 3% bias with a 2% uncertainty implies that there is a possibility that a 3D anemometer may correctly measure the true wind speed.

- The shape of the wind speed distribution is unlikely to be affected by this issue, and so a 0% uncertainty for k_M can be assumed due to this uncertainty in wind speed measurements.
- At sites with more complex terrain, with higher values of the vertical turbulence intensity, Curvers and van der Werff found as much as a 7% difference in U, \bar{M} between different anemometers [66]. In this case, a larger uncertainty and bias is needed for anemometers with 3D angular response characteristics, unless some site calibration is done to quantify the overestimation. Tentatively, a 4% bias for U, \bar{M} , with a 2% uncertainty can be assumed (again using Eq. 9), although this is a very rough estimate. In this way, the mean wind speed is biased by approximately half of the maximum observed bias.

To summarize:

- Vertical turbulence causes 0% bias and 1% uncertainty in IEC approved anemometers with 2D angular response characteristics.
- For non-IEC approved anemometers, such as the NRG Max 40, in flat terrain, vertical turbulence causes an approximately 3% bias and a 2% uncertainty in U, \bar{M} .

- For non-IEC approved anemometers in complex terrain, vertical turbulence causes an approximately 4% bias and a 2% uncertainty in U, \bar{U}_M .

Using IEC approved anemometer

δU_4	δk_4	Bias U_4	Bias k_4
1%	0%	0%	0%

Using NRG Maximum 40 Anemometer

δU_4	δk_4	Bias U_4	Bias k_4
2%	0%	3% or 4%	0%

5. Tower Effects – The tower used in wind resource measurement can significantly affect the flow of air near the anemometers that measure the wind speed. This effect is often referred to as “tower shadow,” and it is especially pronounced when the anemometer is in the wake of the tower. The work of Kline is used to evaluate the uncertainty due to tower effects [68]. Several conclusions and recommendations can be drawn:

- There is some controversy concerning the choice of top-mounted booms versus side-mounted booms. Top-mounted anemometers are generally used in power performance testing. When the anemometer is positioned far above the tower top, there are negligible tower effects, and therefore the anemometer is very closely measuring the undisturbed free-stream flow. However, a top-mounted position has numerous potential drawbacks. First, lightning rods are usually used to protect the equipment, and to be effective the lightning rod should be the highest point on the tower. The presence of a lightning rod can therefore disturb the flow near the top-mounted anemometer. Second, in order to measure wind shear at a location, multiple measurement heights are used. So while a top-mounted

anemometer can be used for the highest height, side mounted anemometers at lower heights are needed as well. Thus, using a top-mounted anemometer would result in inconsistent anemometer configurations, and therefore different tower effects at different heights. Finally, if top-mounted anemometers are not positioned far above the tower, then they are subject to speed-up effects. Kline finds that top-mounted booms on average caused a 2.7% overestimation of the mean wind speed, U, \bar{M} , with a 1% standard deviation for five different meteorological masts [68]. Again, this effect is highly dependent on the distance above the tower that the anemometer is mounted. Overall, it is clear that top-mounted anemometers should be used with care in resource assessment.

- RERL chooses to use a configuration with two anemometers placed on side-mounted booms at each height that is being measured [69]. The two anemometers are positioned 180 degrees from each other. This redundancy helps to minimize the effect of tower shadow. Also, if one anemometer fails, it is still possible to measure at that height. The booms should be long enough to position the anemometers at a significant distance from the tower. RERL generally uses booms that are at least 6 tower diameters long [69].
- RERL chooses to select the higher reading of the two anemometers at each height as the value of the measured wind speed, U_M , for each averaging period (usually 10 minute or hourly averages) during the data processing [70]. Kline recommends this procedure as well [68]. In this way, if one of the anemometers is in the tower shadow for much of the averaging period and therefore biased low, its reading is ignored, and instead the reading from the anemometer in the

unobstructed flow is used. Essentially, this processing method is needed to combat the potential low biasing effects of tower shadow.

- Basic potential flow fluid dynamic theory can be used to investigate this processing method. The investigation seeks to determine if the processing method, by using the higher of the two readings, would bias the measured wind speed and cause an overestimate. Potential flow can be used to model the resulting flow field when a cylinder is placed in a uniform free stream flow. In front of the cylinder (i.e., at a position of 0 degrees from the free stream flow direction), the velocity of the flow decreases below that of the free stream. Meanwhile, the flow accelerates around the tower, reaching a maximum speed, greater than the free stream speed, at a position of 90 degrees from the free stream direction. For a boom length of 6 tower diameters (which RERL uses, and is fairly standard), the potential flow theory indicates that the flow is decelerated by 0.8% in front of the tower (0 degrees) and accelerated by 0.8% to the sides of the tower (90 degrees). If the wind comes uniformly from one of these directions, then the wind speed is biased by +/- 0.8%. Thus, 0.8% is a maximum possible deviation between the free stream wind speed and the measured wind speed for a boom length of 6 tower diameters. Using Eq. 9, the standard uncertainty is therefore 0.5%. This uncertainty is due to an unknown bias, so it is a Type B uncertainty. In practice, the wind does come uniformly from one direction, and so the tower effects are less than this. Overall, this investigation indicates that the processing method used by RERL, in which the higher of the two readings is used, does not introduce large errors into the measurement of the free stream wind

speed, and in fact provides a fairly accurate means of removing the effects of tower shadow. The uncertainty in k_M due to this processing technique can be assumed to be 0% because it does not affect the shape of the wind speed distribution.

- If the RERL method for processing the data is used, then an uncertainty of 0% for k_M should be used, since the effects of tower shadow do not change the shape of the wind speed distribution.
- If one anemometer fails, or if only one anemometer is positioned at a given height, tower shadow becomes a pronounced effect, and readings are systematically biased low. The estimate for this effect is a bias of 1.5% on the mean wind speed, U_M^- , with an uncertainty of 1.0%, for tubular towers. These values come from analyzing ten anemometers, mounted in pairs, which RERL has installed at five sites in Massachusetts. Each of the pairs of anemometers is mounted 180 degrees away from each other, on side-mounted booms. When the ratio of one anemometer to the maximum anemometer reading is plotted as a function of direction, a pronounced dip occurs when the anemometer is in the tower shadow. The mean wind speed of each anemometer is then calculated, along with the mean wind speed of the maximum of the two anemometers. The average decrease in mean wind speed of the anemometers compared to the maximum of the two readings is 1.5%, and the standard deviation of the decrease is 1.0%. Thus, U_M^- should be increased by 1.5% during times of anemometer failure, and this adjusted value should have a 1.0% uncertainty.

- This analysis finds a different effect on k_M when only one anemometer is present. On average, k_M is unchanged, but with a standard deviation of 1.0%. Thus, when one anemometer is present, k_M should have a 1.0% uncertainty.

Two Side-Mounted Anemometers

δU_5	δk_5	Bias U_5	Bias k_5
0.5%	0%	0%	0%

One Side-Mounted Anemometer

δU_5	δk_5	Bias U_5	Bias k_5
1.0%	1.0%	-1.5%	0%

6. Boom and Mounting Effects – The boom that supports the anemometer and connects it to the tower can also affect the reading of the anemometer. Moreover, if an anemometer is not positioned exactly vertically, it measures a different wind speed than a vertical anemometer. Pedersen and Hansen that look at the influence of the boom on anemometer measurements [71]. They conclude that the boom could have a significant effect on the anemometer measurement if they are not adequately separated vertically. However, if the anemometer is positioned 12-15 boom diameters from boom, there is a fairly small effect. They measure a 1% overestimate of the mean wind speed for some wind directions, but no underestimate for any direction. The RERL usually positions their anemometers 15-18 inches above the 1-inch boom pipe, and so only a slight overestimate from certain wind directions is likely.

Mounting effects are also difficult to estimate. Even with a level, it is almost impossible to perfectly position an anemometer. A 5-degree misalignment is certainly possible. For the IEC-approved 2D anemometers described above, a 5-degree

misalignment causes approximately a 1% maximum underestimate of the wind speed for some wind directions.

Both the boom effects and the mounting effects are unavoidable. On the other hand, the effects are only relevant for certain wind direction. For a site with a normal wind rose, with wind blowing from all directions, these effects are likely to be small. The maximum bias due to boom effects is approximately 1% and the maximum bias due to mounting effects is approximately -1%. These biases tend to cancel each other out, producing a net 0% bias. There is some uncertainty due to these affects as well. The range of each effect is 0.5% (range is discussed in Section 2.0), and so there is a standard uncertainty of approximately 0.3% for each effect. These uncertainty sources are independent, so they can be combined using RSS to give an overall uncertainty due to boom and mounting effects of 0.5%.

These effects should not change the shape of the wind speed distribution, and so a value 0% can be used for δk_6 .

For the RERL Boom Setup

δU_6	δk_6	Bias U_6	Bias k_6
0.5%	0%	0%	0%

7. Data Reduction Accuracy – In general, raw wind data are processed prior to the calculation of U, \bar{c}_M , and k_M . This data reduction involves removing data when icing has taken place on the sensors, or when the sensors have failed for other reasons [58]. These gaps in the data could potentially cause errors in the estimation of U, \bar{c}_M . To investigate this effect, seven data sets of at least a year are selected. For each data set, a random time point in the data set is selected. For each random time point, a certain amount of data from this point forward is removed from the data set. The amount

removed is increased from 0% to 20% in increments of 0.5%. Then the ratio of the mean wind speed with the segment removed to the mean wind speed of the full data set is calculated. For each data set, this process is carried out ten times, so that for each percentage amount of data removed, there are ten random initial time points selected. Then, the average and the standard deviation of the results for the seven data sets are calculated. Figure 13 shows the percentage standard deviation of the ratio of the mean to the true mean as a function of the amount of data removed.

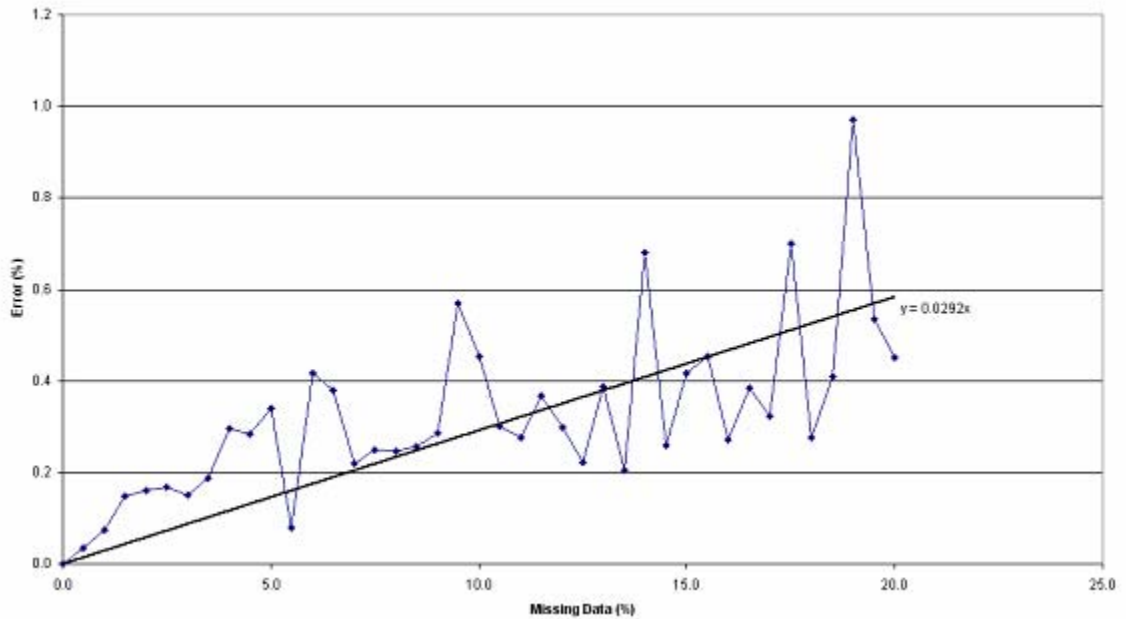


Figure 13 – Effect of Data Removal

In effect, this is a measure of the uncertainty of the estimate of the mean wind speed as a function of the amount of missing data. Clearly, the error in the calculation of the mean increases as the amount of data removed increases. While there is a large amount of scatter in the plot, a linear fit is made in order to determine the approximate relationship between the length of data removed and the error produced in the calculation of U_M^- . The results indicate that the percentage error is approximately 0.03 times the

percentage of missing data. Thus, if 5% of the data set is missing due to icing or failed sensors, then a data reduction accuracy of 0.15% can be assumed. In general, this uncertainty is likely to be negligible, unless large amounts of data are missing. This is also a Type B uncertainty. For any given data set, it is unknown if the missing data would have caused a higher or lower value of U_M^- . Thus, the missing data introduces an unknown bias. The same analysis is carried out for k_M , and the results are very similar. Thus, this relationship can be assumed for both U_M^- and k_M .

δU_7	δk_7	Bias U_7	Bias k_7
0.03 * (% Missing)	0.03 * (% Missing)	0%	0%

3.2 Long-term Resource Estimation Uncertainty

These uncertainty sources arise when the measured wind resource data are used to estimate the long-term wind resource at a site. While wind resource measurement typically lasts for one year, the measured resource during this particular year may not be representative of the actual long-term resource at the site [3],[6],[7],[72]. The long-term resource is characterized by the mean wind speed and wind speed distribution that exists at a site over a very long period of time. Typically, twenty years is assumed to be a long enough time period to characterize the long-term wind resource. Since a twenty year measurement campaign is far too long for practical purposes, the long-term resource must be estimated from the measured data. The measured data, along with long-term data from a nearby site (the “reference site”), are generally used in a process called Measure-Relate-Predict (MRP) to estimate the long-term wind resource at a site [7],[51]. The long-term mean wind speed and Weibull parameters are labeled U_{LT}^- , c_{LT} , and k_{LT} .

respectively. The estimation of the long-term Weibull parameters in the MCP step contributes an additional uncertainty. Finally, global climate change, whether anthropogenic or naturally caused, can cause additional uncertainty [72].

Thus, additional uncertainty arises when the measured data are used to estimate the long-term wind resource at a site. The three uncertainty sources that arise in long-term resource estimation are labeled δU_8 , δU_9 , δU_{10} and δk_8 , δk_9 , δk_{10} . They are:

8. MCP Correlation Uncertainty.
9. Weibull Parameter Estimation Uncertainty.
10. Changes in the Long-term Average.

8. MCP Correlation – Wind measuring campaigns at a specific site usually last for one year. A process called “Measure-Correlate-Predict” is often employed that uses a longer data set from a nearby site (reference site) to obtain the estimate of the long-term wind resource at the site (target site). The MCP procedure begins by using the concurrent data set to determine a statistical relationship between the target and reference site data. This relationship estimates the speed at the target site as a function of the speed at the reference site. The relationship is then applied to the long-term reference site data set to estimate the target site data over this long-term period. In this way, the long-term target site wind resource can be estimated. It is important to use a reference site data set that has high quality, consistently measured wind speed data, with a high correlation with the target site, in order to obtain good estimates of the target site wind resource [7].

The utility of the MCP step is that it incorporates data sets longer than the one year of measured target site data, and therefore provides a more accurate estimate of the long-

term wind resource at the target site [51],[52]. Often a linear regression MCP model is used, which can also be used to estimate the standard deviation of the prediction of the mean wind speed. However, as shown by Rogers et al., “this approach significantly underestimates the actual standard deviation in all cases studied, often by a factor of 10” [52]. This is because the wind data relationship between two sites is serially correlated, and so linear regression theory cannot be used to estimate the uncertainty associated with MCP. An alternative approach to estimating the uncertainty is proposed by Rogers et al. that uses a jackknife estimate of variance. While the details of the jackknife approach are not discussed here, in essence the jackknife method “assesses the prediction uncertainty using the variability of the MCP predictions made by dropping out segments of the concurrent data” [52]. The results of the investigation indicate that the jackknife estimate provides a significant improvement over linear regression theory in estimating the uncertainty associated with MCP. It is important to note that the current RERL jackknife estimate includes correction factors that adjust a slight underestimation by the original jackknife method. The uncertainty due to MCP is a Type B uncertainty, as the process introduces an unknown bias into the estimate of the long-term wind resource. In sum, whenever MCP is used to provide an estimate of the long-term wind resource at a site, the jackknife method should be used to estimate the uncertainty of U_{LT}^- and k_{LT} . Typical values for MCP uncertainties using the jackknife method are between 5% and 10% for δU_8 and δk_8 , although these values are very site dependent.

δU_8	δk_8	Bias U_8	Bias k_8
Jackknife Estimate	Jackknife Estimate	0%	0%

9. Weibull Parameter Estimation Uncertainty – As discussed above, the MCP step is used to estimate U , c_{LT} , and k_{LT} , and the jackknife method can be used to estimate the uncertainty in these quantities. An additional uncertainty arises when Weibull parameters are fit to the output of the MCP step. Since the output data of MCP is not a perfect Weibull distribution, different estimation methods yield different values of the Weibull parameters. The result is an additional uncertainty in the values of c_{LT} , and k_{LT} .

There are several methods of estimating the Weibull parameters from a wind speed time series. These methods include: empirical methods, method of moments, maximum likelihood estimates, least square linear regression, and chi-squared methods. Furthermore, each method produces a slightly different estimate of the parameters, depending on the data set. When estimating the long-term Weibull parameters, one could use any of these methods. If one person chose one particular method, and another person chose a different method, they would come up with different estimates for the Weibull parameters. Since the long-term Weibull parameters are used to estimate AEP , the result is that these two people would estimate different values for the AEP despite using identical measured wind speed data. Clearly, the estimation of Weibull parameters introduces an added uncertainty into the process.

The variation in the estimate of the Weibull parameters is investigated in order to estimate this uncertainty. Fourteen data sets of lengths ranging from one year to five years are used in this investigation. Seven different methods are used to calculate both Weibull parameters from these data sets, and a pooled estimate of the standard deviation of the estimates is calculated. The result is a 5% standard deviation between the various methods for estimating the shape factor k , but a nearly 0% standard deviation for the

scale factor, c . This result is not surprising, since c is proportional to the mean wind speed, and there is no uncertainty in calculating the mean of a wind speed time series. Thus, the estimation of the Weibull parameters during the MCP step introduces no added uncertainty in $U, ^-_{LT}$ or c_{LT} , but it does cause an additional 5% uncertainty in the estimate of k_{LT} . This is a Type B uncertainty, as using a single method for estimating the Weibull parameters does not reveal the variation between methods.

δU_9	δk_9	Bias U_9	Bias k_9
0%	5.0%	0%	0%

10. Changes in the Long-Term Average – Natural climate changes and anthropogenic climate change can potentially cause the long-term wind resource to change at a given site over the turbine lifetime [6],[72]. Breslow and Sailor use climate models to estimate the potential change in mean wind speeds due to climate change [73]. The models predict that over the next 50 years, average annual wind speeds could change from 1% to 3%. Since wind turbines are likely to last for approximately 20 years, a value of 1% uncertainty for $U, ^-_{LT}$ seems reasonable for now. A value of 1% should also be used for k_{LT} since climate change could affect the distribution of wind speeds as well.

δU_{10}	δk_{10}	Bias U_{10}	Bias k_{10}
1.0%	1.0%	0%	0%

3.3 Wind Resource Variability Uncertainty

When the wind resource at a site is evaluated, a finite number of years of reference site data are used to estimate the long-term wind resource. Essentially, a sample of

yearly wind resources is used to estimate the long-term wind resource at the site. Thus, the potential for random error exists, since the years of data used to estimate the long-term parameters might not, in fact, be representative of the true long-term values [6],[72]. As discussed in Section 2.0, random error decreases as the number of samples increases. This implies that the longer the reference site data set used to estimate the long-term parameters, the less uncertainty in these estimates. Thus, the potential for random error exists, and it causes uncertainty in two ways. These two uncertainties are therefore Type A uncertainties, and they are labeled δU_{11} , δU_{12} and δk_{11} , δk_{12} . They are:

11. Inter-Annual Variability Uncertainty.

12. Uncertainty over Turbine Lifetime.

11. Inter-Annual Variability Uncertainty – The annual mean wind speed and k at a given site vary from year to year. These variations are referred to as inter-annual variations. Twenty years is often accepted as the time period necessary to accurately characterize the mean wind speed and Weibull parameters, and thereby average out any inter-annual variations. Consequently, when one uses site monitoring and MCP to estimate U , c_{LT} , and k_{LT} from a certain number of years of reference site data, there is a risk that the estimated value does not equal the historical long-term value. The standard deviation (uncertainty) associated with these inter-annual variations depends on the specific location that is being assessed. Justus et al. investigate forty sites with at least ten years of data in the U.S [9]. They find a range of inter-annual variations between 3% and 12% for annual mean wind speeds. He does not investigate the variation of k . For the six sites located in the northeast United States, the inter-annual variations of the

annual mean wind speed have an average value of 6%. Klink determines the inter-annual variation of the annual mean wind speed and k at seven sites in Minnesota [11]. The average standard deviation at these sites is 5% for the annual mean wind speed, and approximately the same value for k . Thus, based on the empirical data in the papers of Justus et al. and Klink, a 6% inter-annual variation in Massachusetts appears to be a reasonable value for both U_{LT} and k_{LT} . In regions other than the northeast United States, one can use the results of Justus et al., or other studies that estimate the inter-annual variability of the wind resource for that region. The uncertainty associated with assessing a particular site can then be determined from basic statistical theory. The uncertainty due to inter-annual variations is simply equal to 6% divided by the square root of the number of years of reference site data that are used to estimate the long-term wind resource at the site, as shown in Eq. 13.

$$\delta U_{11} = \delta k_{11} = 6\% / \sqrt{N} \quad \text{Eq. 13}$$

The number of years used in this calculation is the length of the long-term reference data set used in the MCP calculations, and not the approximately one year of actual measured data at the target site.

δU_{11}	δk_{11}	Bias U_{11}	Bias k_{11}
$6\% / \sqrt{N}$	$6\% / \sqrt{N}$	0%	0%

12. Uncertainty over Turbine Lifetime – This uncertainty is similar to, but distinct from, the inter-annual variability uncertainty. The actual wind resource at a site during the operation of the turbine may be different from the true wind resource at the site. Once again, this uncertainty is simply the long-term inter-annual variability at the site

(6% in Massachusetts) divided by the square root of the wind turbine lifetime in years, which is usually estimated at twenty years. According to Eq. 13, this value should be taken at approximately 1% for U_{LT}^- and k_{LT} , as both could potentially vary over this period.

δU_{12}	δk_{12}	Bias U_{12}	Bias k_{12}
1.0%	1.0%	0%	0%

3.4 Site Assessment Uncertainty

Wind speed measurements usually take place at heights significantly lower than the hub height of a typical modern wind turbine. Because wind speeds typically increase with height, a wind shear model is used to extrapolate the estimated long-term wind resource to the hub height [17]. The wind shear model is created using the measured wind speed data. The use of a wind shear extrapolation introduces uncertainty [12],[54]. Furthermore, the tower used to measure the wind speed is often not at the exact location of the wind turbine(s). Topographic effects can cause the wind speeds at separate locations at a site to differ. When multiple wind turbines are installed at a site, the wind resource may vary between each turbine due to topography [7],[8]. In complex terrain, this effect can be significant. Thus, it is critical to estimate the hub height wind resource at each of the turbine locations.

Site assessment uncertainties arise when estimating the long-term, hub height mean wind speed and Weibull parameters at the probable turbine location(s), $U_{LT_HUB}^-$, c_{LT_HUB} , and k_{LT_HUB} , from the long-term mean wind speed and Weibull parameters at the

measurement height and the measurement location, U_{LT}^- , c_{LT} , and k_{LT} . The two factors contributing to this uncertainty are labeled δU_{13} , δU_{14} and δk_{13} , δk_{14} . They are:

13. Topographic Effects

14. Wind Shear Model Uncertainty

13. Topographic Effects – If the proposed wind turbine and the measurement tower are positioned in different locations, or when multiple turbines are installed, then local topography can cause different wind conditions at the various turbine locations, even if they are quite close together. These effects can range from negligible to very significant, and obviously depend on the specific site being assessed [7]. Flow modeling is used to estimate the wind resource across the project area at each turbine location, based on the measured wind resource and the local terrain and topography. The numerical models include equilibrium and dynamic models, such as WAsP or Site Wind [8].

The uncertainty associated with this process is also very site dependent. Brower notes that the variation in the prediction of the wind speed at the turbine locations can be used to estimate the uncertainty in the modeling [8]. He notes that a typical range for the uncertainty due to topographic corrections is between 2% and 10%. This uncertainty is Type B, since the potential error in the topographic correction is an unknown bias.

δU_{13}	δk_{13}	Bias U_{13}	Bias k_{13}
Site Dependent	Site Dependent	Site Dependent	Site Dependent

14. Wind Shear Model Uncertainty – Meteorological towers that measure wind speeds at potential sites typically have heights significantly shorter than the hub heights

of modern wind turbines [12]. Consequently, the measured wind resource, U_{LT}^- , has to be extrapolated up to the hub height to get an estimate of the wind resource at the hub, $U_{LT_HUB}^-$. This extrapolation is a significant source of error, often the largest source. The accuracy of the shear extrapolation is highly dependent on the particular shear model that is used. However, one does not know beforehand which shear model provides the most accurate extrapolation. Elkinton et al. explore the accuracy of shear models in flat, forested, and complex terrain [16]. In this analysis, there are three to five data sets for each type of terrain. Each data set contains multiple years of data, and each has wind speed data at three heights. The analysis uses data from the two lower heights to predict the mean wind speed at the highest height. In this way, the accuracy of shear models is evaluated against real data. Both the log law model and the power law model are used. For each type of terrain and each model, the average prediction error and the standard deviation of the prediction error are calculated. These results can be used to estimate the average bias and uncertainty associated with shear extrapolation for each terrain type. However, it should be emphasized that these results are based on a limited number of sites, and any particular site could have very different shear properties. To be conservative, one could use a margin of safety of 1.5 for the uncertainty to compensate for the limited number of data sets, although the numbers quoted below do not contain this margin of safety. The principal findings of the study are summarized here:

- For all types of terrain, the power law and the log law yield similar results, with no particular model being significantly better than the other. The difference between them is so small compared to the scatter of the estimates that either model can be used.

- In flat terrain, the shear models underestimated the mean wind speed at hub height by an average of 1%. This data is based on three sites. It is recommended that a -1% bias be assumed for $U, \overline{LT_HUB}$.
- For sites with hills but no trees, the shear models overestimate the mean wind speed at hub height by an average of 6%. This data is based on five sites. It is recommended that a 6% bias be assumed for $U, \overline{LT_HUB}$.
- For forested and complex terrain sites, the shear models overestimate the mean wind speed at hub height by an average of 2% in forested terrain. This data is based on four sites. It is recommended that a 2% bias be assumed for $U, \overline{LT_HUB}$.
- The standard deviation of the prediction error for all twelve sites is approximately 5%. Thus, an uncertainty of 5% for the value of $\delta U, \overline{LT_HUB}$ can be used for all shear predictions. Again, this data is based on a limited number of samples. Especially in complex terrain, either hilly or forested, a margin of safety may be appropriate and a value of 7.5% could be used.
- It is recommended that at least 200 days of data be used in the shear extrapolation to get a useful average shear value. As one would expect, the shear errors decrease with data length. The results from Elkinton et al. presented above are based on multi-year data sets. However, Elkinton et al. also note that with more than 200 days of data, the scatter between individual 200-day segments is less than 1%.
- Elkinton et al. do not investigate the extrapolation of the shape factor k with height. However, a paper by Justus proposes a model for extrapolating k with height. The model proposed is shown in Eq. 14, where the subscripts 1 and 2

denote the lower and higher heights, respectively. The model indicates a weak dependence of k with height. For example, with a measurement height of 50 m, and a hub height of 80 m, the ratio is 1.05.

$$\frac{k_2}{k_1} = \frac{1 - 0.0881 * \ln\left(\frac{z_1}{10}\right)}{1 - 0.0881 * \ln\left(\frac{z_2}{10}\right)} \quad \text{Eq. 14}$$

Doran and Verholek use data sets from approximately 70 different sites to investigate the accuracy of the model proposed by Justus [74]. The results show that the ratio of the estimated k value to the true k value has a standard deviation of 18% and that the estimate over-predicted k by an average of 6%. Unfortunately, the investigation by Doran and Verholek does not differentiate the sites by terrain type, which could be useful in reducing the scatter of the predictions. Furthermore, the data sets used in the evaluation of the model are from nuclear power plant sites, where the measurement heights are probably low to the ground and turbulence from the power plant possibly affects the measurements. Because of these factors, the results are suspicious, and it is not recommended that they be used either to estimate k at hub height or to estimate the uncertainty of k due to shear.

- Wieringa also investigates the variation of k with height [75]. He determines that k increases with height up until a reversal height, at which point k begins to decrease. This reversal height is typically on the order of 60-100 m (depending on terrain), which is also the range of hub heights for modern wind turbines. These results indicate that extrapolating k with height is a highly uncertain

process, as k can either increase or decrease depending on the hub height and the reversal height. Furthermore, Wieringa notes that the large scatter found in Doran and Verholek's results using the Justus model is partially due to the mathematical formulation of the Justus model. That is, the Justus model, which is a multiplicative equation, is affected by the "large-scale wind climate" at the site, which is unrelated to the local variation of k with height. Essentially, the Justus model is highly dependent on the value k_1 , and k_1 is unrelated to the actual height variation of k , which therefore causes the scatter. In sum, the 18% standard deviation found by Doran and Verholek is not an appropriate value for the uncertainty in k_{LT_HUB} . Instead, Wieringa proposes a model that accounts for the reversal height, so that k decreases after the reversal height. In practice, the Wieringa model provides a better means of predicting k than the Justus model, for a very limited number of sites. This model is shown in Eq. 15, where z_r is the reversal height and c_k is an empirical constant equal to 0.0228.

$$k_2 = k_1 + c_k (z_2 - z_1) \exp \left[-\frac{z_2 - z_1}{z_r - z_1} \right] \quad \text{Eq. 15}$$

The use of this model can be investigated. A measurement height of 50 m and a hub height of 80 m are assumed. The reversal height is then varied between 60 m and 100 m, and k_2 is estimated. The standard deviation of k_2 as a function of reversal height is 6% for a value of $k_1=2$. If the values of k_1 , hub height, and measurement height are varied, then the standard deviation varies slightly. The maximum value of the standard deviation for realistic values of k_1 , hub height, and measurement height is 9%. This value is half of the variation found by Doran and Verholek, and is probably more realistic as it is less dependent on the "large-

scale wind climate” discussed above. Thus, one can assume that the shear extrapolation introduces a 5% uncertainty for k_{LT_HUB} (The 9% range is divided by the square root of three, as shown in Eq. 8). However, the Wieringa model cannot be used in practice for extrapolating k because the reversal height is unknown. Furthermore, the model is based on a limited number of sites, and so it may not be appropriate for all sites. Wieringa also provides a simple linear model that does not depend on reversal height, but this model is only accurate when extrapolating to heights below the reversal height, and once again it relies on a small number of data sets. Overall, when the highest measurement height of k is on the order of 50 m, and the hub height is on the order of 80 m, both the Justus model and the simplified Wieringa model predict small increases in k with height. In practice, it appears to be reasonable to assume that k remains constant with height (so $k_{LT} = k_{LT_HUB}$), or increases a small amount on the order of 5-10% using a linear scaling factor. Future work could investigate k extrapolation further. Again, to account for the potential variability of this assumption, one can assume that the shear extrapolation introduces a 5% uncertainty for k_{LT_HUB} . All of these uncertainties are Type B, since they are due to unknown bias introduced in the shear extrapolation step.

Flat Terrain

δU_{14}	δk_{14}	Bias U_{14}	Bias k_{14}
5.0%	5.0%	-1%	0%

Hilly Terrain

δU_{14}	δk_{14}	Bias U_{14}	Bias k_{14}
5.0%	5.0%	6.0%	0%

Forested Terrain

δU_{14}	δk_{14}	Bias U_{14}	Bias k_{14}
5.0%	5.0%	2%	0%

3.5 Summary of Wind Resource Uncertainties

The tables below summarize the four categories of bias and uncertainty discussed above.

I. Wind Speed Measurement Uncertainty

	δU_i	δk_i	Bias U_i	Bias k_i
1	1.5%	0%	0%	0%
2	0.3%	0%	0.5%	0%
3	0.5%	0%	0%	0%
4	1% or 2%	0%	0%, 3%, or 4%	0%
5	0.5% or 1.0%	0% or 1.0%	0% or -1.5%	0%
6	0.5%	0%	0%	0%
7	0.03 * (% Missing)	0.03 * (% Missing)	0%	0%

II. Long-Term Resource Estimation Uncertainty

	δU_i	δk_i	Bias U_i	Bias k_i
8	Jackknife Estimate	Jackknife Estimate	0%	0%
9	0%	5.0%	0%	0%
10	1.0%	1.0%	0%	0%

III. Wind Resource Variability Uncertainty

	δU_i	δk_i	Bias U_i	Bias k_i
11	$6\% / \sqrt{N}$	$6\% / \sqrt{N}$	0%	0%
12	1.0%	1.0%	0%	0%

IV. Site Assessment Uncertainty

	δU_i	δk_i	Bias U_i	Bias k_i
13	Site Dependent	Site Dependent	Site Dependent	Site Dependent
14	5%	5%	-1%, 6%, or 2%	0%

3.6 Estimation of the Wind Resource and the Wind Resource Uncertainty

Once the wind speed measurements at the site are completed and the fourteen sources of wind resource uncertainty are estimated, an estimate can be made of the long-term hub height wind resource and the associated uncertainty in this estimate. This Section describes the process that should be used for estimating U_{LT_HUB} , c_{LT_HUB} , and k_{LT_HUB} , and their respective uncertainties.

3.6.1 Estimation of U_{LT_HUB} , c_{LT_HUB} , and k_{LT_HUB}

The steps that should be used to determine the long-term, hub height wind resource are listed below.

1. Apply the bias estimates from Group I (Wind Speed Measurement Uncertainty) to U_M . The anemometer vertical sensitivity, the anemometer overspeeding, the anemometer vertical turbulence effects, and the tower effects can introduce a bias into the measurement of the wind speed. Thus, the measured wind speed data, U_M , should be scaled by these values. If a 3% bias due to anemometer vertical sensitivity is used, then all values of U_M should be multiplied by 0.97.
2. Use U_M to determine the appropriate shear parameter. If the power law is used, then solve for α . If the log law is used, then solve for z_0 .
3. Use U_M and data from a long-term reference site in an MCP algorithm. The output of the MCP algorithm is U_{LT} , and k_{LT} . The Weibull shape parameter can be estimated in a variety of ways, as described in Section 3.2.
4. Either utilize the assumption that k does not change with height, and therefore $k_{LT} = k_{LT_HUB}$, or apply a small correction factor to account for an increase in k with height.

5. Apply the chosen shear model to U, \overline{LT} . For example, if one is utilizing the power law, then after determining α in Step 2, Eq. 16 could be used to calculate $U, \overline{LT_HUB}$. h_3 is the probable hub height, and h_2 is the highest measuring height.

$$\overline{U}_{LT_HUB} = \overline{U}_{LT} (h_3 / h_2)^\alpha \quad \text{Eq. 16}$$

6. If multiple turbines are likely or if the met tower and turbine location are not identical, utilize flow modeling software to adjust the estimated hub height wind resource at the met tower site to the various turbine locations.
7. Apply the bias estimates from Group IV (Site Assessment Uncertainty) for the mean wind speed to $U, \overline{LT_HUB}$. For example, if the site is in flat terrain, and a -1% shear bias from above is used, then $U, \overline{LT_HUB}$ should be increased by a factor of 1.01.
8. Calculate the value of c_{LT_HUB} at each turbine location from the values of $U, \overline{LT_HUB}$ and k_{LT_HUB} . This can be done using Eq. 17, where Γ is the gamma function.

$$c = \overline{U} / \Gamma(1 + 1/k) \quad \text{Eq. 17}$$

These eight steps should be used to estimate $U, \overline{LT_HUB}$, c_{LT_HUB} , and k_{LT_HUB} from the measured wind speed data.

3.6.2 Estimation of δk

Once the long-term wind resource is determined as described in Section 3.6.1, the uncertainties can then be estimated using Eq. 11. This Section describes the estimation of δk ; the estimation of δU and δc is described next in Section 3.6.2.

The uncertainty of the Weibull shape factor, δk , is easily calculated because either no shear extrapolation is applied to k or a simple scale factor is used to extrapolate k with

height. In these cases, the sensitivity factors for each uncertainty source and category of uncertainty equal one. Thus, the fourteen sources of uncertainty for the shape factor can simply be combined using the RSS method to yield δk . This is shown in Eq. 18. If a more complex extrapolation method is utilized, it may not be possible to calculate δk in this way.

$$\delta k = \sqrt{(\delta k_1)^2 + (\delta k_2)^2 + \dots + (\delta k_{14})^2} \quad \text{Eq. 18}$$

3.6.3 Estimation of δU and δc

The steps to determine δU and δc are now listed.

1. Use the “root-sum-square” (RSS) method to combine the uncertainty values for each category of uncertainty. This is shown in Eq. 19. The subscripts “ M ”, “ LT ”, “ V ”, and “ SA ” correspond to uncertainty in the four categories of uncertainty.

Within each category of uncertainty, the sensitivity factors are equal to one.

$$\begin{aligned} I : \delta U_M &= \sqrt{(\delta U_1)^2 + \dots + (\delta U_7)^2} \\ II : \delta U_{LT} &= \sqrt{(\delta U_8)^2 + (\delta U_9)^2 + (\delta U_{10})^2} \\ III : \delta U_V &= \sqrt{(\delta U_{11})^2 + (\delta U_{12})^2} \\ IV : \delta U_{SA} &= \sqrt{(\delta U_{13})^2 + (\delta U_{14})^2} \end{aligned} \quad \text{Eq. 19}$$

The general equation to determine δU , which is the long-term hub height mean wind speed uncertainty, is derived from Eq. 11. The result is shown in Eq.

20. The sensitivity factors for each category of uncertainty are $SF_{U,M}$, $SF_{U,LT}$, $SF_{U,V}$, and $SF_{U,SA}$.

$$\delta U = \sqrt{(SF_{U,M} \cdot \delta U_M)^2 + (SF_{U,LT} \cdot \delta U_{LT})^2 + (SF_{U,V} \cdot \delta U_V)^2 + (SF_{U,SA} \cdot \delta U_{SA})^2} \quad \text{Eq. 20}$$

2. Determine the sensitivity factors for each category of uncertainty. The sensitivity factor for the wind resource variability uncertainty and the site assessment

uncertainty are both equal to one. Thus, $SF_{U,V} = SF_{U,SA} = 1$. If a linear model is used in the MCP step, then the sensitivity factor for the long-term resource estimation, $SF_{U,LT}$, is also equal to one. RERL uses a linear MCP model, dubbed the “Variance Ratio” method, described in Chapter II, Section 5.2. From an uncertainty perspective, using a linear model helps simplify the calculation of the overall wind resource uncertainty.

The sensitivity factor for the measurement uncertainty, $SF_{U,M}$, is not equal to one. This is identified by Taylor et al. [76]. $SF_{U,M}$ is not equal to one because the measured wind speed is used to calculate the shear parameter (Step 2 in Section 3.6.1), and the shear parameter is then used to estimate $U_{LT_HUB}^-$ (Step 5 in Section 3.6.1). The result is that error in the measurement of the wind speed causes error in the shear parameter calculation, which then causes additional error in the estimate of $U_{LT_HUB}^-$. Thus, the contribution of measurement uncertainty to the total uncertainty is magnified due to shear extrapolation, and so the sensitivity factor for the measurement uncertainty is greater than one. It is important to emphasize that this effect is not due to any error in the wind shear model. Rather, it is a mathematical byproduct of using uncertain data to determine an extrapolation parameter.

$SF_{U,M}$ can be calculated as follows. h_1 , h_2 , and h_3 are the heights of the lower measurement anemometer, the higher measurement anemometer, and the hub height, respectively. U_{M1}^- and U_{M2}^- are the measured mean wind speeds at the lower and upper anemometer, respectively. When the power law is used, the measured data can be used to calculate the shear parameter, α , using Eq. 21.

$$\alpha = \ln(\bar{U}_{M2} / \bar{U}_{M1}) / \ln(h_2 / h_1) \quad \text{Eq. 21}$$

The predicted hub height mean wind speed, \bar{U}_{HUB} , can then be calculated using Eq. 22.

$$\bar{U}_{HUB} = \bar{U}_{M2} (h_3 / h_2)^{\ln(\bar{U}_{M2} / \bar{U}_{M1}) / \ln(h_2 / h_1)} \quad \text{Eq. 22}$$

If it is assumed that the uncertainties in the mean wind speeds are normally distributed, and there is no uncertainty in the three heights, then the uncertainties can be related using Eq. 23. The uncertainties in Eq. 23 are absolute uncertainties.

$$\delta \bar{U}_{HUB}^* = \sqrt{\left(\frac{\partial \bar{U}_{HUB}}{\partial \bar{U}_{M1}} \delta \bar{U}_{M1}^* \right)^2 + \left(\frac{\partial \bar{U}_{HUB}}{\partial \bar{U}_{M2}} \delta \bar{U}_{M2}^* \right)^2} \quad \text{Eq. 23}$$

Next, it is assumed that the fractional standard uncertainty of \bar{U}_{M1} and \bar{U}_{M2} ($\delta \bar{U}_{M1}$ and $\delta \bar{U}_{M2}$), are both equal to the fractional standard measurement uncertainty, δU_M , as shown in Eq. 24. That is, it is assumed that the measurement uncertainties at both heights are identical.

$$\delta U_M = \delta \bar{U}_{M1} = \delta \bar{U}_{M2} = \delta \bar{U}_{M1}^* / \bar{U}_{M1} = \delta \bar{U}_{M2}^* / \bar{U}_{M2} \quad \text{Eq. 24}$$

Finally, after substituting Eq. 24 into Eq. 23, and after some algebraic manipulation, the ratio of the fractional uncertainty in the predicted mean wind at height h_3 , $\delta \bar{U}_{HUB}$, to the fractional standard measurement uncertainty, δU_M , can be written using Eq. 25. This ratio is also equal to the sensitivity factor for the measurement uncertainty, $SF_{U,M}$.

$$SF_{U,M} = \frac{\delta \bar{U}_{HUB}}{\delta U_M} = \sqrt{\left(\frac{\partial \bar{U}_{HUB}}{\partial \bar{U}_{M1}} \frac{\bar{U}_{M1}}{\bar{U}_{M2}} \right)^2 + \left(\frac{\partial \bar{U}_{HUB}}{\partial \bar{U}_{M2}} \right)^2} \cdot \left(\frac{\bar{U}_{M2}}{\bar{U}_{HUB}} \right) \quad \text{Eq. 25}$$

The partial derivatives can be calculated using Eq. 22. The ratios U_{M1}^-/U_{M2}^- and U_{M2}^-/U_{HUB}^- can be calculated using Eq. 22. When these calculations are substituted into Eq. 25, $SF_{U,M}$ can be written as an analytic function of only the three measurement heights. The final result for $SF_{U,M}$ is shown in Eq. 26.

$$SF_{U,M} = \sqrt{\frac{2\left(\ln\left(\frac{h_3}{h_2}\right)\right)^2 + \left(\ln\left(\frac{h_2}{h_1}\right)\right)^2 + 2\ln\left(\frac{h_2}{h_1}\right)\ln\left(\frac{h_3}{h_2}\right)}{\left(\ln\left(\frac{h_2}{h_1}\right)\right)^2}} \quad \text{Eq. 26}$$

$SF_{U,M}$ can be determined for any configuration of measurement heights and turbine hub height. $SF_{U,M}$ increases as the two measurement anemometer heights are closer together. Therefore, the anemometers should be spaced as far from each other as possible. Overly close spacing of anemometers can cause very large values of $SF_{U,M}$, and so larger values of δU . On the other hand, the lower level anemometer should not be placed too close to the ground, as obstructions and surface roughness changes can distort the wind speed at these low heights.

3. Calculate the overall uncertainty in the long-term hub height mean wind speed, δU . This is accomplished using Eq. 27.

$$\delta U = \sqrt{(SF_{U,M} \cdot \delta U_M)^2 + (\delta U_{LT})^2 + (\delta U_V)^2 + (\delta U_{SA})^2} \quad \text{Eq. 27}$$

4. Determine δc . δc can then be calculated based on δU and δk using Eq. 17. The general equation for δc is shown in Eq. 28.

$$\delta c = \sqrt{(SF_{c,U} \cdot \delta U)^2 + (SF_{c,k} \cdot \delta k)^2} \quad \text{Eq. 28}$$

$SF_{c,U}$ is simply equal to one due to the linear dependence shown in Eq. 17.

The formula for $SF_{c,k}$ is shown below in Eq. 29, where ψ is the Psi function.

$$SF_{c,k} = \frac{\partial c}{\partial k} \frac{k}{c} = \psi(1 + 1/k)/k \quad \text{Eq. 29}$$

3.7 Example Calculation of δU , δc , and δk

An example calculation of δU , δc , and δk helps illustrate the process described in Section 3.6. The tables below indicate the values of δU_i and δk_i that are used in the calculation. The assumptions that generate these values are:

- $\delta U_4 = 1\%$: IEC approved anemometer used for site assessment
- $\delta U_7 = \delta k_7 = 0.03\%$: 1% of the measured data set is missing.
- $\delta U_8 = \delta k_8 = 5\%$: Example result of the jackknife estimate.
- $\delta U_{11} = \delta k_{11} = 2.4\%$: 6 years of long-term data are available for MCP, so $N = 6$.
- $\delta U_{13} = \delta k_{13} = 0\%$: No topographic effects, and the turbine is positioned at the met tower location.
- $\delta U_{14} = 5.0\%$, $\delta k_{14} = 5.0\%$: Flat terrain.
- k is assumed to be constant with height.
- Lastly, assume $h_1 = 35$ m, $h_2 = 50$ m, and $h_3 = 80$ m.

I. Wind Speed Measurement Uncertainty

	δU_i	δk_i	Bias U_i	Bias k_i
1	1.5%	0%	0%	0%
2	0.3%	0%	0.5%	0%
3	0.5%	0%	0%	0%
4	1%	0%	0%	0%
5	0.5%	0%	0%	0%
6	0.5%	0%	0%	0%
7	0.03%	0.03%	0%	0%

II. Long-Term Resource Estimation Uncertainty

	δU_i	δk_i	Bias U_i	Bias k_i
8	5%	5%	0%	0%

9	0%	5.0%	0%	0%
10	1.0%	1.0%	0%	0%

III. Wind Resource Variability Uncertainty

	δU_i	δk_i	Bias U_i	Bias k_i
11	2.4%	2.4%	0%	0%
12	1.0%	1.0%	0%	0%

IV. Site Assessment Uncertainty

	δU_i	δk_i	Bias U_i	Bias k_i
13	0%	0%	0%	0%
14	5%	5.0%	0%	0%

The steps to calculate δU are:

1. Calculate the uncertainty for each group of uncertainty by using the RSS method.

The result is:

$$I: \delta U_M = \sqrt{(1.5)^2 + (0.3)^2 + (0.5)^2 + (1.0)^2 + (0.5)^2 + (0.5) + 0.03^2} = 2.02\%$$

$$II: \delta U_{LT} = \sqrt{(5.0)^2 + (0)^2 + (1.0)^2} = 5.10\%$$

$$III: \delta U_V = \sqrt{(2.4)^2 + (1.0)^2} = 2.60\%$$

$$IV: \delta U_{SA} = \sqrt{(0)^2 + (5.0)^2} = 5.00\%$$

2. Calculate $SF_{U,M}$ using h_1, h_2, h_3 and Eq. 26: $SF_{U,M} = 2.67$.
3. Calculate the overall uncertainty in $U, {}^{-}_{LT_HUB}, \delta U$, using Eq. 27.

$$\begin{aligned} \delta U &= \sqrt{(SF_{U,M} * \delta U_M)^2 + (\delta U_{LT})^2 + (\delta U_V)^2 + (\delta U_{SA})^2} \\ &= \sqrt{(2.67 * 2.02)^2 + (5.1)^2 + (2.60)^2 + (5.00)^2} \\ &= 9.3\% \end{aligned}$$

The steps to calculate δk are:

1. Combine all fourteen sources of uncertainty using the RSS method

$$\begin{aligned}\delta k &= \sqrt{(\delta k_1)^2 + (\delta k_2)^2 + \dots + (\delta k_{14})^2} \\ &= 9.1\%\end{aligned}$$

The steps to calculate δc are:

1. Calculate $SF_{c,k}$ using Eq. 29. If $k_{LT_HUB} = 2.5$, then:

$$\begin{aligned}SF_{c,k} &= \psi(1 + 1/k)/k \\ &= -0.025\end{aligned}$$

2. Calculate δc using Eq. 28. Because $SF_{c,k}$ is so small, δU and δc are almost exactly equal.

$$\begin{aligned}\delta c &= \sqrt{(\delta U)^2 + (SF_{c,k} \cdot \delta k)^2} \\ &= 9.3\%\end{aligned}$$

Thus, once all fourteen sources of uncertainty are estimated, they can be combined to yield a total uncertainty for the long-term values of U , c_{LT_HUB} , and k_{LT_HUB} . For this example, $\delta c = \delta U = 9.3\%$ and $\delta k = 9.1\%$. If $SF_{U,M}$ is assumed to equal one, then δc and δU are reduced to 7.9%.

3.8 Summary of Wind Resource Uncertainty

Overall, this Section describes a comprehensive method for handling uncertainty for this type of wind resource assessment. Along with describing the uncertainty sources that arise in this process, a method for estimating the long-term hub height wind resource and its respective uncertainty is provided. The techniques for estimating uncertainty rely on the use of sensitivity factors. Specifically, an explicit formula to calculate the measurement uncertainty sensitivity factor is provided. This magnification of the

measurement uncertainty due to shear extrapolation should not be ignored, as it can affect the overall wind resource uncertainty.

In general, other sources of uncertainty are possible in the site assessment process, although they are not likely to be large relative to those identified above. Furthermore, alternative methods of performing a site assessment are also viable; for instance mesoscale and microscale modeling can be used instead of MCP [77]. These alternative site assessment methods would necessitate modification to the uncertainty analysis approach outlined above. However, many of the techniques would still be applicable.

4.0 Wind Turbine Power Production and Uncertainty

Section 3.0 focuses on the process of evaluating the wind resource at a site and the associated uncertainty. Like the wind resource, the determination of the power curve and power production of a wind turbine are also potentially subject to error, which then causes uncertainty in the estimate of *AEP*. This Section investigates the uncertainty in the power production of a wind turbine. The process of adjusting a power curve for a specific site is also described.

4.1 Power Curve and Power Production Uncertainty Sources

There are three sources of power curve and power production uncertainty discussed in this Section labeled δP_1 , δP_2 , and δP_3 :

- I. Wind Turbine Specimen Variation Uncertainty.
- II. Power Curve Uncertainty.
- III. Air Density Uncertainty.

Each of these uncertainties is due to Type B errors. The bias of the power curve is not estimated in this Section, so only the uncertainty is presented in the tables after each source or error. In general, when power curves are discussed in this Section, it is assumed that the wind turbine is a variable speed, pitch controlled turbine with constant power output above rated wind speed.

4.1.1 Wind Turbine Specimen Variation Uncertainty

Frandsen and Christensen note that within a particular model of a wind turbine, individual turbines could have power curves that vary from the “reference” power curve quoted by the manufacturer [57]. These variations are likely due to manufacturing variations. They state that no thorough investigation of these variations has taken place, and so they choose a tentative estimate of 5% uncertainty due to “specimen variation” [57]. A report by Risø estimates that the variation of power curves for a given wind turbine model is 2%-3% [36]. A value of 3% is recommended here, unless there is information to suggest another value.

This uncertainty is assumed to be Type B. One could argue that if the turbines are randomly selected from the population of turbines, then the uncertainty should decrease as the total number of turbines increases. This supposition would assume a Type A error. However, the manufacturing variations of the turbines could be localized in a specific batch of turbines (e.g., a specific machine produced slightly different blades), so that all of the turbines at a wind farm varied from the reference power curve by the same amount (i.e., the same bias). Thus, to be conservative, it is assumed that the uncertainty due to specimen variation is 3% regardless of the number of turbines at the wind farm.

δP_1
3.0%

4.1.2 Power Curve Uncertainty

When power curves for wind turbines are measured, several factors contribute to the uncertainty in this “measured power curve”. The primary factor is uncertainty in the wind speed that the turbine is responding to, as the uncertainty in the actual power being produced is quite small. While the wind speed at the hub height is known to a fairly high accuracy, the effects of turbulence and shear across the rotor face are not taken into account, and consequently the mean wind speed averaged over the rotor face is uncertain. This uncertainty is reflected in the power curve, as there are vertical error bars around the power value for a given wind speed, as shown in Figure 14 [13].

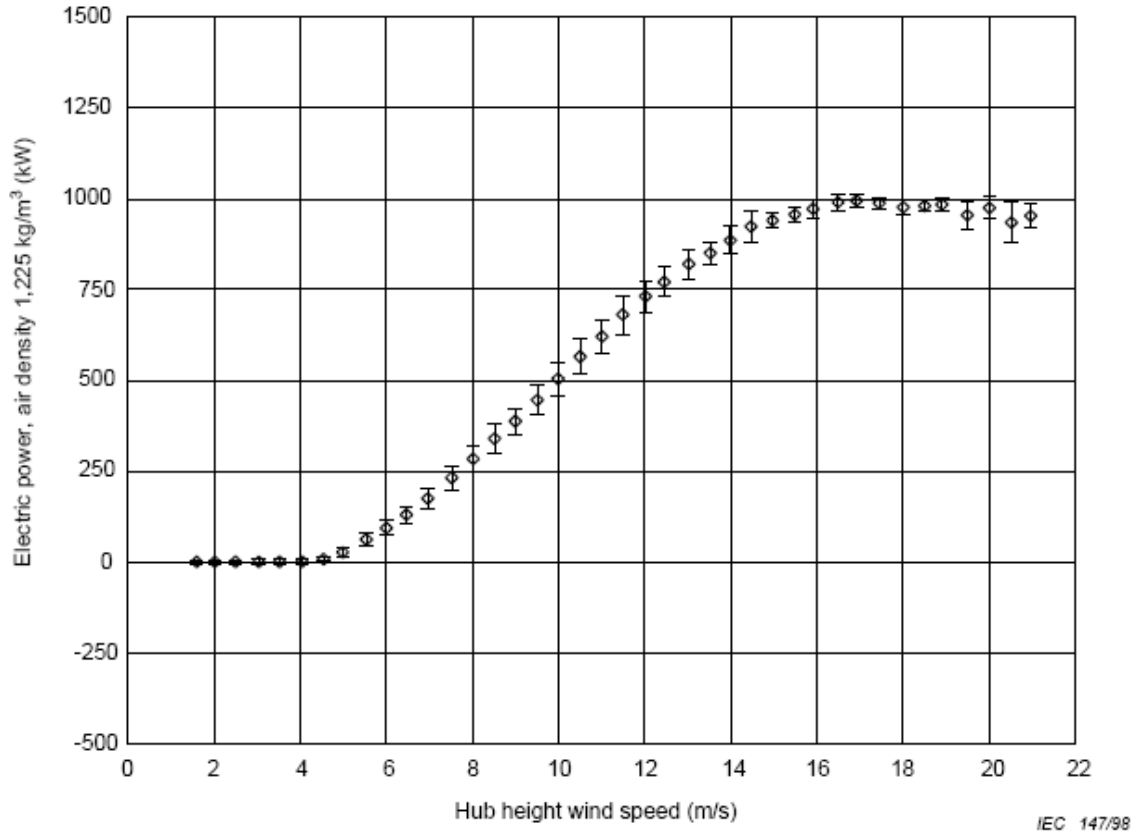


Figure 14 – Example Power Curve with Error Bars

Moreover, for variable speed, pitch controlled turbines the error bars are smaller for wind speeds above the rated wind speed and for low wind speeds. On the other hand, there is more uncertainty for moderate wind speeds. For simplicity, these uncertainties at each speed can then be converted into an overall power curve uncertainty, which is assumed to be constant across all speeds. While the IEC standards require manufacturers to calculate the uncertainty of the power curve of a turbine during testing, these values are not readily available from the manufacturers. Contact with industry sources indicated an approximate overall value of 5%. Pedersen et al. estimate a value between 6%-8% [36]. Frandsen and Christensen estimate a value between 5% and 10% [57]. The Danish Wind Energy Association likewise quotes a value of 10% [78]. A value of 7.5% can be

assumed for the uncertainty of the measured power curve, as it is in the middle of the range of values discussed above.

This issue is complicated because the power curve of a wind turbine is site dependent, and not solely a function of the hub height wind speed. The turbulence, air density, and shear characteristics of a site affect the power curve of a turbine, with the result that a turbine at a specific site could produce either more or less power than the power curve indicates at a given wind speed. The measured power curve specifically corresponds to a site that meets the IEC standards, which require a flat site with very low turbulence [13]. Thus, a site-specific power curve is needed to estimate energy production at a site, especially when the terrain is complex. The manufacturer generally determines this site-specific power curve, based on the turbulence, air density, and shear characteristics of the site. The manufacturer and the developer then agree on this “warranted power curve”. The method by which the manufacturer estimates the site-specific warranted power curve is proprietary and likely depends on the control system of the turbine, as well as the legal language in the contract. A manufacturer often performs a site calibration and power performance test after installation to demonstrate that the turbines do in fact meet the requirements of the warranted power curve and the contract. In regards to site assessment and uncertainty, several remarks can be made:

- A developer should certainly obtain an estimate of the site-specific power curve from the manufacturer before any final financial decisions are made. The discrepancy between the warranted power curve and the measured power curve could make the difference between a successful and failed development. Site

calibration and power performance testing can then confirm the accuracy of the estimated site-specific power curve.

- The site calibration and power performance testing procedure is subject to similar uncertainty as the original measurement of the power curve. Therefore, after verification of the power curve at the site, the uncertainty can be assumed to be 7.5%.
- During development, before the actual installation of the turbines, the developer utilizes the estimated site-specific power curve from the manufacturer to estimate the energy production at the site, and ultimately the profitability. That is, the decision of whether or not to develop a site is made with an estimated site-specific power curve, before power performance verification is possible. This estimated site-specific power curve is derived from the measured power curve. Also, as stated above, the method used by individual manufacturers to adjust the measured power curve to a specific site is proprietary and unavailable. At a minimum, the uncertainty in the site-specific power curve is at least as large as the uncertainty in the measured power curve. In actuality, it is likely to be appreciably larger due to added uncertainty in taking the turbulence, air density, and shear characteristics into account. To date, no value for this uncertainty is determined, primarily due to the confidential nature of the method. With no better option, a 10% uncertainty can be assumed, as it is larger than the 7.5% uncertainty of the measured power curve. In the future, this value can hopefully be determined based on actual data.
- In the very early stages of development, a developer may wish to obtain a “ballpark” estimate of the energy production. A simple method to adjust for the

air density at the site can be used to estimate the site-specific power curve. This method is described in Section 4.2. The method does not take the turbulence or shear characteristics of the site into account, nor does it consider the control strategy of the turbine. Thus, this estimated power curve is subject to even more uncertainty than the site-specific power curve. Again, no data are currently available to estimate this uncertainty. A value of 12.5% is recommended here with no justification.

δP_2
7.5%, 10.0%, or 12.5%

4.1.3 Air Density Uncertainty

Seasonal variations in air density could potentially affect the accuracy of the energy production estimate. The uncertainty due to air density variations is therefore explored. In most locations in the world, the density changes with the seasons, causing the power production to be different in different seasons, even at identical wind speeds. This issue is investigated and two major conclusions can be drawn.

- Wind turbine annual energy production calculations are fairly insensitive to seasonal density effects. That is, the calculated energy output of a turbine does not change greatly if the average yearly density is used to adjust the calculation, or if the seasonal fluctuations are taken into account. For a sample power curve, the *AEP* can be estimated for two cases: one where the average density of the year is used and one where seasonal fluctuations are taken into account. Even when large seasonal density fluctuations are used (and typical seasonal wind speed variations at Massachusetts Sites), the effect on *AEP* estimates is less than or

equal to 1%. Thus, for simplicity, one could adjust the power curve using the average annual air density, and therefore ignore seasonal variations. A 0.5% uncertainty in the power output can be assumed, using Eq. 9. Thus, $\delta P_3 = 0.5\%$.

- If there is an error in the calculation of the average annual density, then this error causes an error in the *AEP* estimate of approximately half the magnitude of the density error. For example, a 1% error in the calculation of density causes a 0.5% error in the *AEP*. In essence, the sensitivity factor for the air density measurement uncertainty is approximately 0.5. This is because at higher wind speeds, above the rated wind speed of a turbine, an error in the density estimate has no effect on the *AEP* calculation (for variable speed, pitch controlled turbines). To date, no determination of the uncertainty in the actual density estimate is made, although one would assume that the annual density could be calculated with high accuracy. In practice, this error is likely to be negligible and is assumed so for this Chapter.

δP_3
0.5%

4.2 Air Density Normalization

In general, power curves are given for atmospheric conditions corresponding to standard temperature and pressure (STP) at sea level. The air density at these conditions is the rated air density for the power curve, and it usually equals 1.225 kg/m^3 . The density of the air has a direct effect on the power production of the turbine, and so if the turbine is sited at a location with an average air density different than the rated air density, the power curve must be adjusted (normalized) for the site. When a developer is purchasing turbines from a manufacturer, the manufacturer most likely adjusts the power

curve for the air density at the site to provide a site-specific power curve to the developer. However, when a preliminary site assessment is being performed, the manufacturer adjustments may not be available, and one must normalize the power curve on one's own in order to then estimate *AEP*. This Section describes one method for normalizing the power curve at a site with a different annual air density than the rated value. This method does not take the site-specific turbulence and shear characteristics into account.

For variable speed, pitch-regulated turbines, the IEC power performance standards recommend adjusting the wind speed values from the power curve data to normalize the power curve [13]. That is, the value of the power output of the turbine is not changed; rather the corresponding wind speed for each power output value is adjusted. This normalization equation is shown in Eq. 30, where V_n is the normalized velocity value, V_0 is the original velocity value, ρ_n is the actual density at the site, and ρ_0 is the rated density value for the turbine (usually the STP value of 1.225 kg/m³).

$$V_n = V_0 * (\rho_0 / \rho_n)^{1/3} \quad \text{Eq. 30}$$

Thus, each value of wind speed in the power curve data is adjusted using Eq. 30, which results in a normalized power curve that is specific to the density value at the site. An example is shown in Figure 15. Figure 15 shows a GE 1.5 MW power curve under three conditions: rated density of 1.225 kg/m³, a low density site with a value of 1.0 kg/m³, and a high density site with a value of 1.45 kg/m³.

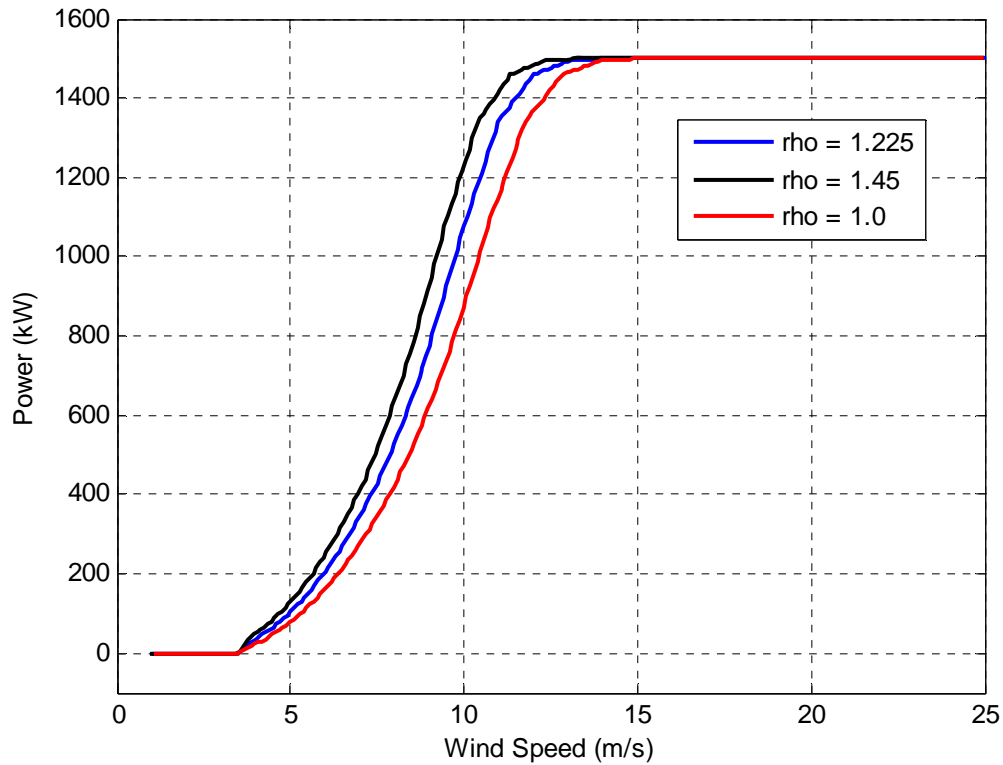


Figure 15 – Power Curves for Different Density Sites

The effect of the density normalization is seen clearly in Figure 15. When the density is higher than the rated density, the power curve is shifted to the left, which results in more power being produced for wind speeds below rated wind speed and the turbine reaching rated power at a lower wind speed than the rated wind speed. Conversely, when the density is lower than the rated density, the power curve is shifted to the right, which results in less power being produced for wind speeds below rated wind speed and the turbine reaching rated power at a higher wind speed than the rated wind speed. However, the cut-in and cut-out wind speeds are unaffected. This method does not take the control system of the turbine into account, and therefore is potentially subject to significant error. But, as a “back of the envelope” method, it is very useful. In sum, the effect of air

density clearly must be taken into account when it differs from the rated value, and this Section describes one method for accomplishing this task.

4.3 Summary of Power Curve and Power Production Uncertainties

The estimated values of the uncertainty for the three uncertainty sources discussed above are summarized in the table below.

	δP_1
1	3%
2	7.5%, 10%, or 12.5%
3	0.5%

4.4 Combination of Power Curve and Power Production Uncertainty

The three sources of uncertainty discussed in Section 4.1 can then be combined into a total uncertainty in the power output, δP . The uncertainty sources are assumed to be independent, and sensitivity factor for each uncertainty source is equal to one, so the RSS method can be used, as shown in Eq. 31.

$$\delta P = \sqrt{(\delta P_1)^2 + (\delta P_2)^2 + (\delta P_3)^2} \quad \text{Eq. 31}$$

4.5 Example Calculation of δP

For this example, it is assumed that a manufacturers site-specific power curve is supplied, so $\delta P_2 = 10\%$. The total power output uncertainty, δP , is simply:

$$\begin{aligned} \delta P &= \sqrt{(\delta P_1)^2 + (\delta P_2)^2 + (\delta P_3)^2} \\ &= \sqrt{(3.0)^2 + (10)^2 + (0.5)^2} \\ &= 10.5\% \end{aligned}$$

5.0 Energy Production Losses and Uncertainty

This Section describes the factors that contribute to uncertainty in the estimate of energy losses. These factors are distinct from those described in the previous Section, which related to uncertainty in the instantaneous power output. Those factors that contribute to lost energy production are referred to as the “energy loss factors.” Essentially, they quantify the deviation between the actual turbine performance, and the ideal turbine performance, due to specific sources of energy loss. The three energy loss factors identified in this Section are:

- I. Availability Losses
- II. Fouling Losses
- III. Array Losses

For each of the three energy loss factors discussed in this Section, a general description is provided first. Next, the expected value or range of expected values is given. It should be noted that other sources of energy loss are possible, such as electrical losses and high wind speed hysteresis. These losses are not considered in this Section.

The energy loss factors are assumed to be normally distributed quantities, so the uncertainty values are once again the percentage standard uncertainty. This assumption of a normal distribution must be justified.

5.1 Justification for Normally Distributed Energy Loss Factors

The assumption of a normal distribution must now be justified. The energy loss factors, by definition, have a range between 0% and 100% (i.e. 0 and 1). A normal distribution is defined between $[-\infty, \infty]$. This is a clear contradiction, as a normally

distributed energy loss factor implies the possibility for a value less than 0 or greater than 1. Despite this contradiction, normally distributed energy loss factors are used, and there is a sound mathematical basis for their use.

The yearly availability of a wind farm is not a normally distributed quantity about its expected value. This can be seen clearly in the histogram in Figure 16. The data in Figure 16 show the number of occurrences of yearly availability values for 25 different wind farms, with a total of 104 wind farm-years of operation. The mean availability is approximately 94%, and the distribution is clearly asymmetrical, with an upper limit of 100%. These data are compiled from a variety of North American wind farms by Jones [79].

The data in Figure 16 can be fit with a Weibull distribution, for example. The choice of a Weibull distribution is fairly arbitrary, though it does provide a good fit to the empirical data. The Weibull approximation to the data is also shown in Figure 16. The result for the shape factor is a value of $k=1.5$. Thus, based on empirical data, the yearly availability of a wind farm can be approximated by a Weibull distribution with a shape factor value of $k=1.5$.

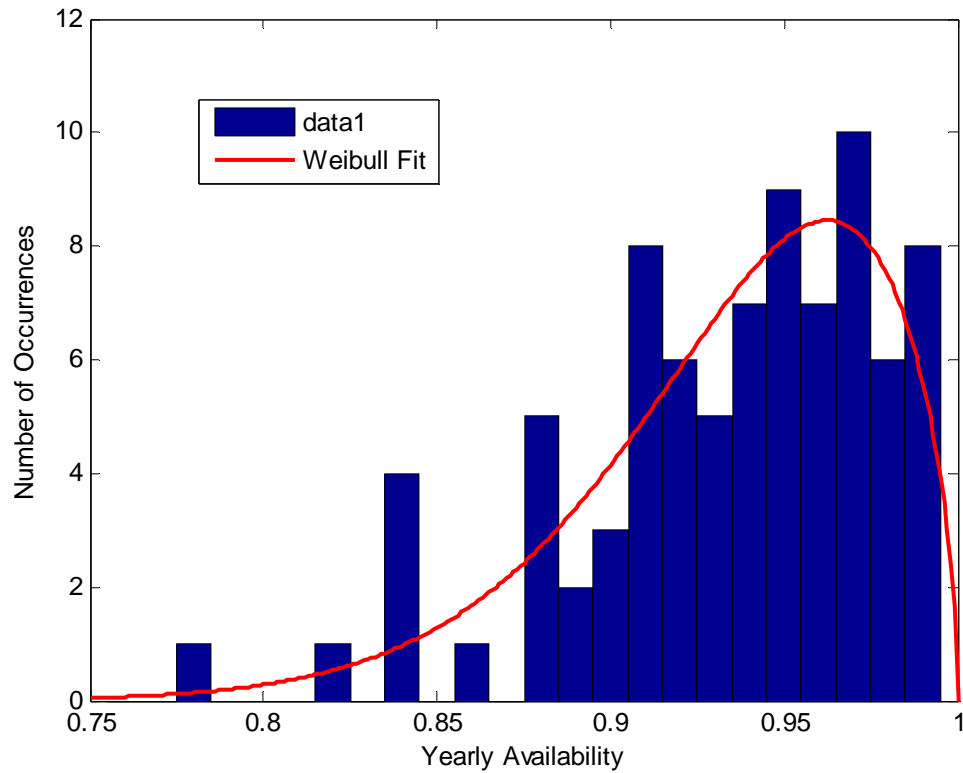


Figure 16 – Wind Farm Availability Data

However, the yearly availability is not the quantity used in energy production estimates. A developer is interested in the average availability over the approximately twenty year lifetime of the project. Thus, the quantity of interest is the lifetime availability of the wind farm, or the average of the twenty yearly availabilities. The distribution of the lifetime availability can be determined using a “Monte Carlo” simulation. The simulation proceeds as follows:

1. Using a Matlab function, twenty values are randomly sampled from the Weibull distribution fit shown in Figure 16. These twenty values represent a random set of wind farm yearly availability values.
2. The twenty yearly availability values are averaged to get the lifetime availability.
3. This process is repeated 100,000 times.

The distribution of the lifetime availability values can then be plotted in a histogram. This is shown in Figure 17. A normal distribution can be fit to the data. This is shown in Figure 17 as well. The mean is 0.94 and the standard deviation is 0.009.

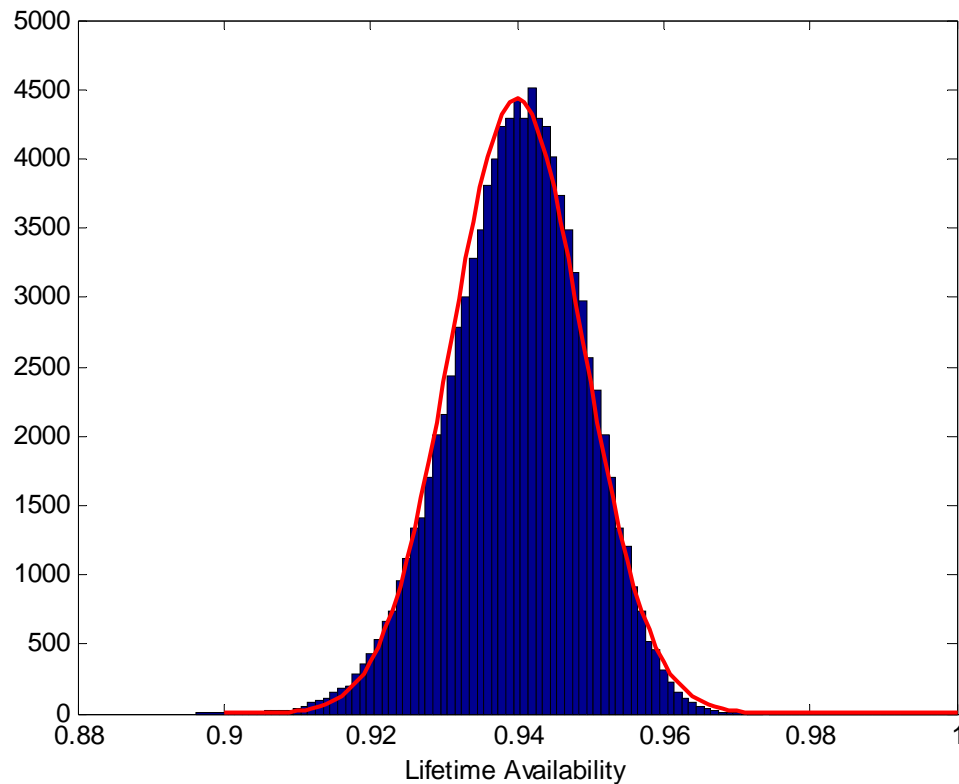


Figure 17 – Distribution of Lifetime Availability Data

Thus, while the distribution of yearly availability values can be approximated by a Weibull distribution, the distribution of lifetime availability values is very closely approximated by a normal distribution. This result should not be surprising, and it follows directly from the central limit theorem. The theorem states that the distribution of the mean of random samples taken from any other distribution is normally distributed as the number of samples becomes large. In the case of the yearly availability data, only

twenty samples are taken from the Weibull distribution, which causes the resulting distribution of the mean to be not exactly normal. However, there are still enough samples that a normal distribution provides a good approximation.

This result makes intuitive sense as well. The yearly availability distribution from Figure 16 indicates that there is approximately a 10% chance of getting an availability value less than 0.90 in a single year. However, the chance of getting availability values less than 0.90 over the lifetime of the project is extremely small, and this is reflected in Figure 17. Over a twenty year period, it's unlikely that the average availability is much different than the expected value.

This result is applied to all three energy loss factors. Like the availability, the yearly distributions of the fouling and array loss energy loss factors are probably not normally distributed. Instead, they most likely follow a similar asymmetrical distribution, with an upper limit of one. However, the distribution of the twenty year average once again follows a normal distribution, due to the central limit theorem. Thus, all three energy loss factors are characterized by normal distributions.

There is still the possibility for values greater than one when normally distributed energy loss factors are assumed, and so a contradiction remains. However, in general the probability of a value greater than one is so small that it is completely negligible. In the availability example, the probability of a lifetime availability value greater than one is $2 \times 10^{-9}\%$. Clearly the contradiction can be ignored in this case.

5.2 Availability Losses and Uncertainty

Wind turbines are sometimes shut down for scheduled inspection and maintenance, or for unscheduled repair. During these shut downs, the wind turbine clearly cannot

produce any energy, and so the *AEP* is reduced. The availability is simply defined as the percentage of time that a turbine is operable. It is generally assumed that modern wind turbines have availabilities on the order of 97% [78]. On the other hand, Jones finds that that wind farms in North America have an average availability of about 94% [79]. However, the issue is not so simple, as the average value of the availability does not tell the whole story. Availability does not necessarily affect energy production linearly. For example, scheduled maintenance is usually performed in the summer time, when the days are longer and the wind speeds are lower, and so the turbines may be producing very little power. In this way, even though the wind turbine is shut down 3% of the time (for example) for maintenance, the reduction in the turbines' energy production can be nearly negligible. On the other hand, unscheduled repairs can cause a decrease in energy production disproportionate to the actual time that the turbine is not operating. If a component breaks and causes a turbine to shut down, it is more likely to occur during high wind speeds, perhaps in the winter. So even if the turbine repair results in 97% availability, the energy production would be reduced by more than 3%. Also, in the case of offshore turbines, repairs may be greatly delayed due to weather-related and scheduling issues, causing an even larger loss in energy production. Thus, to truly determine how availability affects energy production, the relative energy loss due to scheduled and unscheduled maintenance must be determined.

Jones finds that, on average, the larger lost energy production during unscheduled maintenance outweighs the smaller lost energy production during scheduled maintenance. Thus, the energy production is reduced by more than just the value of the availability. In this Chapter, the actual amount that *AEP* is reduced due to maintenance is labeled ELF_{AV} .

ELF_{AV} is equal to the actual AEP divided by the AEP if no maintenance or repairs are done on the turbine. ELF_{AV} is distinct from the typical definition of availability, as it accounts for the reduction in energy production due to maintenance and repairs, and is not simply calculated based on the annual reduction in operating time. The value of ELF_{AV} has a clear upper and lower limit. The upper limit is 100%. In the lower limit, the largest possible energy loss occurs if the turbine is operating at rated power during the entire time it is shut down for repairs and maintenance.

Overall, for modern wind turbines with availabilities around 97%, ELF_{AV} is typically around 95%-96% because of the disproportionately large energy production loss during unscheduled maintenance. To be conservative, a value of 95% is assumed here. This value is larger than the 94% quoted by Jones. However, there is little information available concerning the types of turbines in Jones's study. Presumably, the turbines in the study encompass a range of ages. In general, the more modern a turbine is, the better its availability, and so in the future one may expect better availabilities for wind farms than the data in Jones's study indicates. Regardless of the actual value estimated for the availability, there is likely some uncertainty in this estimate. A value of 1% for the uncertainty in the expected value of the availability is reasonable, given the range of values quoted for the expected availability.

Additional uncertainty arises due to the variability of yearly availability values, seen in the data provided by Jones in Figure 16. That is, there is a potentially large variation in the availability from year to year, and so the lifetime availability of a wind farm may not equal the expected value of the availability. Thus, there is additional uncertainty in the estimate of the availability. The Monte Carlo simulation above indicated that the

uncertainty due to this variability is approximately 1% as well. These two distinct uncertainties for the availability can then be combined using the RSS technique to give an overall availability uncertainty of 1.5%.

ELF_{AV}	δELF_{AV}
95.0%	1.5%

5.3 Fouling Losses and Uncertainty

Ice, dirt, and insects can attach to the surfaces of wind turbine blades, reducing the aerodynamic performance of the blades, and thereby reducing the power output and AEP of a turbine. In the northeast United States, icing is an especially important factor due to the cold winters. Moreover, along with reducing the power output of a wind turbine, icing can cause a complete loss of production, overloading, and fatigue [80]. Anecdotal evidence from the Searsburg, Vermont wind farm indicates icing losses reducing AEP by between 2-6% [81]. The evaluation of the proposed East Haven Wind Farm in Vermont estimates an 8% reduction in AEP due to fouling (which includes icing), while the evaluation of Sheffield Wind Farm in Vermont estimates a 3% reduction due to icing [81],[82]. The degree to which fouling decreases AEP depends on a number of factors including: the frequency of blade cleaning, the amount of rain at a site, the likely amount of ice accumulation at a site, the ice mitigation efforts, the particular airfoil used in the turbine blades, and more. Moreover, the effect of fouling varies year-to-year depending on the weather. Finally, fouling reduces the energy production in stall-controlled turbines more than pitch-controlled turbines. Thus, the effect of fouling is highly site dependent and very uncertain.

The energy loss factor due to fouling is labeled ELF_{FOUL} , and it is equal to the actual AEP divided by the AEP if no fouling occurs. In the northeast United States, ELF_{FOUL} is likely between 90-95% based on the Searsburg wind farm and the estimates for the two proposed Vermont wind farms, although it certainly could vary outside of this range. Based on this data, a reasonable uncertainty in the expected value of the fouling is 2%.

This value of ELF_{FOUL} obviously is not constant from year to year over the lifetime of the wind farm. Like availability, there is probably a yearly fouling distribution with a large amount of spread. Thus, there is variability in the fouling from year to year, which causes additional uncertainty in the estimate of the effect of fouling. Some years fouling may decrease the AEP substantially, and other times not at all. Unlike the availability, however, no empirical data are available with which to model the yearly availability distribution. A conservative approach can be taken to approximate the fouling uncertainty. This approach assumes a large amount of spread in the yearly fouling distribution, which is modeled by assuming a value of $k=1.01$ for the Weibull approximation. For an expected value of $ELF_{FOUL} = 0.90$, the uncertainty in the lifetime fouling is 2%. The overall fouling uncertainty, ELF_{FOUL} , can be found by combining the uncertainty of the expected value and the uncertainty due to yearly variability using the RSS method. The result is a value for ELF_{FOUL} of 3%.

For sites in warmer climates, where icing occurrences are rare, the uncertainty is likely quite a bit smaller. A value of $ELF_{FOUL} = 1\%$ can be used, since the amount of bugs, dirt, and rain (and others) may still causes some variation in the value of ELF_{FOUL} .

Sites where icing is likely

ELF_{FOUL}	δELF_{FOUL}
Site Dependent	3%

Sites where icing is unlikely

ELF_{FOUL}	δELF_{FOUL}
Site Dependent	1%

5.4 Array Losses and Uncertainty

When multiple wind turbines are arrayed to form a wind farm, the wakes of upwind turbines can decrease the wind speed seen by downwind turbines. This reduction in the wind speed seen by downwind turbines causes a reduction in power production. Therefore, on average, a wind farm with N turbines at a certain site produces less energy than a single turbine at that site, multiplied by N . Array losses can be estimated using wake models. This estimate is necessary whenever a wind farm is being considered. Software packages such as WindPro or WindFarmer are used for estimating the array losses at a wind farm.

The reduction in AEP depends on a number of factors, including the wind farm layout, the turbine spacing, the distribution of wind directions, the wind speed, and more. The magnitude of array losses is therefore highly site dependent, and uncertain. The energy loss factor due to array losses is labeled ELF_{ARRAY} , and it is equal to the actual AEP divided by the AEP if no array losses occur. ELF_{ARRAY} is often referred to as the “array efficiency.” For a single turbine, ELF_{ARRAY} is 100%.

Uncertainty in the array losses is due to many possible sources of error. Some of these are:

- Wake model error. The wake model used to estimate the array losses may not be accurate.
- Incorrect estimation of the wind direction probability distribution. The measured wind direction distribution may differ from the long-term wind direction

distribution. This could lead to errors in the estimated array losses. This is an error due to an unknown bias.

- Inter-annual wind direction variability. Even if the long-term wind direction distribution is correctly estimated, the wind direction distribution may vary from year to year. This is a random error.
- Wind speed estimation error and wind speed inter-annual variability. The wind speed affects the wake losses as well, although it is likely a relatively small effect. Errors in the estimation of the wind speed, as well as the natural variability in the wind speed can potentially lead to errors in the estimation of the array losses.

Unfortunately, it is not possible to provide a specific value for the array loss uncertainty, ELF_{ARRAY} . It is far too site dependent and layout dependent. For example, a uniformly spaced, square grid wind farm (e.g., 5x5) in flat, uniform terrain is likely to have a small array loss uncertainty. Even if the wind direction distribution is completely misestimated, the resulting error is fairly small. The uncertainty would therefore be quite small, perhaps on the order of 1%. On the other extreme, a wind farm comprised of a single row of turbines could have a very large array loss uncertainty. If the wind direction distribution is misestimated, this could have a very large effect on the magnitude of the array losses. The uncertainty in the estimate of the array losses would then be very large, perhaps even on the order of 8-10%.

One method to obtain a “ballpark” estimate of the array loss uncertainty is a bracketing method. First, the wake model program is run with the best estimate of the wind speed and direction distribution. Next, the program can be rerun using synthesized

wind direction data. The program can be run once when the wind direction comes 100% of the time from the direction corresponding to maximum array losses, and once from the direction of minimum array losses. In this way, the best-case and worst-case scenarios are identified. This would provide a maximum possible range of array loss values. The uncertainty is certainly less than this range, but this method at least provides a means of bracketing the uncertainty.

ELF_{ARRAY}	δELF_{ARRAY}
Site Dependent	Site Dependent

5.5 Combination of Energy Losses and Uncertainties

The three energy loss factors each reduce the energy production of a turbine or wind farm linearly. Thus, the overall energy loss, ELF , is simply the product of the three individual energy loss factors, as shown in Eq. 32.

$$ELF = ELF_{AV} \cdot ELF_{FOUL} \cdot ELF_{ARRAY} \quad \text{Eq. 32}$$

The overall energy loss factor uncertainty, δELF , can be determined using the RSS method to combine the uncertainty values of the three individual energy loss factors, as shown in Eq. 33. The sensitivity factor for each uncertainty source is equal to one.

$$\delta ELF = \sqrt{(\delta ELF_{AV})^2 + (\delta ELF_{FOUL})^2 + (\delta ELF_{ARRAY})^2} \quad \text{Eq. 33}$$

5.6 Example Calculation of ELF and δELF

For this example, it is assumed that:

- $ELF_{AV} = 95\%$, $\delta ELF_{AV} = 1.5\%$.
- $ELF_{FOUL} = 92\%$, $\delta ELF_{FOUL} = 3\%$. The site is likely to experience icing.
- $ELF_{ARRAY} = 90\%$, $\delta ELF_{ARRAY} = 2\%$.

The overall energy loss factor, ELF , is found using Eq. 32:

$$\begin{aligned} ELF &= ELF_{AV} \cdot ELF_{FOUL} \cdot ELF_{ARRAY} \\ &= 0.95 * 0.92 * 0.90 \\ &= 0.787 = 78.7\% \end{aligned}$$

The overall energy loss factor uncertainty, δELF , is found using Eq. 33:

$$\begin{aligned} \delta ELF &= \sqrt{(\delta ELF_{AV})^2 + (\delta ELF_{FOUL})^2 + (\delta ELF_{ARRAY})^2} \\ &= \sqrt{(0.015)^2 + (0.03)^2 + (0.02)^2} \\ &= 3.9\% \end{aligned}$$

6.0 Combining Uncertainty – The Capacity Factor Uncertainty

Once the wind resource at a site is determined for each turbine location ($U, \bar{c}_{LT_HUB}, k_{LT_HUB}$), it is combined with a selected power curve and the energy losses (ELF) to yield an estimate of the energy production. This process is depicted graphically in Figure 18. The yellow boxes represent processes or calculations, and the blue parallelograms represent sources of data.

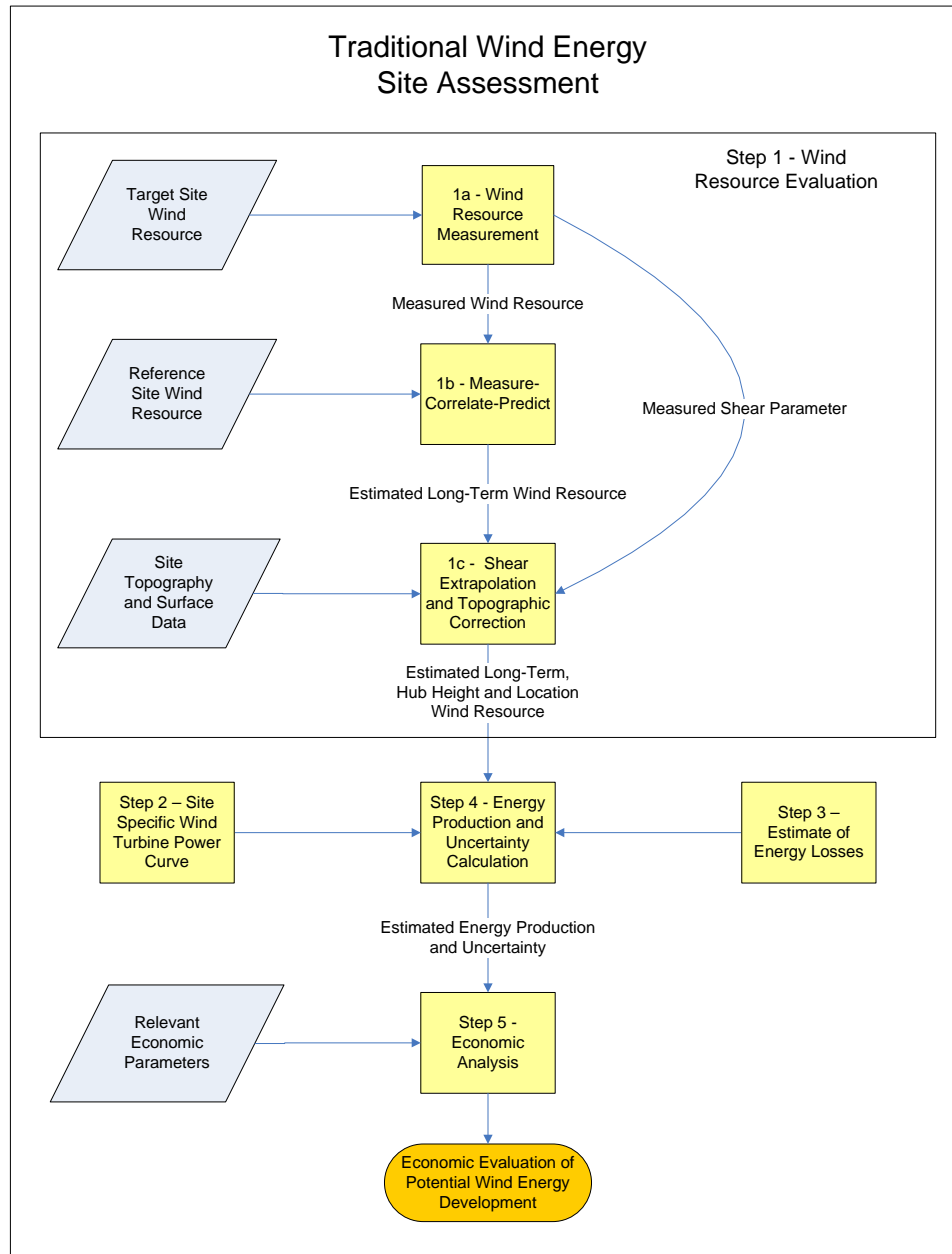


Figure 18 – Flow Chart of the Site Assessment Process

The uncertainty in the wind resource (δU , δc , δk), the uncertainty in the power production (δP), and the uncertainty of the energy loss factor (δELF) contribute to an overall uncertainty in the energy production.

Often, it is more convenient to use the “Capacity Factor” as a measure of energy production. The capacity factor is simply equal to the average turbine power output, $\overline{P_W}$, divided by the rated turbine power output, P_R , and it is a non-dimensional quantity. The capacity factor is labeled CF . The relationships between CF , AEP , and $\overline{P_W}$ are shown in Eq. 34. CF is used exclusively as a measure of energy production for the rest of this Section. It must be emphasized that the goal of site assessment is not maximizing CF [83]. Minimizing the cost of energy is generally the goal of site assessment, and CF is one component of the cost of energy. Instead, CF is a useful metric for representing the energy production of a site because it is non-dimensional.

$$CF = \overline{P_W} / P_R, \quad AEP = \overline{P_W} \cdot (8766 \text{ hours}) \quad \text{Eq. 34}$$

This Section reviews:

- How the wind resource, the power curve, and the overall reduction in the energy production are combined to estimate CF .
- A new method to determine the capacity factor uncertainty, δCF .

In general, this process cannot be performed analytically, and so a program that uses numerical integration or a simplified summation method must be used to determine the capacity factor and its uncertainty.

6.1 Method for Estimating the Capacity Factor

The capacity factor, CF , can be calculated using c_{LT_HUB} and k_{LT_HUB} along with a wind turbine power curve, $P_W(U)$, and the energy losses, ELF , as shown in Eq. 35 and Eq. 36. Note, in all the equations in this Section, c_{LT_HUB} and k_{LT_HUB} are simply labeled c

and k . When there are multiple turbines in a wind farm, the hub height estimate of the Weibull parameters may be different for each turbine.

$$CF_{IDEAL} = f(c, k, P_w, ELF) \quad \text{Eq. 35}$$

The actual functional dependence can be found by integrating the product of the wind speed distribution and the power curve over all values of wind speed, U , and then multiplying by the energy losses, and dividing by the rated power. This can be done for each turbine in the wind farm when there are multiple turbines. The capacity factor for the entire wind farm is simply the average of the CF values for each turbine. The result when using a Weibull wind speed distribution, with probability density function $p(U)$, is shown in Eq. 36 [21].

$$CF = \frac{ELF}{P_R} \int_0^{\infty} P_w(U) p(U) dU = \frac{ELF}{P_R} \int_0^{\infty} P_w(U) \left(\frac{k}{c}\right) \left(\frac{U}{c}\right)^{k-1} \exp\left[-\left(\frac{U}{c}\right)^k\right] dU \quad \text{Eq. 36}$$

The integral in Eq. 36 can be approximated by numerical integration. RERL uses a Simpson's method integration scheme in Matlab. A simplified version of a trapezoid scheme is shown in Eq. 37, in which N_B speed bins (often 25 of them) are utilized, and U_j is the wind speed for the j th bin.

$$CF = \frac{ELF}{P_R} \sum_{j=1}^{N_B} \left\{ \exp\left[-\left(\frac{U_{j-1}}{c}\right)^k\right] - \exp\left[-\left(\frac{U_j}{c}\right)^k\right] \right\} P_w\left(\frac{U_{j-1} + U_j}{2}\right) \quad \text{Eq. 37}$$

The IEC standards specify a similar, but simplified formula that uses a Rayleigh distribution instead of a Weibull distribution [13].

6.2 Method for Estimating Capacity Factor Uncertainty

While the uncertainties δc , δk , δP , and δELF are known, the non-linear dependence of CF on k and c makes the calculation of the total uncertainty of CF , δCF , fairly complicated. The general equation for the uncertainty of CF is given in Eq. 38.

$$\delta CF = \sqrt{\left[\left(\frac{\partial CF}{\partial c} \frac{c}{CF} \right) \delta c \right]^2 + \left[\left(\frac{\partial CF}{\partial k} \frac{k}{CF} \right) \delta k \right]^2 + \delta P^2 + \delta ELF^2} \quad \text{Eq. 38}$$

This is derived from the general uncertainty formula for fractional uncertainties, shown in Eq. 11. δc , δk , δP , and δELF are the fractional standard uncertainties, and some example values are given in Sections 3.7, 4.4, and 5.6.

The terms multiplying δc and δk in Eq. 38 are the sensitivity factors for c and k . Like the uncertainties, the sensitivity factors are non-dimensional. The sensitivity factors for c and k are labeled $SF_{CF,c}$ and $SF_{CF,k}$, respectively. The sensitivity factors for δP and δELF are 1, as expected. In general, the sensitivity factors may be positive or negative to indicate if a change in the individual variable causes an increase or a decrease in CF . The sign is not particularly important however, since the terms are then squared.

To calculate the sensitivity factors for c and k , one needs to start with Eq. 36. Using the Leibniz integration rule [84]:

$$SF_{CF,c} = \frac{\partial CF}{\partial c} \frac{c}{CF} = \frac{1}{CF} \frac{ELF}{P_R} \int_0^\infty P_w(U) \frac{\partial p(U)}{\partial c} c dU \quad \text{Eq. 39}$$

$$SF_{CF,k} = \frac{\partial CF}{\partial k} \frac{k}{CF} = \frac{1}{CF} \frac{ELF}{P_R} \int_0^\infty P_w(U) \frac{\partial p(U)}{\partial k} k dU \quad \text{Eq. 40}$$

After the derivatives are taken and some algebraic manipulation is carried out, the sensitivity factors can be written in the form:

$$SF_{CF,c} = \frac{1}{CF} \frac{ELF}{P_R} \int_0^\infty P_W(U) k \left(\left(\frac{U}{c} \right)^k - 1 \right) p(U) dU \quad \text{Eq. 41}$$

$$SF_{CF,k} = \frac{1}{CF} \frac{ELF}{P_R} \int_0^\infty P_W(U) \left(1 + k \ln \left(\frac{U}{c} \right) \left(1 - \left(\frac{U}{c} \right)^k \right) \right) p(U) dU \quad \text{Eq. 42}$$

These two equations are similar to the last expression in Eq. 36. Again, a numerical integration scheme can be used to determine the values of the sensitivity factors. Also, a similar summation approximation can be made for Eq. 41 and Eq. 42. This approximation yields:

$$SF_{CF,c} = \frac{k * ELF}{CF * P_R} \sum_{j=1}^{N_B} \left\{ \exp \left[- \left(\frac{U_{j-1}}{c} \right)^k \right] - \exp \left[- \left(\frac{U_j}{c} \right)^k \right] \right\} * P_W \left(\frac{U_{j-1} + U_j}{2} \right) \left(\left(\frac{U_{j-1} + U_j}{2c} \right)^k - 1 \right) \quad \text{Eq. 43}$$

$$SF_{CF,k} = \frac{ELF}{CF * P_R} \sum_{j=1}^{N_B} \left\{ \exp \left[- \left(\frac{U_{j-1}}{c} \right)^k \right] - \exp \left[- \left(\frac{U_j}{c} \right)^k \right] \right\} * P_W \left(\frac{U_{j-1} + U_j}{2} \right) \left(1 + k \ln \left(\frac{U_{j-1} + U_j}{2c} \right) \left(1 - \left(\frac{U_{j-1} + U_j}{2c} \right)^k \right) \right) \quad \text{Eq. 44}$$

Thus, the sensitivity factors for c and k can be calculated using Eq. 43 and Eq. 44. This calculation is very similar to the calculation of CF using Eq. 37. Once again, a more complicated numerical integration scheme, like the Simpson's method used by RERL, could be used to solve Eq. 41 and Eq. 42.

Finally, the total uncertainty of CF can be calculated using the general equation given in Eq. 38. Again, δCF , δc , δk , δP , and δELF are all fractional uncertainties.

$$\delta CF = \sqrt{(SF_{CF,c} * \delta c)^2 + (SF_{CF,k} * \delta k)^2 + \delta P^2 + \delta ELF^2} \quad \text{Eq. 45}$$

In sum, CF is the estimated value for the capacity factor. It is calculated using the long-term hub height estimates of c and k , the chosen power curve, and the energy losses. The uncertainty of this estimate is δCF , which is the fractional standard uncertainty of CF .

The utility of this new method for estimating the uncertainty of the energy production in the site assessment process rests in the ability to explicitly calculate sensitivity factors using Eq. 41 and Eq. 42, rather than assuming values. The method recommended in IEC 61400-12, while equally valid, utilizes a bin method, which may be more cumbersome and less elegant than the method presented here [13]. Furthermore, the values of the sensitivity factors give insight into the contribution of the component uncertainty sources to the overall uncertainty.

6.3 Summary of Method for Estimating CF and δCF

The estimation of the capacity factor and its uncertainty is a multi-step process, and it is fairly complicated. The steps below are meant to summarize the process of estimating these quantities, and guide the reader to the relevant Sections of this Chapter. Section 6.4 provides an example calculation to help clarify the process outlined here.

1. Estimate c_{LT_HUB} and k_{LT_HUB} . The process to estimate these values is outlined in Section 3.6. This process combines the measured wind resource with an MCP algorithm, a shear extrapolation, and a topographic correction to produce the final long-term, hub height estimates of the Weibull parameters at the site for each wind turbine.
2. Estimate δc and δk . Fourteen different uncertainty sources contribute to the overall uncertainty of the estimate of the long-term Weibull parameters at the hub

location of the turbine. These uncertainty sources are the subject of Section 3.0. Sections 3.1-3.4 provide descriptions of each uncertainty source, as well as estimated values or ranges of estimated values. They are then summarized in Section 3.5. The individual uncertainty sources can then be combined using the process outlined in Section 3.6, which yields the desired parameters: δc and δk . An example calculation is provided in Section 3.7.

3. Choose a wind turbine power curve. If available, use a site-specific power curve provided by the manufacturer. If this is not available, scale the power curve for the average density at the site using Eq. 30
4. Estimate δP . Three uncertainty sources, identified in Section 4.0, contribute to the overall uncertainty in the power curve and power production. Section 4.1 describes each of these uncertainty sources, and a summary is provided in Section 4.3. These uncertainty sources are easily combined using the RSS method to yield an estimate of δP .
5. Estimate the value of the three energy loss factors. Approximate values for the energy loss factors or guidelines for choosing the values are given in Section 5.0. The three energy loss factors can then be combined into an overall energy loss factor, ELF , using Eq. 32.
6. Estimate the energy loss factor uncertainty, δELF . This can be calculated using the recommended values for the individual energy loss factor uncertainties, and Eq. 33.
7. Estimate the capacity factor, CF , for the wind farm. This is calculated using Eq. 36, and it depends on c_{LT_HUB} , k_{LT_HUB} , the chosen power curve, and ELF .

8. Estimate $SF_{CF,c}$ and $SF_{CF,k}$. The sensitivity factors for c and k can be calculated using Eq. 41 and Eq. 42.
9. Estimate δCF . Using the results of Steps 1-8, δCF can be estimated using Eq. 45.

6.4 Example calculation of CF and δCF

An example calculation helps to clarify the process, as it can be quite complicated. Example values of δc , δk , δP , ELF , and δELF are calculated in Sections 3.7, 4.4, and 5.6. Thus, Steps 2, 4, 5, and 6 from Section 6.3 above have already been performed. This calculation is for a single wind turbine. These values are again shown in the table below.

δc	δk	δP	δELF	ELF
9.3%	9.1%	10.5%	3.9%	78.7%

The remaining steps from Section 6.3 needed to calculate CF and δCF are given below.

1. For this example, it is assumed that $c_{LT_HUB} = 9$ m/s, and $k_{LT_HUB} = 2.5$.
3. A GE 1.5 MW wind turbine power curve is used for this example. This power curve is shown below in Figure 19. It is assumed that the power curve does not need to be adjusted for the specific site.

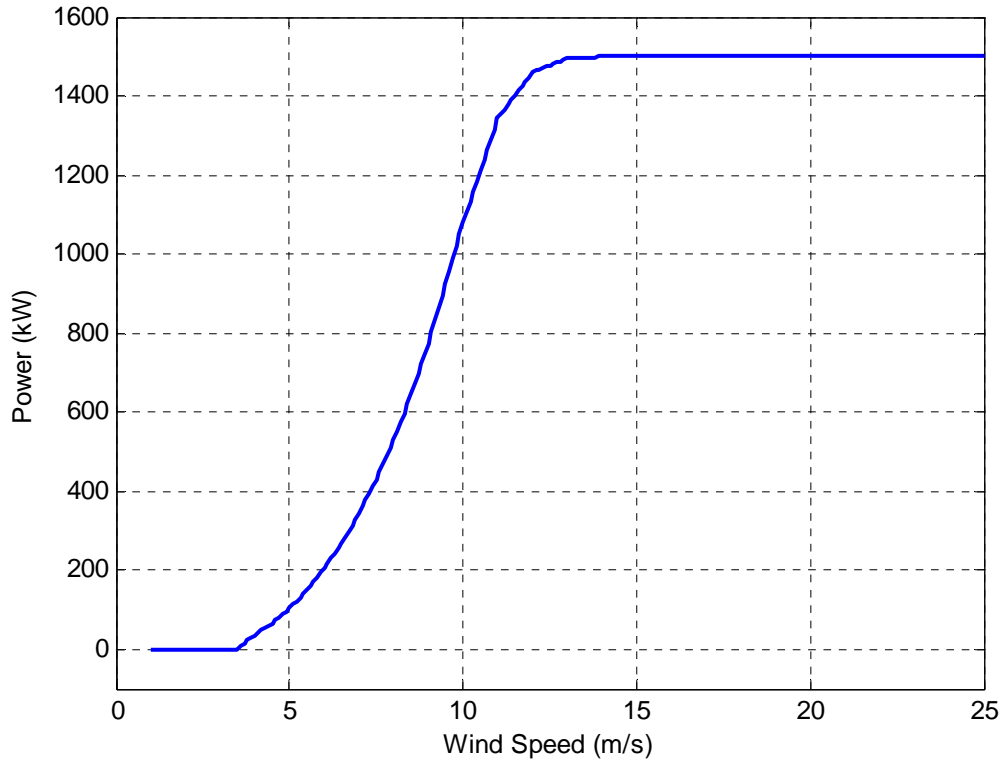


Figure 19 – GE 1.5 MW Power Curve

7. The capacity factor is calculated using Eq. 36. An RERL program that uses Simpson's Rule for the numerical integration is used. The result is a value of $CF=33.2\%$. A simplified version of Eq. 36 is given in Eq. 37, and this can also be used to calculate CF .
8. The sensitivity factors are calculated using Eq. 41 and Eq. 42. This calculation depends on the value of CF , as well as the power curve, ELF , c_{LT_HUB} , and k_{LT_HUB} . The result is values of $SF_{CF,c} = 1.85$ and $SF_{CF,k} = 0.07$. Once again, an RERL program that uses a numerical integration scheme is used. A simplified calculation can be made using Eq. 43 and Eq. 44.
9. The values of the uncertainty and sensitivity factor for each of the parameters that contribute to δCF are shown in the table below.

Parameter	c	k	P_w	ELF
Uncertainty (%)	9.3%	9.1%	10.5%	3.9%
Sensitivity Factor	1.85	0.07	1.0	1.0

The overall capacity factor uncertainty, δCF , is calculated using Eq. 45, and is shown below.

$$\begin{aligned}
\delta CF &= \sqrt{(SF_{CF,c} * \delta c)^2 + (SF_{CF,k} * \delta k)^2 + \delta P^2 + \delta ELF^2} \\
&= \sqrt{(1.85 * .093)^2 + (0.07 * .091)^2 + 0.105^2 + 0.039^2} \\
&= 20.6\%
\end{aligned}$$

6.5 Discussion of the Example Calculation

Several important observations arise from this example calculation.

6.5.1 The Calculation of CF

The value of CF is 0.331 (i.e., 33.1%). This value is a reasonable value of the capacity factor at a site with a good wind resource. In general, capacity factors greater than 30% are promising sites. The value of CF is dependent on the value of both c and k . This dependency is illustrated in Figure 20, which shows the value of the capacity factor for ranges of values of c and k , using the same power curve and ELF value as the example.

Two major trends can be seen. First, the capacity factor increases as c increases. This comes as no surprise, as the value of c is directly proportional to the mean wind speed, which is by far the most important parameter in assessing a site and estimating energy production. Second, CF tends to increase as k increases, except when c is very small. As k increases, the Weibull distribution becomes less spread out and therefore

more concentrated about its expected value. At very low values of c , this means that the distribution is concentrated about very low values of the wind speed, and so the turbine is producing very little power, even when it is above the cut-in wind speed. But, for moderate to high values of c , a high k value results in the wind speed being above the cut-in value for a very high percentage of the time, and therefore a high capacity factor.

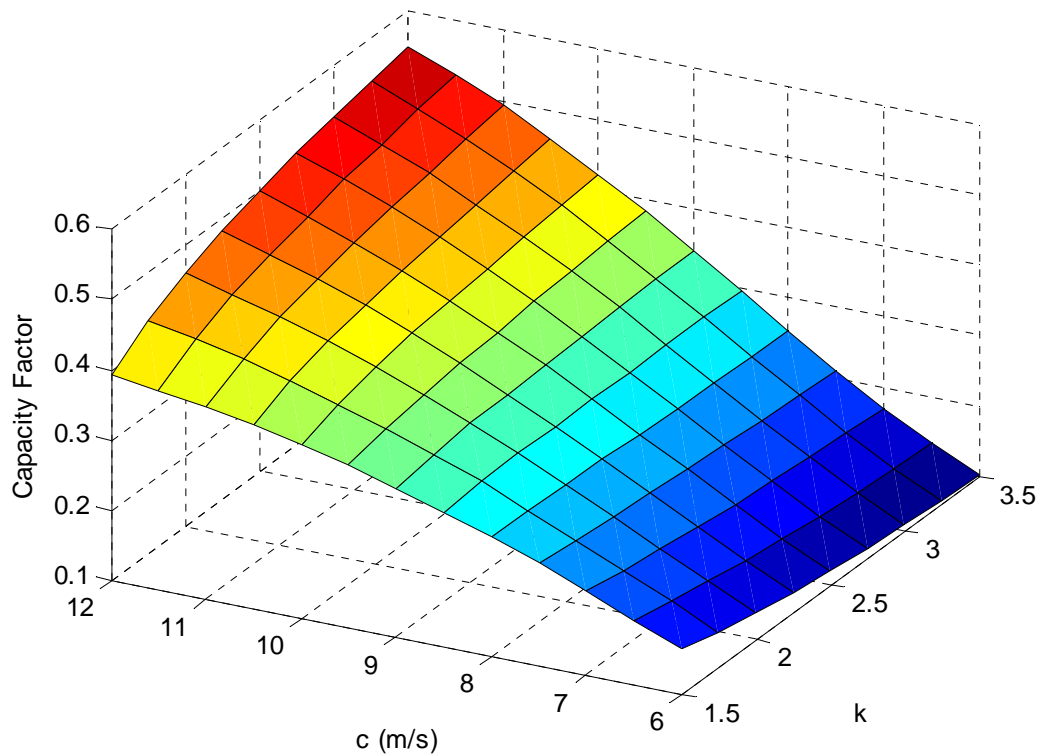


Figure 20 – Capacity Factor for Various Values of c and k

6.5.2 The Calculation of δCF

The uncertainty in CF , δCF , is 20.6%. Once again, this is the fractional standard uncertainty. To obtain the absolute standard uncertainty, δCF is multiplied by CF . The result is an absolute standard uncertainty of 0.07. Thus, the estimate of CF is: $CF = 0.331 \pm 0.07$.

The magnitude of δCF depends predominantly on the value of δc . In fact, if δk , δP , and ELF are all 0%, the uncertainty in CF is 17.2%. This is due to the large magnitude of $SF_{CF,c}$. Thus, reducing the uncertainty in c provides the best opportunity for reducing the overall capacity factor uncertainty.

6.5.3 The Sensitivity Factor $SF_{CF,c}$

The sensitivity factor for c is 1.85. This is lower than is generally assumed. It is sometimes assumed that a percentage increase in c (or the mean wind speed) causes between 2 and 3 times the percentage increase in CF , i.e., a sensitivity factor between 2 and 3 [57]. However, this is a gross oversimplification, and the results indicate that this assumption could lead to large errors. For example, if one assumes that $SF_{CF,c} = 2.3$ (a common value), then δCF would be 24.2% instead of 20.6%. This could mean the difference between an acceptable and unacceptable risk level for a potential wind energy venture.

In actuality, the sensitivity factor for c is highly dependent on the value of c . $SF_{CF,c}$ decreases as c increases. Furthermore, $SF_{CF,c}$ is dependent on the value of k . $SF_{CF,c}$ increases as k increases. The dependence of $SF_{CF,c}$ on c and k (for this example) is shown below in Figure 21. The plot indicates $SF_{CF,c}$ approximately decreases proportionally to the square of c .

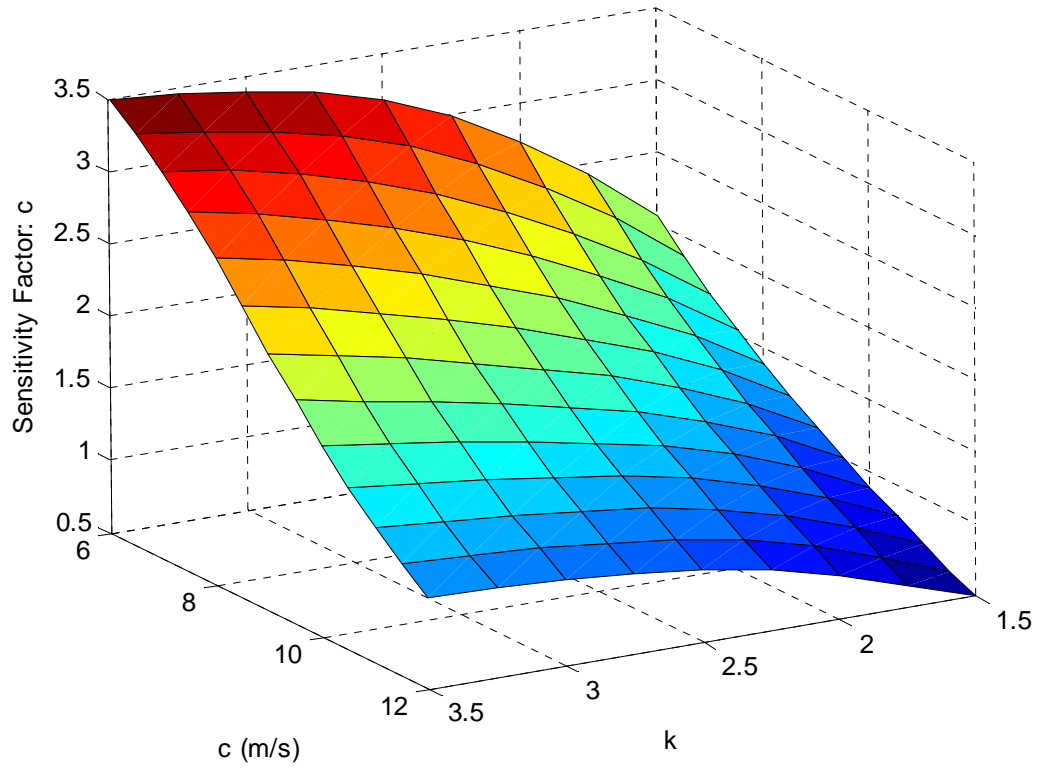


Figure 21 – Sensitivity Factor for c

Figure 22 is useful in understanding the behavior of the sensitivity factors. It shows five different Weibull distributions, for various values of c and k , including the values used in this example. It also shows the power curve used in this example. In the case of $SF_{CF,c}$, Figure 22 shows that as c increases, the wind speed is above the rated wind speed more and more frequently. Therefore any error in the estimation of c affects the value of CF less, since the turbine produces constant power above rated wind speed, regardless of the actual wind speed.

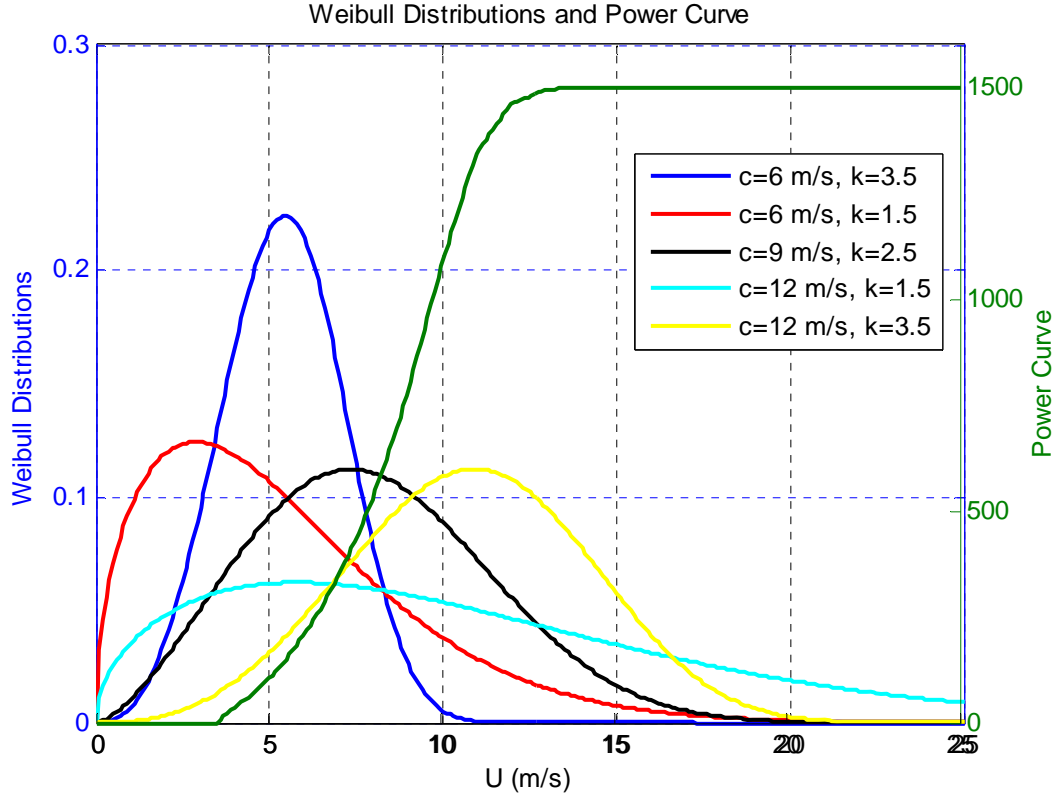


Figure 22 – Various Weibull Distributions and Power Curve

$SF_{CF,c}$ also increases as k increases as shown in Figure 21. As k increases, the Weibull distribution becomes less spread out, resulting in the wind speed being close to the mean value more frequently. The effect of the value of k on the Weibull distribution is shown again in Figure 22. The result is that for a given value of c (for example compare the two plots for $c=6$ m/s in Figure 22), a higher value of k results in the wind speed being less than the rated wind speed more often, and therefore the capacity factor is more dependent on the value of c , and so $SF_{CF,c}$ is larger (as stated above, the more often the wind speed is above the rated value, the less the value of $SF_{CF,c}$).

The common assumption that $SF_{CF,c}$ is between 2 and 3 is only valid for values of c between approximately 6 m/s and 8 m/s. Thus, in practice, a value of the sensitivity factor should never be assumed. Instead, a calculation similar to this example calculation

should be carried out, using the appropriate power curve, wind resource, and energy losses.

6.5.4 The Sensitivity Factor $SF_{CF,k}$

In this example, $SF_{CF,k}$ is fairly small relative to the other sensitivity factors, indicating that CF has a weak dependence on k . For example, a 10% increase in k would only change CF by 0.7%. This is not a surprising result, as generally the shape of the wind speed distribution is considered to be much less important for CF estimates than the mean wind speed value (or c). However, $SF_{CF,k}$ is also highly dependent on the value of both c and k . Figure 23 shows this dependence for this example. Several important observations can be made.

First, for moderate values of c near 8-9 m/s, $SF_{CF,k}$ is very close to zero. At these conditions, the wind speed tends to be above the cut-in wind speed, and below rated conditions most of the time, regardless of the value of k , and therefore regardless of how spread out the wind speed distribution is. Thus, CF is nearly independent of the value of k for these values of c .

Second, for small values of c , $SF_{CF,k}$ is negative, and so increasing k when c is small causes CF to decrease. This effect can be explained using Figure 22, which shows two Weibull functions with values of $c=6$ m/s (the red and the blue plots). For these two plots, when k is small ($k=1.5$) the wind speed distribution is very spread out, and so the wind blows at higher wind speeds (greater than 8 m/s) much more frequently than when $k=3.5$ and the distribution has much less spread. Third, for large values of c , $SF_{CF,k}$ is positive. Thus, increasing k when c is large causes CF to increase. In this situation, when c is large, a higher value of k , and so less spread in the distribution, results in the

wind speed being greater than the cut-in wind speed, and less than the cut-out wind speed, nearly all the time. On the other hand, a small value of k results in frequent wind speeds below cut-in or greater than cut-out.

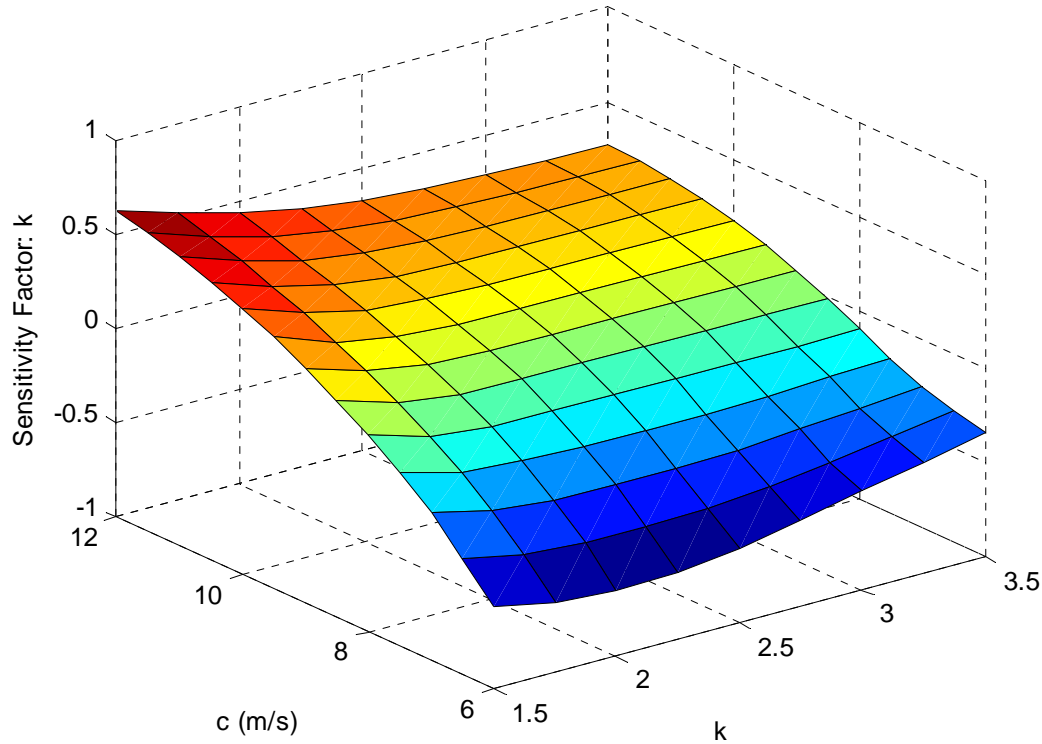


Figure 23 – Sensitivity Factor for k

6.5.5 The Weibull Shape Factor, k

The value of k is often assumed to be approximately 2, although it can vary widely, with values that may be as low as 1.5 or as high as 3.5 at some sites. For low values of k , the sensitivity factor is much larger than it would be for high values of k . Furthermore, the sensitivity factor changes more rapidly for low values of k . This result has important practical implications. For this example, if one assumes that k is equal to 2, but in fact it is equal to 1.5, the capacity factor would be calculated as 0.325 or 0.311, respectively. This may seem like a small difference, but it corresponds to a 4% change in AEP , which

can make the difference between a successful venture and a failure. Thus, assuming a value of k has dangerous consequences, as it could lead to a significantly incorrect estimation of CF (or AEP). This point further reinforces the utility of using the two parameter Weibull distribution to approximate the wind speed distribution rather than the one parameter Rayleigh distribution (the Rayleigh distribution is equivalent to the Weibull with a value of $k=2$). By estimating a value of k , and therefore taking the shape of the wind speed probability distribution into account in AEP estimation, one can avoid the significant errors that may arise when k is assumed to be a certain value.

7.0 Conclusions

Wind energy site assessment is a complex multi-step process, with a high degree of uncertainty. This Chapter seeks to present a comprehensive means for understanding and estimating uncertainties in this process. Important conclusions and results include:

- Fourteen sources of uncertainty are identified that arise during the wind resource assessment process. Estimates of the bias due to the sources or error are also made. A method for estimating the long-term wind resource is presented. Also, a means of combining the uncertainties and biases is shown, which takes into account the magnification of the measurement uncertainty.
- Significant uncertainty arises when assessing the wind resource at a site. In an example calculation with reasonable values, the uncertainty of $U_{LT_HUB}^-$ and c_{LT_HUB} is 9.3%, and the long-term Weibull shape parameter, k_{LT_HUB} , has an uncertainty of 9.1%.

- Wind measurement devices capable of measuring at hub height offer an opportunity to significantly reduce wind resource assessment uncertainty. These devices, discussed in Chapter II, Section 2.0, eliminate errors due to shear model uncertainty, and tower/boom effects. They also reduce the measurement uncertainty sensitivity factor to 1. In fact, a LIDAR or SODAR with 5% measurement uncertainty would still reduce the uncertainty in $U_{LT_HUB}^-$ and c_{LT_HUB} to 7.6%, and the overall uncertainty in the capacity factor, δCF , to 18%. Reliable LIDAR or SODAR measurements should be used for site assessment whenever possible.
- The power production from a wind turbine is also uncertain for a variety of reasons. The estimate of the total power production uncertainty is 10.5% in the example calculation.
- Three energy loss factors are identified which directly reduce the energy production of a turbine or wind farm. In the example calculation, these terms cause a total reduction in the energy production of 21.3%. The uncertainty of these terms in the example calculation is 3.9%.
- A means of combining the estimated long-term wind resource, the power curve, and the energy losses in order to estimate the capacity factor is presented. By using the 2-parameter Weibull distribution to represent the long-term wind resource, the shape of the wind speed distribution can be taken into account in the calculations of CF . This yields a more accurate estimate of CF , as the value of the Weibull shape parameter k can noticeably affect the value of CF . In the example calculation, the calculated capacity factor is 33.1%.

- A means of combining wind resource uncertainty, power production uncertainty, and energy loss uncertainty into an estimate of the capacity factor (or *AEP*) uncertainty is presented. This method relies on a Weibull wind speed distribution, and employs sensitivity factors. Equations to calculate the sensitivity factors are given, as well as a final equation that yields the *CF* uncertainty. This method provides an analytical means for calculating the sensitivity factors, as opposed to assuming their value, which can lead to significant errors. An example calculation yields an estimate of the *CF* uncertainty at 20.6%. The new methods for uncertainty analysis presented in this Chapter are in contrast to those recommended in IEC 61400-12, which recommend a bin method [13]. Neither approach is inherently more correct than the other; they are instead different approaches to the same problem. In general, it is unlikely that they produce significantly different results. The methods presented in this Chapter are potentially more easily implemented, as a single equation is needed to calculate each sensitivity factor, which can be less cumbersome than dealing with many bins.

CHAPTER IV

OBJECTIVE DECISION MAKING IN SITE ASSESSMENT

1.0 Introduction

Traditionally, wind energy site assessment is performed using meteorological towers (met towers) equipped with cup anemometers and wind vanes. This process is described in detail in Chapter I, Section 1.1. In order to estimate the long-term wind resource at a site, the measured wind data are often incorporated into a process called “Measure-Correlate-Predict” (MCP). MCP is also described in detail in Chapter I, Section 1.1 and Chapter II, Section 5.0. A full year of data is often measured on-site to reduce the uncertainty in the estimate of the long-term wind resource [52].

At many sites, however, where the wind resource is either very good or very bad, a decision to cease measurement and either build or not build a wind farm may be possible well before a full year of measurement has taken place, despite the larger uncertainty due to the shorter measurement period. The MCP process can be executed with any length of measured data, not just one year, and so an estimate of the long-term wind resource, and therefore an evaluation of the site, can be made after any length of measurement

This Chapter describes the development of an approach for making objective decisions for wind resource monitoring. The basic question that is addressed by this research is: When and how can one decide to stop measuring the wind resource at a site and either build or not build a wind farm? The goal of this approach is to accelerate the site assessment process, saving time and money in the process.

2.0 Motivation

This research develops an objective decision making framework that can be used to reduce the necessary measurement period in the site assessment process. There are several reasons why this is desirable.

First, monitoring the wind resource on-site is an expensive process. The installation of a met tower requires a crew of several people at least a full day to both raise and lower the met tower. Most met towers are approximately 40 m to 60 m tall, and towers of this height (including labor and sensors) cost approximately \$20,000 [3],[20]. Taller towers, with heights of 80 m and greater, are significantly more expensive than traditional met towers (at least \$100,000). Moreover, it is sometimes necessary to install multiple towers at a large site. Furthermore, the cost of data collection, processing, and reporting can also be quite expensive. Overall, a standard wind resource monitoring campaign at a site using a single met tower costs approximately \$30,000.

Second, along with the potentially lengthy permitting and construction phase of a wind energy project, the measurement of the wind resource adds more time to the overall process of wind energy development. The uncertain nature of federal and state subsidies in the United States, along with unpredictable turbine availability, encourages rapid development of wind energy projects, which is potentially in direct conflict with a lengthy wind resource measurement time.

Lastly, wind energy consulting firms or state-wide wind energy assessment programs often have multiple candidate sites for site assessment but limited equipment, and so there is a strong motivation for quick measurement campaigns. Essentially, there is an

opportunity cost to measuring at a given site, as the resources committed to that site could potentially be better served at another location.

Overall, there are compelling reasons to accelerate the wind resource measurement process, even if there is an associated increase in uncertainty. Furthermore, ground-based devices, such as SODAR and LIDAR, are especially well suited to rapid site assessment campaigns. These devices are described in detail in Chapter II, Section 2.0. One notable feature of these devices is that they are portable and easy to install, especially when compared to met towers. Their portability makes the process of stopping measurement at one location and commencing at another significantly easier than if met towers are being employed.

While the methods developed in this Chapter do not presuppose the use of a ground-based device, their portability makes them the logical choice in practice. Portable met towers (also called “jack-up” towers) that are quickly installed could also be used for this application. Nonetheless, this approach can be applied when standard met towers are used for the wind resource measurement. However, the high fixed cost of using a met tower for wind resource measurement makes this approach less compelling than when ground-based devices are used.

3.0 Objective Decision Making Framework

This Section describes the decision framework used for this analysis. This description provides an overview of the process, and the details of the actual data analysis are provided in the next Section. The framework assumes that while the wind resource is monitored at a site, at any point in the process one is faced with a decision consisting of three choices:

1. Stop on-site measuring and build a wind farm.
2. Stop on-site measuring and do not build a wind farm.
3. Continue on-site measuring and decide at a later point.

This is the basic set of options available, which clearly depend on the estimate of the wind resource and the relevant economic parameters for the particular site. The actual decision made is based on maximizing some utility function. Economic profit is one such option for evaluating the options, and a version of it, net present value (NPV), is used in this analysis. The basic decision framework can be summarized in the following steps:

1. Measure the wind resource on-site for a limited number of continuous days, N_{Days} (i.e., significantly less than 365 days).
2. Use this limited on-site measured data set in an MCP algorithm, in conjunction with long-term data from a nearby reference met tower. This yields an estimate of the long-term mean wind speed and also the uncertainty in this estimate at the site. The estimate of the long-term mean wind speed at the site is used to characterize the wind resource throughout this Chapter, and is labeled U_{LT} . As stated above, MCP can be executed with any length of measured on-site data, including lengths less than one year. While the full seasonal variation in the wind resource is not captured in the measured data in these cases, the reference site data set does contain data for the entire season, as well as several more years of data. Thus, MCP is utilized to account for variations in the wind resource at time scales longer than the measured data length.

3. Evaluate the three choices.

- a. For the first choice, stop measuring on-site and build the wind farm: the annual energy production and its uncertainty are first estimated from U_{LT} , and then the economic success of the project is evaluated. Because the energy production is an uncertain quantity, it is actually the expected value of the economic success that is calculated.
- b. For the second choice, stop measuring on-site and do not build the wind farm: the cost of the wind resource monitoring is the only factor contributing to the economic evaluation.
- c. For the third choice, continue to measure: all future possible choices are considered, and so in essence this process repeats itself and begins again at Step 1.

The process is therefore recursive, as the “continue to measure” choice considers future repetitions of the process. The process terminates at the end of one year of measurement.

3.1 Example Decision Tree

An example helps to clarify this process. The example assumes that the wind resource can be continuously measured over the course of one year, and reported twice: after 180 days, and then at the end of one year. A visualization of this sample decision tree is shown below in Figure 24.

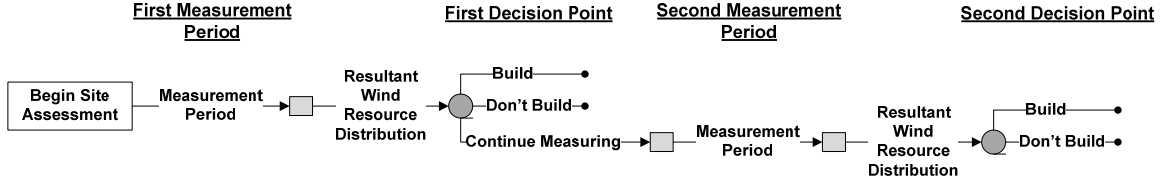


Figure 24 – Sample Decision Tree

When 180 days of measurement have passed, the first on-site measurement period is complete, and the data are reported. An estimate is made of the long-term mean wind speed using the measured data and MCP, which is labeled U_{LT_1} . U_{LT_1} is an uncertain quantity, and in this Chapter it is assumed to be normally distributed [85]. Thus, U_{LT_1} is a random variable, characterized by a mean, $\mu(U_{LT_1})$, and standard deviation, $\sigma(U_{LT_1})$, and the probability density function (pdf) is $p(U_{LT_1})$. Next, the long-term annual capacity factor is estimated, as well as the uncertainty of the long-term annual capacity factor. The estimated long-term annual capacity factor is simply the estimated long-term annual energy production, appropriately normalized by the number of hours in a year and the wind turbine rated power. Like U_{LT_1} , the long-term annual capacity factor, CF_{LT_1} , is assumed to be normally distributed, with probability density function $p(CF_{LT_1})$.

At this stage, the first decision point is reached, and a decision can be made. The expected value of the first two choices, building or not building the wind farm after the first measurement period of 180 days, can then be calculated directly, as functions of CF_{LT_1} and the relevant economic parameters. The formula for calculating the expected value of building the wind farm, $E[NPV(Build)]_1$ is shown in Eq. 46.

$$E[NPV(Build)]_1 = \int_0^1 p(CF_{LT_1}) \cdot NPV(CF_{LT_1}) \cdot dCF_{LT_1} \quad \text{Eq. 46}$$

The subscript “1” indicates that this calculation takes place for one measurement period. The details of this calculation, such as the functional dependence of NPV on

CF_{LT_1} , are described later. The expected value of not building, $E[NPV(Not_Build)]_1$ is simply equal to the net present value of the total cost of measurement up to the end of the first measurement period. A specific value for this cost is given later.

To calculate the third choice, continue measuring, all future outcomes must be considered and evaluated as well. There is not the luxury of actually measuring; instead, the probability of each possible outcome is calculated as well as the expected value of each outcome, and these are combined to yield the expected value of measuring. Thus, a second hypothetical measurement period is considered (but not yet measured), which, including the first measurement period, would result in a full year of measured data. The full year of measured data could then be used, along with MCP, to estimate the long-term mean wind speed. The second estimate of the long-term mean wind speed would be a normally distributed random variable, U_{LT_2} , characterized by a mean, $\mu(U_{LT_2})$, and standard deviation, $\sigma(U_{LT_2})$. The probability of a given mean of the pdf of U_2 , $\mu(U_{LT_2})$, depends on the pdf of U_{LT_1} , $p(U_{LT_1})$. That is, given $p(U_{LT_1})$, the probability of any value of $\mu(U_{LT_2})$ can be calculated. This probability is labeled $P(\mu(U_{LT_2}) | p(U_{LT_1}))$. In practice, the probability of $\mu(U_{LT_2})$ occurring in some finite bin is calculated. The specifics of this binning are discussed later.

The uncertainty of U_{LT_2} , $\sigma(U_{LT_2})$, must also be considered, as it is needed to define the pdf of U_{LT_2} . A model for the behavior of future uncertainties can be used to estimate $\sigma(U_{LT_2})$. A description of the model used in this Chapter is given later. Thus, each possible value of the mean of the pdf of U_{LT_2} , $\mu(U_{LT_2})$, can be considered and the uncertainty modeled, with the resulting pdf being $p(U_{LT_2})$. The probability of a certain $p(U_{LT_2})$ occurring is $P(\mu(U_{LT_2}) | p(U_{LT_1}))$.

Then, for any given $p(U_{LT_2})$, the pdf of the capacity factor can be calculated, which is $p(CF_{LT_2})$. The second decision point has now been reached, and since this is the terminal decision, only the first two choices are possible: either build or do not build the wind farm. Thus, the expected values of building and not building are calculated. The expected value of building after the second measurement period, $E[NPV(Build)]_2$, is calculated using Eq. 47.

$$E[NPV(Build)]_2 = \int_0^1 p(CF_{LT_2}) \cdot NPV(CF_{LT_2}) \cdot dCF_{LT_2} \quad \text{Eq. 47}$$

Once again, the expected value of not building after the second measurement period, $E[NPV(Not_Build)]_2$, is simply equal to the net present value of the total cost of measurement up to the end of the second measurement period. For any given $\mu(U_{LT_2})$, and so any given $p(U_{LT_2})$ and $p(CF_{LT_2})$, the decision to build or not build the wind farm depends on which choice has the higher $E[NPV]$. This decision is based on the maximum $E[NPV]$ for a given $\mu(U_{LT_2})$, and so it is labeled $\text{Max}\{E[NPV] \mid \mu(U_{LT_2})\}_2$.

The purpose of considering these future choices is to determine the expected net present value of continuing to measure after the first measurement period is complete, $E[NPV(Measure) \mid p(U_{LT_1})]_1$. Thus, all the future choices can then be integrated using the probability of each possible outcome, $P(\mu(U_{LT_2}) \mid p(U_{LT_1}))$, and the expected value of each outcome, $\text{Max}\{E[NPV] \mid \mu(U_{LT_2})\}$, which allows for $E[NPV(Measure) \mid p(U_{LT_1})]_1$ to be calculated after the first measurement period, as shown in Eq. 48. It is important to note that this value is dependent on $p(U_{LT_1})$.

$$E[NPV(Measure) | p(U_{LT_1})] = \int P(\mu(U_{LT_2}) | p(U_{LT_1})) \cdot \text{Max}\{E[NPV] | \mu(U_{LT_2})\} \cdot d\mu(U_{LT_2}) \quad \text{Eq. 48}$$

In this way, the expected value of the continue to measure, build, and not build choices after the first measurement period are calculated, and the choice with the maximum expected value can be chosen as the optimal strategy.

If the choice with the largest expected value after the first measurement period is the continue measuring option in Figure 24, then the wind resource is measured for the rest of the year, and the entire year of measured wind data is used along with MCP to estimate the long-term mean wind speed. New values of $\mu(U_{LT_2})$ and $\sigma(U_{LT_2})$ are therefore estimated, yielding a new pdf for U_{LT_2} , and also a new pdf for CF_{LT_2} . The second decision point has then been reached, which is a terminal decision, and so only the options to build or not build are considered. Eq. 47 is once again used to determine $E[NPV(Build)]_2$, and once again, the expected value of not building after the second measurement period, $E[NPV(Not_Build)]_2$, is simply equal to the net present value of the total cost of measurement up to the end of the second measurement period. The option with the larger expected value is then chosen.

This basic decision-tree framework is used later in the actual data analysis, and can be expanded to include more measurement periods.

4.0 Data Analysis

This Section describes the details of the data analysis that is used to evaluate the decision making framework with actual wind speed data.

4.1 Data Sets Used

Fifteen pairs of long-term data sets are used in this investigation. Table 1 summarizes each of the data set pairs. Each data set pair consists of two sites, located near each other, each with long-term periods of concurrent wind speed and direction data. The concurrent data length for the sets ranges from three years to seventeen years. These data sets come from locations all over the United States, including coastal and offshore sites.

For each pair of sites, the site that is listed first in the table is used as the reference site. The “Distance” column gives the distance between sites in kilometers. In many cases, the distance is much larger than is desirable for the MCP process in practice. However, for the purpose of investigating the statistics of the predictions, the large distances between sites are not important.

These data sets are comprised of either 10-minute or hourly wind speed data. For many of the sites, two anemometers are positioned at each of the measurement heights. In these cases, for each 10-minute or hourly average, the higher of the two measured wind speeds from the anemometers is selected as the wind speed at that height, to combat the effects of tower shadow [68]. The data are also subjected to quality control tests to attempt to remove any data corrupted by icing or other issues [69]. Overall, there is reasonable confidence in the quality of the data. Nonetheless, tower shadow effects and other obstructions are difficult to identify in many cases, and so there is still some potential for the data to be corrupted [86].

Data Set	Name	State/Region	Distance	Years of Good Data
1	Buoy 44013	NE	365 km	6
	Buoy 44011	NE		
2	Buoy 46005	NE	390 km	3
	Buoy 46002	NE		
3	Cornucopia	WI	180 km	3
	Rib Lake	WI		
4	Currie	MN	253 km	8
	Breckenridge	MN		
5	Currie	MN	90 km	5
	Montevideo	MN		
6	Hatfield	MN	35 km	7
	St. Killian	MN		
7	Buoy 44007	NE	87 km	17
	Buoy 44005	NE		
8	Buoy 44008	NE	231 km	14
	Buoy 44013	NE		
9	Buoy BUZM3	NE	178 km	15
	Buoy IOSN3	NE		
10	Buoy MDRM1	NE	62 km	17
	Buoy MISM1	NE		
11	Cedar	IA	219 km	5
	Red Oak	IA		
12	Estherville	IA	100 km	4
	Forest City	IA		
13	Sibley	IA	66 km	5
	Inwood	IA		
14	Sutherland	IA	186 km	3
	Radcliffe	IA		
15	Buoy 51001	Pacific	497 km	14
	Buoy 51003	Pacific		

Table 1 - Summary of Data Sets

4.2 Measure-Correlate-Predict

The estimation of the long-term mean wind speed from the measured wind speed data is accomplished using measure-correlate-predict. As stated above, MCP can be utilized with any length of measured data, including data lengths less than one year. The reference site data is utilized to account for variations in the wind speed at longer time scales than the length of measured data, such as seasonal and annual variations. This investigation utilizes the “Variance Ratio” method [37]. This method is described in

detail in Chapter II, Section 5.0. Along with using MCP to predict the long-term mean wind speed, the long-term value of the Weibull shape parameter k is also estimated.

The uncertainty in the MCP estimate of the long-term annual mean wind speed is calculated using the jackknife estimate of variance method [52]. This predicted uncertainty is the standard uncertainty (i.e., the standard deviation of the uncertainty), as the prediction is assumed to be normally distributed. This method is an effective means of estimating the uncertainty of MCP predictions, on average. The uncertainty in the Weibull k parameter is not considered as it generally has a negligible effect on the overall uncertainty [85].

The issue of uncertainty is complicated by the objective decision making framework. Future branches of the decision tree are calculated after each measurement, and the calculations in these future branches depend on the uncertainty in the long-term mean wind speed estimate, as described in the decision tree example above. It is not appropriate to assume that the uncertainty in the estimated long-term mean wind speed is constant in all future branches, as the uncertainty in MCP prediction decreases with increased measurement periods [52].

This situation is resolved as follows. Figure 25 shows the average percentage uncertainty when estimating the long-term mean wind speed using MCP for the data sets used by Rogers et al. [52]. These data are labeled “Jackknife Data.” The data are modeled with a power law function, and the least square fit to the data that also passes through the first data point has an exponent of -0.33, and is also shown in Figure 25.

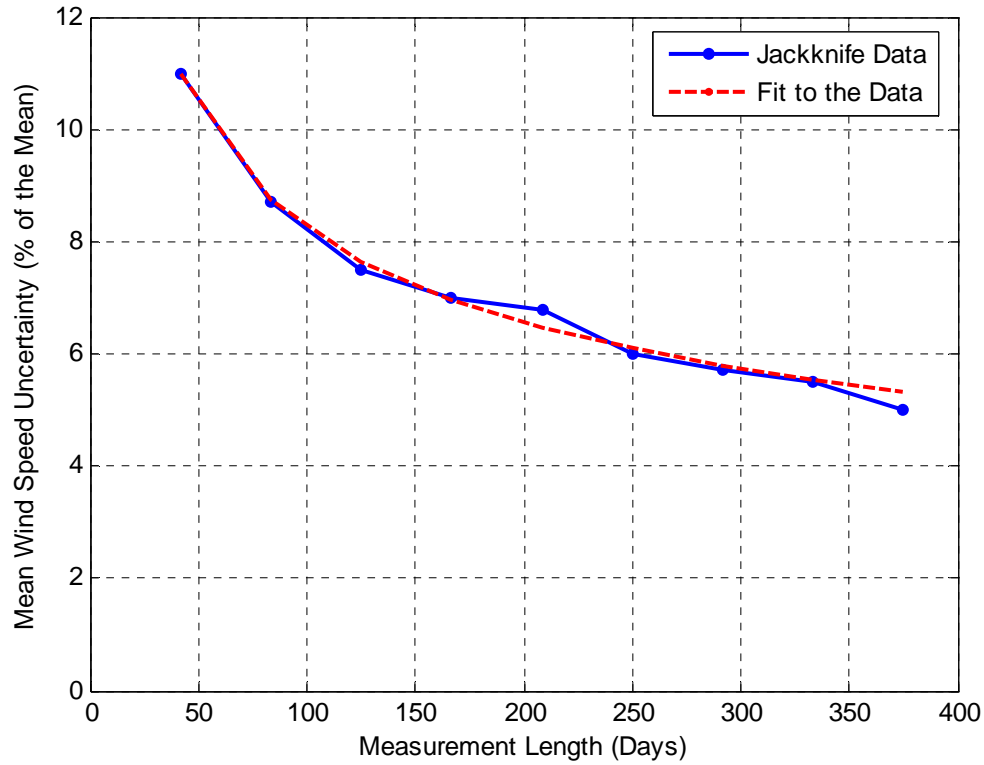


Figure 25 – Mean Wind Speed Uncertainty

This power law function is used to model the decrease in uncertainty in future branches. Obviously, the model is not appropriate for all situations, but it does provide a good representation of the average behavior of the uncertainty in future measurements. In function form, this fit is described using Eq. 49, where δU is the long-term annual mean wind speed uncertainty, N is the number of measured days, and C is a constant.

$$\delta U = C \cdot N^{-0.33} \quad \text{Eq. 49}$$

Thus, the model has only one parameter, namely C . When a single measurement is performed, and so there is only one estimate of the long-term mean wind speed uncertainty using the jackknife method, then C is determined exactly. However, when two or more measurements are made, and so there are two or more estimates of the long-

term mean wind speed uncertainty for different measurement lengths, then C is calculated to give the best least square fit to the data.

4.3 Energy Production Estimate

After the long-term annual mean wind speed is estimated, the annual energy production from a wind farm is calculated. This analysis utilizes the capacity factor as a non-dimensional form of the annual energy production. For this analysis, the power curve from a GE 1.5 MW turbine is used. Also, it is assumed that 10% of the energy production is lost per year due to maintenance, dirt and icing, array losses, and other effects. The capacity factor of the wind farm is then calculated as a function of the estimated long-term mean wind speed and k . A larger long-term mean wind speed corresponds to a larger capacity factor.

The uncertainty of the capacity factor is also calculated, and again it is assumed to be normally distributed. First, an additional 7% uncertainty in the estimated long-term mean wind speed (on top of the MCP jackknife uncertainty) is assumed, due to measurement error, shear and topographic effects, and other factors, based on the research in Chapter III. The sensitivity factor of the energy production to the mean wind speed uncertainty is then determined. Next, an 8% power curve uncertainty and 4% uncertainty in the energy losses are assumed, again based on the research in Chapter III. Finally, all of the respective uncertainties are combined to yield an overall capacity factor uncertainty using the methods developed in Chapter III.

4.4 Economic Evaluation

The economics of not building the wind farm are easily evaluated, as they are simply a function of the monitoring costs and the number of days of measurement. It is assumed that the monitoring cost is \$100 per day of measurement (in accordance with the values given previously). This cost model is most appropriate when a ground-based device is used to measure the wind resource. Ground-based devices have minimal installation costs, and so the marginal cost of monitoring for another day is approximately equal to the average cost per day over the entire measurement period. In contrast, a met tower has a high upfront cost due to the installation required, and so the marginal cost of measuring for another day is quite low relative to the average cost per day. Thus, a cost model with a fixed cost per day of measurement is much more representative of a ground-based device measurement campaign. A different type of cost model can be used when considering a met tower.

After each measurement period, the monitoring costs must be paid, and these payments are discounted back to the day that measurement began to get the net present value (NPV). The discount rate used is 8% per year. Thus, if each measurement period is 10 days, then after 10 days, \$1000 is paid. The NPV of this payment is -\$997.89. If another 10 days are measured after that, another \$1000 is paid at the end of that period (20 days total), and the NPV of that payment is -\$995.79. The total NPV of the monitoring costs is -\$1993.69. Whenever monitoring ceases, the total NPV of the monitoring costs is calculated based on the total measurement length, and the number of measurement periods.

The economic success of building the wind farm is evaluated using a cash flow method. This method combines the revenue, expenses, loan obligations, taxes, and subsidies in each year of operation to yield an after-tax net cash flow, and it is described in greater detail in Chapter VII, Section 1.0. In the first year of the cash flow sheet, the cash flow is negative due to the initial capital costs of constructing the wind farm. In all later years, the cash flow is either positive or negative depending on the relative amount of revenue and subsidies compared to the loan payments and expenses. The cash flow in each year is then discounted back to the day that the wind resource measurement commenced, to yield the net present value of the project. The total NPV of building the wind farm is the sum of the NPV of the discounted cash flows and the NPV of the monitoring costs. In this way, all choices are compared on an equal footing.

4.4.1 Cash Flow Example

A simple example helps to clarify the process. Hypothetically, the wind resource is measured at a site for an entire year, and there are two measurement periods. After both 180 days and after 365 days, monitoring costs of \$18,000 and \$18,500 are paid, respectively. The NPV of these costs is -\$34,459. The wind turbine is then built, with initial capital costs of \$1,000,000 in the first year, paid immediately after monitoring ends, and net cash flow of \$300,000 for the next 5 years. These cash flows are shown in Figure 26. The net present value of these cash flows, discounted back to the day that monitoring commenced (not construction) is \$358,207. The total NPV for the monitoring and turbine operation is therefore \$323,748.

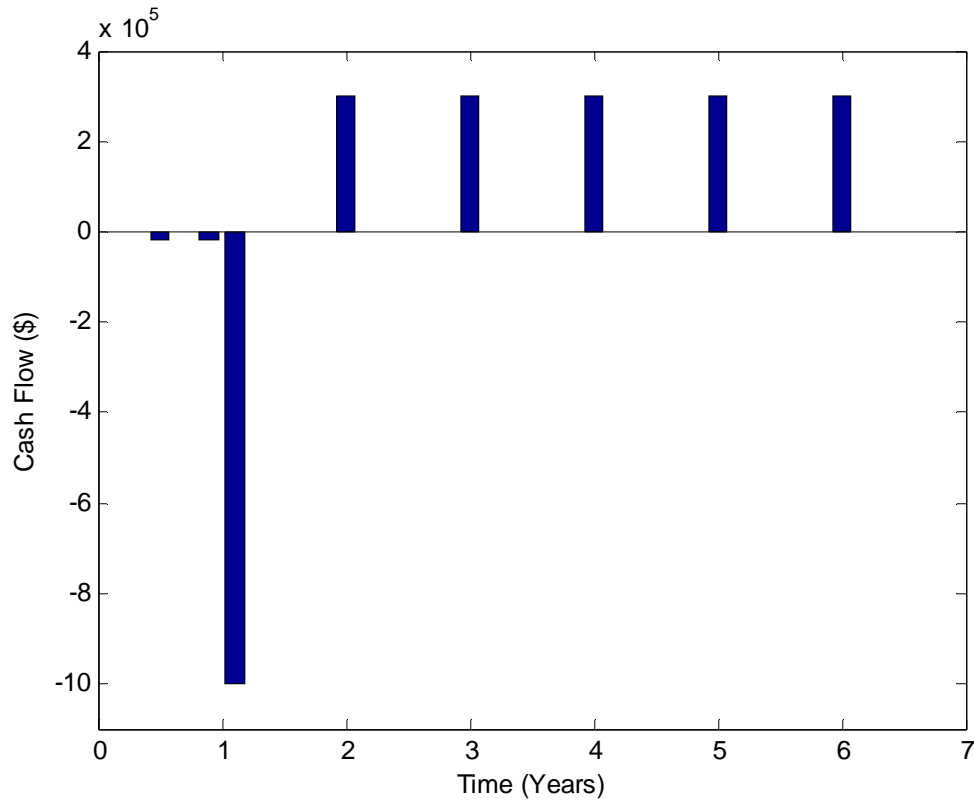


Figure 26 – Cash Flow Example

To emphasize the advantage of building the wind farm rapidly, this same example is considered, except with the decision to build taking place after the first measurement period. In this case, the total NPV of building the wind farm, including the monitoring costs, is \$355,127. This is \$31,378 more than the previous example, and this increase in NPV is due both to a decrease in monitoring costs, and reduced discounting to the cash flow due to the accelerated installation of the turbines.

4.4.2 Economic Assumptions

To calculate the actual NPV of building the wind farm, after any measurement period, numerous economic assumptions are necessary. The important assumptions are:

- Five 1.5 MW turbines are installed, for a total capacity of 7.5 MW.

- A power purchase agreement for 5 cents per kWh is used.
- The construction time is 1 year, and the project life is 20 years.
- The capital costs of the turbines are \$1,200 per kW installed, so the total capital costs are \$9,000,000.
- The yearly expenses (including O&M, leasing fees, etc) are \$285,000.
- A 60% debt, 40% equity mixture is assumed, with a 20 year loan and a 10% interest rate.
- The PTC is 10 years at 1.8 cents per kWh.
- Accelerated 5 year MACRS depreciation is used for the capital costs.
- The total tax rate is 40%.
- The inflation rate for all expenses and revenues is 1%.

While many of these assumptions could have significantly different values, e.g., with inclusion of incentives that increase the value of the exported electricity, different borrowing costs, etc, the analysis is generally applicable for any set of assumptions.

The economic evaluation is complicated by the debt repayment. The ratio of the available cash for the loan payment and the actual loan payment is referred to as the “debt service coverage ratio,” or DSCR. For capacity factors below a certain value, the revenue generated by the wind energy is insufficient to repay the loan obligation for a given year, and so the DSCR is less than 1. Figure 27 shows the minimum DSCR for all the years of wind farm operation, and for the economic assumptions above, as a function of capacity factor. The minimum DSCR is a linear function of capacity factor. For capacity factors below approximately 25%, the minimum DSCR is less than 1. In these

cases, the wind farm is unable to fulfill its loan obligations, and so defaults. The actual consequences of defaulting on the loan are varied, and beyond the scope of this Chapter. This issue is handled as follows: for capacity factors greater than 25%, NPV is positive and also a linear function of capacity factor, as shown in Figure 27. As capacity factor decreases from these larger values, it eventually reaches 25%. At that point, for all capacity factors less than 25%, NPV is forced to the smaller value of either -\$100,000 or the value obtained by extrapolating the linear NPV function to lower capacity factor values. The result can be seen in Figure 27 as well, as there is a “notch” for capacity factors between approximately 21% and 25% where the NPV is forced to -\$100,000.

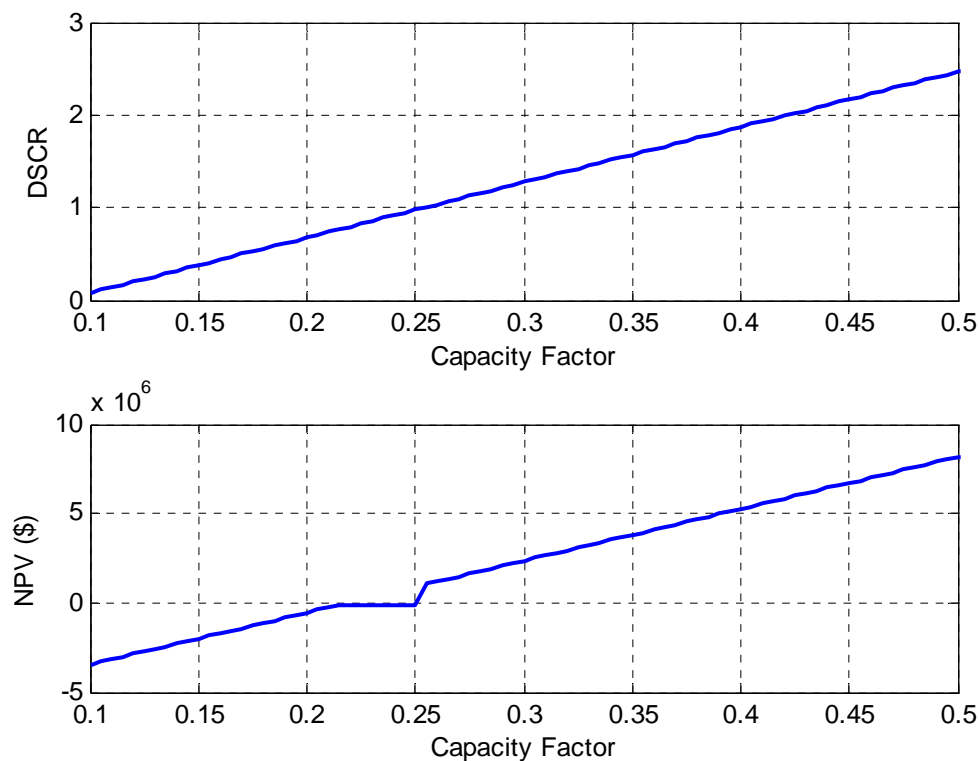


Figure 27 – NPV of building and DSCR as a function of Capacity Factor

It is worth noting that without this adjustment, the break even capacity factor calculated from the NPV line is 22%. However, this is an incorrect result, as the

minimum DSCR at that point is only 0.8, and so the loan cannot be repaid. Once again, the quantitative results of this analysis depend critically on the values used in the assumptions.

This approach is clearly a significant simplification. The value of -\$100,000 is arbitrary, and so is the extrapolation of NPV values to lower capacity factors. The goal is to create a sizable penalty for building the wind farm when the minimum DSCR is less than 1. On the other hand, when the capacity factor is low enough that the minimum DSCR is less than 1, the wind farm would not be built anyway, and so the NPV of the decision is simply the NPV of the monitoring costs. In this way, the actual values of NPV for DSCR values less than 1 are not particularly important, as long as they are low enough to ensure that the decision in these cases is not to build the wind farm.

Lastly, because the capacity factor is an uncertain quantity, the expected value of the NPV, $E[NPV]$, of building the wind farm must be calculated. This is shown in Eq. 46 above, and is repeated here in Eq. 50. $NPV(CF)$ is the function shown in Figure 27, and CF is the capacity factor. $p(CF)$ is the distribution of the capacity factor, which is assumed to be normal. The limits of integration are necessary because of the definition on the capacity factor.

$$E[NPV(Build)] = \int_0^1 p(CF) \cdot NPV(CF) \cdot dCF \quad \text{Eq. 50}$$

4.5 Decision Model Parameters

The parameters that define the objective decision making framework are defined below. The model is qualitatively similar to the example decision tree shown in Figure

24, except with more measurement periods, and the exact economic parameters described above used to calculate the NPV of the various decisions.

- The predicted long-term annual mean wind speed is categorized by 1 m/s bins between 4 m/s and 14 m/s (as opposed to a continuous distribution, which is used in the decision tree example above). There are a total of 12 bins including the bin for values less than 4 m/s, and the bin for values greater than 14 m/s. These extreme values are chosen to encompass the likely range of values at nearly any site.
- There are 4 total measurement periods, each 90 days long.

At the end of each measurement period, the three choices are evaluated, and one of them is selected. The decision to build is more complicated than simply choosing it if it has the largest $E[NPV]$. Because of the risk associated with building a wind farm, a more conservative decision criterion is needed. As stated previously, the capacity factor is an uncertain quantity, and so a range of values are possible. A common method, which is used here, is to require that the minimum DSCR calculated with the 10th percentile capacity factor value is greater than 1 [14]. Thus, the decision to build a wind farm is only made if the expected NPV of building is larger than the other two choices, and if the minimum DCSR using the 10th percentile capacity factor value when building is greater than 1. If one of these criteria is not met, then the decision is limited to the maximum expected NPV between the choices of not building the wind farm and continuing to measure.

4.6 Decision Space Example

An example is useful to demonstrate the basic functioning of the framework. The plot in Figure 28 shows an example decision space. Essentially it shows what decision is made as a function of the predicted long-term mean wind speed and the number of measured days of data. Figure 28 is created by assuming that the uncertainty behaves according to the data in Figure 25. A few important observations about Figure 28 are:

- For actual sites, the decision space would be qualitatively similar, but would differ due to different estimates of the uncertainty in the long-term mean wind speed.
- As the measurement length increases, and so the uncertainty in the prediction of the long-term mean wind speed decreases, the boundaries narrow indicating that there is a smaller region in which the decision would be to continue measurement. Essentially, increased certainty in the estimate makes a decision more likely.
- The actual values of the boundaries are also highly dependent on the economic parameters used in this analysis.
- At the end of 1 year of measurement, a decision is always made, and so there is no longer any space occupied by the option to continue measurement.
- The upper boundary between building and continuing to measure is fairly flat relative to the lower boundary. This is likely due to the conservative DSCR requirement decision criteria.

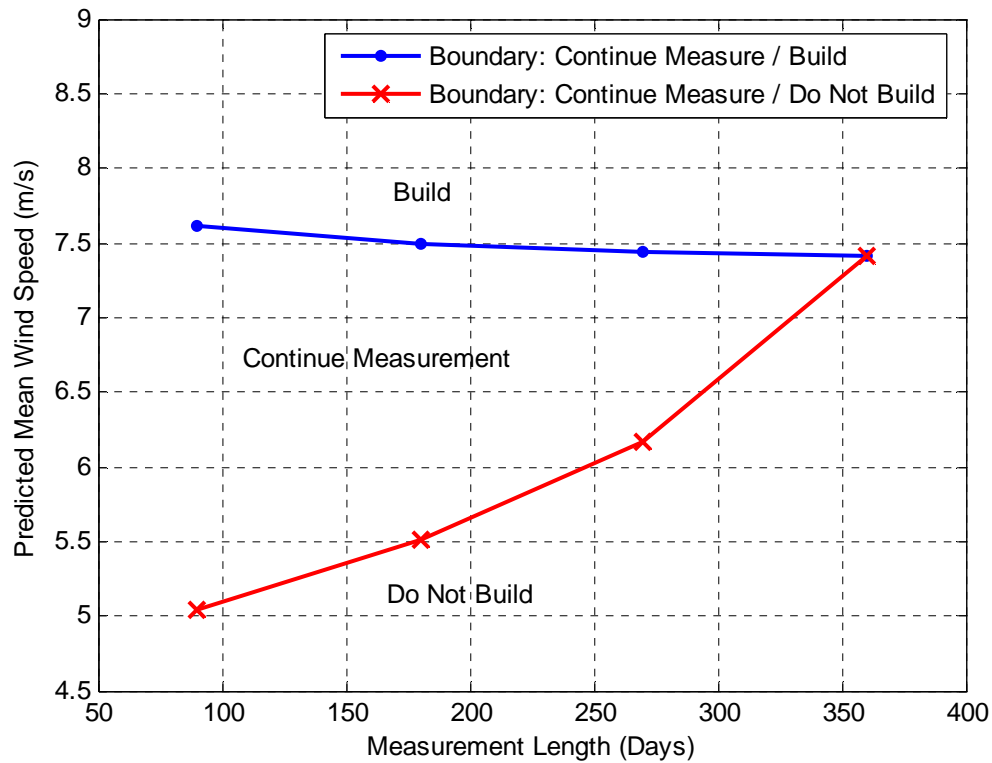


Figure 28 – Decision Space for Example

4.7 Data Set Analysis Procedure

The 15 data sets are each analyzed using a recursive dynamic program that solves the decision tree using the actual wind data and MCP predictions. The goal is to compare the objective decision making results to the results of using the traditional method of an entire year of measured data. Also, because long-term target site data is available in this analysis, it is also possible to calculate the target site capacity factor based on the long-term target site wind resource. This is an estimate of the true capacity factor at the site, and it can be used to calculate the true decision that would be made if this target site data are available. This true decision serves as a useful comparison, and the full target site wind resource enables the consequences of the various decisions to be calculated as well.

The program functions as follows:

1. For each data set, N random starting points are selected in the target site data set, where N is equal to the number of years of concurrent data. These are the hypothetical starting points for a measurement campaign at the site. The starting points must be at least 180 days apart from all other starting points to ensure that the data sets used are dissimilar. The starting points are random instead of sequential to avoid any potential biasing due to starting at the same time of a year each time.
2. The program runs, using the reference site data for MCP predictions, and the decision framework outlined above. An MCP prediction of the long-term mean wind speed is made at the end of each measurement period, and the program stops when a decision to either build or not build is made. At the end of the four measurement periods, a decision is made no matter what. The measurement period of the decision and the decision itself are stored. This is referred to as the “objective decision.”
3. For the same starting point, a full year of measured data is also used to predict the long-term mean wind speed and make a decision of whether or not to build the wind farm. This is referred to as the “one-year decision.” This serves as a useful comparison, as it represents the status quo method for site assessment.
4. The actual NPV of the objective decision and the one-year decision are calculated using the entire target site wind resource. In this way, the true results of the decisions are calculated, as the full target site wind resource is representative of the true wind resource at the site. This is referred to as the “true decision.”

5. The average measured days saved, the percentage of correct objective decisions and one-year decisions relative to the true decisions, and the average amount of money saved using the objective decision are then calculated for each site, by averaging across the N runs.

5.0 Results

In using the decision making framework for this application, there are two primary priorities. First, it is desirable that the decisions made are identical to the true decision, which is made with the full target site wind resource. This indicates the accuracy of the decisions, and it is important to compare the decisions to the true decision, as the decisions made using one year of measured data may be incorrect as well. Second, it is desirable that the decisions be made as rapidly as possible. These two effects contribute to the overall amount of money that is saved using the decision making approach. Incorrect decisions result in lost money due to either building a wind farm when the wind resource is not actually good enough to build, or not building a wind farm when the wind resource is good enough. Either way, money is lost with an incorrect decision. Furthermore, more rapid decisions result in lower monitoring costs, and less discounting of the cash flows. The two priorities are often in conflict with each other, as rapid decisions are accompanied by more uncertainty in the estimate of the long-term mean wind speed. Thus, this approach can only be successful if a balance is struck, resulting in accurate and rapid decisions. These results are shown below in Table 2. They are the average over the 15 sites, with a total of 130 separate simulations.

Correct Percentage - Objective Decisions (%)	97.7%
Correct Percentage - One Year Decisions (%)	96.9%
Overall Average Measurement Length (Days)	199
Overall Average NPV Saved (\$)	\$121,600

Table 2 – Analysis Results

The results indicate:

- Approximately 98% of the time, the objective decision results in the identical decision as the true decision, while approximately 97% the one-year decision results in the same decision as the true decision. These decisions can be either to build or not to build. Overall, the objective decision has slightly better accuracy than the one-year decision. This difference is not statistically significant, however, and so in essence the two methods appear to have equivalent accuracy.
- 99.2% of the objective decisions and the one-year decisions are identical.
- The average measurement length using the objective decision making approach is approximately 199 days. This is slightly larger than half of a full year, and so there is a 45% reduction in measurement length using this approach.
- The result is an average savings of approximately \$122,000 per site assessment using the objective decision making approach. This savings is enabled by both accurate decisions and rapid measurement.

Figure 29 shows the fraction of correct decisions at each site using the objective decision making approach compared to the true decision. The fraction is plotted as a function of the long-term capacity factor at the target site, to investigate how the results depend on the windiness of the site (the more windy the site, the larger the capacity factor). Each data point corresponds to one of the 15 sites. For 12 of the 15 sites, the

objective decision making approach is correct 100% of the time. Only 3 sites have even a single incorrect decision, and at each of these three sites, only a single simulation results in an incorrect decision. Overall, of the 130 simulations, there are only three instances of incorrect decisions using the objective decision making method.

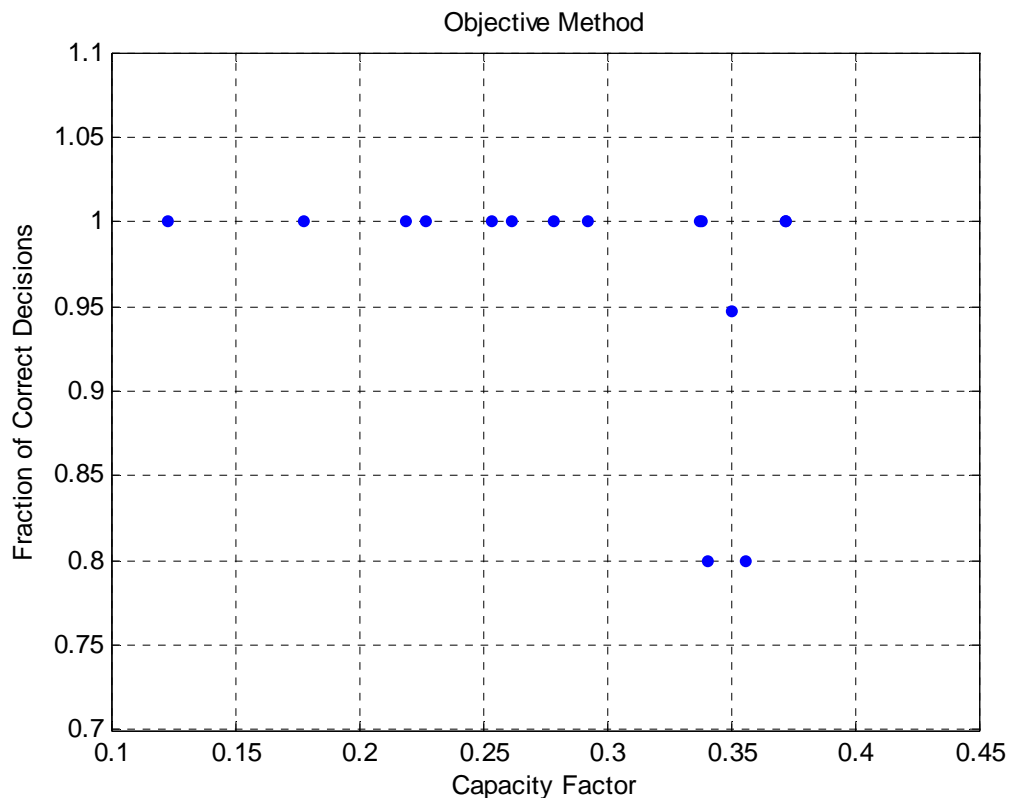


Figure 29 – Correct Decision Percentage for Each Site

The average measurement length for each site as a function of the long-term capacity factor is shown in Figure 30, again to investigate how the results depend on the windiness of the site. It indicates that the average measurement length at each site ranges from as short as 90 days, to as long as 315 days. Also, while it is not a very strong pattern, the longer measurement lengths tend to occur at sites with moderate capacity factors. These sites are only somewhat windy, with capacity factors near the break even value of 25-26%. The results indicate that it is more difficult to make definitive decisions at these

sites, presumably because it is uncertain whether or not building a wind farm will be successful. In these situations, it appears that collecting more data and reducing uncertainty is the appropriate option, and therefore longer measurement lengths occur. For sites with either very good or very bad wind resources (greater than 30% or less than 20% long-term capacity factor), the measurement length tends to be shorter overall. Because the capacity factor is not close to the break-even value at these sites, decisions can be made early on, despite the larger uncertainty due to a short measurement length.

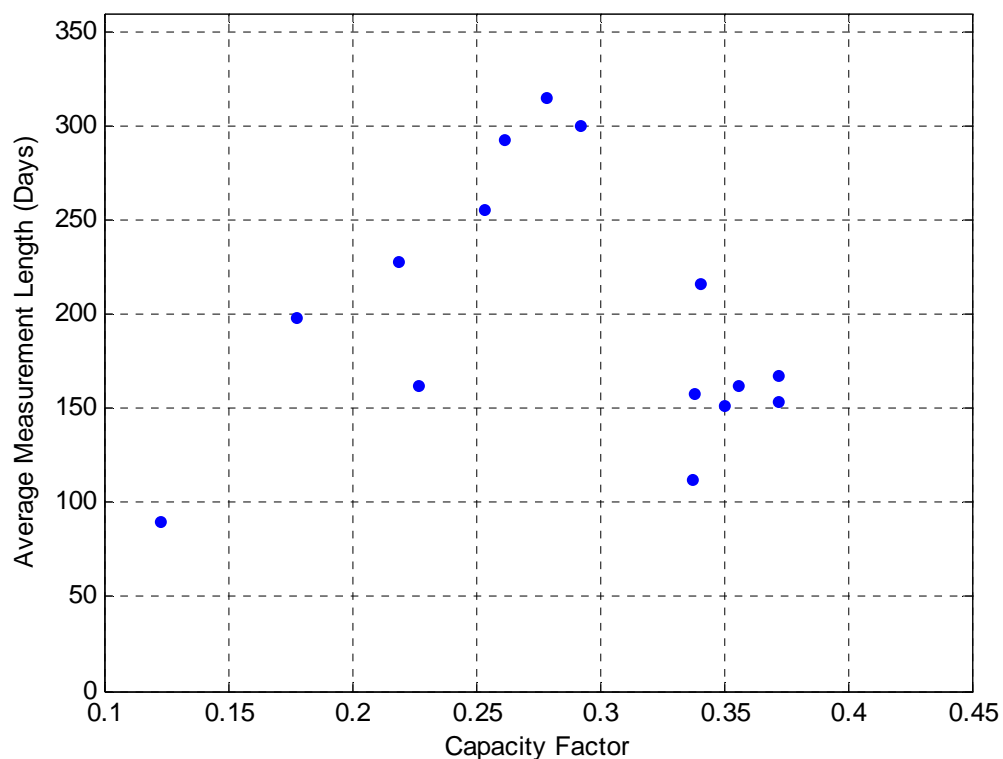


Figure 30 – Average Measurement Length for Each Site

Finally, the average NPV saved per simulation for each site as a function of the long-term capacity factor at each site is shown in Figure 31. Figure 31 indicates that for bad sites, with very small capacity factors (i.e., not very windy), a modest amount of savings is possible (~\$25,000) as a result of reduced measurement lengths. At moderate sites

with capacity factors between 20% and 30%, the savings are actually least, because the average measurement length tends to be longest at these sites. But, as the long-term capacity factor gets larger for the windy sites, the average NPV saved also gets larger. This is due both to reduced monitoring costs and reduced discounting of the cash flows due to shorter measurements. In general, the better the wind resource at a site, the more money saved using the objective decision making approach. Finally, the average NPV saved for all sites is positive.

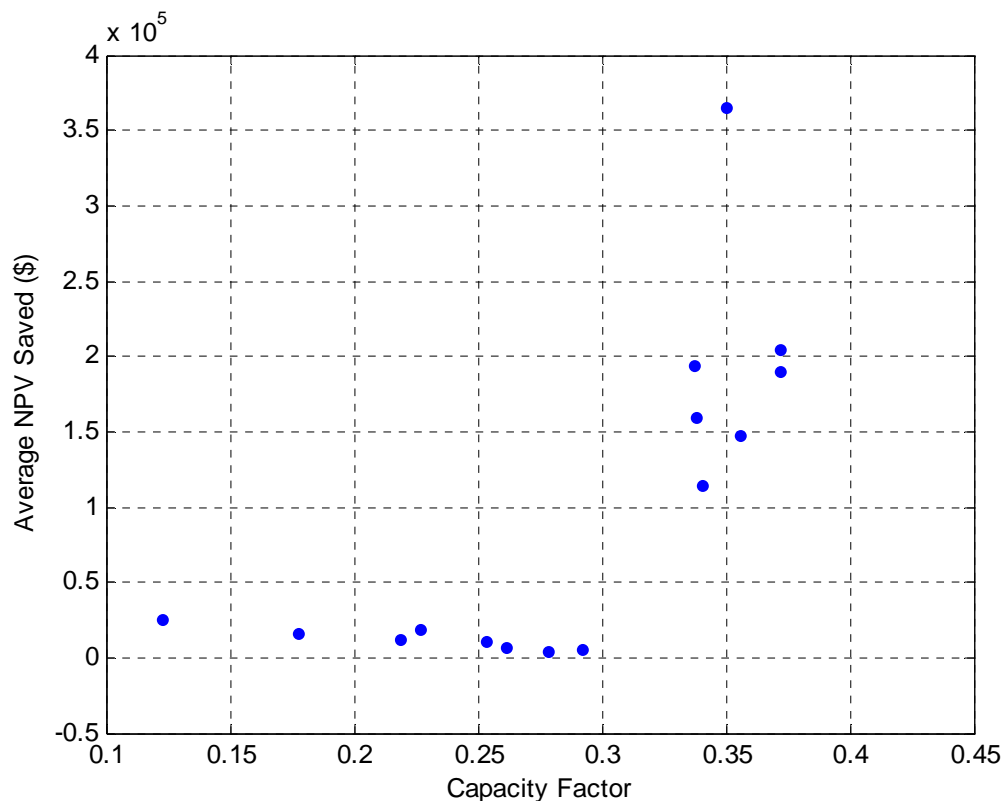


Figure 31 – Average NPV Saved for Each Site

6.0 Conclusions and Recommendations

The results presented above demonstrate that the objective decision making approach for wind energy site assessment can be an extremely effective means of accelerating the

site assessment process and saving money without a sacrifice in the accuracy of the decisions. Some important conclusions and recommendations on implementation of this approach are now given.

- The objective decision making approach is uniformly effective, and is especially effective for either very good (i.e., windy) or very bad sites. At marginal sites, the savings are less because the required measurement length tends to be very long, nearly a full year. At these sites, because of the lengthy measurement using the objective decision making method, it may be worthwhile to measure for an entire year, as the savings are very small. This is a somewhat circular recommendation: it requires knowing that the long-term capacity factor is marginal before measurement begins. One solution is to utilize either wind maps, atlases, or near by reference site data to get a “ballpark” estimate of the long-term capacity factor at the site of interest. If it is very close to the break-even capacity factor, then the traditional method of measuring a full year of data can be employed. For sites that appear promising beforehand, or sites that are likely not promising, then the objective decision making approach can be utilized exclusively.
- An advantage of ground-based devices that is also touched upon in Chapter II, Section 2.0, is their ability to measure the wind resource at the turbine hub height, and so they obviate the need for shear extrapolation. Shear extrapolation uncertainty is often the largest source of uncertainty in the estimation of the wind resource [16]. While the relevant uncertainties are modeled in this research, they are not compared to the uncertainty that occurs in the traditional site assessment approach, when a met tower is used to measure the wind resource. While the

objective decision making approach may be accompanied by larger uncertainty due to shorter measurement periods, this effect is potentially much less severe than the shear extrapolation uncertainty that arises when a met tower is used. Overall, utilizing this approach with a ground-based device does not necessarily imply that the uncertainty in the wind resource estimate is larger than if a met tower is used to measure the wind resource for an entire year.

- Because of the 10th percentile debt service coverage ratio constraint, reducing the uncertainty in the process causes a decision to build a wind farm to become more likely. Reduced uncertainty makes this constraint less restrictive, and therefore decisions to build are more common. This effect can be visualized in Figure 32, which shows the same decision space from Figure 28 (the solid lines), and a new decision space (the dashed lines). The new decision space is created by reducing the additional wind resource uncertainty from 7% to 5.4% and the power curve uncertainty from 8% to 5%. These original values are discussed in Section 4.3. In Figure 32, the upper boundary is lowered noticeably, indicating that a decision to build the wind farm is more likely. The lower boundary remains fairly constant, except for the final measurement period, which is lowered as well. The overall effect of reducing uncertainty in the process is to narrow the “Continue Measurement” space, and to expand the “Build” space, while keeping the “Do Not Build” space relatively constant until the final measurement period. There are numerous possible means of reducing uncertainty, including reduced measurement uncertainty, reduced power curve uncertainty, and reduced economic uncertainty via more secure revenue guarantees or more secure

subsidies. Regardless of the means of reducing uncertainty, there is a strong motivation to do so, as it has a direct effect on the likelihood of wind energy development occurring. While there are some uncertainty sources that are purely physical byproducts of the site assessment process, many uncertainties in the process are derived from state and federal policies on subsidies. These results indicate that not only the actual value of a subsidy, but also the certainty of it can affect the rate and likelihood of wind energy development. More certain long-term subsidies, like the feed-in tariffs that are used in Europe, can have a pronounced long-term effect and accelerate the development of wind energy.

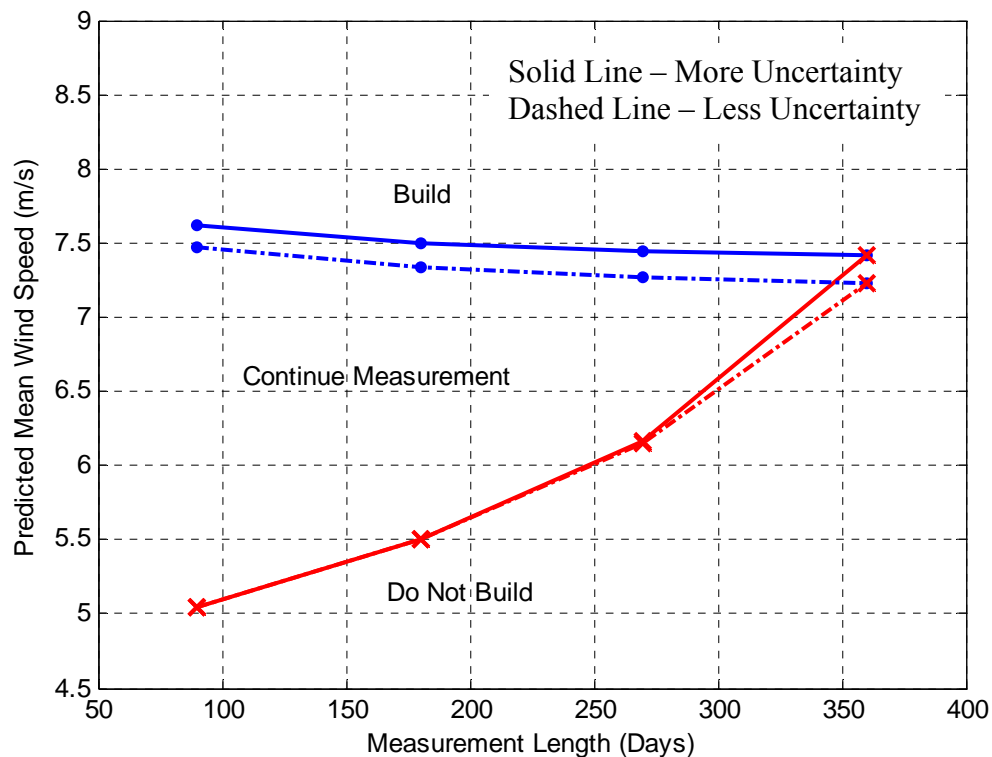


Figure 32 – Effect of Uncertainty on Decision Space

- From a practical perspective, initially this objective decision making approach may be difficult to implement on a large scale because of the issue of

“bankability.” Because wind farms are such large capital investments, almost all wind farms require financing from some type of bank or lending institution. These loans are often conditional on an independent assessment from a consultant, and because of the risk averse nature of these lending institutions, a full year of measured data is likely required or strongly preferred. The result is that even in instances when the objective decision making approach is both appropriate and correct, it may not be adopted. While this conservative approach may be unavoidable, it would also be a missed opportunity and an inefficient path to pursue, as it would ignore the substantial potential savings in time and money indicated by these results.

- On the other hand, government sponsored site assessment programs, in which a government body is financing both the monitoring and the wind farm, may be an ideal application for this approach. These programs often have priorities other than making money, such as rapid growth of renewable energy and diversification of the energy generation portfolio. Strict requirements for site assessment practices may not be relevant in these cases.
- In the long-term, as experience is gained with this approach, and its effectiveness is validated, it is hoped that this method can become much more commonly used. The results are extremely compelling, and a transition towards more effective and efficient site assessment methods can increase wind energy development.

Overall, the approach developed in this Chapter offers an innovative means of accelerating the site assessment process. The results indicate an impressive accuracy

along with substantial savings in the cost of wind energy development. While the initial implementation of this approach may be difficult, eventually it may offer a viable alternative to the traditional one year measurement period utilized in site assessment today.

CHAPTER V

THE ROUND ROBIN SITE ASSESSMENT STRATEGY

1.0 Introduction

In the traditional site assessment process, the wind resource is typically measured at a site for at least one year. This feature of site assessment, discussed in Chapter I, Section 1.2, is due to seasonal variations in the wind resource. Measurement periods less than one year can also be used in the MCP process, although the accuracy and precision of the predictions of the long-term wind resource generally decreases as the measurement period decreases [52]. This Chapter describes the development of a new technical approach for wind resource measurement, which relies on ground-based devices, that seeks to shorten the required measurement length at a site, without the associated decrease in the accuracy and precision of the estimate of the long-term wind resource.

Ground-based measurement devices, such as SODARs or LIDARs, are beginning to be used as alternatives to met towers for wind resource assessment. These devices, discussed in Chapter II, offer numerous potential advantages compared to traditional met towers. Specifically, they are portable and easy to install, especially when compared to met towers. Their portability offers a further advantage beyond convenience: it can be exploited to allow for alternative monitoring strategies. Met towers are completely stationary, and therefore measure continuously at one location for the duration of their deployment. Conversely, SODARs and LIDARs are easily transported between sites, allowing for discontinuous measurement periods. In practice, the portability of these devices has not been consistently capitalized upon in the site assessment process.

This Chapter investigates the use of a new technical approach for wind resource assessment, which is dubbed the “round robin site assessment method”. The premise of the round robin site assessment method is to measure the wind resource at multiple sites in a single year using a single portable device (capable of measuring at the hub height of a turbine), and to distribute the measurement time at each site over the whole year. The measurement period at each site is not continuous when using the round robin site assessment method. Rather, the total measurement period is comprised of smaller segments of measured data, discontinuously distributed over the course of one year.

An example of the round robin site assessment method helps to clarify this premise: in one year, one wishes to measure the wind resource at two sites, spaced within a few hours drive of each other. One could measure at the first site for the first six months of the year, and then at the second site for the remaining six months of the year. This is the standard, continuous measuring method. However, because of seasonal fluctuations in the wind speed, measuring for only six months at each site can lead to mischaracterization of the wind resource at both sites, and therefore large errors and uncertainty. The round robin site assessment method approaches the monitoring strategy differently. The wind resource is measured at the first site for some fraction of six months (e.g., one month). This is the “round robin measurement period.” When the initial round robin measurement period is complete, the portable measurement device is transported to the second site, where the wind resource is again measured for the duration of the round robin measurement period. This process is repeated, with the measurement device being transported back and forth between sites, until the year is completed.

By using the round robin site assessment method, the wind resource at both sites can be assessed in a single year, and the seasonal fluctuations in the wind speed are captured in the data as well. Essentially, the round robin site assessment method aims to increase the number of sites that can be assessed in a single year, and therefore the efficiency of the site assessment process, without the sacrifice in accuracy and precision that usually accompanies measurement periods less than one year. The portability of the remote measurement devices enables this potential combination of increased efficiency and high performance.

In this Chapter, fifteen pairs of long-term data sets are used to investigate the efficacy of the round robin site assessment method. The traditional continuous wind monitoring approach is compared to the discontinuous round robin approach, for various total measurement lengths and for various round robin measurement periods. The results demonstrate that the round robin site assessment method is an effective monitoring strategy that improves the accuracy and reduces the uncertainty of MCP predictions for measurement periods less than one year. In fact, the round robin site assessment method compares favorably to the accuracy and uncertainty of a full year of resource assessment. While there are some tradeoffs to be made by using the round robin site assessment method, it is potentially a very useful strategy for wind resource assessment.

2.0 Data Sets Used

Fifteen pairs of long-term data sets are used in this investigation. These data sets, including the steps that are taken to process the data, are discussed in detail in Chapter IV, Section 4.1. Table 3 summarizes each of the data set pairs.

Long-term target site data are critical to any test involving MCP predictions, because it offers a means of objectively evaluating the MCP method. When long-term target site data are available, the long-term wind resource can be determined (e.g., the long-term mean wind speed and Weibull parameters), and these values are considered to be the true values of the target site wind resource. The goal is for the MCP method to closely predict these true values of the target site wind resource. The long-term target site data set can be divided into smaller segments of data, and each of these segments is considered to be a hypothetical “measured data set”. The reference site data along with the hypothetical measured data can be used to predict the long-term target site wind resource. Therefore, each hypothetical measured data set produces a prediction of the target site wind resource, and so there are multiple MCP predictions. Finally, each of the MCP predictions of the long-term target site wind resource can be compared to the true target site values. In this way, long-term target site data is used to objectively evaluate MCP methods, since it offers a means of comparing the predictions to the true values. Furthermore, multiple MCP predictions can be made with a single pair of long-term data sets, which allows for the variability of the predictions to be assessed.

Data Set	Name	State/Region	Distance	Years of Good Data
1	Buoy 44013	NE	365 km	6
	Buoy 44011	NE		
2	Buoy 46005	NE	390 km	3
	Buoy 46002	NE		
3	Cornucopia	WI	180 km	3
	Rib Lake	WI		
4	Currie	MN	253 km	8
	Breckenridge	MN		
5	Currie	MN	90 km	5
	Montevideo	MN		
6	Hatfield	MN	35 km	7
	St. Killian	MN		
7	Buoy 44007	NE	87 km	17
	Buoy 44005	NE		
8	Buoy 44008	NE	231 km	14
	Buoy 44013	NE		
9	Buoy BUZM3	NE	178 km	15
	Buoy IOSN3	NE		
10	Buoy MDRM1	NE	62 km	17
	Buoy MISM1	NE		
11	Cedar	IA	219 km	5
	Red Oak	IA		
12	Estherville	IA	100 km	4
	Forest City	IA		
13	Sibley	IA	66 km	5
	Inwood	IA		
14	Sutherland	IA	186 km	3
	Radcliffe	IA		
15	Buoy 51001	Pacific	497 km	14
	Buoy 51003	Pacific		

Table 3 – Summary of Data Sets

3.0 Data Analysis

The premise of the round robin site assessment method is to measure the wind resource at multiple sites in a single year, with the measured data at each site distributed over the course of the year in smaller discontinuous segments. It is important to emphasize that in all cases in this analysis, the measurement of the wind resource at any site takes place within a one year time frame. Since there are multiple years of target site data for the data sets, each one year time frame is analyzed individually.

An example illustration of the round robin site assessment method is shown in Figure 33. In this example, two sites are assessed in the one year time frame between January 1, 1999 and January 1, 2000. The wind resource is measured at each site for a total of six months, and the six months of measured data at each site are comprised of six smaller segments of data, each one month in length and each separated by one month. The arrows in Figure 33 indicate the individual segments of measured data. The ground-based device is transported between sites at the end of each month over the course of one year.

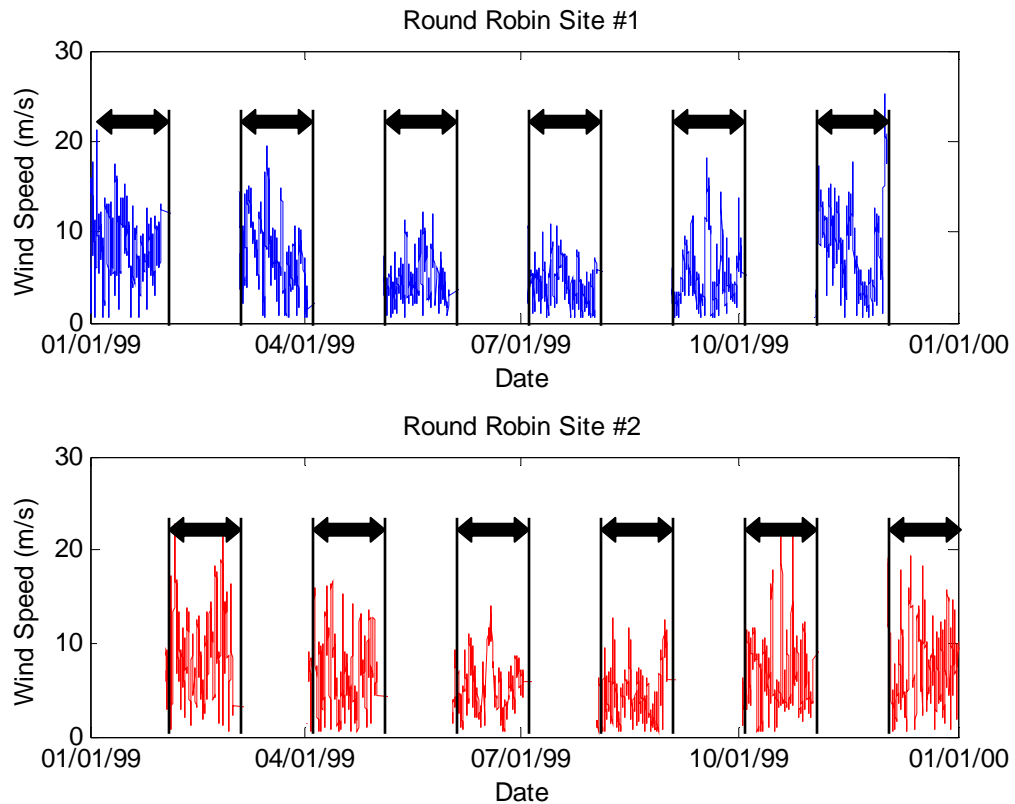


Figure 33 – Example of Measurements at Two Sites

The goal of this analysis is to assess the utility of the round robin site assessment method. Specifically, two important questions are addressed in this analysis:

1. How does the round robin site assessment method, for a given measured data length per site, compare to the standard method, which uses a continuous measurement period, for that same measured data length per site? For example, one could employ the round robin site assessment method as shown in Figure 33, with a total of six months of measured data at each site, and with the measurement device alternating between sites every month. This would produce a discontinuous measured data set at each site. Alternatively, one could use the standard method and measure the wind resource continuously for six months at one site, and then six months at the other site. This question aims to determine the relative performance between these two methods, when the same amount of data is measured at each site.
2. How does the round robin site assessment method, for a given measured data length at a site, compare to the standard method using a full year of measured data at that site? For example, one could again use the two-site round robin site assessment method, and so a total of six months of data are measured at each site. These results can then be compared to the results when a full year of continuous data is measured at the target sites.

The first question assesses the merits of the round robin site assessment method relative to equally short measured data lengths using the standard method. Initially, it seems likely that the round robin site assessment method would be an improvement over the standard method with the same measured data length, due to the ability of the round robin site assessment method to encompass seasonal variations in wind speed. The

second question addresses a more important point: whether or not the round robin site assessment method, given its increased efficiency, provides enough accuracy and precision relative to a full year of measured data to make it a useful strategy. Section 4.0 utilizes these two questions as a framework for the discussion of the results.

The performance of a given method in this analysis is evaluated on its ability to predict the long-term wind resource at a site. The two factors that are used to characterize the long-term wind resource are:

- The mean wind speed.
- The Weibull shape parameter, k .

Both the accuracy and the variance of the predictions are important. The methods are assessed based on both the error of the predictions, as well as the standard deviation of the predictions. In all cases, the predictions of the mean wind speed and k are compared to the respective true long-term values of the mean wind speed and k for the particular target site data that is being predicted.

3.1 Primary Analysis Parameters

While many parameters are assessed in this analysis, there are two that are particularly interesting and relevant to the utility of the round robin site assessment method. These are:

1. The number of sites evaluated in a year, and therefore the measured data length per site. The measured data length per site is labeled *MDL*. In general, *MDL* at each site, in months, is simply equal to twelve months divided by the total number of sites measured in the year. Therefore, when two sites are evaluated in a year,

MDL at each site is six months, as in the example in Figure 33. Similarly, if three sites are evaluated, then *MDL* at each site is 4 months. In this Chapter, both two site and three site scenarios are tested.

2. The round robin measurement period, which is labeled *RRMP*. This time frame is defined as the period of time that the measurement device is kept at an individual site before being moved to another site. In the example in Figure 33, *RRMP* is equal to one month, and so over the course of one year, the device is moved between sites in one-month increments. *RRMP* can conceivably range from as small a time period as a few days, to as long as one half of the measured data length. Thus, when using two sites, and *MDL* is six months, the maximum *RRMP* value is three months. The lower limit is only restricted by the transport time between sites, and the inconvenience of moving the device frequently. In practice, it is unlikely that one would be inclined to move the device more than once per week. In this Chapter, *RRMP* values of 10 days, 30 days, and 60 days are investigated.

3.2 Data Analysis Procedure

Each of the fifteen data sets shown in Table 3 is analyzed as follows:

1. For each data set, the round robin site assessment method is assessed for values of *MDL* of 4 months and 6 months, and values of *RRMP* of 10 days, 30 days, and 60 days. Also, the standard method, where the measured data set is continuous, is considered for values of *MDL* of 4 months, 6 months, and 12 months.
2. Each one year time frame of data at the target site is considered.

3. Within each one year time frame, N measured data sets are selected, where N is simply equal to 12 months divided by the value of MDL . Thus, values of $N=2$ and $N=3$ are considered for the round robin site assessment method, and values of $N=1$, $N=2$, and $N=3$ are considered for the standard method. These measured data sets are discontinuous for the round robin site assessment method (like in Figure 33), and continuous for the standard method.
4. For each measured data set, the concurrent data between the target site and the reference site are determined.
5. MCP is performed using the Variance Ratio method, which is described in Chapter II, Section 5.0. The mean wind speed and k at the target site are predicted for each measured data set. The percentage errors in the prediction from the true long-term value of the mean wind speed and k at the target site are calculated for each measured data set.
6. The mean and standard deviation of the percentage error of the predictions is then calculated for each data set, and for each value of MDL and $RRMP$. For a given value of MDL and a given data set, the total number of predictions is equal to N multiplied by the number of years of target site data. So, for a site with 5 years of target site data, and a value of MDL equal to 4 months (so $N=3$), there would be 15 total predictions, and the mean and standard deviation of the percentage error in each of these predictions is then calculated.

Finally, the results from the analysis of each data set are consolidated across all the data sets. First, the root-mean-square of the mean percentage error for each site is

calculated. Second, to consolidate the standard deviation of the percentage error for each site, σ_i , a pooled estimate is used. The overall pooled standard deviation σ_P , consolidated across the data sets, is calculated using Eq. 51, where σ_i is the standard deviation of the percentage error at the i th site, and there are m total sites.

$$\sigma_P = \sqrt{\frac{\sum_{i=1}^m \sigma_i^2}{m}} \quad \text{Eq. 51}$$

These values are calculated for both the predictions of the mean wind speed and k , for both the round robin site assessment method and the standard method, and for each value of MDL and $RRMP$ (when the round robin site assessment method is utilized). For the mean wind speed predictions, the root-mean-square of the mean percentage error is labeled $RMSE(U)$, and for k it is labeled $RMSE(k)$. Likewise, the pooled standard deviation of the percentage error is labeled $PSTD(U)$ and $PSTD(k)$ for the mean wind speed and k , respectively.

RMSE indicates the accuracy of the predictions for a particular method and set of parameters. Smaller values of RMSE correspond to better results. PSTD indicates the uncertainty of the predictions for a particular method and set of parameters. Smaller values of PSTD signify instances when there are smaller amounts of variability in the MCP predictions, and therefore less uncertainty in the predictions. These results are presented in the next Section.

4.0 Results and Discussion

The results of the analysis described in Section 3.0 are now discussed. The results relevant to the prediction of the mean wind speed are discussed first, followed by the

results relating to the prediction of the Weibull parameter k . In general, the two questions raised at the beginning of Section 3.0 are utilized as a framework for the discussion, as they specifically address the performance of the round robin site assessment method in relation to the standard data measurement method.

4.1 Prediction of the Mean Wind Speed

All of the results in this Section relate to the prediction of the mean wind speed. Both $RMSE(U)$ and $PSTD(U)$ are discussed in this Section.

4.1.1 Accuracy of the Prediction of the Mean Wind Speed

The plot in Figure 34 shows the results for $RMSE(U)$ across all data sets for the two data measurement methods, and for various values of MDL and $RRMP$. The results for the standard method are labeled as such, and the results for the round robin site assessment method are labeled by their respective values of $RRMP$. Note that $RMSE(U)$ is less than 1.1% in all cases. In all cases, a smaller value of $RMSE(U)$ corresponds to a better result. Also, the standard method has data for a value of MDL of 12 months, whereas the round robin site assessment method does not.

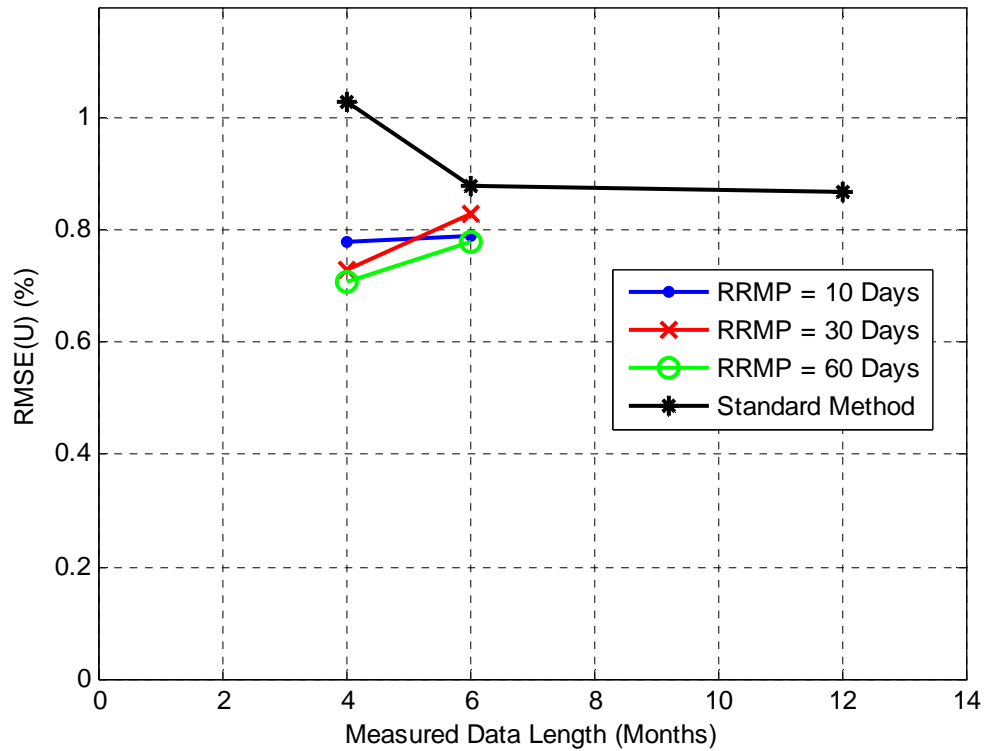


Figure 34 – Accuracy of the Mean Wind Speed Predictions

The two questions raised at the beginning of Section 3.0 are now addressed.

1. The round robin site assessment method often greatly reduces the value of the $RMSE(U)$ relative to the standard measuring method using the same measured data length, and never produces an increase in the value of $RMSE(U)$. The round robin site assessment method produces an especially dramatic improvement for a value of MDL of 4 months. For a value of MDL of six months, the round robin site assessment method still produces an improvement, but it is less pronounced.
2. The round robin site assessment method also always reduces the value of $RMSE(U)$ relative to the standard method when a full year of concurrent data is used. This result is somewhat surprising, as one would assume that a full year of

data would produce the smallest value of $RMSE(U)$ in all cases. However, for this analysis, that is not the case.

The results are also summarized in Table 4, which shows the values of $RMSE(U)$ in Figure 34.

Round Robin Measurement Period (Days)	Measured Data Length (Months)		
	4	6	12
10	0.78	0.79	-
30	0.73	0.83	-
60	0.71	0.78	-
Standard Method	1.03	0.88	0.87

Table 4 – $RMSE(U)$ for Round Robin Site Assessment Method and Standard Method

The round robin site assessment method always decreases, often to a significant degree, the value of $RMSE(U)$, both relative to the same value of MDL , and relative to a full year of measured data. The improvement is especially pronounced for a value of MDL of 4 months. It appears that a value of 60 days for $RRMP$ produces the best results, but this is not a particularly strong effect.

Overall, the difference in the accuracy of the predictions using the round robin site assessment method and a full year of measured data is small, and is not likely to be significant. The more important general point is that the round robin site assessment method produces equivalent accuracy in predicting the mean wind speed, compared to a full year of measured data.

4.1.2 Uncertainty of the Prediction of the Mean Wind Speed

$PSTD(U)$ is shown below in Figure 35. $PSTD(U)$ is used as a measure of the uncertainty in the prediction of the mean wind speed. In this discussion, these two terms are used interchangeably. Thus, smaller values of uncertainty correspond to better

methods. In all cases, the uncertainty of the prediction of the mean wind speed is between 3% and 6%. Again, the results for the standard method are labeled as such, and the results for the round robin site assessment method are labeled by their respective values of *RRMP*.

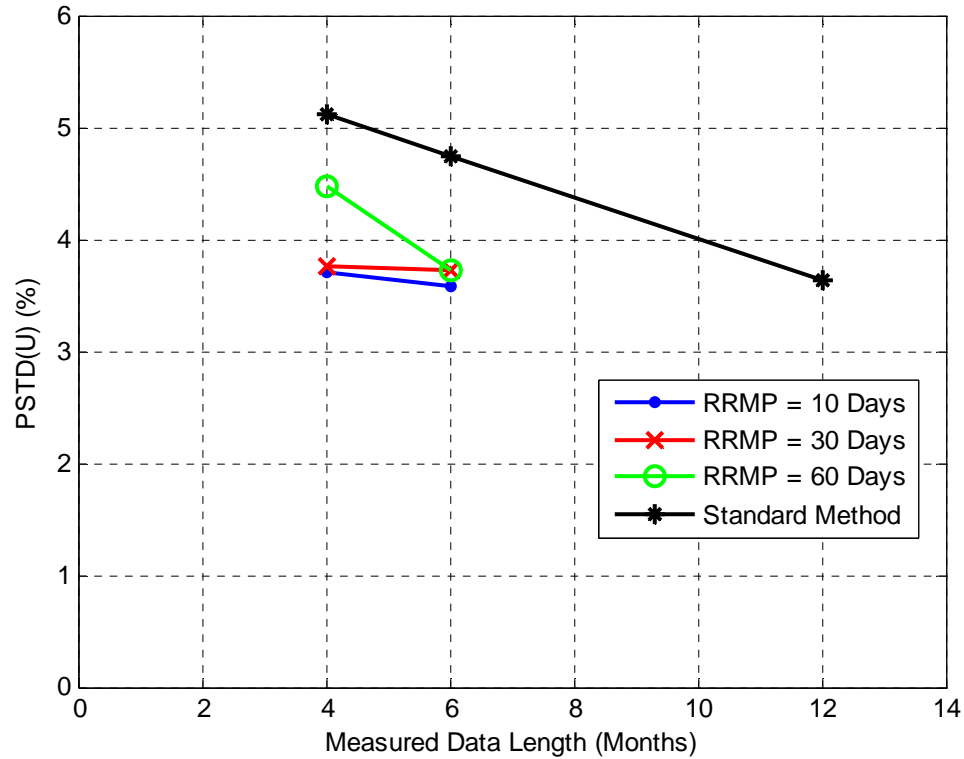


Figure 35 – Uncertainty of the Mean Wind Speed Predictions

Figure 35 shows two very consistent patterns. First, the uncertainty of the predicted mean wind speed decreases with increasing values of *MDL*. Second, the uncertainty of the predicted mean wind speed decreases with decreasing values of *RRMP*. Once again, the results can be discussed in the framework of the two questions posed at the beginning of Section 3.0.

1. For *MDL* values of both 4 months and 6 months, the round robin site assessment method significantly reduces the uncertainty of the prediction of the mean wind

speed compared to the standard method. Furthermore, the magnitude of the reduction increases with decreasing values of $RRMP$. Thus, the lowest value of $PSTD(U)$ occurs for a value of $RRMP$ of 10 days. Finally, for any given value of $RRMP$, the uncertainty decreases with increasing values of MDL , so that the uncertainty is always smaller for MDL of 6 months compared to 4 months.

The relationship between the uncertainty of the predicted mean wind speed and the round robin measurement period length can be further investigated using Figure 36. Figure 36 shows the values of the uncertainty as a function of $RRMP$, for MDL values of 4 months and 6 months. Figure 36 again indicates that $PSTD(U)$ decreases with a decreasing value of $RRMP$. This effect is especially pronounced when MDL is 4 months. The results indicate that when MDL is 4 months, for large values of $RRMP$, decreasing $RRMP$ causes a larger reduction in the uncertainty than for smaller values of $RRMP$. When MDL is 6 months, $PSTD(U)$ is nearly constant as a function of $RRMP$.

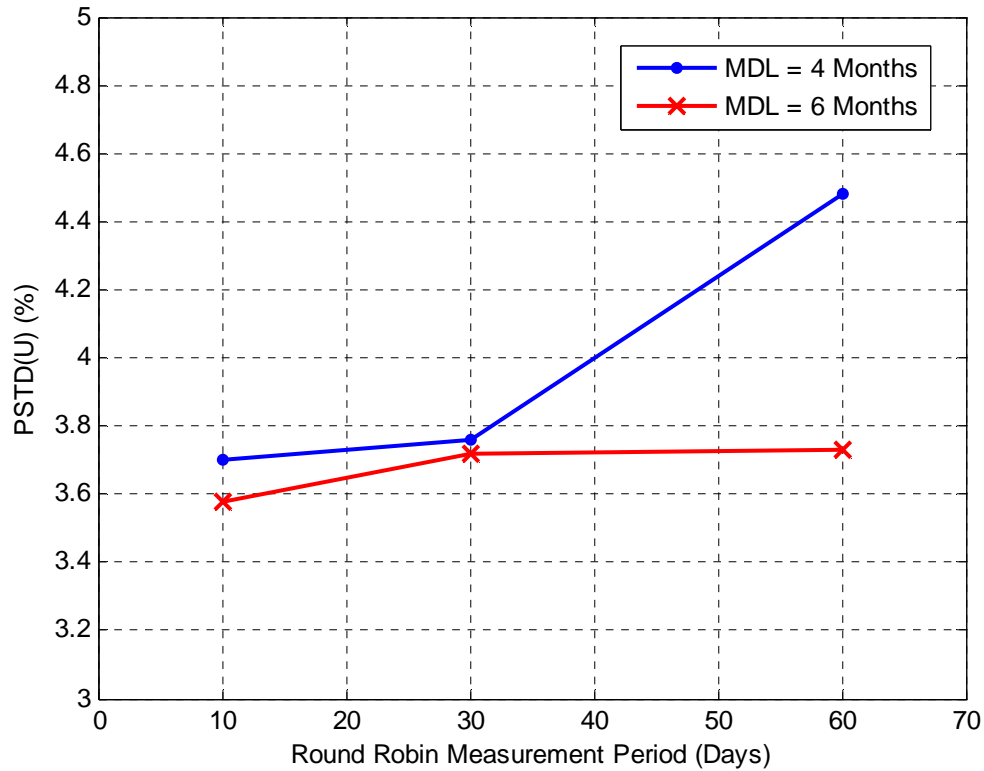


Figure 36 – Effect of the Round Robin Measurement Period

In practice, this plot indicates that there are diminishing returns associated with decreasing the round robin measurement period. When MDL is 4 months, decreasing $RRMP$ beyond 30 days results in very little improvement in the uncertainty of the prediction of the mean wind speed. When MDL is 6 months, $PSTD(U)$ is nearly independent of $RRMP$ and so there is little incentive to decrease the value of $RRMP$.

This effect can be viewed in terms of the number of trips required to move the ground-based device. The total number of trips in a year is simply equal to 365 days divided by the round robin measurement period in days, plus 1. Thus, smaller values of $RRMP$ correspond to a larger number of trips. Figure 37 shows $PSTD(U)$, for both values of MDL , as a function of the total number of trips

required in one year. Again, the diminishing returns associated with decreasing *RRMP* and therefore increasing the number of trips can be seen in Figure 37. As a comparison, when the standard method is used, there are 3 trips for a value of *MDL* of 6 months, and the value of $PSTD(U)$ is 4.8%. There are 4 trips for a value of *MDL* of 4 months, and the value of $PSTD(U)$ is 5.1%.

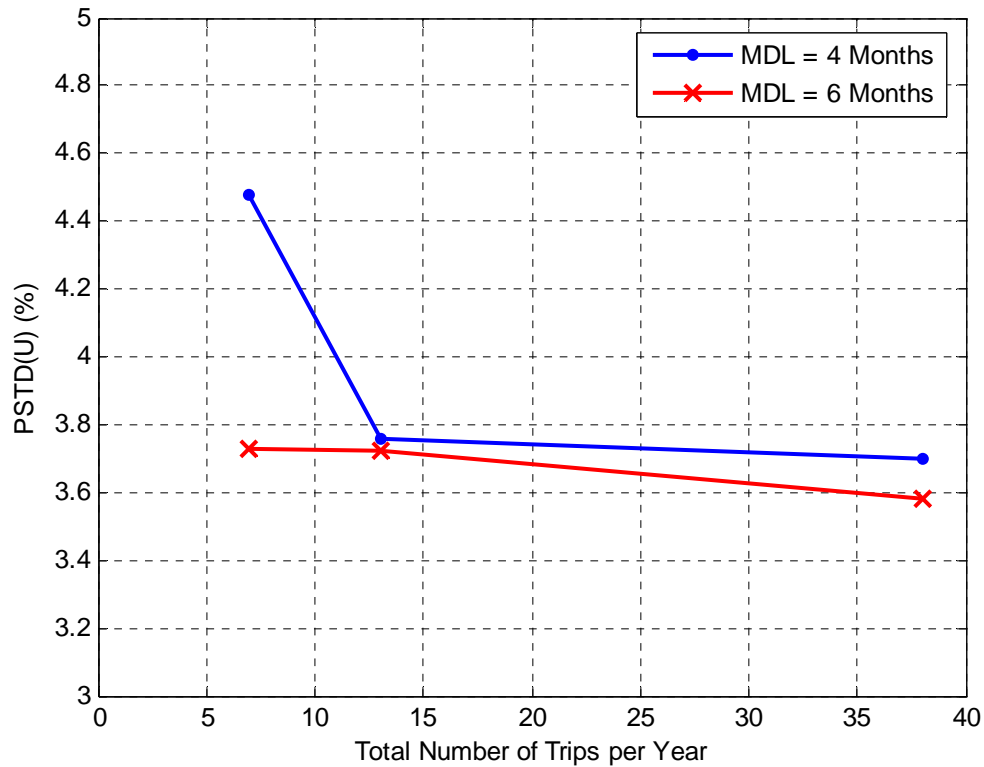


Figure 37 –Number of Trips in the Round Robin Site Assessment Method

2. In almost all cases, the value of $PSTD(U)$ when the round robin site assessment method is used is nearly identical to the value of $PSTD(U)$ for the standard method with a full year of measured data. Only when *MDL* is 4 months and *RRMP* is 60 days is the uncertainty in the predictions using the round robin site assessment method significantly larger than the uncertainty for the standard method. Overall, compared to a full year of concurrent data using the standard

method, the round robin site assessment method performs nearly equivalently well.

The results are also summarized in Table 5, which shows the values of $PSTD(U)$ in Figure 35.

Round Robin Measurement Period (Days)	Measured Data Length (Months)		
	4	6	12
10	3.70	3.58	-
30	3.76	3.72	-
60	4.48	3.73	-
Standard Method	5.12	4.75	3.63

Table 5 - $PSTD(U)$ for Round Robin Site Assessment Method and Standard Method

The round robin site assessment method appears to be extremely effective at reducing $PSTD(U)$ for a given value of MDL less than 1 year. Moreover, $PSTD(U)$ for the round robin site assessment method is often very similar to $PSTD(U)$ when a full year of measured data is used.

4.1.3 Summary of Mean Wind Speed Predictions

Figure 34 and Figure 35 indicate that the magnitude of the uncertainty of the predictions, $PSTD(U)$, is significantly larger than the magnitude of the accuracy of the predictions, $RMSE(U)$. The result is that the accuracy of all predictions are essentially equivalent, as small differences in $RMSE(U)$ are negligible compared to the magnitude of $PSTD(U)$. The various methods and parameter values can then be compared strictly in terms of the values of $PSTD(U)$.

The overall point is that the round robin site assessment method provides uncertainty values comparable to a full year of measured data in almost all cases, and so the two methods are interchangeable in terms of the uncertainty of the predictions. This

equivalence is the primary result of this analysis; namely, the round robin site assessment method, in which multiple sites are evaluated in a single year, yields comparable prediction uncertainty to a full year of measured data. The implication of these results is discussed further in Section 5.0.

4.2 Prediction of k

All of the results in this Section relate to the prediction of k , and both $RMSE(k)$ and $PSTD(k)$ of the predictions are discussed.

4.2.1 Accuracy of the Prediction of k

The plot in Figure 38 shows the results for $RMSE(k)$ across all data sets for the two data measurement methods, and for various values of MDL and $RRMP$. The results for the standard method are labeled as such, and the results for the round robin site assessment method are labeled by their respective values of $RRMP$. Note that $RMSE(k)$ is less than 2% in all cases. In all cases, a smaller value of $RMSE(k)$ corresponds to a better result. Also, the standard method has data for a value of MDL of 12 months, whereas the round robin site assessment method does not.

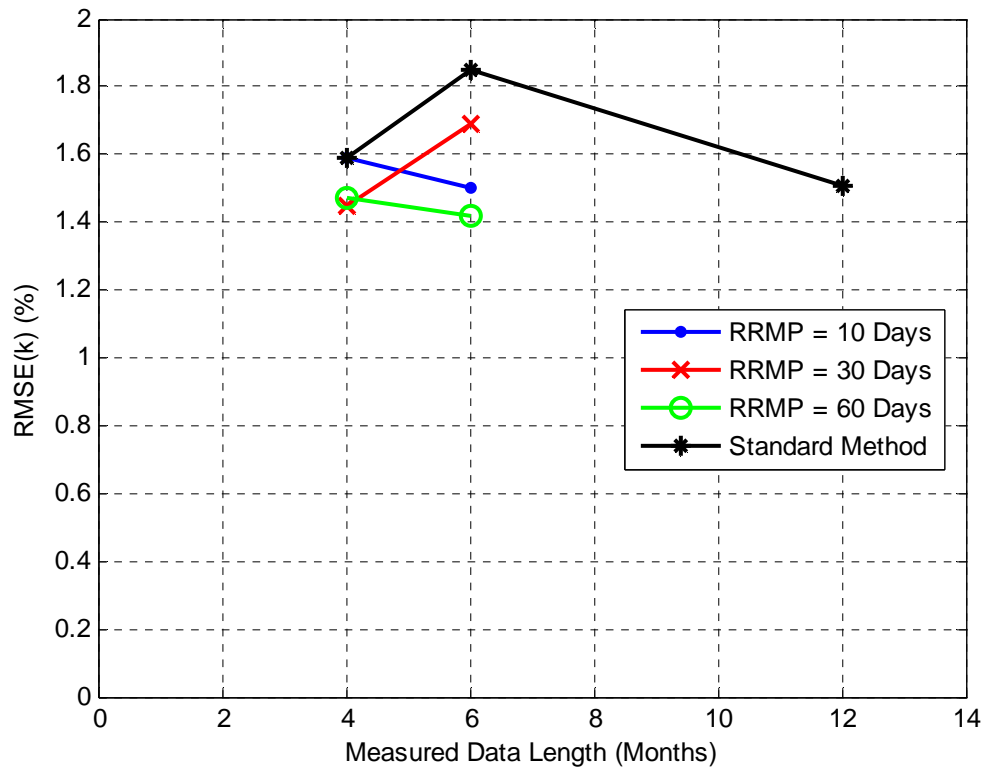


Figure 38 – Accuracy of the Predictions of k

The two questions raised at the beginning of Section 3.0 can again be used to analyze the results.

1. The round robin site assessment method uniformly reduces $RMSE(k)$ relative to the standard method using the same value of MDL , in some cases dramatically so. There does not appear to be a strong pattern with regards to the value of MDL or $RRMP$.
2. The round robin site assessment method has mixed results relative to using a full year of measured data. In four of the six cases, the round robin site assessment method reduces the value of $RMSE(k)$ compared to a full year of measured data. There does not seem to be a pattern with regards to the value of MDL or $RRMP$.

However, a value of $RRMP$ of 60 days is the only instance where the error is reduced for both values of MDL .

The results are also summarized in Table 6, which shows the values for $RMSE(k)$ from Figure 38.

Round Robin Measurement Period (Days)	Measured Data Length (Months)		
	4	6	12
10	1.59	1.50	-
30	1.45	1.69	-
60	1.47	1.42	-
Standard Method	1.59	1.85	1.51

Table 6 - $RMSE(k)$ for Round Robin Site Assessment Method and Standard Method

The round robin site assessment method appears to improve $RMSE(k)$, relative to the standard method with a measured data set of the same length. When the round robin site assessment method is compared to the standard method with a measured data length of one year, the results are mixed, with the round robin site assessment method sometimes offering an improvement over the standard method, and other times not. While the results with a value of $RRMP$ of 60 days are best, there is no discernable pattern to indicate how the accuracy depends on $RRMP$. In general, there appears to be more randomness in the predictions of k compared to those of the mean wind speed.

4.2.2 Uncertainty of the Prediction of k

The results for $PSTD(k)$ are shown below in Figure 39. $PSTD(k)$ is used as a measure of the uncertainty in the prediction of the mean wind speed. Smaller values of uncertainty correspond to better methods. In all cases, the uncertainty of the prediction of k is between 4% and 7%. Again, the results for the standard method are labeled as such,

and the results for the round robin site assessment method are labeled by their respective values of *RRMP*.

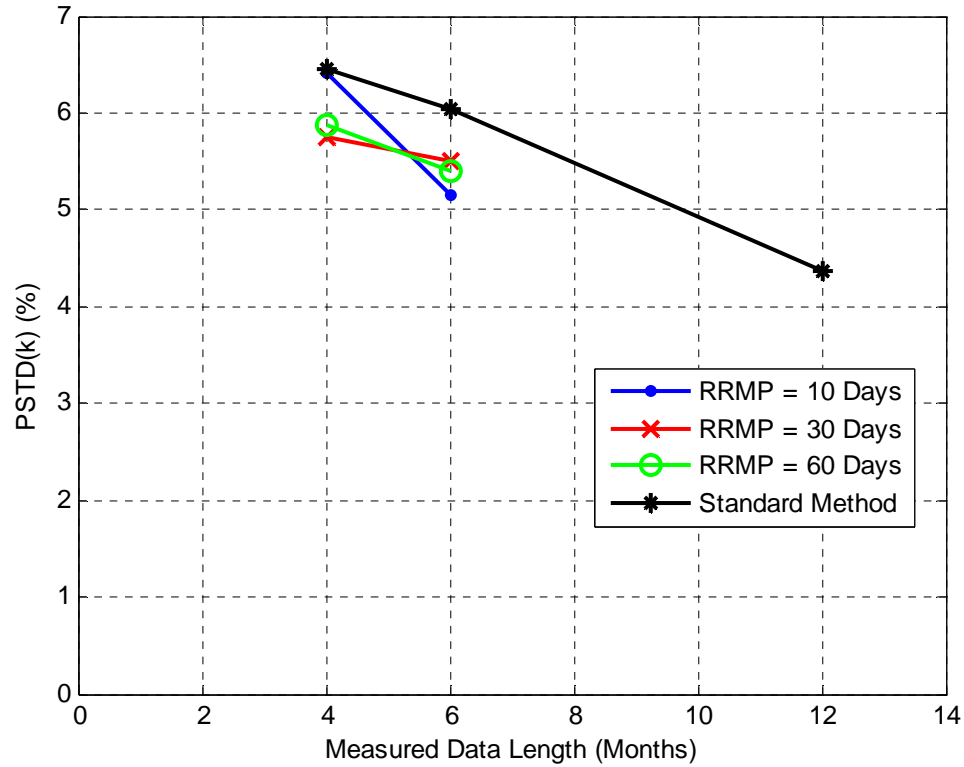


Figure 39 – Uncertainty of the Predictions of k

The two questions raised at the beginning of Section 3.0 are used to analyze the results.

1. In all cases, the round robin site assessment method reduces the average uncertainty of the prediction of k relative to the standard method for the same measured data length. There does not appear to be a pattern with regards to the value of *RRMP*. However, the uncertainty of the prediction of k uniformly decreases with increasing values of *MDL* for a given value of *RRMP*. This result is similar to the result for the mean wind speed.

2. Using a full year of measured data results in the minimum uncertainty in the prediction of k . Thus, the round robin site assessment method always results in a higher uncertainty compared to a full year of measured data. In general, the uncertainty decreases with increasing values of MDL , and so the results for MDL values of 6 months have smaller uncertainties than results for MDL values of 4 months.

The results are also summarized in Table 7, which shows the values for $RMSE(k)$ from Figure 39.

Round Robin Measurement Period (Days)	Measured Data Length (Months)		
	4	6	12
10	6.41	5.16	-
30	5.75	5.50	-
60	5.88	5.41	-
Standard Method	6.46	6.04	4.37

Table 7 - $PSTD(k)$ for Round Robin Site Assessment Method and Standard Method

The round robin site assessment method appears to be effective at reducing $PSTD(k)$ for a given measured data length. However, the $PSTD(k)$ is minimized when a full year of measured data is used. Overall, while the round robin site assessment method causes the uncertainty of the prediction of k to decrease in general, the use of measured data lengths less than one year still results in increased uncertainty.

4.2.3 Summary of Mean Wind Speed Predictions

Figure 38 and Figure 39 indicate that the magnitude of the uncertainty of the predictions, $PSTD(k)$, is significantly larger than the magnitude of the accuracy of the predictions, $RMSE(k)$, which is also the case for the mean wind speed predictions. Once again, the accuracy of all predictions are essentially equivalent, as small differences in

$RMSE(k)$ are negligible compared to the magnitude of $PSTD(k)$. The various methods and parameter values can then be compared strictly in terms of the values of $PSTD(k)$.

Unlike the case with the mean wind speed, the uncertainty of the predictions of k using the round robin site assessment method are larger than the uncertainty when using a full year of measured data. The implication of these results is discussed further in Section 5.0.

5.0 Conclusions and Recommendations

The results and discussion from Section 4.0 can be used to summarize the findings in this investigation of the round robin site assessment method, and to provide a basis for determining when and how the round robin site assessment method should be employed. This investigation used the root-mean-square of the percentage error and the pooled standard deviation of the percentage error of the predictions of the mean wind speed and k as metrics to determine the accuracy and uncertainty of the two measurement methods for various parameters. The major findings of this Chapter are discussed below, followed by general recommendations for how the round robin site assessment method can be implemented.

5.1 Choice of the Round Robin Measurement Period

- The value of $RRMP$ has a pronounced effect on the uncertainty of the prediction of the mean wind speed as decreasing $RRMP$ reduces the uncertainty of the predictions. However, decreasing $RRMP$ also dramatically increases the total number of trips required to move the measurement device over the course of one year. This can result in larger fuel costs and increased person-hours of labor.

There are diminishing returns associated with decreasing the *RRMP*, such that there is likely an optimum point at which the uncertainty of the predictions is low but the number of trips required to move the device is not prohibitive.

- The particular value of the *RRMP* appears to have no discernable effect on the accuracy of the predictions of the mean wind speed and k , as well as the uncertainty of the prediction of k , as long as the round robin site assessment method is being used. Any of the three values of *RRMP* could result in better or worse results relative to the other two possibilities.
- Overall, a reasonable choice for the value of *RRMP* when three sites are being assessed in a single year, and so *MDL* is 4 months, is approximately 30 days. When two sites are being assessed in a single year, and so *MDL* is 6 months, then a value for *RRMP* of 60 days seems appropriate.

5.2 Choice of the Measured Data Length

- When using the round robin site assessment method, the accuracy of the predictions of both the mean wind speed and k appears to have a weak dependence on the measured data length. In some cases, increasing the measured data length results in increased accuracy, and in other cases it resulted in decreased accuracy. For the standard method, increased measured data length generally results in increased accuracy, which is to be expected based on most previous MCP investigations. Thus, based strictly on the accuracy of the predictions, two or three site round robin measurement strategies appear to be equally effective compared to each other.

- The uncertainty of the predictions of the mean wind speed and k has a strong dependence on the measured data length. In all cases, whether using the round robin site assessment method or the standard method, increasing the measured data length results in decreased uncertainty in the predictions for a given value of *RRMP*.

5.3 Comparing Methods with Equal Measured Data Length

- When predicting the mean wind speed and k , the round robin site assessment method improves the accuracy of the predictions compared to the standard method when the same measured data length is used, in all cases.
- Furthermore, when predicting the mean wind speed and k , the round robin site assessment method reduces the uncertainty of the predictions compared to the standard method when the same measured data length is used, in all cases.
- Whenever multiple sites are going to be measured in a single year using a portable measurement device, the round robin site assessment method should be employed (assuming the sites are close enough together for logistical reasons). The round robin site assessment method increases the accuracy and decreases the uncertainty of the predictions of the mean wind speed and k , on average.

5.4 Comparing Methods to 1 Year of Measured Data

- The accuracy of the round robin site assessment method compares favorably with the standard method when an entire year of data is measured at each site. On average, the accuracy of the predictions is better for the round robin site assessment method than for the standard method with an entire year of concurrent

data, although the difference is small. Compared to the magnitude of the uncertainty of the predictions, the differences in the accuracy are negligible, and so the round robin site assessment method and the standard method with a full year of measured data result in equivalent accuracy.

- For the predictions of the mean wind speed, the round robin site assessment method results in uncertainty values that are equivalent to the uncertainty for the standard method when a full year of data is used. For the prediction of k , a full year of measured data using the standard method results in the lowest uncertainty of the predictions.

5.5 Recommendation for Implementing the Round Robin Site Assessment Method

The round robin site assessment method can dramatically alter the nature of wind energy site assessment. The traditional site assessment process entails measurement of the wind speed for one year using a met tower, whereas in the round robin site assessment method the wind resource is measured at multiple sites in a year using a single ground-based device. The results indicate that the accuracy and the uncertainty of the prediction of the mean wind speed for the round robin site assessment method are equivalent to using a full year of measured data in the standard method. For the prediction of k , the accuracy is likewise equivalent, but the uncertainty is somewhat higher using the round robin site assessment method. On the other hand, the contribution of uncertainty of k to the overall uncertainty in energy production is generally very small relative to the uncertainty in the mean wind speed, and so this slight increase is negligible in the larger process of estimating the overall energy production uncertainty in the site assessment process [85].

There is an additional and significant advantage to using the round robin site assessment method compared to the traditional site assessment process using a met tower: the lack of shear extrapolation due to the use of ground-based devices for wind speed measurement. Typically shear extrapolation is the largest form of uncertainty in the site assessment process, and its elimination reduces the overall uncertainty in the estimate of the long-term hub height wind resource, often to a significant extent [16],[85]. This point is also discussed in Chapter III.

From a broad perspective, taking into account the entire site assessment process, and all the component uncertainties, these results have dramatic consequences. The round robin site assessment method results in an overall reduction in the uncertainty of the estimate of the long-term hub height wind resource, while allowing for multiple sites to be assessed in a single year. While this is a fundamental departure from the standard site assessment process, the results in this Chapter indicate that there is little downside to using the round robin site assessment method in terms of the accuracy and uncertainty of the predictions, and there is tremendous upside in terms of the rapidity of the site assessment and the reduced overall uncertainty due to the lack of shear extrapolation.

A reevaluation of the traditional site assessment process seems appropriate. Rather than continue to evaluate the wind resource using met towers, a process hindered by shear extrapolation uncertainty and one year measurement lengths, ground-based devices can be employed to dramatically increase the efficiency and decrease the uncertainty of site assessment. Future wind resource assessment campaigns should give strong consideration to utilizing the round robin site assessment method.

CHAPTER VI

THE SHORT-TERM SHEAR MEASUREMENT STRATEGY

1.0 Introduction

One of the primary goals of wind energy site assessment is the characterization of wind shear. The importance of wind shear determination for wind turbine siting is noted many times [87],[88],[89]. These authors and others note that there are numerous reasons that the wind shear should be accurately determined at a specific site [90]. These include:

- Accurate wind speed predictions and subsequent energy production estimates.
- Minimization of potential wind turbine damage in high wind shear sites.

For the purposes of energy production estimation, the estimate of the wind resource at the hub height of a wind turbine is of critical importance. In wind energy site assessment, the measurement height of a met tower is usually positioned significantly below the hub heights of modern wind turbines (~50 m), which typically range from 70 m to 100 m. Shear extrapolation is also often the largest source of error and uncertainty that arises when evaluating the wind resource, and so there is a clear need to improve the accuracy of hub height wind resource estimates using shear extrapolation [16],[85].

1.1 Background of Shear Modeling for Wind Energy Applications

As discussed in Chapter II, Section 6.0, shear extrapolation is a critical component of site assessment. It is often a large source of error, and there is strong motivation for improved methods of shear extrapolation. Furthermore, errors in the estimation of the wind resource propagate through the calculation of the energy production, which results

in even larger errors in the energy production estimate. In fact, any error in the estimation of the wind resource results in approximately twice the error in the energy production estimate [85].

1.2 Wind Resource Measurement Approaches

While ground-based devices are becoming more commonly used for wind resource measurement, it is often not feasible to deploy a SODAR or LIDAR at a site for a full year, despite the clear advantage of hub height measurements. These devices are still quite expensive, so if multiple sites must be assessed, it could become prohibitively expensive to use ground-based devices exclusively. SODARs are also noisy, which may preclude their deployment at certain sites, at least for long periods of time. Finally, a site may already have a met tower installed, making the presence of a SODAR or LIDAR at the site for a full year redundant. Regardless, a met tower is often the only practical long-term method for site assessment.

This Chapter assumes that ground-based devices produce unbiased measurements equivalent to those that would be measured by a cup anemometer, as discussed in Chapter II, Section 2.0.

2.0 Scope and Objectives

This Chapter presents methods for improving the estimate of the hub height wind resource from met tower data through the use of measurements from ground-based devices. The methods leverage the two major advantages of these devices: their portability and their ability to measure at the wind turbine hub height. Specifically, the methods rely on augmenting the one year of met tower measurements with short-term

measurements from a ground-based device. The goal is to improve the accuracy of shear extrapolation from met tower data without the need to deploy a ground-based device at a site for a long period of time.

2.1 Wind Shear Modeling

The power law and the log law are the two most commonly used models for extrapolating wind speeds to higher heights at a site. This Chapter considers both models. Elkinton et al. show that the two models perform equivalently in shear extrapolation predictions on average, although at any particular site one model may be better than another [16]. The power law is shown in Eq. 52 and a version of the log law is shown in Eq. 53 [21]. This particular version of the log law assumes neutral stability and no displacement height, and so it is a simplification in many cases. The implications of these assumptions are discussed later.

$$\frac{U(z)}{U(z_r)} = \left(\frac{z}{z_r} \right)^\alpha \quad \text{Eq. 52}$$

$$\frac{U(z)}{U(z_r)} = \frac{\ln(z / z_0)}{\ln(z_r / z_0)} \quad \text{Eq. 53}$$

- $U(z)$ is the wind speed at height z .
- $U(z_r)$ is the reference wind speed at the reference height z_r .
- α is the power law exponent.
- z_0 is the surface roughness height.

The shear parameters can be calculated when the wind speed is measured at two heights. This Chapter uses Eq. 54 to calculate α , and Eq. 55 to calculate z_0 .

$$\alpha = \frac{\ln(U_2 / U_1)}{\ln(h_2 / h_1)} \quad \text{Eq. 54}$$

$$z_0 = \left(\frac{h_1^{U_2/U_1}}{h_2} \right)^{\frac{1}{U_2/U_1 - 1}} \quad \text{Eq. 55}$$

- h_1 and h_2 are the two measurement heights, with $h_2 > h_1$.
- U_1 and U_2 are the mean wind speeds at h_1 and h_2 , respectively.

It is important to emphasize that U_1 and U_2 in Eq. 54 and Eq. 55 are the mean wind speeds measured at each height. Unless otherwise stated, all wind speed variables in this Chapter can be assumed to be the mean value of 10-minute or 1-hour wind speed data over a period of time, such as 10 days or 1 year.

For the models shown in Eq. 52 and Eq. 53, the shear parameters depend only on the measurement height and wind speed. In general, however, the shear parameters may also depend on the surface roughness and the stability, among others [91],[92]. Therefore, more complex methods for wind shear modeling are also possible. These models may account for stability, utilize local topography, and estimate the shear parameters from multiple direction sectors. Numerical models such as WAsP may also be utilized [93]. The possibility of using these more complex models is discussed later.

2.2 Selected Data Sets

Long-term SODAR or LIDAR data near met towers are not plentiful. Consequently, tall tower data are used as a surrogate for long-term data from a ground-based device in this Chapter. Tall towers are met towers with upper measurement heights significantly higher than those of standard met towers. These upper measurement heights are typically

on the order of 80-100 m, which are much higher than standard met towers, which typically have upper measurement heights near 50 m.

This Chapter uses data from tall towers that have three measurement heights, with the highest height at approximately the hub height of a modern turbine, and the lower two heights at approximately the measurement heights of standard met towers. The data from the lower two measurement heights can be considered to be the data that one would obtain from a standard met tower. The data from the upper measurement height can be used as a proxy for ground-based device data. As discussed above, recent advances using ground-based device result in very good agreements between measurements from these devices and cup anemometers on tall towers, and so it is assumed that the tall tower data are very similar to what would be measured if a ground-based device is used instead. Tall tower data has the further advantage that any shear extrapolation method can be verified with the data from the highest height.

Ten data sets, each with one year of wind speed data at three measurement heights, are used in this analysis. These data sets are compiled from a regional database of wind speed data for thirteen states in the central United States [94]. The location, surrounding terrain, and measurement heights of each data set are presented in Table 8. The terrain is classified as either “Flat, No Trees,” “Hills, No Trees,” or “Forested”.

These data sets are comprised of either 10-minute or hourly wind speed data. At each site, two anemometers are positioned at each of the measurement heights. For each 10-minute or hourly average and each height, the higher of the two measured wind speeds from the anemometers is selected as the wind speed at that height, to combat the effects of tower shadow [68]. The data are also subjected to quality control tests to attempt to

remove any data corrupted by icing or other issues [70]. Overall, there is reasonable confidence in the quality of the data, and the uncertainty in the estimate of the mean wind speed is likely on the order of 2-3% standard uncertainty, as discussed in Chapter III. Nonetheless, tower shadow effects and other obstructions are difficult to identify in many cases, and so there is still some potential for the data to be corrupted [86]. The majority of the data sets do not contain sufficient temperature data for stability to be considered.

Site Name	State	Description	h1 (m)	h2 (m)	h3 (m)
Boulder	CO	Hills, No Trees	20	50	80
Detroit Lakes	MN	Forested	30	50	85
Fountain	MN	Forested	30	60	90
Glenmore	WI	Flat, No Trees	37	60	83
Hatfield	MN	Flat, No Trees	30	60	90
Hilman	MN	Forested	30	60	90
Hobart	OK	Flat, No Trees	40	70	100
Isabella	MN	Forested	30	50	75
Marshall	MN	Hills, No Trees	30	60	90
St. Killian	MN	Hills, No Trees	30	60	90

Table 8 – Data Set Information

Again, for each data set, the lower two measurement heights are considered to be standard met tower data, while the upper measurement height is considered to be data taken from a ground-based device.

2.3 Motivation for Improved Wind Shear Extrapolation Methods

The need for improved shear extrapolation methods can be highlighted using the statistics from the data sets used in this Chapter, shown in Table 9. For each data set, the mean wind speeds at the lower two heights, U_1 and U_2 , are calculated (the second and third column of Table 9). Next, the power law exponent and roughness length are calculated for each site, using Eq. 54 and Eq. 55 (the fourth and fifth column). The calculated power law exponent and roughness length are then used to predict the mean wind speed, U_3^* , at the highest height, h_3 , using Eq. 52 and Eq. 53 (the seventh and ninth

column). h_2 is used as the reference height and U_2 is used as the reference wind speed. From now on, predicted quantities are labeled with a superscript *. The predicted mean wind speed is then compared to the actual calculated mean wind speed, U_3 , at h_3 (the sixth column). Finally, the percentage error of the prediction of the mean wind speed at h_3 is calculated (the eighth and tenth column).

Site Name	U1 (m/s)	U2 (m/s)	Alpha	z ₀	Actual U3 (m/s)	Predicted U3 (m/s) - Power Law	% Error Power Law	Predicted U3 (m/s) - Log Law	% Error Log Law
Boulder	3.9	4.6	0.19	0.14	4.8	5.1	6.0	5.0	5.0
Detroit Lakes	4.4	5.4	0.40	3.18	6.0	6.6	11.7	6.4	7.6
Fountain	5.1	6.0	0.24	0.65	6.7	6.6	-0.4	6.6	-1.6
Glenmore	5.8	6.7	0.31	1.77	7.3	7.4	0.5	7.3	-0.6
Hatfield	5.9	7.0	0.25	0.73	7.9	7.7	-1.7	7.6	-2.9
Hilman	3.8	4.8	0.33	2.11	5.9	5.6	-5.3	5.4	-7.3
Hobart	6.7	7.5	0.21	0.42	8.1	8.1	-0.6	8.0	-1.2
Isabella	3.9	5.1	0.53	5.80	6.1	6.3	4.4	6.1	0.1
Marshall	6.4	7.7	0.25	0.82	8.2	8.5	4.2	8.4	2.8
St. Killian	6.1	7.9	0.38	3.06	7.9	9.2	16.2	9.0	13.1

Table 9 – Mean Wind Speed Predictions

The eighth and tenth columns of Table 9 indicate that significant error can occur in the prediction of the mean wind speed when using shear extrapolation. The root-mean-square of the error (RMSE) is 7.1% using the power law, and 5.7% using the log law.

The average value of the percentage errors is 3.5% and the standard deviation is 6.5% using the power law. Using the log law, the average value of the percentage errors is 1.5% and the standard deviation is 5.8%. Moreover, errors in the estimation of the mean wind speed disproportionately affect errors in the calculation of the energy production. Overall, the results of Table 9 demonstrate the need for an improved method for shear extrapolation.

It is also worth noting that the error in the prediction of U_3^* is consistently small for the sites with terrain classified as “Flat, No Trees”. For the sites with more complex terrain, the errors in the predictions tend to be larger. This is not surprising, as complex

terrain can greatly affect the shear profile, and cause profiles that are not as easily fit with the models. Another pattern is that the calculated values of α and z_0 tend to be larger at sites with “Forested” terrain. This is also a logical result, as the trees at lower heights tend to reduce U_1 relative to U_2 and therefore cause larger values of the shear parameters.

It also should be pointed out that at the St Killian, Minnesota site, the mean wind speeds at 60 m and 90 m are nearly identical. This is a curious result, and helps explain the large prediction error for this site. To date, no explanation has been determined for this result. If this site is ignored, the RMSE using the power law would be reduced to 5.2%, which is still a substantial amount of error.

A more complex method for extrapolating wind speeds is also considered, in which the shear parameters are calculated for each of eight direction sectors. The purpose of this method is to account for varying topography and roughness with direction, and therefore calculate more appropriate shear parameters for each direction sector. Despite the logic of this method, the results are nearly identical to the methods described above that did not sort the data by direction. This method is not utilized in later analysis.

In general, the power law and log law methods are not necessarily the most advanced methods for performing wind shear extrapolation. On the other hand, they are often the only available methods. Accurate temperature data at multiple heights is not generally available for stability considerations. Furthermore, these models are very commonly used by wind energy developers and consultants [93]. Therefore, these models are used in later analyses for comparison, and so the predictions from Table 9 are the baseline predictions.

2.4 Objectives

The goal of the research is to develop methods that can be applied to wind resource measurement campaigns in order to improve the accuracy and precision of wind shear extrapolation predictions. Two distinct scenarios are analyzed in this Chapter. Each represents a situation in which short-term hub height measurements may be able to improve the shear extrapolation estimate. They are:

- Scenario 1: Short-term hub height measurements from a ground-based device are used in conjunction with a full year of data from a standard met tower, with two measurement heights. In this scenario, the short-term hub height data can be used to adjust the calculated shear parameter from the lower met tower measurement heights.
- Scenario 2: In this scenario, there is only a single lower measurement height. Once again, short-term hub height measurements from a ground-based device are used. While standard met towers that measure at two heights are cumbersome and difficult to install, one could instead utilize “jack-up” towers or other shorter towers that are much easier to deploy. The drawback of these towers is that they are shorter than standard met towers. In this scenario, it is assumed that these portable towers can only measure at a single height. The short-term hub height measurements are therefore the only data available for estimating the shear characteristics at the site.

3.0 Data Analysis

The data sets in Table 8 are used to explore improved methods for shear extrapolation. Two scenarios are considered: a standard met tower with two measurement heights, and a shorter portable tower with a single measurement height. For each scenario, short-term hub height measurements are used to improve the shear extrapolation. This Section describes the analysis that is performed for each scenario.

3.1 Primary Analysis Parameters

In the analysis of each scenario, two important parameters are considered. These parameters define how the short-term hub height measurements are performed. These are:

1. Total short-term measurement length, N_{Days} . This parameter defines the total length of time, measured in days, that the short-term measurement is performed at the site using the ground-based device. This parameter is varied from a minimum of 10 days to a maximum of 100 days.
2. Total number of measurement segments, N_{seg} . This parameter indicates the total number of measurement segments that constitutes the total short-term measurement length. One segment and two segments are considered. For one segment, a single continuous measurement with the ground-based device is carried out for a length of N_{Days} . When two segments are used, then two discontinuous measurements are performed, each with a length of one half of N_{Days} . The two measurement periods are separated by 180 days.

This parameter is explored due to the potential for variations in the shear profile over the course of the year to affect the results. The shear profile at a site

is not constant during the year. Instead, seasonal variations can cause the shear profile to vary substantially in time. Figure 40 shows the monthly power law exponent for five of the sites listed in Table 8. While not shown, the surface roughness length also displays pronounced monthly variations. These variations can be caused by a number of factors, including seasonally dependent stability characteristics or prevailing wind direction at the site. The causes of the variations in Figure 40 are not investigated due to the lack of temperature data at the sites, which therefore precludes the stability from being evaluated.

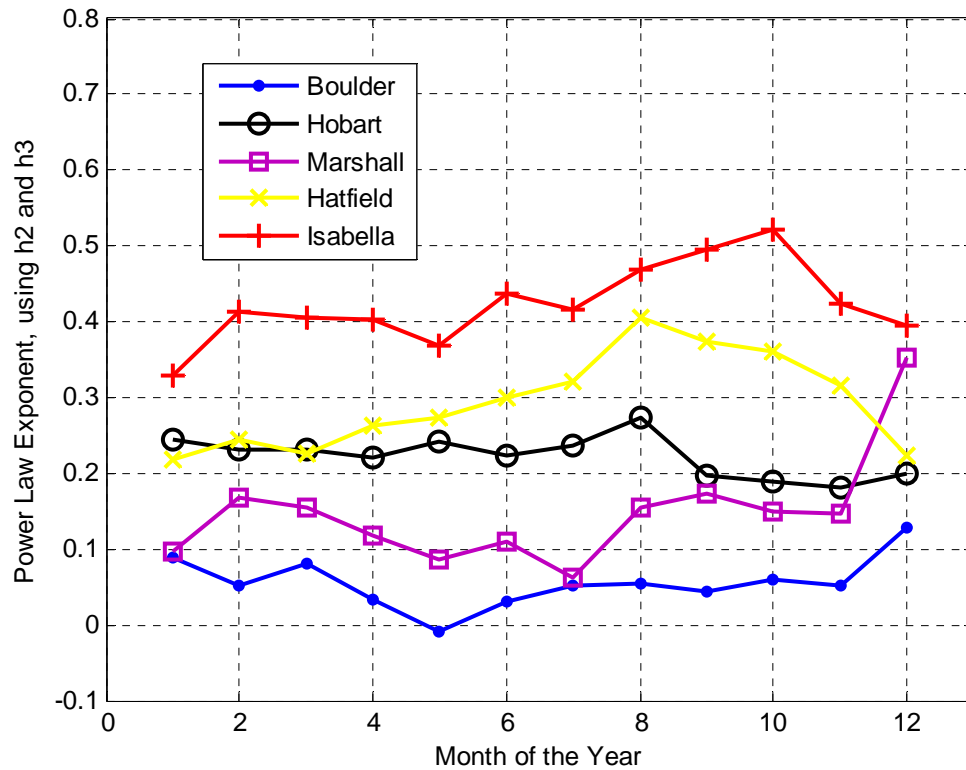


Figure 40 – Monthly Power Law Exponent

Regardless of the source of the variations in the shear characteristics at a site, they can cause significant effects when short-term data are used for shear extrapolation. Two measurement segments can potentially help average out these

variations and provide a better representation of the shear profile at a site than a single measurement segment.

3.2 Choice of Wind Shear Model

For all of the data analysis, the power law is used exclusively, and the log law is not used, despite the fact that the log law performs slightly better in the predictions in Table 9. The power law is chosen because the calculation of the power law exponent, α , is more robust than the calculation of the surface roughness height, z_0 . This can be seen by comparing Eq. 54 and Eq. 55. A singularity occurs in Eq. 55 as U_2/U_1 goes towards 1. No such singularity occurs in the calculation of α . Figure 41 shows the surface roughness height as a function of U_2/U_1 , when $h_2 = 50$ m, and $h_1 = 30$ m. Clearly, as U_2/U_1 approaches 1, a singularity in z_0 occurs, and since z_0 is in the denominator twice in Eq. 53, this can cause shear extrapolation using the log law to have widely varying results if U_2/U_1 is close to 1. Overall, both methods display nearly identical results in many cases, but for a few sites this issue in calculating z_0 causes difficulty in the shear extrapolation.

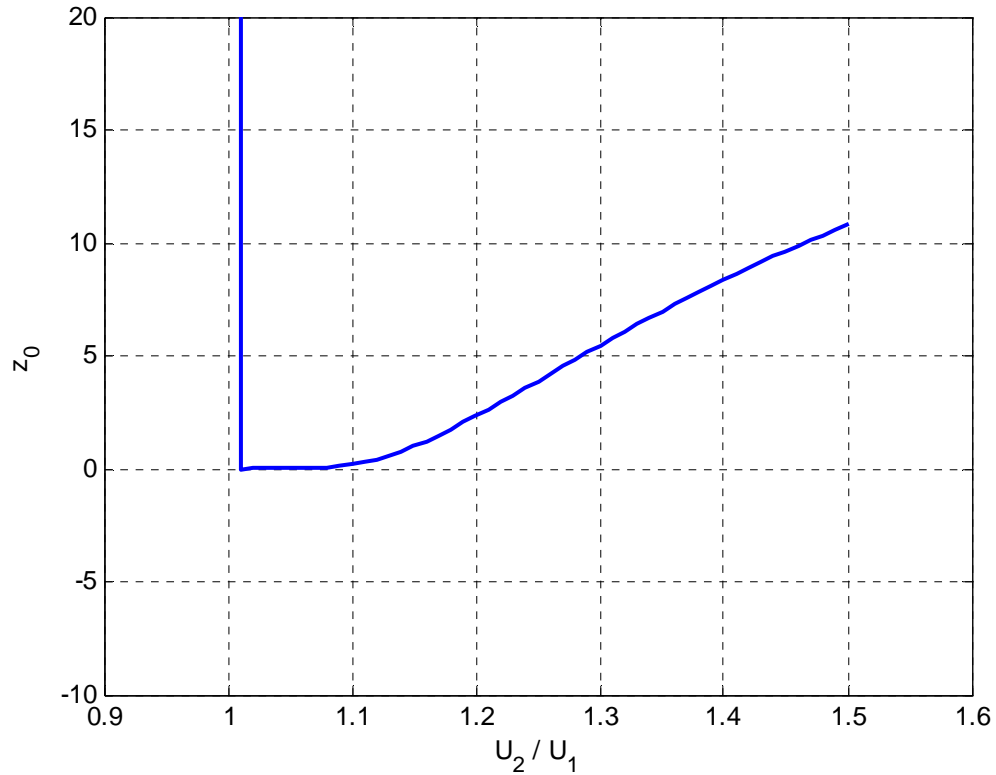


Figure 41 - z_0 versus U_2/U_1

3.3 Scenario 1 Analysis

In scenario 1, a standard met tower, with two measurement heights positioned well below a turbine hub height, measures the wind resource at a site for an entire year. The power law exponent that is calculated using the full year of data from the two lower met tower measurement heights, h_1 and h_2 , is labeled α_L (The subscript “L” indicates that α is based on data from the “lower” heights).

In order to improve the shear extrapolation estimates, a shear correction factor (*scf*) for α_L can be calculated using the short-term hub height measurement from the ground-based device. The overall goal of shear extrapolation is to accurately estimate the wind resource at the turbine hub height. Ideally, the shear relationship between the wind speed at h_2 , and the wind speed at h_3 would be known perfectly. Since the wind speed cannot

be measured at h_3 using a met tower, however, this relationship is usually approximated with the shear relationship between h_1 and h_2 . For a variety of reasons, the shear relationship between h_1 and h_2 may differ from the shear relationship between h_2 and h_3 . An obvious possibility for a discrepancy is trees and other obstructions, which can reduce the wind speed at the lowest measurement height. In this case, the power law exponent that is calculated using data from h_1 and h_2 is larger than the true value, causing an overestimation of the mean wind speed at h_3 . There are a variety of other factors that could lead to a discrepancy as well, causing either over- or under-prediction of the mean wind speed at h_3 .

By using a shear correction factor, the aim is to correct for the potentially different shear relationships between h_1 and h_2 , and h_2 and h_3 . While the shear relationship between h_2 and h_3 is only calculated for a short period of time in this Chapter, the hope is that the shear correction factor adequately scales the year long power law exponent, α_L .

As stated previously, the highest measurement height tall tower data can be used as a proxy for the hub height measurement data from the ground-based device. The equation for the shear correction factor is given in Eq. 56.

$$scf = \alpha'_H / \alpha'_L \quad \text{Eq. 56}$$

- scf is the shear correction factor.
- α'_H is the power law exponent calculated using Eq. 54, and the short-term data from the ground-based device measurement height and the upper met tower height (h_3 and h_2). The apostrophe indicates that the power law exponent is based on a short-term period of data of length N_{Days} , and the subscript “ H ” indicates that α is based on data from the “higher” heights.

- α'_L is the power law exponent calculated using Eq. 54, and the short-term data from the two lower met tower heights (h_1 and h_2). The apostrophe again indicates that the power law exponent is based on a short-term period of data of length N_{Days} .

The shear correction factor is then used to scale α_L , the power law exponent using the full year of wind speed data from h_1 and h_2 . The corrected power law exponent, α_C , is calculated using Eq. 57.

$$\alpha_C = scf \cdot \alpha_L \quad \text{Eq. 57}$$

This method makes no assumptions concerning the nature of the shear profile. It is assumed to be generally applicable to any site, not just those with smooth shear profiles. It relies on a single basic assumption; namely, that there is some systematic relationship between the shear parameter calculated using the lower two heights, and the shear parameter calculated using the higher two heights. While a power law model is used in this case, this approach is applicable to any shear model that relates the wind speed at different heights.

The efficacy of the shear correction factor method is evaluated using the data sets in Table 8. The parameters, N_{Days} and N_{Seg} , are used to investigate the method. For each data set, the following steps are performed:

1. The total short-term measurement length, N_{Days} , is varied from 10 days to 100 days in increments of 10 days for $N_{seg} = 1$, and from 20 days to 100 days in increments on 20 days for $N_{seg} = 2$.

2. For $N_{seg} = 1$, non-overlapping continuous segments of wind speed data are used as the short-term measurement data set. For $N_{seg} = 2$, non-overlapping discontinuous segments of wind speed data are used as the short-term measurement data set. These discontinuous segments are separated by 180 days, and are each half the length of N_{Days} .

If $N_{Days} = 20$, then there are 18 individual short-term measurement data sets in a year, either continuous or discontinuous depending on the value of N_{seg} . The number of individual measurement segments is labeled n for convenience, and n is equal to 365 days divided by N_{Days} (rounded down). If $N_{seg} = 1$, then each of the n short-term measurement data sets is a continuous 20 day segment. If $N_{seg} = 2$, then each short-term measurement data set is comprised of two 10 day segments, separated by 180 days.

3. For each of the n short-term measurement data sets, the wind speed data at h_1 and h_2 during the short-term period are used to calculate α'_L , and the wind speed data from h_2 and h_3 during the short-term period are used to calculate α'_H .
4. The scf is calculated using Eq. 56.
5. α_C is calculated using Eq. 57.
6. The estimated mean wind speed at h_3 , U_3^* , is then calculated using α_C and Eq. 52 (where h_2 is used as the reference height and U_2 is used as the reference wind speed). There are n total predictions.
7. The percentage error for each of the n estimated values of U_3^* is calculated.
8. Then for each value of N_{Days} , the mean and standard deviation of the percentage error are calculated across the n total values of the percentage error.

The results of this analysis are the mean and standard deviation of the percentage error for the prediction of U_3 for each site, for each value of N_{Days} , and for both values of N_{Seg} . The results are presented and discussed below.

3.4 Scenario 2 Analysis

In scenario 2, a shorter portable tower with a single measurement height h_1 measures the wind resource at a site for an entire year. Thus, the tall tower data from h_2 is ignored (as opposed to Scenario 1); only the data from h_1 and h_3 are used. In this case, a year long power law exponent (α_L) cannot be calculated, since there is only a single measurement height. Instead, the power law exponent is approximated by calculating its value using the data from the ground-based device measurement height and the portable tower measurement height during the short-term period in which the ground-based device is deployed at the site. This estimated power law exponent is α'_{2H} . Again, the apostrophe indicates that the power law exponent is based on a short-term period of data, and the subscript “ H ” indicates that α is based on data from the “higher” height.

The efficacy of the Scenario 2 method is evaluated using the data sets described above. The parameters N_{Days} and N_{seg} are used to investigate the method. For each data set, the following steps are performed:

1. The total short-term measurement length, N_{Days} , is varied from 10 days to 100 days in increments of 10 days for $N_{seg}=1$, and from 20 days to 100 days in increments on 20 days for $N_{seg}=2$.
2. For $N_{seg} = 1$, non-overlapping continuous segments of wind speed data are used as the short-term measurement data set. For $N_{seg} = 2$, non-overlapping discontinuous

segments of wind speed data are used as the short-term measurement data set.

These discontinuous segments are separated by 180 days, and are each half the length of N_{Days} . Again, the number of individual measurement segments is labeled n , and n is equal to 365 days divided by N_{Days} (rounded down).

3. For each of the n short-term measurement data sets, the wind speed data from h_1 and h_3 are used to calculate α'_{2H} .
4. The estimated mean wind speed at h_3 , U_3^* , is then calculated using α'_{2H} and Eq. 52, where h_1 is used as the reference height and U_1 is used as the reference wind speed. There are n total predictions.
5. The percentage error for each of the n estimated values of U_3^* is calculated.
6. Then for each value of N_{Days} , the mean and standard deviation of the percentage error are calculated across the n total values of the percentage error.

The results of this analysis are the mean and standard deviation of the percentage error for the prediction of U_3 for each site, for all values of N_{Days} , and for both values of N_{Seg} . The results are presented and discussed below.

4.0 Results and Discussion

The results from the analysis for both scenarios are now presented. The analysis yields the mean and standard deviation of the percentage error in the prediction of U_3 , for each data set, and for the ranges of values of N_{Days} and N_{seg} . The results are then consolidated across all the data sets. First, the root-mean-square of the mean percentage error is taken across all the data sets. Second, to consolidate the standard deviation of the

percentage error for each site, a pooled estimate is used. The overall pooled standard deviation σ_P , consolidated across the data sets, is calculated using Eq. 58.

$$\sigma_P = \sqrt{\frac{\sum_{k=1}^m \sigma_k^2}{m}} \quad \text{Eq. 58}$$

The root-mean-square of the mean percentage error of the prediction of U_3 is a measure of the accuracy of the prediction. It is the average across all ten data sets. This quantity is labeled $RMSE(U_3)$, which is a function of N_{Days} and N_{seg} for both Scenario 1 and Scenario 2.

The pooled standard deviation of the percentage error of the prediction of U_3 is a measure of the uncertainty of the predictions. This quantity is labeled $PSTD(U_3)$. “PSTD” stands for the “pooled standard deviation”, where the standard deviation is the standard deviation of the percentage error at each site. $PSTD(U_3)$ is a function of N_{Days} and N_{seg} for both Scenario 1 and Scenario 2.

4.1 Scenario 1 Results

Scenario 1 utilizes a shear correction factor to adjust the year long power law exponent calculated using the met tower data, α_L . From Table 9, the RSME of the prediction of U_3 without correcting α_L is 7.1%. $RSME(U_3)$ for $N_{seg} = 1$ and $N_{seg} = 2$ is plotted in Figure 42, as a function of N_{Days} . Again, these values are consolidated across all ten data sets. The $RSME(U_3)$ value of 7.1% when α_L is not corrected is also plotted in Figure 42. This value is not a function of N_{Days} ; rather it is included as a comparison to the shear results using the method described here.

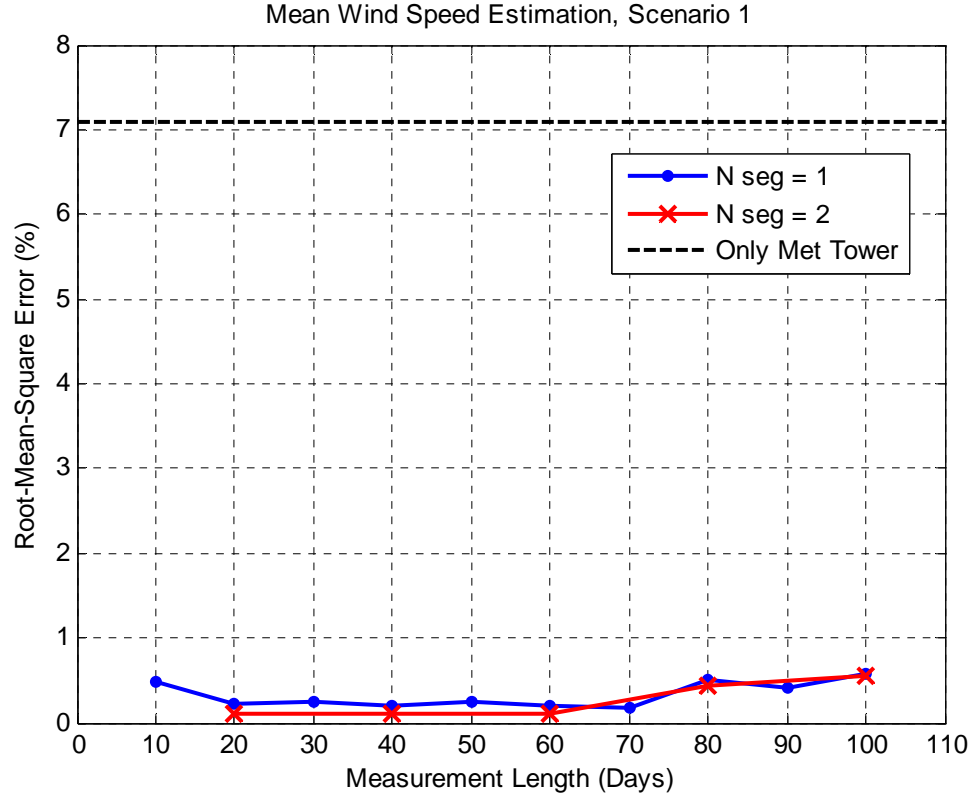


Figure 42 – Accuracy of the Predictions, Scenario 1

Several comments can be made regarding Figure 42:

- $RMSE(U_3)$ is significantly reduced when using a shear correction factor. For both $N_{Seg} = 1$ and $N_{Seg} = 2$, $RMSE(U_3)$ is less than 1.0%, for all values of N_{Days} . This is a substantial improvement over the uncorrected value of 7.1%, indicating that the shear correction factor drastically improves the accuracy of the prediction of U_3 .
- The average value of the percentage error across all data sets and all values of N_{Days} is less than 0.2%, indicating that there is almost no bias in the predictions.
- The results for $N_{Seg} = 1$ and $N_{Seg} = 2$ are nearly identical.
- The value of $RMSE(U_3)$ when using the shear correction factor is fairly independent of N_{Days} . This is not surprising, as the average of 36 predictions using 10 days of measured data should approximately equal the average of 18

predictions using 20 days of data, and so forth (they are not exactly equal due to non-linearities in the calculation of α , and other minor factors). The same wind speed data are used in all the predictions, the difference lies only in the averaging period. These results do not imply, therefore, that an arbitrarily small value of N_{Days} can be used. This point is revisited below when the uncertainty of the predictions is discussed.

The effect of using a shear correction factor can be highlighted using Figure 43. It indicates that the value of the shear correction factor is less than 1.0 for the six sites in Table 9 that over-predict of the mean wind speed, and it is greater than 1.0 for the four sites that under-predict the mean wind speed. This reinforces the logic behind the use of the shear correction factor, as it serves to decrease the prediction of the mean wind at sites where the mean wind speed is over-predicted, and vice-versa.

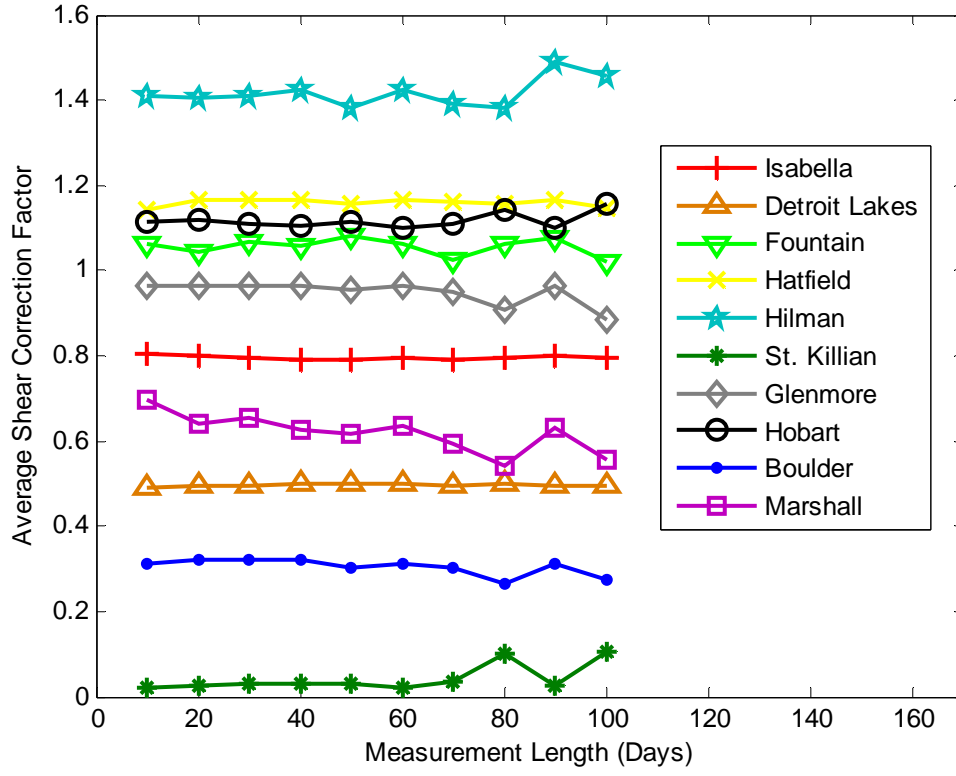


Figure 43 - Average Shear Correction Factor, $N_{Seg} = 1$, Scenario 1

While $RMSE(U_3)$ is used to measure the accuracy of the predictions, $PSTD(U_3)$ is used as a measure of the uncertainty of the predictions. $PSTD(U_3)$ for $N_{Seg} = 1$ and $N_{Seg} = 2$ is plotted in Figure 44, as a function of N_{Days} .

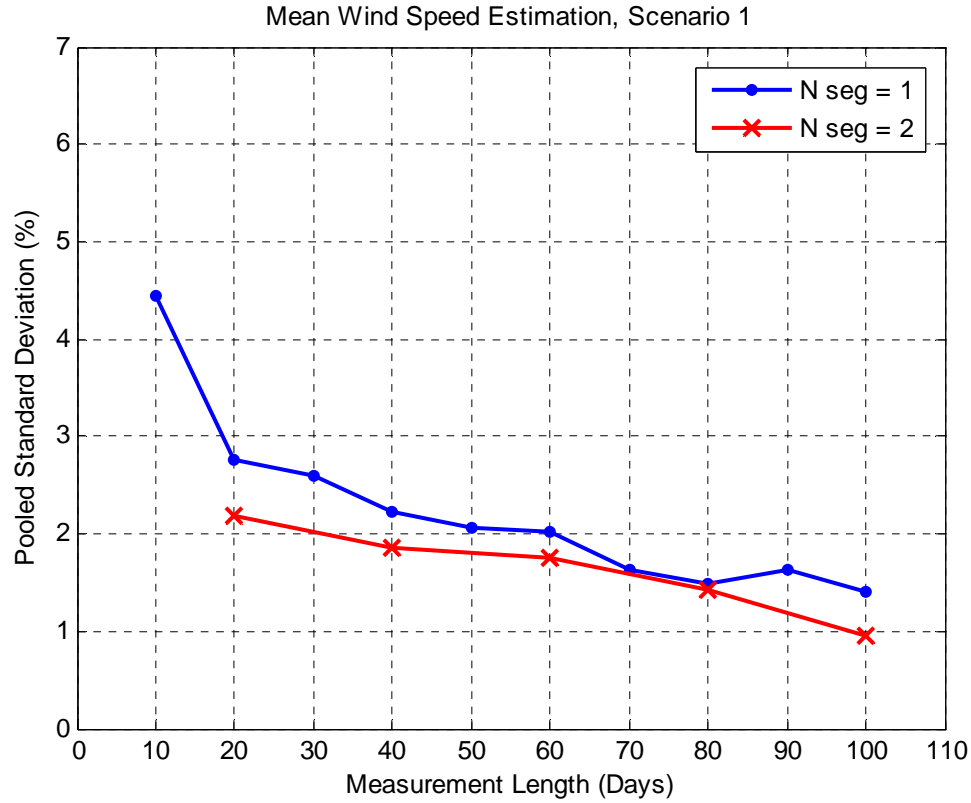


Figure 44 – Uncertainty of the Predictions, Scenario 1

Several comments can be made regarding Figure 44:

- For both $N_{Seg} = 1$ and $N_{Seg} = 2$, the uncertainty in the predictions decreases as N_{Days} increases. Even though Figure 42 indicates that the accuracy of the predictions is not affected by the value of N_{Days} , Figure 44 demonstrates that the uncertainty of the predictions does in fact depend on N_{Days} .
- Overall, it appears that higher values of N_{Days} are preferable. This is a critical result, and confirms the initial supposition that longer measurement lengths would improve the predictions. While smaller values of N_{Days} yield accurate predictions on average, the variability is high compared to larger values of N_{Days} . Thus, longer measurement lengths are indeed beneficial as it results in lower variability in the predictions, and therefore more confidence in an individual prediction.

- Some caution should be used in interpreting Figure 44. The number of samples used to calculate the standard deviation decreases as N_{Days} increase. While there are 36 samples used to calculate the standard deviation for a given site when $N_{Days} = 10$, there are only 3 samples when $N_{Days} = 100$. Figure 44 is still useful in that it indicates the variability in the predictions; there are some limitations, however, in using the results to generalize about the uncertainty of the predictions.
- The uncertainty in the predictions is somewhat lower when $N_{Seg} = 2$, compared to $N_{Seg} = 1$. This is to be expected, as the use of multiple short-term measurement segments should help average out the variability in the predictions.

4.1.1 Scenario 1 Individual Site Predictions

While the shear correction factor is highly effective on average, an actual application of this method results in a single prediction for the hub height mean wind speed at the site, which may or may not be an improvement over the prediction using only met tower data. It is therefore informative to consider each of the individual predictions for a site. This also helps elucidate the magnitude of the uncertainty values shown in Figure 44 by demonstrating the scatter in the predictions.

Figure 45 and Figure 46 show each of the predictions of the mean wind speed at the Isabella and Glenmore sites, respectively, as a function of N_{Days} , for $N_{Seg} = 1$ and $N_{Seg} = 2$. Also shown in each of the plots are the actual mean wind speed at the site and the predicted mean wind speed when only the met tower data are used to make the prediction. Several comments can be made regarding Figure 45 and Figure 46:

- For Isabella, nearly all of the predicted values of the mean wind speed using the shear correction factor are improvements over the predicted value using only met

tower data, for $N_{Seg} = 1$ and $N_{Seg} = 2$. The percentage error in the prediction of the mean wind speed for Isabella when only the met tower data are used is 4.4%.

- For Isabella, the standard deviation of the predictions using the shear correction factor is approximately 3.2% for $N_{Days} = 10$, and 1.2% for $N_{Days} = 100$, when $N_{Seg} = 1$. When $N_{Seg} = 2$, the standard deviation of the predictions using the shear correction factor is approximately 2.6% for $N_{Days} = 20$, and 1.9% for $N_{Days} = 100$. The scatter in the predictions is small relative to the error in the prediction when only the met tower data are used.

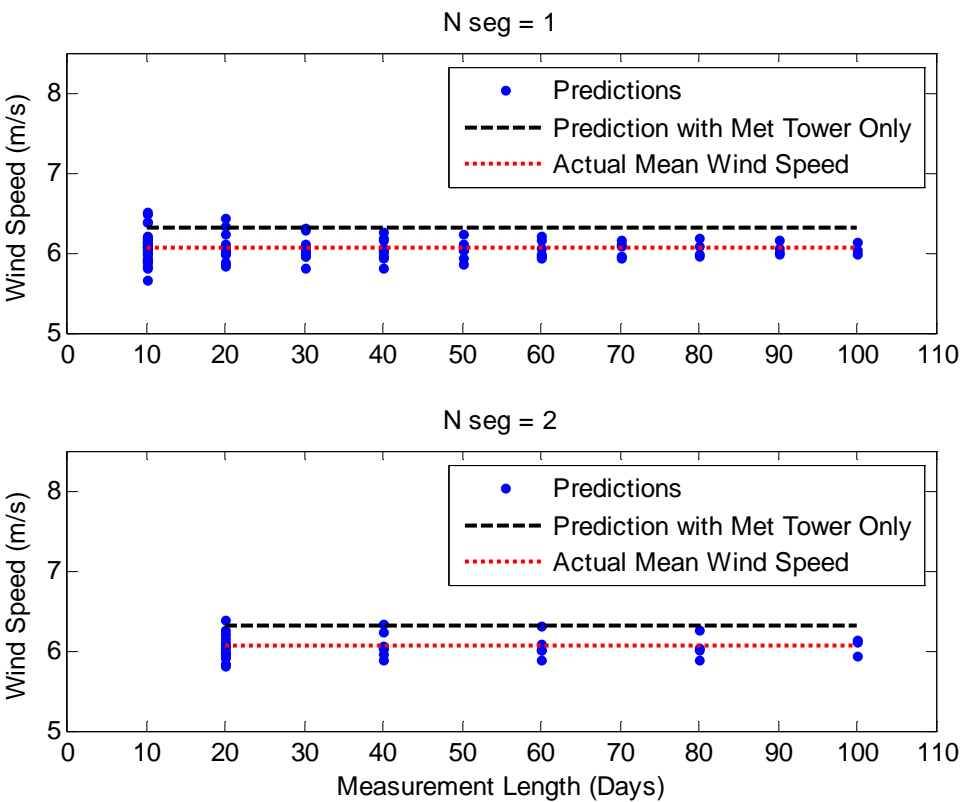


Figure 45 – Mean Wind Speed Predictions for Isabella, Scenario 1

- For Glenmore, few predictions using the shear correction factor are improvements over the predicted value using only met tower data, because the percentage error in the prediction of the mean wind speed when only the met tower data are used is

only 0.5%. The result is that most of the predictions using the shear correction factor are worse than the predicted value using only met tower data.

- For Glenmore, the standard deviation of the predictions using the shear correction factor is approximately 3.0% for $N_{Days} = 10$, and 1.5% for $N_{Days} = 100$, when $N_{Seg} = 1$. When $N_{Seg} = 2$, the standard deviation of the predictions using the shear correction factor is approximately 1.7% for $N_{Days} = 20$, and 0.6% for $N_{Days} = 100$.
- For Glenmore, while the majority of the predictions are worse than the predicted value using only met tower data, the small amount of scatter in the predictions results in most of the predictions still being close to the true value.

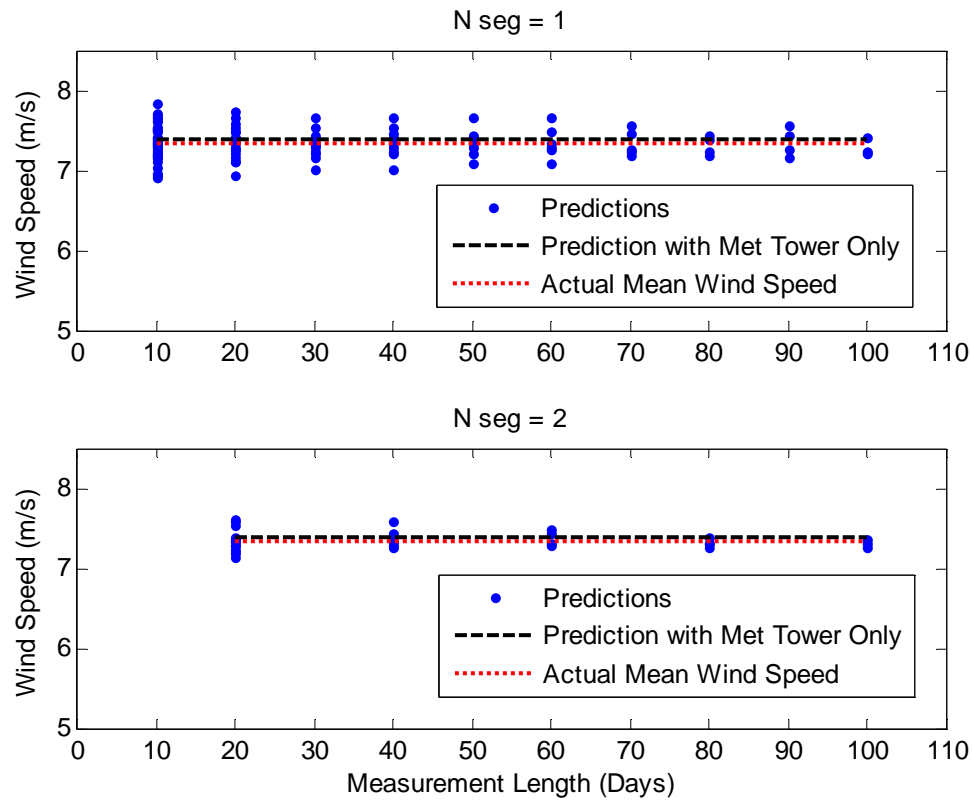


Figure 46 – Mean Wind Speed Predictions for Glenmore, Scenario 1

- The standard deviation of the predictions is slightly less when $N_{Seg} = 2$, which reinforces the logic behind the use of multiple measurement segments.

The shear correction method for Scenario 1 appears to be an effective method for improving the accuracy of shear extrapolations, on average. While there is no guarantee that the shear correction method is effective every time it is applied, it is extremely effective on average, and produces far more accurate predictions of the hub height mean wind speed the majority of the time. Furthermore, even in situations when this method does produce slightly worse predictions, the substantially reduced uncertainty when using this method is far more valuable. That is, this method produces predictions with no bias and small scatter, compared to the standard shear predictions, which contained a large amount of error and scatter. While the standard method may produce accurate predictions in some cases, the uncertainty in these predictions is large, and there is no way of knowing beforehand if the predictions are actually accurate. Thus, much of the value of the shear correction factor method lies in the substantially reduced uncertainty in the predictions.

4.2 Scenario 2 Results

Scenario 2 uses short-term measurements of the power law exponent to approximate the year long power law exponent. $RMSE(U_3)$ for $N_{Seg} = 1$ and $N_{Seg} = 2$ is plotted in Figure 47, as a function of N_{Days} . Again, these values are consolidated across all ten data sets. The $RMSE(U_3)$ value of 7.1% when α_L is not corrected is also plotted in Figure 47. This value is not a function of N_{Days} and it is calculated using two measurement heights; rather it is included as a comparison.

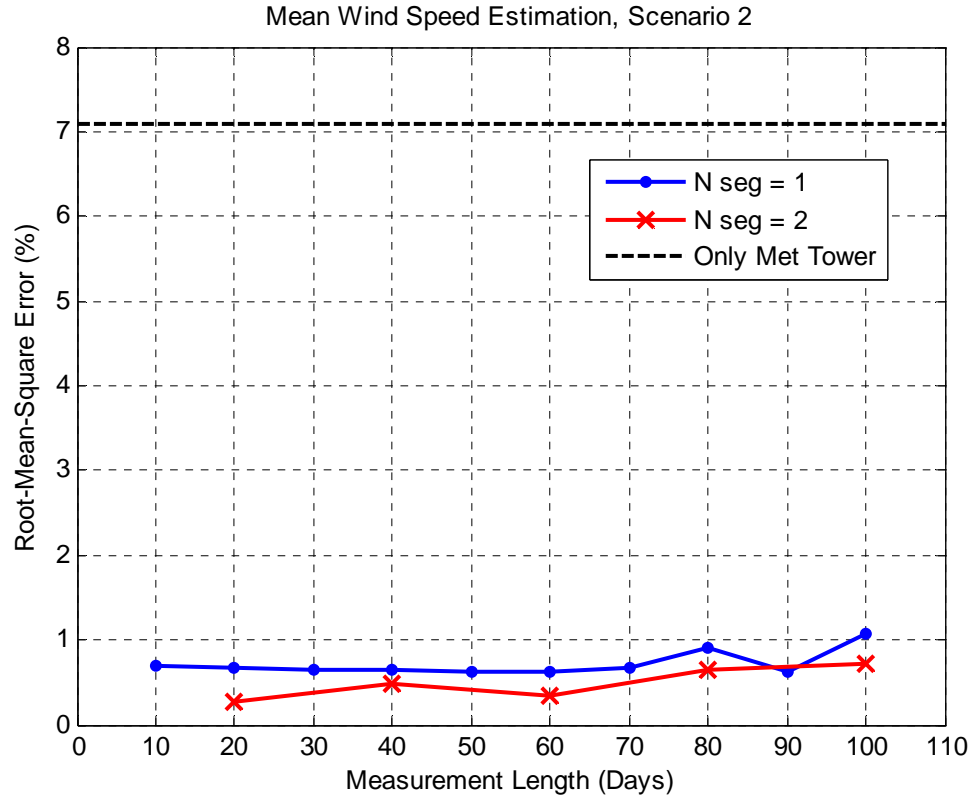


Figure 47 – Accuracy of the Predictions, Scenario 2

Several comments can be made regarding Figure 47:

- $RMSE(U_3)$ is significantly reduced when using the short-term power law exponent to approximate the long-term value. For both $N_{seg} = 1$ and $N_{seg} = 2$, $RMSE(U_3)$ is less than 1%, for nearly all values of N_{Days} . The uncorrected value is 7.1%. This is a substantial reduction in the error, although less than the reduction in error seen in Scenario 1. This is not surprising, as less information about the shear profile is available in Scenario 2.
- The average value of the percentage error across all data sets and all values of N_{Days} is less than 0.2%, indicating that there is essentially no bias in the predictions.

- $RMSE(U_3)$ does not depend strongly on the value of N_{Seg} . The results are very close together for the two values of N_{Seg} .
- The value of $RMSE(U_3)$ is once again fairly independent of N_{Days} .

$PSTD(U_3)$ for $N_{Seg} = 1$ and $N_{Seg} = 2$ is plotted in Figure 48, as a function of N_{Days} , for Scenario 2. Again, these values are consolidated across all ten data sets.

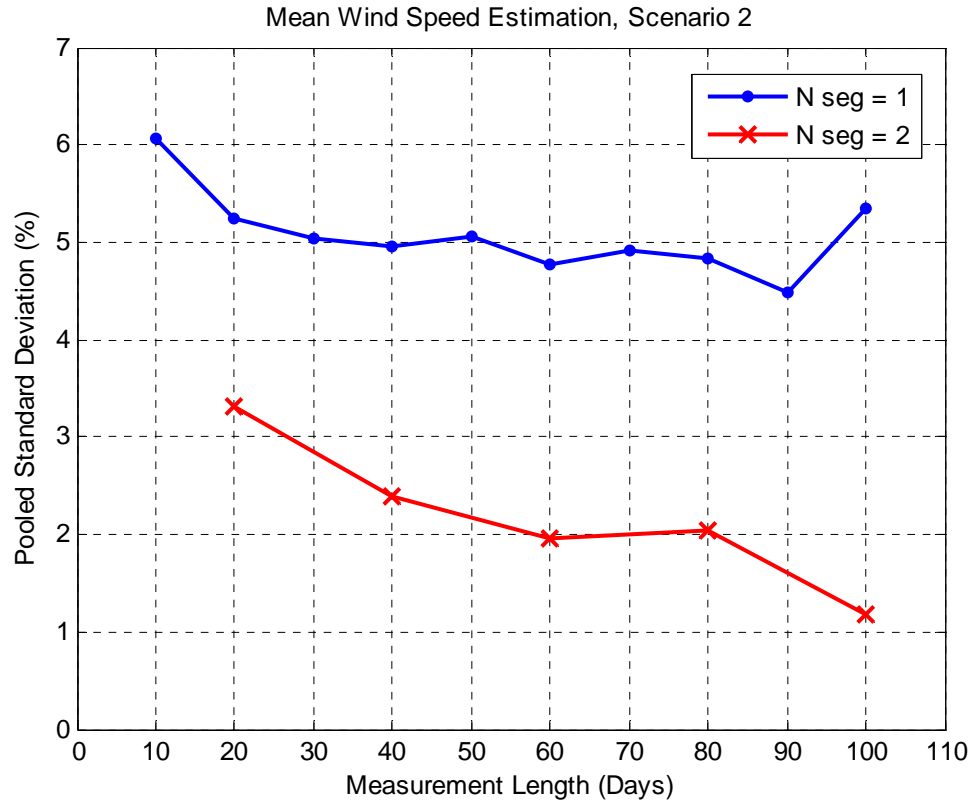


Figure 48 – Uncertainty of the Predictions, Scenario 2

Several comments can be made regarding Figure 48:

- For both $N_{Seg} = 1$ and $N_{Seg} = 2$, the uncertainty in the predictions decreases as N_{Days} increases. Again, it appears that higher values of N_{Days} are preferable. (The increase in uncertainty between $N_{Days} = 90$ and $N_{Days} = 100$ when $N_{Seg} = 1$ is likely

not a real effect and instead is simply due to the small number of samples for large values of N_{Days} .)

- As is the case for Scenario 1, these results indicate that while smaller values of N_{Days} yield accurate predictions on average, the variability is high compared to larger values of N_{Days} . Longer measurement lengths are preferable as it results in lower variability in the predictions, and therefore more confidence in an individual prediction.
- The uncertainty for Scenario 2 is higher than the uncertainty for Scenario 1, seen in Figure 44, especially when $N_{Seg} = 1$. This is not surprising, as less information about the shear profile is available in Scenario 2.
- Once again, some caution should be used in interpreting Figure 48, as the values for the standard deviation are often based on a very small number of samples. Figure 48 is still useful in that it indicates the variability in the predictions; however, there are some limitations in using the results to generalize about the uncertainty of the predictions.
- The uncertainty in the predictions is significantly lower when $N_{Seg} = 2$, compared to $N_{Seg} = 1$. This result is in contrast to those shown in Figure 44, in which the uncertainty is reduced only slightly due to the use of two short-term measurement segments. In the case of Scenario 2, it appears that using two segments of measurement data can cut the uncertainty approximately in half.

Once again, it is informative to consider each of the individual predictions for a site using the Scenario 2 method to understand the performance of a single prediction, and to

illuminate the scatter in the predictions of the mean wind speed. Figure 49 and Figure 50 show each of the predictions of the mean wind speed at the Isabella and Glenmore sites, respectively, as a function of N_{Days} , for $N_{Seg} = 1$ and $N_{Seg} = 2$. Also shown in each of the plots is the actual mean wind speed at the site and the predicted mean wind speed when only the met tower data are used to make the prediction (i.e., no shear correction factor is employed). Again, Figure 49 and Figure 50 are all plotted using the same y-axis scale, in order to facilitate comparisons of the scatter in the predictions. Several comments can be made regarding Figure 49 and Figure 50:

- For Isabella, most of the predicted values of the mean wind speed using short-term hub height measurements are improvements over the predicted value using only met tower data, for $N_{Seg} = 1$.
- When $N_{Seg} = 2$ for Isabella, however, nearly all of the predictions are improvements over the predicted value using only met tower data. Thus, the lower uncertainty that results from using two measurement segments results in a higher number of improved predictions.
- For Isabella, the standard deviation of the predictions using the Scenario 2 method is approximately 5.5% for $N_{Days} = 10$, and decreases to 4.3% for $N_{Days} = 100$, for $N_{Seg} = 1$. When for $N_{Seg} = 2$, the standard deviation of the predictions using the Scenario 2 method is approximately 3.5% for $N_{Days} = 20$, and decreases to 1.7% for $N_{Days} = 100$.
- The uncertainty in the predictions at Isabella is substantially higher than the Scenario 1 analysis when $N_{Seg} = 1$. When $N_{Seg} = 2$, the increase in uncertainty in

the Scenario 2 analysis is small. Also, the uncertainty tends to decrease less rapidly as N_{Days} increases for Scenario 2.

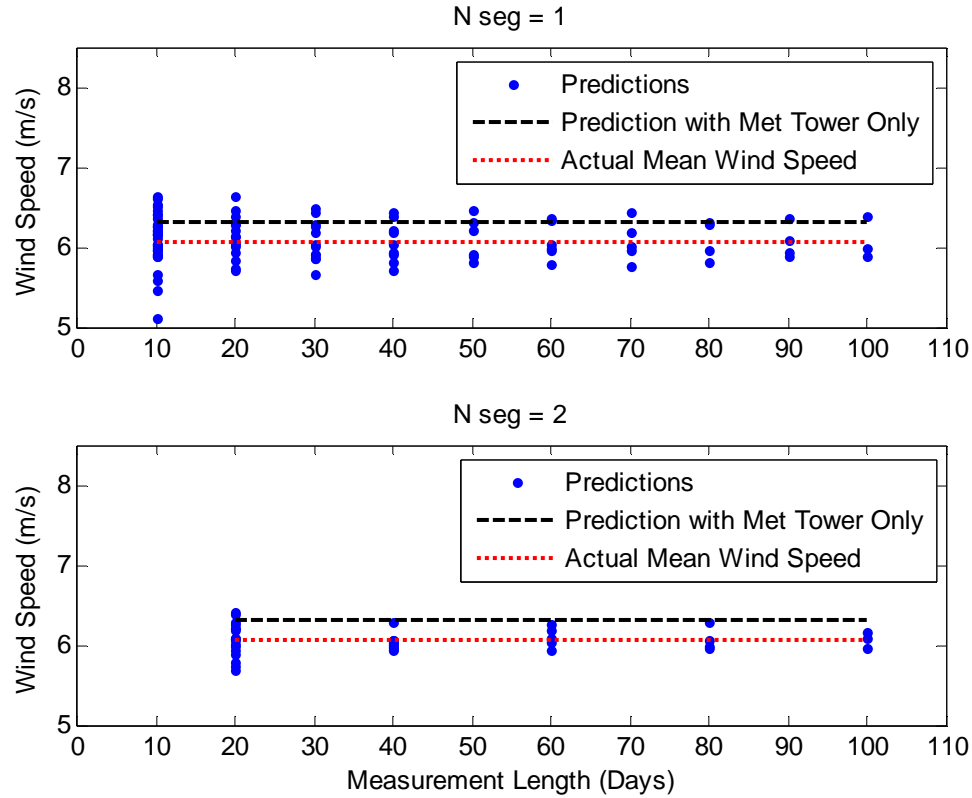


Figure 49 – Mean Wind Speed Predictions for Isabella, Scenario 2

- For Glenmore, few predictions using the Scenario 2 method are improvements over the predicted value using only met tower data, for both $N_{Seg} = 1$ and $N_{Seg} = 2$. This is due to two factors. First, the percentage error when only the met tower data are used is only 0.5%. Second, the scatter in the predictions is higher when using the Scenario 2 method compared to Scenario 1. The result is that most of the predictions using the Scenario 2 are worse than the predicted value using only met tower data.
- For Glenmore, the standard deviation of the predictions using the Scenario 2 is approximately 3.7% for $N_{Days} = 10$, and decreases to 2.9% for $N_{Days} = 100$, for

$N_{Seg} = 1$. When for $N_{Seg} = 2$, the standard deviation of the predictions using the Scenario 2 method is approximately 2.4% for $N_{Days} = 20$, and decreases to 1.5% for $N_{Days} = 100$.

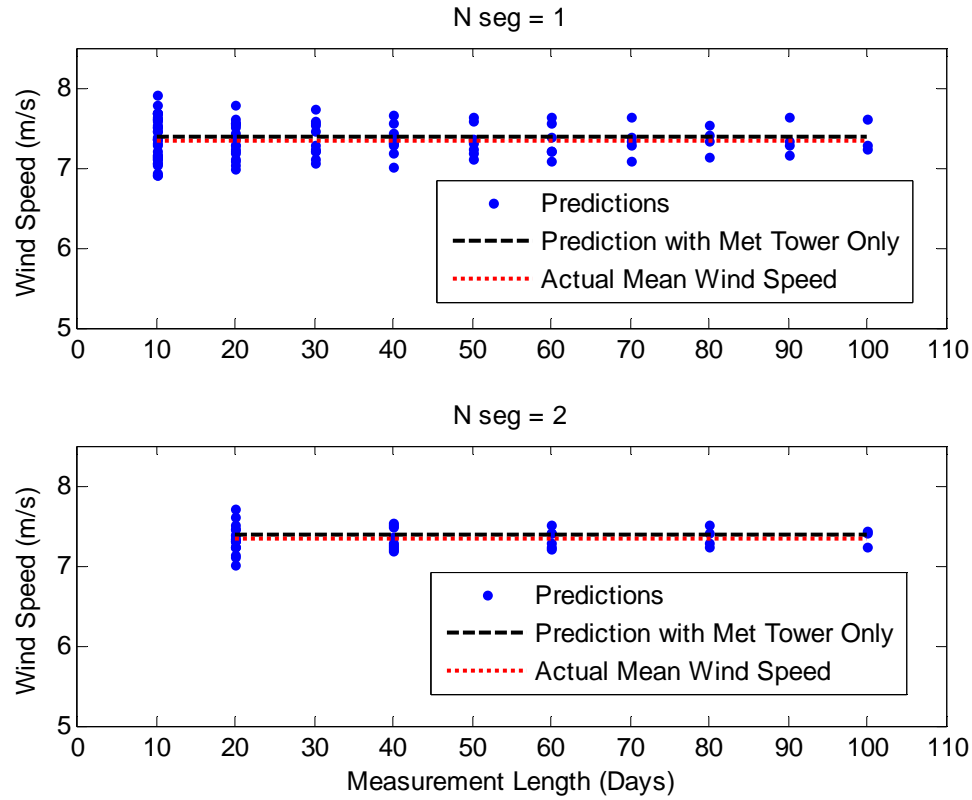


Figure 50 – Mean Wind Speed Predictions for Glenmore, Scenario 2

- Overall, the scatter in the predictions of the mean wind speed is larger in Scenario 2, with standard deviations that are often similar to or greater than the actual percentage error in the prediction of the mean wind speed when only the met tower data are used. The result is that in some cases, individual predictions of the hub height mean wind speed are improvements over the prediction when only the met tower data are used, and in other cases they are not.
- The use of two measurement segments has a much more pronounced effect in Scenario 2 than it did in Scenario 1. The uncertainty in the predictions decreases

significantly in most cases when $N_{Seg} = 2$, and so the predictions tend to be better in general when $N_{Seg} = 2$.

The short-term shear data used in Scenario 2 appears to be an effective method for estimating the hub height wind resource, on average. Compared to Scenario 1, however, the uncertainty in the predictions can be significantly higher, resulting in predictions of the mean wind speed that are worse than the prediction using just the met tower in many cases. This effect is especially pronounced when $N_{Seg} = 1$. Thus, there is no guarantee that the Scenario 2 method is effective every time it is applied. On the other hand, it is very effective on average, and produces more accurate predictions of the hub height mean wind speed the majority of the time. Even when the Scenario 2 method does result in worse predictions, the magnitude of the error is small. Lastly, the use of multiple measurement segments is especially effective for Scenario 2.

5.0 Conclusions

Shear extrapolation is often the most uncertain aspect of wind resource assessment, leading to large errors in the estimate of the hub height wind resource and therefore the energy production. This Chapter has presented two methods that can be used to improve shear extrapolation predictions. The specific conclusions of this Chapter are:

- Short-term measurements from ground-based devices at met tower sites can be used to drastically improve the accuracy of shear predictions on average.
- The uncertainty of the predictions decreases as the short-term measurement length increases.

- At a site with a standard met tower, with two measurement heights, the number of segments of measured data does not affect the accuracy or the uncertainty of the predictions appreciably.
- At a site with a smaller portable tower, with only a single measurement height, increasing the number of measurement segments from one to two reduces the uncertainty of the predictions substantially, but has no appreciable affect on the accuracy of the predictions.
- The true value in this method lies in the substantially reduced uncertainty that it produces in shear extrapolation predictions. Utilizing this approach allows for substantially more confidence in hub height mean wind speed predictions.

More generally, these results demonstrate that hub height wind speed measurements, even those that are relatively short in length, can provide valuable information for improving the accuracy of wind shear extrapolation. While this Chapter used the shear correction factor method, many other potential methods for utilizing hub height data are possible.

One possible source of error in the method described above is the potential for pronounced seasonal variations in the wind shear at time scales longer than the short-term hub height measurement length. For example, at sites with pronounced seasonal stability variations, utilizing short-term data may lead to substantial errors, as the corrected shear exponent would not be representative of the annual shear characteristics. Seasonal dependent prevailing wind directions coupled with varying topography with direction

could also lead to errors. Future work in this area could look at incorporating these seasonal effects, and correcting for the resulting errors.

On the other hand, the results from the data sets used in this Chapter do not seem to indicate that these seasonal effects produce substantial error. The relatively simple methods discussed in this Chapter produce very encouraging results on their own, and demonstrate how valuable hub height wind speed measurements are for improving the accuracy and reducing the uncertainty in shear extrapolation. These results are especially applicable to situations when the log law or the power law is used for the shear extrapolation (as opposed to more complex methods such as numerical models mentioned previously). Because these simple models are so commonly utilized, the results in this Chapter are quite relevant.

6.0 Recommendations

These results suggest that a reevaluation of the traditional site assessment process may be appropriate. The potential to use of ground-based devices for short-term hub height measurements presents a new approach to site assessment. This new approach offers two distinct strategies for site assessment.

First, whenever the wind resource is evaluated at a site using a standard met tower, with two measurement heights, a LIDAR or SODAR should be used to measure the hub height wind resource at the site, for some short-term period of time (this obviously requires that a LIDAR or SODAR is available). The methods presented here could be especially useful when multiple sites are being assessed simultaneously with met towers, and only a single ground-based device is available. In this case, the ground-based device should be brought to each site.

Second, the results also offer an alternative monitoring strategy when multiple sites must be assessed. Ground-based devices are expensive, but so are standard met towers. Conversely, shorter portable towers are much cheaper and easier to install than met towers. The towers can be used in conjunction with short-term ground-based measurements to produce estimates of the hub height wind resource that are substantially better than the estimates one would obtain using a standard met tower. For institutions or companies that assess numerous sites concurrently, this new strategy can be employed to improve the accuracy and decrease the costs of site assessment. When this approach is taken, the results suggest that two measurement segments should be used to help reduce the uncertainty of the predictions.

In general, for either approach, only a single prediction on the hub height mean wind speed is made when these methods are actually applied. While the results in this Chapter show impressive accuracy of the predictions on average for very short measurement lengths with a ground-based device, the uncertainty of the predictions for these short measurement lengths is significantly higher than for longer measurement lengths. In order to ensure a reasonable level of confidence in the prediction, a longer measurement length with the ground-based device is appropriate. For Scenario 1 with either one or two measurement segments, and Scenario 2 with two measurement segments, a 60 day measurement length with the ground-based device results in uncertainty less than 2%. While there is nothing particularly noteworthy about this value of 60 days, it seems like a reasonable benchmark. A 2% uncertainty due to shear extrapolation is a dramatic improvement over the standard method for shear extrapolation, which has a standard deviation of 6.5% for the predictions using the data used in this Chapter. Furthermore,

using a 60 day measurement length for the ground-based device enables a total of six sites to be evaluated in a single year using a these approaches.

In the future, one particular aspect of this research deserves further consideration. Namely, for what measurement length with the ground-based device would one be better off not using a met tower at all? This question addresses the tradeoff between uncertainty due to shear extrapolation when a met tower and the methods described in this Chapter are employed, and uncertainty due to a measurement length less than one year when a ground-based device only is used for wind resource assessment and so no shear extrapolation is needed. An investigation into these tradeoffs would further illuminate how the methods developed in this Chapter can be incorporated into the site assessment process.

CHAPTER VII

WIND ENERGY ECONOMIC ANALYSIS

The estimate of the energy production from a wind farm is one of the primary goals of the site assessment process. However, a decision of whether or not to build a wind farm is not possible until an economic analysis is performed as well. Economic analysis of wind energy takes on a variety of forms, ranging from very simple methods to advanced financial analyses. Whenever a wind farm is under consideration, an economic analysis of the project is likely.

This Chapter does not describe any original research, but instead presents a sampling of some important aspects of the economic analysis of wind energy and the development of a useful tool for economic analysis. It is divided into two Sections. First, the development of a “Wind Energy Financial Calculator” is described. This tool provides a useful means for analyzing proposed wind energy developments in the United States. The analysis methods used in this tool are also described in detail. Second, some interesting new and alternative methods for valuing wind energy, especially in relation to other energy sources, are presented. These particular methods are by no means exhaustive; instead this summary is meant to highlight a few particular areas in which alternative methods of analysis provide insight or different perspectives on the merit of wind energy from an economic perspective. In general, the topics described in this Chapter are especially applicable to the United States, as opposed to Europe and the rest of the world.

1.0 The Wind Energy Financial Calculator

The wind energy financial calculator is a general tool for analyzing wind energy finances. The WEFC utilizes cash flow methods for determining the relevant economic results. These cash flow methods calculate the relevant revenues, expenses, debt payments, depreciation allowances, subsidies, and tax liabilities in each year of operation of the wind farm. These methods are desirable because they closely mimic the actual financial operation of the wind farm, including the specific depreciation allowances and subsidies available to wind farms. While there is no “correct” method for analyzing the economics of a wind farm (e.g., payback methods, levelized cost method, EPRI-TAG, etc), the cash flow method is similar to how a business or utility would evaluate a potential development. Furthermore, a cash flow method analysis is not particularly easy to implement, at least in relation to other methods. It requires iteration, and so it lends itself well to “canned” programs that perform the iterations automatically.

The specific cash flow analysis methods in the WEFC are derived from the work of Wiser and Kahn, in their paper “Alternative Windpower Ownership Structures: Financing Terms and Project Costs” [95]. The authors identify three types of ownership structures for wind energy development: Independent Power Producers (IPP), Investor Owned Utilities (IOU), and Government Owned Utilities (GOU). These represent the three major categories of wind farm developers, and each has different financial structures, tax and subsidy situations, and therefore each requires its own cash flow method. A more detailed description of the important details of each ownership structure follows. Again, the cash flow methods described in this Section are particularly applicable in the United States.

Lastly, while the descriptions below provide good summaries of the various ownership structures and their financial operations, the descriptions are by no means exhaustive, or uniformly applicable. Instead, these descriptions approximate the functioning of the most common ownership structures, and are qualitatively similar to many developments in the United States. However, deviations from these structures are common, and more complex financial arrangements, such as “Minnesota-Style Flips” and others, are used as well. Also, many states have specific subsidy programs, such as renewable energy credits (RECs), which may be incorporated into specific analyses, but are not described here.

1.1 Independent Power Producer

An IPP is the most common type of wind farm development in the U.S. IPPs are privately owned companies that own and run a wind farm with the goal of making some desired return on their equity investment. IPPs almost always borrow money to help finance the project. The debt fraction is typically on the order of 60-80%, although this can vary [95]. The underlying projected cash flows and assets of the specific project dictate the terms of the loan; i.e., it is judged on a stand-alone basis. The lender must decide if the project is capable of servicing the debt payments. Some of the other important characteristics of IPPs are:

- They qualify for the 5-year MACRS accelerated depreciation, and so the equipment cost for the wind farm can be depreciated over the first six years of operation [96].
- They can qualify for the production tax credit, or PTC, which is currently valued at 1.8 cents per kW-hour. It is important to point out that the full benefit of the

PTC can only be used if the IPP has a tax liability large enough to absorb the full subsidy. For a small company, it is possible that only a fraction of the PTC can be utilized, bringing the tax liability to zero.

- The loan interest rate is higher for IPPs because of perceived risk by the lender.
- The loan payment type is usually either a constant principal repayment, or a constant mortgage style repayment.

The analysis of an IPP uses a cash flow method that yields the after-tax net cash flow in each year of operation of the wind farm (an example is shown in the next Section). This is the cash flow that would be returned to the equity investors. The analysis is “solved” by using the price of electricity as a variable. That is, the cash flow is dependent on the electricity price, and so the electricity price can be varied to satisfy the constraints of the analysis. The minimum electricity price that satisfies all of the constraints is the levelized cost of energy (LCOE).

Typically, there are several constraints that must be satisfied when analyzing an IPP. The most common constraints are:

- Equity rate of return: The equity investors typically require a certain rate of return. This is ensured by determining the internal rate of return of the cash flows and ensuring it is equal to or higher than the required equity rate of return.
- Debt service coverage ratio: The lenders typically require that the projected operating income (revenue minus expenses) is larger than the loan payment by some amount in every year of operation. The ratio of the operating income to the loan payment is the debt service coverage ratio (DSCR), and a common

requirement is that the minimum DSCR across all years of operation is greater than or equal to 1.4 [14].

Thus, LCOE can be calculated for a wind farm by adjusting the value so that it is minimized and satisfies the imposed constraints. This process requires some type of iteration or root finder to determine the solution.

1.1.1 IPP Example

A simple example helps to illuminate the process. This example closely mimics how IPPs are analyzed in the WEFC, except that some simplifying assumptions are made. The major assumptions of this example are:

- Twenty 1.5 MW turbines, operating for twenty years.
- The capacity factor is 30%, and *AEP* is approximately 79,000 MWh per year.
- Installed capital costs (*CC*) are \$36 million.
- Yearly operating expenses (*OE*) are \$500,000.
- The loan interest rate (r_b) is 8%, the debt fraction (f_b) is 60%, and the loan term (N_b) is 20 years. A level mortgage payment is assumed, so that the loan payment (*LP*) each year is \$2.2 million, calculated using Eq. 59.

$$LP = \frac{CC \cdot f_b \cdot r_b}{1 - 1/(1 + r_b)^{N_b}} \quad \text{Eq. 59}$$

- The inflation rate is 0%.
- Tax rate is 40%.
- The minimum required DSCR is 1.4.
- The required internal rate of return on equity is 18%.

The cash flow sheet for this example is shown in Figure 51. In Year 0, the capital costs are paid by the loan and the equity investment. In all subsequent years, the wind farm operates, generating revenue. The quantities in each row are calculated as follows.

- Operating Revenue (OR): $OR = AEP * \text{Price}$.
- Operating Income (OI): $OI = OR - OE$.
- Loan Balance at Beginning of Year ($LBBOY$): In Year 1, $LBBOY$ equals $CC * f_b$, while in all later years it equals the remaining principal from the previous year.
- Loan Payment: LP is calculated using Eq. 59 and is constant in every year.
- Interest Payment (IP): $IP = LBBOY * r_b$.
- Principal Repayment (PR): $PR = LP - IP$.
- Remaining Principal (RP): $RP = LBBOY - PR$.
- Debt service coverage ratio ($DSCR$): $DSCR = OI / LP$.
- Total Accelerated Depreciation (TAD): TAD equals the MACRS depreciation allowance for a given year multiplied by CC . For wind turbines, all of the depreciation occurs in the first six years of operation.
- Taxable Income (TI): $TI = OI - IP - TAD$.
- Income Taxes (IT): IT equals the tax rate multiplied by the taxable income, TI .
- Production Tax Credit (PTC): PTC equals AEP multiplied by the value of the credit, which is \$0.018 per kWh.
- Tax Savings (TS): $TS = PTC - IT$.
- After-Tax Net Equity Cash Flow (CF): $CF = OI + TS - LP$.

Year	0	1	2	5	10	15	20
Price (\$/kW-hr)		\$0.046	\$0.046	\$0.046	\$0.046	\$0.046	\$0.046
Operating Revenue - OR		\$3,587,220	\$3,587,220	\$3,587,220	\$3,587,220	\$3,587,220	\$3,587,220
Operating Expenses - OE		\$500,000	\$500,000	\$500,000	\$500,000	\$500,000	\$500,000
Operating Income - OI		\$3,087,220	\$3,087,220	\$3,087,220	\$3,087,220	\$3,087,220	\$3,087,220
Financing							
Loan Balance at BOY		\$21,600,000	\$21,127,992	\$19,473,080	\$15,705,776	\$10,170,371	\$2,037,044
Loan Payment - LP		\$2,200,008	\$2,200,008	\$2,200,008	\$2,200,008	\$2,200,008	\$2,200,008
Interest Payment - IP		\$1,728,000	\$1,690,239	\$1,557,846	\$1,256,462	\$813,630	\$162,964
Principal Repayment - PR		\$472,008	\$509,768	\$642,161	\$943,546	\$1,386,378	\$2,037,044
Remaining Principal - RP		\$21,127,992	\$20,618,224	\$18,830,919	\$14,762,231	\$8,783,993	\$0
Debt Service Coverage Ratio - DSCR		1.40	1.40	1.40	1.40	1.40	1.40
Taxes							
MACRS Depreciation Allowance (%)		20.0%	32.0%	11.5%			
Total Accelerated Depreciation - TAD		\$7,200,000	\$11,520,000	\$4,147,200	\$0	\$0	\$0
Taxable Income - TI		-\$5,840,780	-\$10,123,019	-\$2,617,826	\$1,830,758	\$2,273,590	\$2,924,256
Income Taxes - IT		-\$2,336,312	-\$4,049,208	-\$1,047,131	\$732,303	\$909,436	\$1,169,703
Production Tax Credit - PTC		\$1,419,120	\$1,419,120	\$1,419,120	\$1,419,120	\$0	\$0
Tax savings - TS		\$3,755,432	\$5,468,328	\$2,466,251	\$686,817	-\$909,436	-\$1,169,703
Results							
After Tax Net Equity Cash Flow - CF		-\$14,400,000	\$4,642,644	\$6,355,540	\$3,353,463	\$1,574,029	-\$22,224

Figure 51 – Cash Flow Example

To “solve” the cash flow analysis, the price of electricity is varied until it is minimized and the two constraints are satisfied. In this example, the levelized cost of energy is \$0.0455 per kWh, the DSCR is 1.40, and the internal rate of return of the cash flow is 24.5%, as shown in Table 10. Thus, the DSCR constraint is the active constraint, whereas the internal rate on return constraint is more than satisfied. For different assumptions, the active constraint could switch to the required return on equity constraint.

Levelized Cost (cents/kW-hr)	4.55
Minimum DSCR	1.40
IRR	24.5%

Table 10 – IPP Example Results

This example highlights the basic functioning of a cash flow analysis for an IPP. In the WEFC, the solution for the LCOE can be determined for a wider variety on inputs. Issues such as property taxes and inflation can be included in the analysis. Furthermore, the WEFC can analyze an IPP when a power purchase agreement has been secured. In this case, the price of electricity is no longer a variable, but instead is a fixed input.

To be clear, this price of electricity is referred to as the levelized cost of energy. The terms “price” and “cost” are often incorrectly used interchangeably. The price of electricity calculated in the cash flow method is the price that the IPP must charge to satisfy all the necessary requirements. On the other hand, this price can also be viewed as the cost of electricity to the utility that the wind farm sells its power to. In this way, by viewing the price of electricity as the levelized cost of energy, it can be compared on an equal footing to the other ownership structures. In general, one should be precise and cautious when using the terms price and cost, as they are not usually synonymous.

1.2 Investor Owned Utility

IOU wind farms are owned and operated by a utility instead of by a private owner. When IOUs borrow money, it is the income from the entire utility that the loan is based on, and not the specific wind farm operations. Some of the other important characteristics of IOUs are:

- They qualify for the 7-year MACRS accelerated depreciation. The equipment cost for the wind farm can be depreciated over the first eight years of operation.
- They can qualify for the production tax credit, or PTC, which is currently valued at 1.8 cents per kW-hour. It is almost certain that the IOU can absorb the full benefit of the PTC.
- The loan interest rate tends to be lower than IPPs because of the other assets and income streams. Furthermore, there are no explicit debt service coverage requirements, since the company as a whole must pay the debt, not the specific wind farm operation.
- The debt and equity usually make up equal portions of the initial capital outlay.

- A straight-line declining rate base principal repayment schedule is used.

The analysis of an IOU uses a revenue requirement model recommended by Wiser and Kahn, which is representative of actual utility analysis. The revenue requirement model calculates the yearly revenue that is needed to satisfy all of the expenses and debt payments, and that provides a sufficient return to the investors. Then, a nominal levelized cost of energy can be calculated using the estimated energy production in each year, and the required revenue figures. This analysis requires iteration to find the levelized cost of energy.

An example of an IOU cash flow calculation is not included as it behaves qualitatively similarly to the IPP example above. Once again, the WEFC is capable of handling a wide variety of inputs for this ownership structure.

1.3 Government Owned Utility

GOU wind farms differ greatly from IPPs and IOUs. GOU wind farms are run by public utilities, such as a town or municipality. Some of the other important characteristics of GOUs are:

- They are financed by 100% debt, typically via a bond. The interest rate tends to be lower than that of an IPP or IOU.
- There are no specific debt service coverage requirements.
- They pay no income taxes, and typically very low property taxes. Sometimes, they provide “payments in lieu of taxes” instead.

- They do not qualify for the PTC. Instead they qualify for the renewable energy production incentive, or REPI. The REPI is more uncertain than the PTC since Congress must appropriate the funds for it each year.

The analysis of a GOU requires a simple cash flow model. The required revenue for each operating year is simply equal to the total operating expenses and debt payments minus the REPI in each year. This is not an iterative calculation. The required revenue and the annual energy production can then be used to determine the levelized cost of energy of the project.

1.4 WEFC Features

The WEFC is created in Matlab using the graphical user interface (GUI) functionality. The WEFC is created to be easy to use, so that a relative novice could enter all the inputs into the program, and the program could do all of the calculations. The WEFC is then compiled into C-code and turned into an executable file so that it can be run on any computer, even those without Matlab.

The main window of the WEFC is shown in Figure 52. The user begins by either starting a new analysis or continuing a previously saved analysis. Next, the user must choose between the three ownership structures, IPP, IOU, and GOU, which are described in detail in the previous Sections. In the example window shown in Figure 52, an IPP ownership structure is chosen. When an ownership structure has been set, the inputs to the analysis can be selected in the four sub-windows that can be opened by pressing the buttons under the “Input Categories” label. These four input categories, and the accompanying sub-windows, are “General Inputs,” “Capital Costs and Expenses,”

“Financing and Taxes,” and “Economic Inputs and Constraints.” Each of these categories is discussed below.

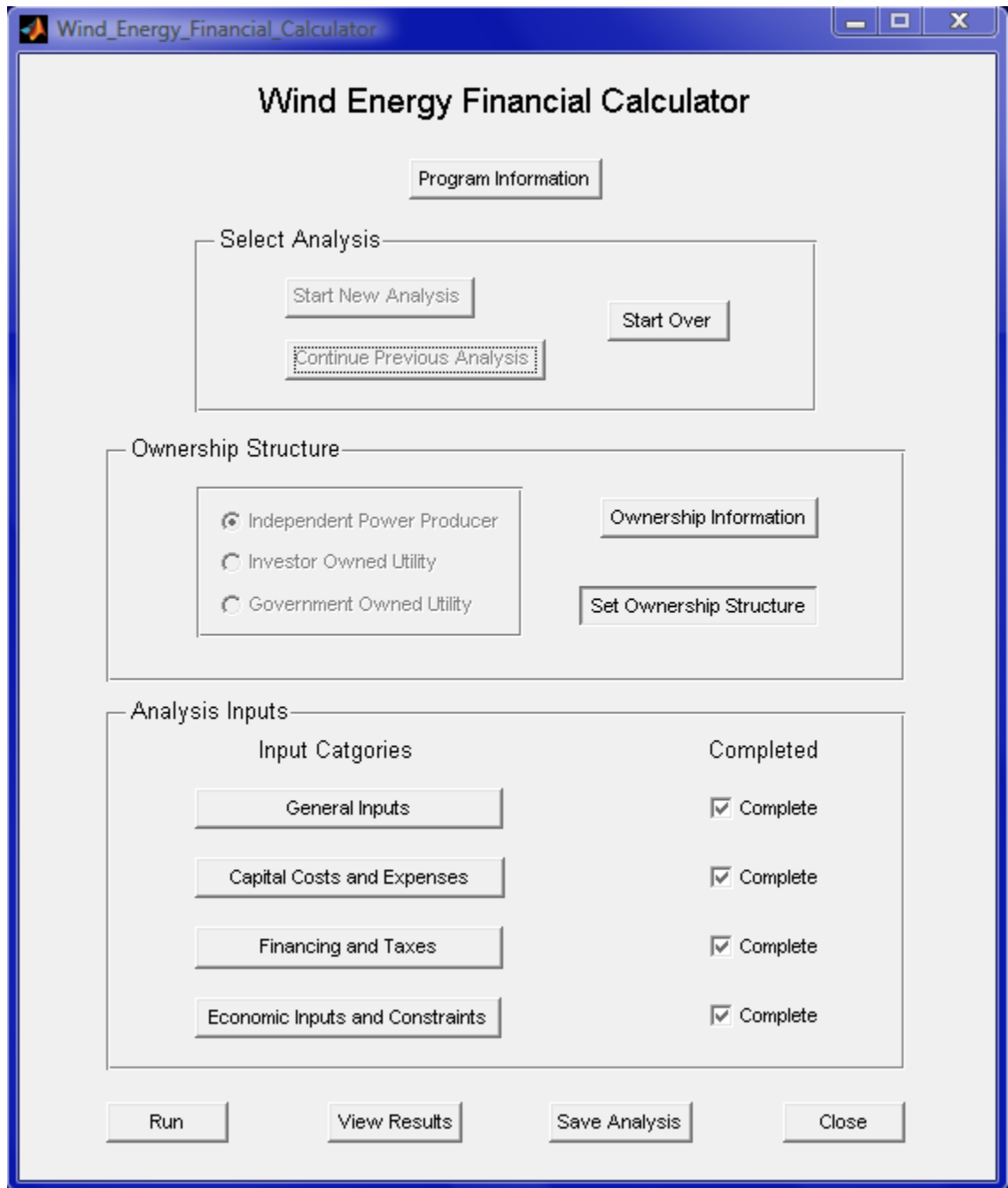


Figure 52 – WEFC Main Window

1. General Inputs. In this sub-window, with an example shown in Figure 53, the user sets the general framework of the wind farm such as number of turbines,

capacity factor, and project lifetime. The user can also choose to analyze a power purchase agreement for an IPP.

The screenshot shows a software window titled "general_inputs_gui" with a subtitle "General Inputs". Inside the window, there is a tab labeled "General Inputs Information". Below the tab, the inputs are organized into three distinct sections. The first section contains four input fields: "Number of Turbines" with the value 5, "Wind Farm Capacity" with the value 10 and unit MW, "Capacity Factor" with the value 34 and unit %, and "Annual Energy Production" with the value 29784 and unit MW-hr/Year. A "Calculate" button is positioned below these fields. The second section contains three input fields: "Project Life" with the value 20 and unit Years, "Construction Time" with the value 1 and unit Years, and "First Operating Year" with the value 2007. The third section contains a "Power Purchase Agreement?" section with two radio buttons, "Yes" (which is selected) and "No", and a "PPA Price" input field with the value 5 and unit Cents/kW-hr. A "Close" button is located at the bottom right of the window.

Input Field	Value	Unit
Number of Turbines	5	
Wind Farm Capacity	10	MW
Capacity Factor	34	%
Annual Energy Production	29784	MW-hr/Year
Project Life	20	Years
Construction Time	1	Years
First Operating Year	2007	
PPA Price	5	Cents/kW-hr

Figure 53 – WEFC General Inputs Sub-Window

2. Capital Cost and Operating Expense Inputs. The user sets the inputs that determine the total capital cost of the wind farm as well as the yearly operating expenses in this sub-window. An example is shown in Figure 54.

Capital Costs and Expenses

Capital Costs and Expenses Information

Capital Costs			Yearly Operating Expenses		
Installed Capital Cost	1200	\$/kW	Fixed O&M Costs	20	\$/kW
Financing Fees	0	\$	Variable O&M Costs	0	\$/kW-hr
Miscellaneous Fees	0	\$	Land Expense	25000	\$
Total Capital Costs	12000000	\$	Insurance	0.5	% of Installed Costs
<input type="button" value="Calculate"/>			Administration and Management Fee	100000	\$
			Property Tax	1	% of Installed Costs
			Total Yearly Expenses	505000	\$
			<input type="button" value="Calculate"/>		
<input type="button" value="Close"/>					

Figure 54 – WEFC Capital Costs and Expenses Sub-Window

3. Finance and Tax Inputs – In this sub-window, the user sets the relevant financing, subsidy, tax, and depreciation inputs. An example is shown in Figure 55.

Financing and Taxes

Financing and Taxes Information

Financing

Grant Amount: 0 % of Installed Costs

Debt Fraction: 60 %

Loan Term: 20 Years

Loan Interest Rate: 10 %

Schedule Type: Level Mortgage

Equity Fraction: 40 %

Equity Return Rate: 18 %

Tax Rates

Federal Tax Rate: 35 %

State Tax Rate: 5 %

Depreciation

Accelerated Depreciation Fraction: 95 %

Accelerated Depreciation Method: 5 Year MACRS

Straight Line Depreciation Fraction: 5 %

Straight Line Depreciation Length: 15 Years

First Year Depreciation Bonus: 0 %

Subsidies

Federal Subsidy Type: ☐ None ☒ PTC ☐ REPI

Federal Subsidy Value: 1.8 Cents/kW-hr

Federal Subsidy Length: 10 Years

Additional Subsidy Value: 0 Cents/kW-hr

Additional Subsidy Length: 0 Years

IPP Tax Base

Is the IPP able to absorb the entire PTC and the accelerated depreciation? ☒ Yes ☐ No

Close

Figure 55 – WEFC Financing and Taxes Sub-Window

4. Economic Assumptions and Constraints – The user sets some economic assumptions, such as discount rate and inflation rate, as well as any requirements for the debt service coverage ratio or the cash flows. In order to account for the risk of the project, the user can choose the uncertainty of the AEP estimate, and constrain the 10th percentile DSCR to be larger than a certain value [14]. An example of this sub-window is shown in Figure 56.

Economic Assumptions and Constraints

Economic Assumptions and Constraints Information

Basic Economic Assumptions		CAPM Discount Rates	
Inflation Rate	1 %	Pre-Tax Riskless Rate	4 %
Energy Price Escalation Rate	1 %	Pre-Tax Cost of Debt	10 %
Nominal Discount Rate	8 %	Pre-Tax Cyclical Discount Rate	10 %
Weighted-Average Cost of Capital	10.8 %		

Constraints	
Minimum P50 DSCR Constraint	<input checked="" type="radio"/> Yes <input type="radio"/> No
Required Minimum P50 DSCR	1.4
Minimum P90 DSCR Constraint	<input checked="" type="radio"/> Yes <input type="radio"/> No
Required Minimum P90 DSCR	1
AEP Standard Uncertainty	15 %
Positive Cash Flow	<input type="radio"/> Yes <input checked="" type="radio"/> No

Close

Figure 56 – WEFC Economic Assumptions and Constraints Sub-Window

Once all of the input categories are completed, the program can analyze the particular wind farm by pressing the “Run” button in the WEFC main window in Figure 52. The results of the analysis can be seen by pressing the “View Results” button in the WEFC main window, which then opens the results sub-window. This sub-window is different for the three ownership structures. The results sub-window for an IPP example is shown in Figure 57. The results window for the IOU and GOU ownership structure is simpler, displaying only the levelized cost of energy and the required price of electricity in each year of wind farm operation.

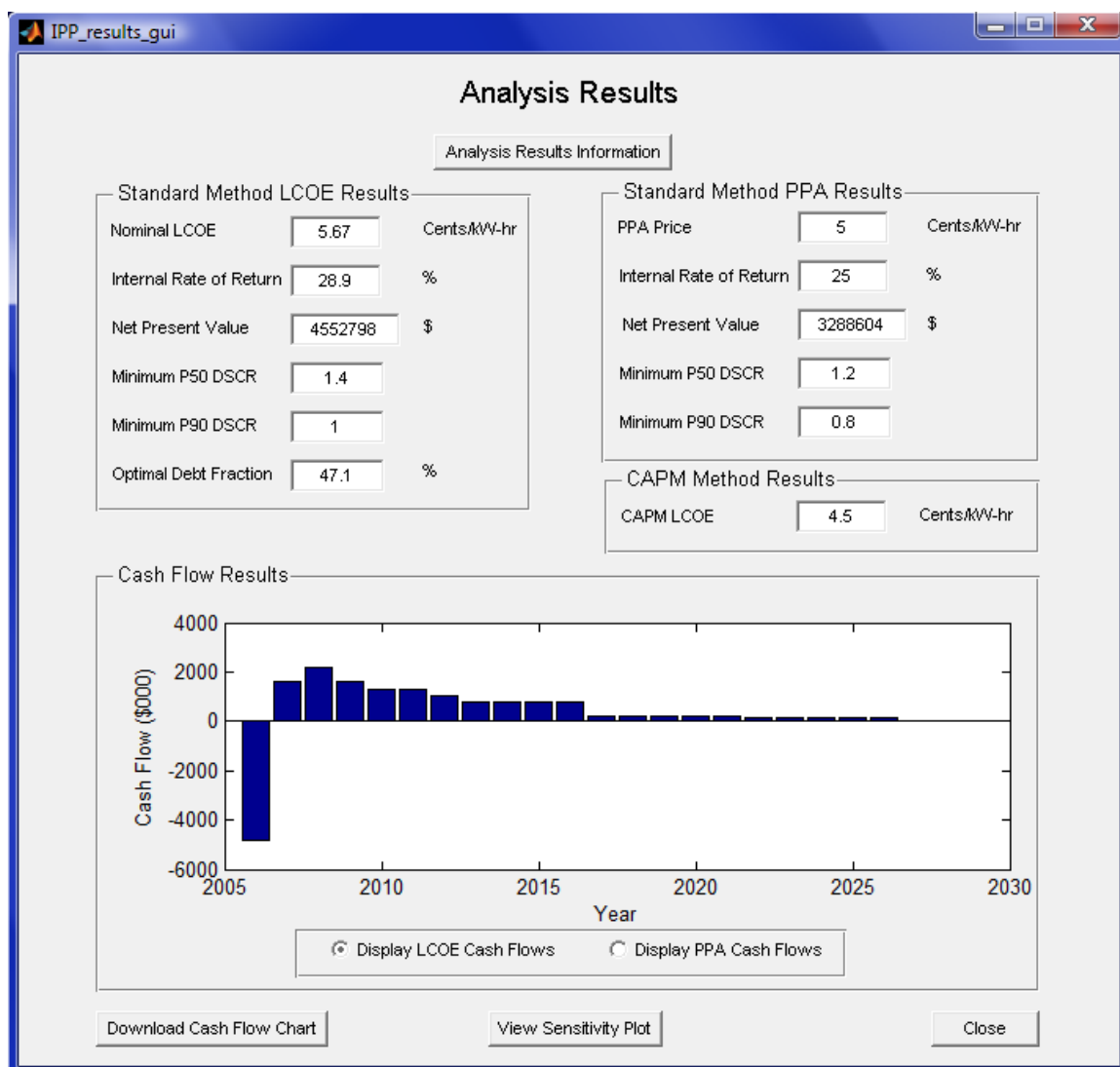


Figure 57 – WEFC IPP Results Sub-Window

The outputs of the program include:

- The levelized cost of energy.
- The internal rate of return.
- For an IPP, the outputs also include the net present value of the project, the minimum and average debt service coverage ratio, and the fraction of capital supplied by debt that minimizes the cost of energy.
- A plot of cash flow for an IPP, and of cost of electricity for an IOU or GOU.

Sensitivity plots, which show the variation in the economic success of the project as various parameters are changed, can be viewed by pressing the “View Sensitivity Plot” button in the results sub-window. An example sensitivity plot is shown in Figure 58.

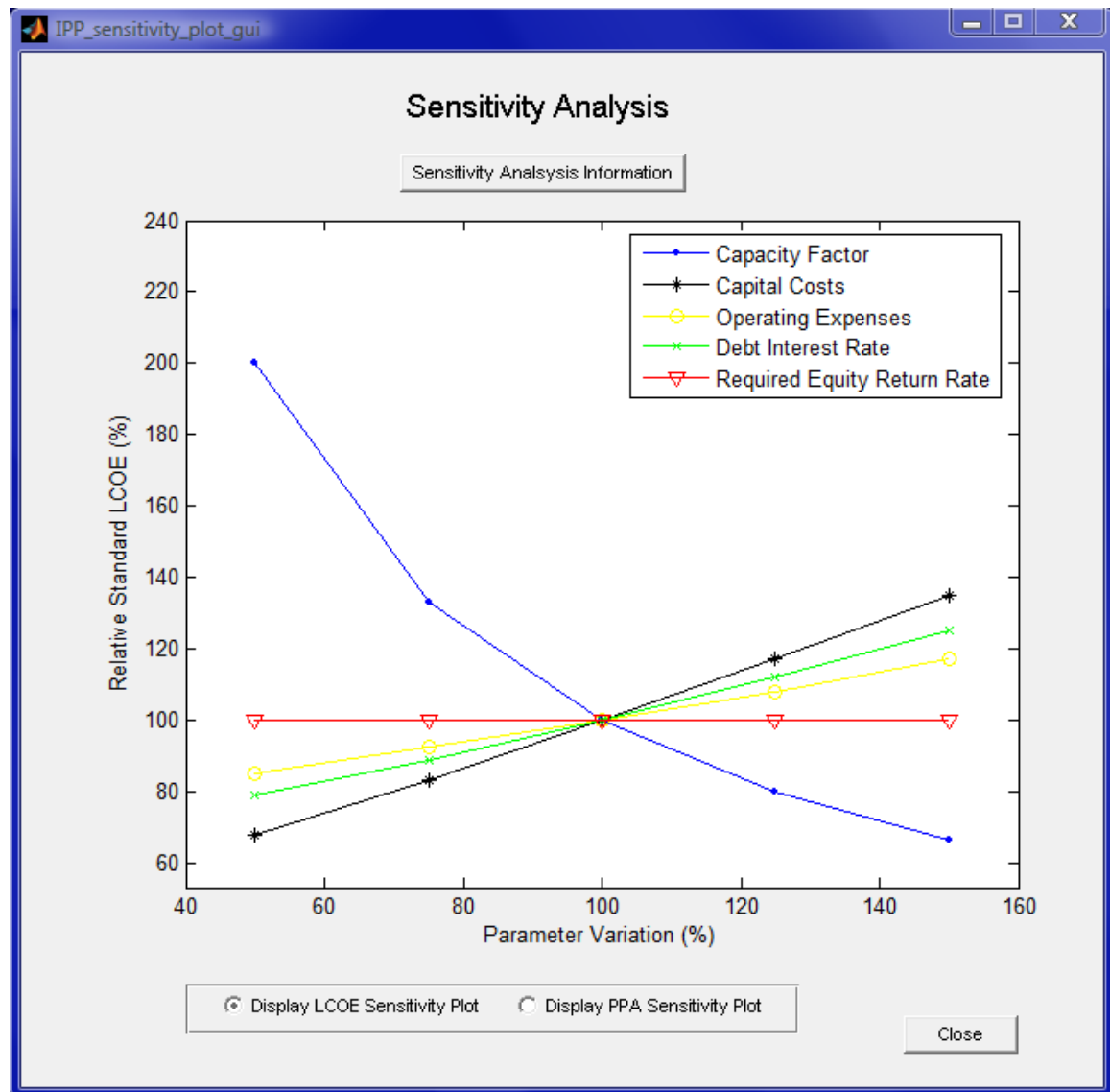


Figure 58 – WEFC Sensitivity Plot

The program also has the capability to:

- Save the inputs from a previous session so that the user does not have to start over each time.

- Download the cash flow spread sheet. This can be loaded into Excel to allow the user to see first hand how the results are calculated.
- Provide fairly detailed descriptions of the various inputs and outputs.

Finally, an alternative analysis technique is added to the WEFC. This method is derived from the work of Awerbuch, specifically his paper “Investing in Renewables: Risk, Accounting, and the Value of New Technology” [97]. Awerbuch advocates using a capital asset pricing model (CAPM) to value all energy production. The CAPM analysis approach is described in detail later in this Chapter in Section 2.2.

Overall, the WEFC hopefully provides a very useful tool for a user interested in wind energy economics. It is easy to use, and implements the most common and representative methods for analyzing the finances of wind energy projects.

2.0 Alternative Wind Energy Evaluation Methods

Along with exploring and implementing the standard methods for wind energy economic analysis, several alternative methods for valuing wind energy are also examined. Again, this is by no means exhaustive. Rather, three different methods that provide a different perspective on wind energy relative to other forms of electricity production are considered. The three methods are:

1. External Cost Analysis
2. Advanced Finance Analysis
 - a. Capital Asset Pricing Model
 - b. Mean Variance Portfolio Theory

3. Energy Balance Analysis

2.1 External Cost Analysis

In a perfectly functioning market economy, the market price of a good reflects the total production cost of that item. However, sometimes the total cost of production is not reflected by the price. These additional costs are passed on to third parties, and are referred to as “externalities,” or external costs. They can be viewed as the additional cost to society for the production of that good. By not including these costs in the market price of the good, society as a whole pays for the external costs [98]. One of the roles of government is to “internalize” these external costs, by means of taxes or subsidies that alter the market price to bring it in line with the true cost.

In particular, there are significant external costs associated with the production of electricity, especially from fossil fuels and nuclear energy. These external costs are due to the release of pollutants into the atmosphere, waterways, and soil due to the construction and operation of the power plant, as well as the protection of sources and supply lines. These pollutants can cause human health issues, environmental destruction, and climate change, as well as many other negative effects. However, valuing these external costs is extremely difficult. The price of human health and human life, the destruction of habitats and pristine environments, and the potential catastrophic damage due to global climate change are very difficult to quantify.

Compared to fossil fuels and nuclear energy, renewable energy and wind energy in particular appear to have much smaller external costs. Hohmeyer is one of the first to attempt to estimate the external costs of various types of electricity production [98]. Using conservative assumptions, he estimates the total social cost of fossil fuels to be

between approximately 2 and 5 cents/kWh. For nuclear energy, the total social cost is between approximately 5 and 10 cents/kWh.

More recently, a European funded commission entitled the “ExternE” project also attempts to quantify the external costs associated with energy production [99]. Some of the important results are:

- If external costs are included, the cost of electricity generated from coal and oil would double, and the cost of electricity from gas would increase 30%.
- The external costs of coal are approximately 5 eurocents per kWh. Gas is approximately 2 eurocents per kWh, and wind is approximately 0.1 eurocents per kWh.

Thus, the external costs of wind energy are much lower than those of fossil fuel generation. If these external costs are included in the price of electricity (i.e., internalized), this would dramatically alter the playing field for wind energy. In many cases, wind energy would likely emerge as the cheapest of all forms of electricity, along with hydropower. In general, considering the external costs of energy production is hugely beneficial to renewables, and makes renewable energy sources a compelling alternative to traditional fossil fuel generated electricity. In practice, certain countries have attempted to internalize these external costs through various policies and subsidies. The feed-in tariff approach, which guarantees a fixed price for generated wind energy and is used in many European countries, is one such attempt at internalization.

2.2 Advanced Finance Analysis

Awerbuch writes extensively about the need to apply modern finance theory to the analysis of energy production. He claims that the classic “engineering” economic methods for analyzing energy production are outdated and inaccurate [100]. He advocates two distinct analysis techniques: the capital asset pricing model (CAPM) and mean variance portfolio (MVP) theory. These methods are not mutually exclusive; rather, they apply to two distinct situations. CAPM analysis is used for the analysis of specific projects, such as a wind farm or coal plant. MVP is applied when analyzing a portfolio of generation, such as a utility or national energy production portfolio.

2.2.1 Capital Asset Pricing Model

At its most basic level, CAPM theory simply dictates that market risk is included in the analysis of the costs of energy production. That is, the risk associated with a particular cost should dictate the discount rate associated with that cost stream, which therefore determines its relative contribution to the total net present value of all the costs. In the classical engineering methods, all costs are discounted at the same rate (typically the weighted average cost of capital or WACC) regardless of the associated risk of the costs. In the CAPM method, for cost streams that are low risk to the energy producer (such as variable O&M, which generally scales with output and therefore with revenue) and higher risk to the provider of the O&M services, a high discount rate should be used, to reflect the relative risk to each party. For high-risk costs to the energy producer (such as fuel prices for a gas turbine company) a low discount rate should be used [101]. There are many simple examples of this phenomenon in his work. By applying different

discount rates to future cost streams, dependent on their level of risk, Awerbuch claims that a more accurate estimation of the cost of electricity is achieved.

One of the consequences of a CAPM analysis for energy production is to drastically alter the relative price of wind energy (and photovoltaics) compared to fossil fuels, especially natural gas. The high level of risk associated with future fuel prices causes those costs to be discounted at a low rate, and therefore to contribute to the total cost more than if they are discounted at the WACC. The result is that the CAPM method generates estimates of fossil fuel levelized costs of energy that are significantly higher than traditional estimates. In one example [97], by using the CAPM method instead of using the WACC for all discount rates, the levelized cost of energy of a 200 MW combined cycle natural gas plant increases from 2.8 cents/kWh to 4.8 cents/kWh, an increase of approximately 70%. On the other hand, the levelized cost of energy of a 50 MW photovoltaic installation decreases from 7.8 cents/kWh to 7.2 cents/kWh when switching from the standard method to the CAPM method. This decrease in the cost of energy for a photovoltaic installation is due to the low risk of future cost streams. Like photovoltaics, the majority of wind energy costs are fixed upfront costs, and the future costs are relatively small and they are low risk. The result is the CAPM method decreases the estimated levelized cost of energy for wind energy (compared to standard methods), and this decrease is a function of the low risk inherent in wind energy. In sum, Awerbuch's use of CAPM analysis, which is the standard in modern financial analysis, makes wind energy a much more attractive energy source, especially when it is compared to fossil fuel generated electricity.

This CAPM method can be utilized for the analysis of wind farms as well. Three discount rates are appropriate:

1. The Riskless Rate of Return – This is generally equal to the interest rate on U.S. Government bonds. This rate is applied to future costs that are deemed risky to the energy producer (and therefore riskless to whomever is collecting on these cost streams). It is also applied to riskless benefits to the producer, such as accelerated depreciation, which is risk free.
2. The Debt Equivalent Discount Rate – This discount rate is applied to future cost streams that behave much like debt. These are fixed costs that must be paid unless the company defaults, and therefore they are moderately risky. This rate is used to discount all future fixed expenses, such as fixed O&M and property taxes.
3. The Cyclical Discount Rate – This discount rate is applied to variable costs. Generally, these costs vary with revenue, and therefore are less risky to the energy producer. Therefore a high discount rate is used for these costs.

Using the CAPM method, all future costs are discounted with the appropriate discount rate. The net present value of the costs is then multiplied by the capital recovery factor and divided by the annual energy production to produce an estimate of the levelized cost of electricity. This value is fundamentally different from the levelized cost of energy calculated using the cash flow sheet. Neither is inherently better than the other; rather, they provide different means of analyzing the financial prospects of a wind farm development, and thus both are useful.

2.2.2 Mean Variance Portfolio Theory

Awerbuch also uses mean variance portfolio (MVP) theory to analyze wind energy. The CAPM analysis focuses on the cost of energy production for wind energy or fossil fuels at the scale of a single power producing entity (i.e. a single power plant or wind farm). MVP analyzes how the addition of a new source of generation affects the portfolio-wide performance. The portfolio could be the generation sources of a utility or a region, or even a country. The question of portfolio performance is therefore very interesting and useful for utility planners and policy decision makers, since overall what one really cares about in planning electricity development is lowering the overall cost of all generation [102].

Awerbuch states that most would intuitively believe that the addition of the least cost source of new generation would be the best choice every time new generation is needed [100]. This is not in fact the case, despite its intuitive appeal. In fact, the risk associated with a new generation source must also be considered when assessing the addition of this new source. Awerbuch points out: “At any given time, some alternatives in the portfolio may have high costs while others have lower costs, yet over time, the astute combination of alternatives serves to minimize overall generation cost relative to the risk” [100]. The result is that in the long-term the addition of a low-risk, but more expensive generation source can lower the overall portfolio cost of electricity generation, while the addition of higher risk, but cheaper generation can raise the overall portfolio cost.

Awerbuch uses MVP theory to analyze the contribution of wind energy on a portfolio wide scale. Because wind energy and other renewables are fixed cost alternatives, they are relatively low risk, especially compared to natural gas generation, which has high fuel

price uncertainty. Furthermore, the price of wind energy is statistically independent from fossil fuel prices, and therefore the costs do not correlate with fossil fuel movements. The result is that adding wind energy, even when it is more expensive than the overall portfolio cost, can lower the overall long-term portfolio cost because of its ability to diversify the generation portfolio and lower the risk of future costs. Awerbuch presents many examples of various portfolios and the change in cost and risk as wind energy is introduced.

The use of MVP analysis reverses a common point of opposition to wind energy, namely its large upfront costs. Because of the large upfront costs, wind energy is perceived as a more expensive alternative to fossil fuel generation, which has lower upfront costs, but higher fuel costs in the future. By using MVP analysis, Awerbuch portrays the high upfront costs of wind energy as an asset, since it reduces the risk associated with uncertain future cost streams of the overall electricity generating portfolio.

2.2.3 Advanced Finance Analysis Summary

Awerbuch's work demonstrates that the traditional methods for analyzing energy production are systematically biased against wind energy and other renewables. This is manifested in two ways. First, the traditional methods for estimating the cost of energy use the same discount rate for all future costs, ignoring the inherent risk in each cost stream. This causes estimates of fossil fuel generation costs to be lower than is warranted, and the estimates of the costs of wind energy to be higher than is accurate. Second, decisions for new generating capacity are based solely on the relative cost of the stand-alone systems, and not on their affect on the overall portfolio cost. Because wind

energy has large fixed upfront costs, it is relatively low risk, and it does not correlate with fossil fuel price changes. Even if wind energy has higher stand-alone costs than fossil fuel generation (and the CAPM analysis makes this assumption very uncertain), the addition of wind energy to the generation portfolio can lower the overall portfolio costs in the long-term. This type of global portfolio scale analysis is rarely carried out, which therefore biases new generation choices against wind energy. The adoption of Awerbuch's suggestions to use modern finance theory in energy production decisions would greatly enhance the perceived costs and benefits of new wind energy development.

2.3 Energy Balance Analysis

Energy production can also be analyzed in terms of its energy balance. Energy balance, sometimes called the energy return on investment (EROI) or energy payback, is a relatively simple concept. The energy balance or EROI is simply equal to the ratio of the energy that is produced from a particular source to the total amount of energy needed to allow that source to produce energy. For electricity generation, "the EROI entails the comparison of the electricity generated to the amount of primary energy used in the manufacture, transport, construction, operation, decommissioning, and other stages of the facility's life cycle" [103]. Energy payback is simply the amount of time it takes for the energy produced by the source to equal the amount of energy needed to allow the source to produce. Energy balance is a compelling way to look at energy production. Because energy is often a scarce resource (e.g., fossil fuels), and because energy has such an important role in economic growth, the more efficiently primary energy is used to deliver energy to society, the better. This is especially important when global climate change is considered.

While energy balance is a simple concept, it can be difficult to accurately quantify all the energy that goes into a particular energy source. For a wind turbine, this is the energy needed to produce the equipment, transport it to the site, install it, maintain it, and finally to decommission it. Numerous studies investigate the energy balance of modern wind turbines. Lenzen reviews 72 operating turbines, and finds a mean energy balance of approximately 16, and a mean energy payback of approximately five months [104]. The Danish Wind Turbine Manufacturing Association estimates energy paybacks on the order of 80, with payback periods as low as 3 months for a modern Danish 600 kW machine [105]. A review of three wind farms in Wisconsin and Minnesota finds energy balances ranging between 17 and 39 [106]. Overall, energy paybacks on the order of 3-4 months seem to be reasonable estimates for modern turbines.

Another interesting result of these studies is that the energy balance tends to increase with increasing turbine size. This is due to a number of factors including increased size and efficiency of modern turbines and economics of scale [103]. The result is that modern turbines have much better energy balances than older turbines, and this trend is likely to continue in the future. Thus, for current modern turbines, energy balances on the order of 50-80 seem reasonable.

This energy balance for wind energy compares very favorably to essentially all other forms of energy production, as shown in Figure 59 [103]. Coal, nuclear, solar, and hydropower all have energy balances on the order of 5-10, which is significantly less than that of wind energy. While there is some uncertainty in these numbers, it seems clear that wind energy compares very favorably to other electricity sources on an energy balance

basis. Furthermore, if one compares energy sources based on their carbon intensity, wind energy would likely compare even more favorably.

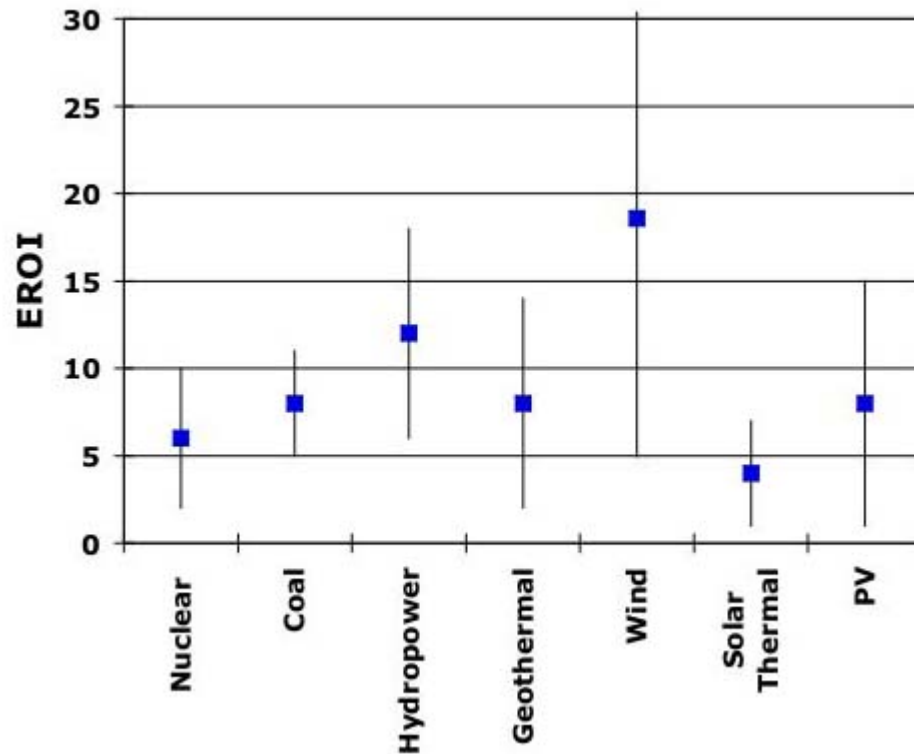


Figure 59 – Energy Return on Investment (EROI) for Various Energy Sources

2.4 Alternative Wind Energy Evaluation Methods Conclusions

The preceding is a summary of three alternative methods for analyzing wind energy and energy production. A common theme of these three methods is that wind energy performs well relative to other forms of energy production in each framework. The external costs of wind energy are significantly lower than most energy sources, and the energy balance is possibly the best of any source. Furthermore, modern finance theory can be used to remove bias from the analysis of wind and other energy sources, which greatly strengthens the case for wind energy. Overall, these alternative methods provide compelling motivations for increased production of energy from wind turbines.

3.0 Conclusions

This Chapter presents both the development of a tool for analyzing the economics of wind energy, and three alternative methods for evaluating wind energy. Presently, these two subjects are quite distinct in a practical sense. The methods used in the WEFC represent the status quo approach to analyzing wind energy economics from a developer's perspective. On the other hand, the alternative evaluation methods have varying degrees of acceptance in the mainstream. That is, these approaches have not been generally adopted or incorporated into the way that wind energy and other renewables are evaluated. In European countries, where the Kyoto Protocol is adopted, the external costs of energy production are considered, and a carbon trading system is now in place. In the United States, no such evaluation has been made.

External mechanisms are needed to incorporate these alternative evaluation methods into the mainstream, which may eventually alter the status quo method of analyzing wind energy development, exemplified by the WEFC. As awareness of global climate change increases, governments may decide to attempt to internalize the external costs of energy production. This decision may be reinforced by issues of energy independence and security. In the United States, the result may be a carbon tax or carbon trading scheme, or some other mechanism for promoting energy sources with low external costs or high energy balances. The net effect of these policies would be to generate additional costs to energy sources that generate a large amount of carbon or with low energy balances, or both. These costs would then have to be incorporated into the analysis of any new energy production development. In the case of wind energy, these new costs would likely be quite small.

Likewise, external mechanisms may lead to the advanced financial methods becoming more common means of analyzing wind energy and other energy developments. If utilities, system operators, or governments begin to confront fuel price risk and volatility, then these approaches are needed to account for the varying degrees of risk among different sources of energy. In this case, the status quo approach to analyzing wind energy and other energy projects would be drastically altered.

No matter what, a drastic change in the analysis of wind energy and other energy sources is likely dependent on external mechanisms which would force the status quo methods to be abandoned or altered. If these changes take place, it appears that wind energy development would benefit substantially.

CHAPTER VIII

THE STREAMLINED SITE ASSESSMENT METHODOLOGY

The research and tools developed in Chapter III through Chapter VII encompass a variety of wind energy site assessment analysis techniques and wind resource measurement strategies. While the research presented in each Chapter can stand alone as an independent subject, the topics comprise one broad strategic approach to wind energy site assessment. This approach has been dubbed the “Streamlined Site Assessment Methodology” or SSAM. The goal of SSAM, which is a unification of the various research subjects and tools presented, is to provide a flexible and comprehensive methodology for executing the site assessment process in which the specific priorities and constraints of the project dictate the approach that is taken.

1.0 SSAM Description

This Section presents a detailed description of the SSAM framework, which is shown graphically in the flow chart in Figure 60. A description of the various choices and paths in Figure 60 that can be taken in the SSAM approach is now provided. In Figure 60, the yellow boxes indicate processes or analyses, and the green diamonds indicate decision points.

When the site assessment process commences, the first choice encountered is whether to use a met tower or a ground-based device, such as SODAR or LIDAR, as the primary method for wind resource measurement. This is the first decision point in Figure 60, “Install Met Tower”. This decision is the most general in SSAM, as it dictates the course of the rest of the site assessment.

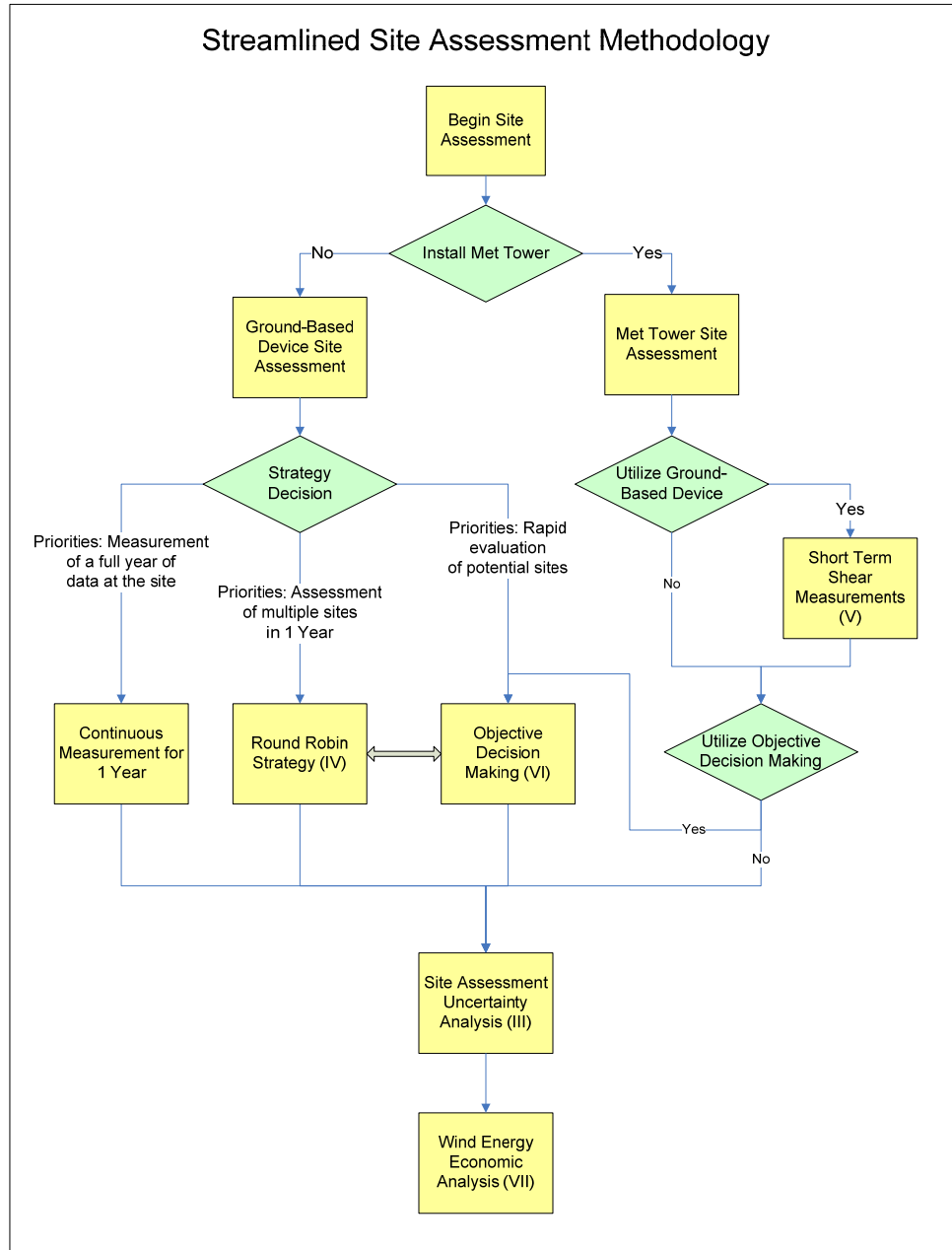


Figure 60 – SSAM Flow Chart

1.1 The Ground-Based Device Site Assessment Option

If a ground-based device is chosen as the primary wind resource measurement device, then the path to the left of the first decision point in Figure 60 is taken. This is the “No” branch of the “Install Met Tower” decision point. Once a ground-based device is chosen, a second decision point is reached, labeled “Strategy Decision” in Figure 60. This

decision determines what strategic approach is taken for wind resource measurement using a ground-based device. Three possible strategies that utilize a ground-based device are possible:

- **Continuous Measurement for 1 Year.** The first possible strategy for ground-based device measurement is to simply measure the wind resource at the site for an entire year, satisfying the priority of obtaining a full year of measured data. This approach is similar to the traditional site assessment method, except that a ground-based device is used in lieu of a met tower. Relative to the traditional site assessment method, this approach has the advantage that the wind resource can be measured at the hub height of a wind turbine, which is usually not possible when using a met tower, as discussed in Chapter I. This strategic approach ensures that seasonal variations in the wind resource are captured in the measured data, which may be an important if minimizing the uncertainty in the estimate of the wind resource is a priority. On the other hand, this approach requires that the ground-based device is deployed at a single site for the entire year, precluding it from being used anywhere else, regardless of the quality of the wind resource at the site.
- **The Round Robin Site Assessment Strategy.** If a primary priority of the site assessment campaign is the measurement of multiple sites in a single year, then the round robin strategy can be employed. This strategic approach is only possible if the sites are relatively near by each other, as the ground-based device is transported back and forth between sites over the course of one year. This approach is described in detail in Chapter V, and the results indicate that it is a

highly effective method of measuring multiple sites in a year using a single ground-based device, without a significant sacrifice in accuracy or uncertainty that usually would accompany measurement lengths less than one year.

- **Objective Decision Making.** The final strategic choice when using a ground-based device is the objective decision making approach described in Chapter IV. In this approach, the wind resource is measured in segments, and after each segment a decision is made whether to stop measurement and build a wind farm, stop measurement and not build a wind farm, or continue measurement. This approach is likely to be implemented when the rapid evaluation of a site is a primary priority. In these cases, the objective decision making approach is an effective method for drastically reducing the required measurement time, on average. It should be pointed out that the analysis in this approach depends on the economic parameters of the wind farm, and so it should be used when those parameters are well known or at least closely approximated. Furthermore, the objective decision making strategy and the round robin strategy are potentially complementary approaches that can be used in parallel. In this case, the objective decision making approach would be utilized after each round robin segment of measured data. While these data segments are discontinuous, the objective decision making framework is still applicable and is implemented in the same way. Finally, as depicted in Figure 60, the objective decision making can also be utilized when a met tower is used as the primary method for wind resource measurement. This possibility is discussed later.

1.2 The Met Tower Site Assessment Option

If a met tower is chosen as the primary wind resource measurement device, then the path to the right of the first decision point in Figure 60 is taken. This is the “Yes” branch of the “Install Met Tower” decision point. Once a met tower is chosen, a second decision point is reached, labeled “Utilize Ground-Based Device” in Figure 60. This decision determines whether or not a ground-based device is used to supplement the primary wind resource measurement using the met tower. Two approaches are therefore possible, “Yes” and “No”:

- Yes, utilize a ground-based device. For this approach, a ground-based device is used as a supplement to the met tower, by measuring the hub height wind resource for short-term period of time with a ground-based device, and applying the short-term shear measurement strategy. In this approach, short-term hub height wind resource data are used to adjust the estimate of the wind shear characteristics at the site. This approach is presented in Chapter VI, and is highly effective at improving the accuracy and decreasing the uncertainty in hub height mean wind speed estimates. The ground-based device can be deployed at the site for as little as a few days, although the uncertainty in the hub height wind resource estimate decreases as the ground-based device is deployed for longer periods of time. Overall, when a ground-based device is available for short-term deployment, this strategy is extremely useful.
- No, do not utilize a ground-based device. In this case, a ground-based device is not utilized as a supplement to the met tower measurement.

As discussed in Chapter IV, it is possible to utilize the objective decision making strategy when a met tower is used to measure the wind resource. Thus, for either of the two branches of the “Utilize Ground-Based Device” option, another decision point is reached. This decision point is the “Utilize Objective Decision Making” green diamond in Figure 60. Two approaches are therefore possible, “Yes” and “No”:

- Yes, utilize the objective decision making strategy. This approach is described in Chapter IV, and may also be used when a ground-based device is the primary method for measuring the wind resource, as described in previously in Chapter VIII, Section 1.1. In this approach, the wind resource is measured in segments, and after each segment a decision is made whether to stop measurement and build a wind farm, stop measurement and not build a wind farm, or continue measurement. This approach is likely to be implemented when the rapid evaluation of a site is a primary priority. While it is more likely that this approach would be used when a ground-based device is the primary method for measuring the wind resource, it can be used in this situation as well. Finally, it is possible to use this approach in conjunction with the short-term shear strategy described in Chapter VI. In this case, a ground-based device would also be brought to the site to measure the hub height wind speed for some short-term period of time. This additional information may help reduce the uncertainty in the estimate of the hub height wind resource, and therefore accelerate the decision making process.
- No, utilize the objective decision making strategy. In this case, the traditional approach to wind energy site assessment is performed. This approach is discussed in detail in Chapter I, including two major drawbacks: the required

measurement length and the low measurement height. Nonetheless, this approach is by far the most common in the United States right now.

1.3 Uncertainty and Economic Analysis

Wind resource measurement can take a variety of forms, using either a ground-based device or a met tower, and with a variety of possible strategies within these two approaches. Regardless of the approach taken, the uncertainty analysis techniques developed in Chapter III are utilized next to determine the uncertainty of the wind resource estimate and the energy production estimate. This is depicted in Figure 60, as all the paths converge at the “Site Assessment Uncertainty Analysis” process. While the material presented in Chapter III focused specifically on the traditional site assessment process in some cases, the majority of the techniques and methods developed in Chapter III are general, and can easily be applied to alternative scenarios that utilize ground-based devices.

Finally, the last step in the SSAM process is an economic analysis, which is depicted in Figure 60 as the “Wind Energy Economic Analysis” process after the “Site Assessment Uncertainty Analysis” process. A commonly used and detailed approach to wind energy economic analysis utilizing cash flow sheets is described in detail in Chapter VII. This is a fairly general approach which can be applied to a variety of wind farm developments and ownership structures, and is independent of the measurement technique and strategy used to evaluate the wind resource.

1.4 SSAM Approach Summary

The above provides a description of the SSAM framework, which is comprised of the strategies, analysis techniques, and tools that are developed in this dissertation. The priorities, constraints, and goals of a given project dictate the particular path, and therefore the particular measurement configuration, measurement strategy, and analysis methods utilized in the site assessment process. SSAM is therefore a flexible process, utilizing both traditional site assessment methods and alternative approaches to site assessment. In particular, SSAM encompasses several techniques that utilize ground-based devices, which are potentially extremely effective substitutes to the standard method of site assessment, and can result in more rapid development, more accurate and certain results, or both.

2.0 SSAM Software

The SSAM approach, described above and depicted graphically in Figure 60, is implemented into a software program. The goal is to create a flexible and detailed tool that can effectively implement all aspects of the SSAM approach, and that can then be applied to specific site assessments. Each of the strategies and analysis methods developed in the SSAM approach are incorporated into this program. The SSAM software is created in Matlab, using the graphical user interface (GUI) functionality. The SSAM software is then compiled into C-code and turned into an executable file so that it can be run on any computer, even those without Matlab.

This Section describes the SSAM software in detail, providing descriptions of the inputs, processes, and outputs of the software. The SSAM main window, the four major sub-windows, and some important features of the software are now presented.

2.1 SSAM Main Window

A view of the SSAM main window is shown in Figure 61. When the SSAM software is first opened, the user begins in the “Select Analysis” section, and chooses between starting a new analysis and continuing a previous analysis. At any point, the user can press the “Start Over” button and begin again. In Figure 61, the previous analysis “test_IPP.mat” is being continued.

Next, the user moves to the “Primary Wind Resource Measurement Technique” section of the main window, as shown in Figure 61. This choice corresponds to the first choice in the flow chart of SSAM in Figure 60. In the SSAM software, the user likewise chooses between a met tower and a ground-based device, which are the right and left branches of Figure 60, respectively. For the “test_IPP.mat” example in Figure 61, a met tower is selected.

Finally, the user may now begin defining the inputs of the site assessment and running the analyses that are used to generate the results. This occurs in the “Inputs and Analysis” section of the main window. There are four main categories of inputs and analysis, and each of these is described in the next Sections.

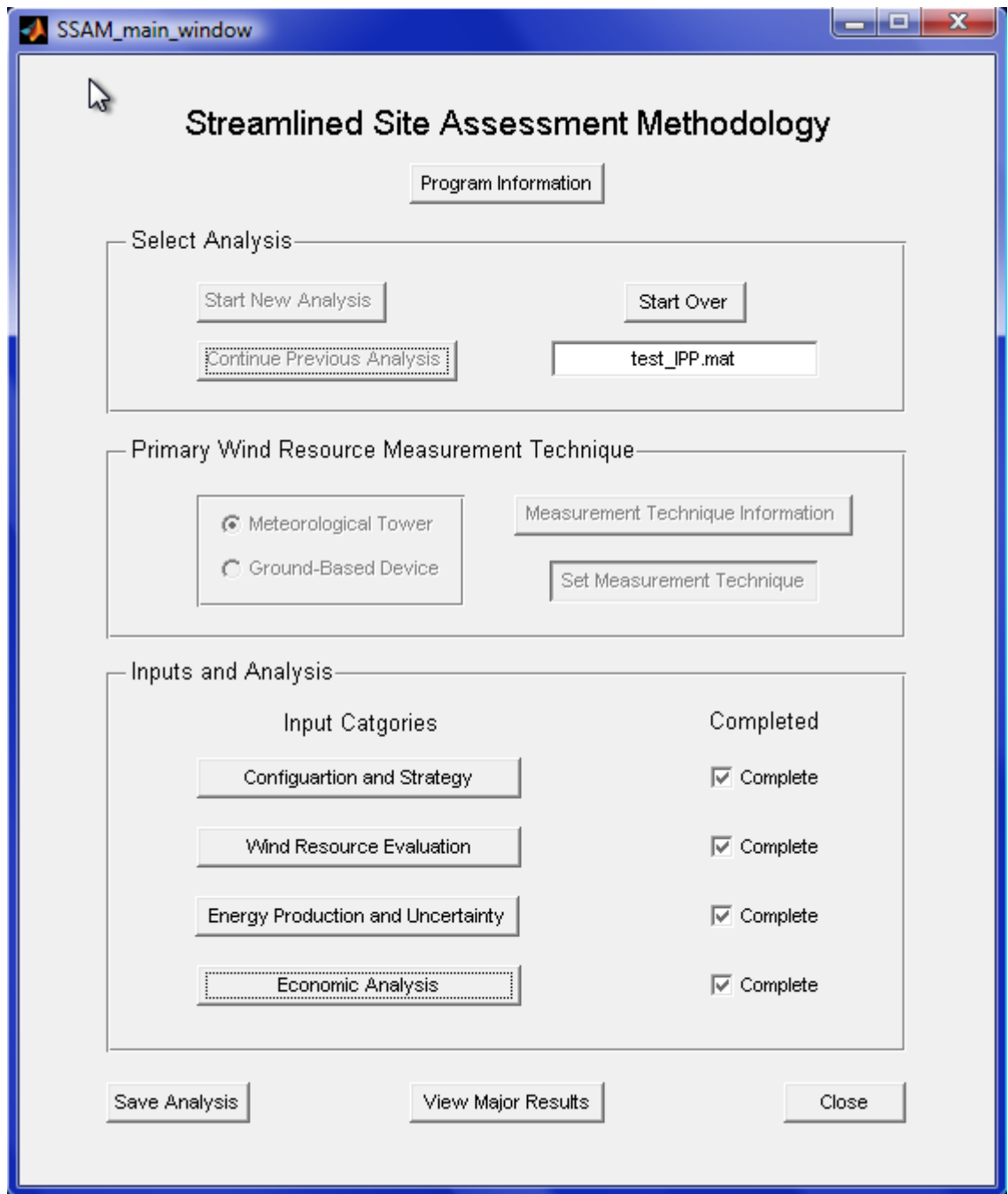


Figure 61 – SSAM Main Window

2.2 Configuration and Strategy Window

In the “Configuration and Strategy” window, the general configuration inputs are chosen. The window for a met tower based site assessment is shown in Figure 62, and the window for a ground-based device site assessment is shown in Figure 63.

met_config_strategy_gui

Meteorological Tower Configuration and Strategy

Information

Wind Turbine Configuration

Number of Turbines	2	
Hub Height of Turbine(s)	80	m
Project Life	20	Years

Met Tower Configuration

Number of Measurements Heights	2	
Upper Met Tower Height	60	m
Lower Met Tower Height	30	m

Ground-Based Device Data

Utilize Short-Term Shear Strategy?

☐ Yes ☒ No

Ground-Based Device Measurement Height		m
--	--	---

Close

Figure 62 – Configuration and Strategy Window for Met Tower

The screenshot shows a software window titled "gbd_config_strategy_gui". Inside, the main heading is "Ground-Based Device Configuration and Strategy". Below this heading is an "Information" button. The window is divided into three main sections:

- Wind Farm Configuration:**
 - Number of Turbines: 1
 - Hub Height of Turbine(s): 80 m
 - Project Life: 20 Years
- Ground Based Device Configuration:**
 - Number of Measurements Heights: 1 (dropdown menu)
 - Upper Measurement Height: 80 m
 - Lower Measurement Height: (empty input field) m
- Objective Decision Making:**
 - Utilize Objective Decision Making Strategy?
 - ☒ Yes
 - ☐ No
 - First Measurement?
 - ☒ Yes
 - ☐ No
 - Load Previous Data button and an empty text input field.
 - Measurement Cost: 100 \$ per Day
 - Measurement Period Length: 90 Days

A "Close" button is located at the bottom right of the window.

Figure 63 - Configuration and Strategy Window for Ground-Based Device

The inputs in these windows include the number of turbines, the turbines' hub heights, and the project length. The configuration of the wind resource measurement is also selected, including the height of each measurement. Finally, when a met tower is used for the wind resource measurement, the option to use the short-term shear strategy is

available. This can be seen in Figure 62, and corresponds to the “Utilize Ground-Based Device” choice in the right branch of Figure 60. When a ground-based device is used for the wind resource measurement, then the option to use the objective decision making strategy is available. This can be seen in Figure 63, and corresponds to the “Strategy Decision” choice in the left branch of Figure 60. There is no option to use the round robin strategy in this window, as it only requires using a discontinuously measured data set.

2.3 Wind Resource Evaluation Window

Once the configuration and strategy are determined, the “Wind Resource Evaluation” window can be selected. In this window, shown in Figure 64, the process of utilizing measured data to estimate the long-term hub height and location wind resource is carried out. There are four more sub-windows in which this process is performed, and a summary of the results is also shown in the “Wind Resource Evaluation” window in Figure 64.

The process begins by loading the measured data in the “Measured Data Set” sub-window. Next, the long-term wind resource can be estimated in the “Measure-Correlate-Predict” sub-window, in which long-term reference site data can be loaded and the Variance Ratio MCP algorithm is used. The long-term resource is then extrapolated to hub height (when applicable) in the “Wind Shear” sub-window. The wind shear characteristics at the site can either be calculated from data from a lower measurement height, or manually fixed to a certain value. Finally, the wind resource at each turbine can be adjusted in the “Topographic Correction” sub-window. This sub-window allows for simple scaling factors to be used to adjust the estimated long-term hub height Weibull

parameters at each turbine. There is no flow modeling capability. Instead, the outputs of flow modeling can be utilized for the topographic correction. The end result of the “Wind Resource Evaluation” window is an estimate of the long-term hub height and location wind resource.

Wind Resource Evaluation

Information

Inputs and Analysis

Completed

Measured Data Set ☒ Complete

Measure-Correlate-Predict ☒ Complete

Wind Shear ☒ Complete

Topographic Correction ☒ Complete

Summary

	Measured Wind Resource	Estimated Long-Term Wind Resource	Estimated Long-Term, Hub Height Wind Resource	
Mean Wind Speed	6.96	6.88	7.41	m/s
Weibull c	7.85	7.76	8.37	m/s
Weibull k	2.43	2.36	2.36	

Close

Figure 64 – Wind Resource Evaluation Window

2.4 Energy Production and Uncertainty Window

The energy production and the uncertainty of the energy production can be determined next, once the wind resource evaluation is complete, by selecting the “Energy Production and Uncertainty” window from the SSAM Main Window. The “Energy

Production and Uncertainty” window is shown in Figure 65. There are three sub-windows that are used to determine the final energy production and uncertainty results; these results are also summarized in the bottom of the “Energy Production and Uncertainty” window in Figure 65.

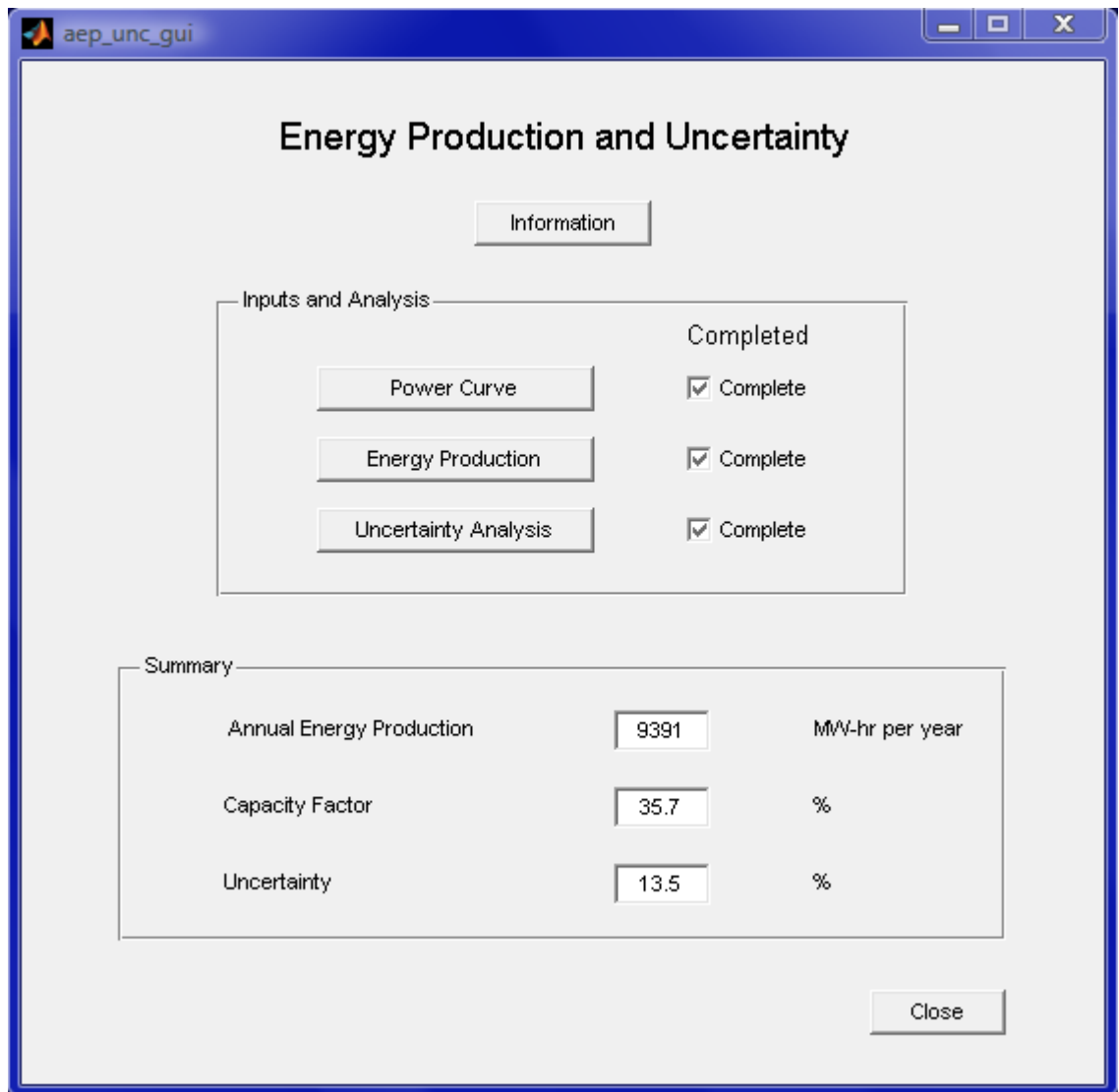


Figure 65 – Energy Production and Uncertainty Window

The analysis in the “Energy Production and Uncertainty” window begins by choosing the power curve of the wind turbines in the “Power Curve” sub-window. The power curve can either be chosen from a database of wind turbine power curves, or the data can

be loaded manually from a text file. Next, the energy loss factors are set and then the energy production and capacity factor are calculated in the “Energy Production” sub-window. Finally, the uncertainty of the energy production is determined in the “Uncertainty Analysis” sub-window, which implements the uncertainty analysis techniques developed in Chapter III. The results of all the analyses are displayed in the summary section of the “Energy Production and Uncertainty” window.

The “Energy Production and Uncertainty” window corresponds to the “Uncertainty Analysis” process from the SSAM framework shown in Figure 60. That is, this process occurs after the wind resource evaluation is complete, and is generally applicable to all possible monitoring strategies.

2.5 Economic Analysis Window

Finally, an economic analysis of the project can be performed by selecting the “Economic Analysis” window in the SSAM main window shown in Figure 61. The “Economic Analysis” window, which is shown in Figure 66, also corresponds to the final process in the SSAM framework shown in Figure 60. In the “Economic Analysis” window, an economic analysis of the wind farm is carried out, and this analysis is based on the material described in Chapter VII. In fact, the “Economic Analysis” window is simply the Wind Energy Financial Calculator, which is described in detail in Chapter VII. The only modification is that many of the inputs to the economic analysis are already determined in previous windows in the SSAM software.

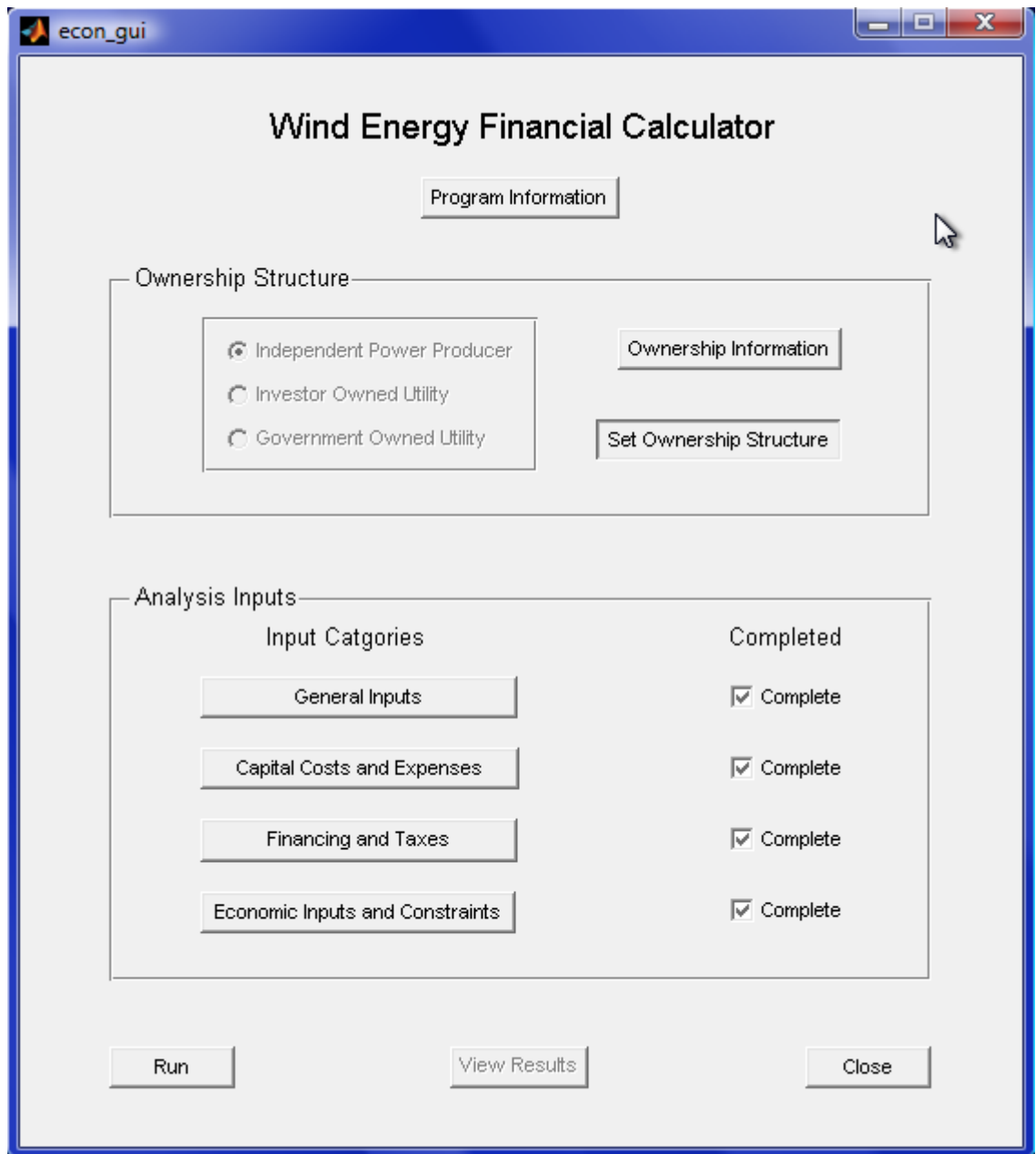


Figure 66 – Economic Analysis Window

An example results window of the “Economic Analysis” window is shown in Figure 67. These results are for an IPP ownership structure, and a wind resource evaluation using a met tower. The results windows when other ownership structures are used, or when the objective decision making strategy is used, are somewhat different than that shown in Figure 67, but provide similar results and information.

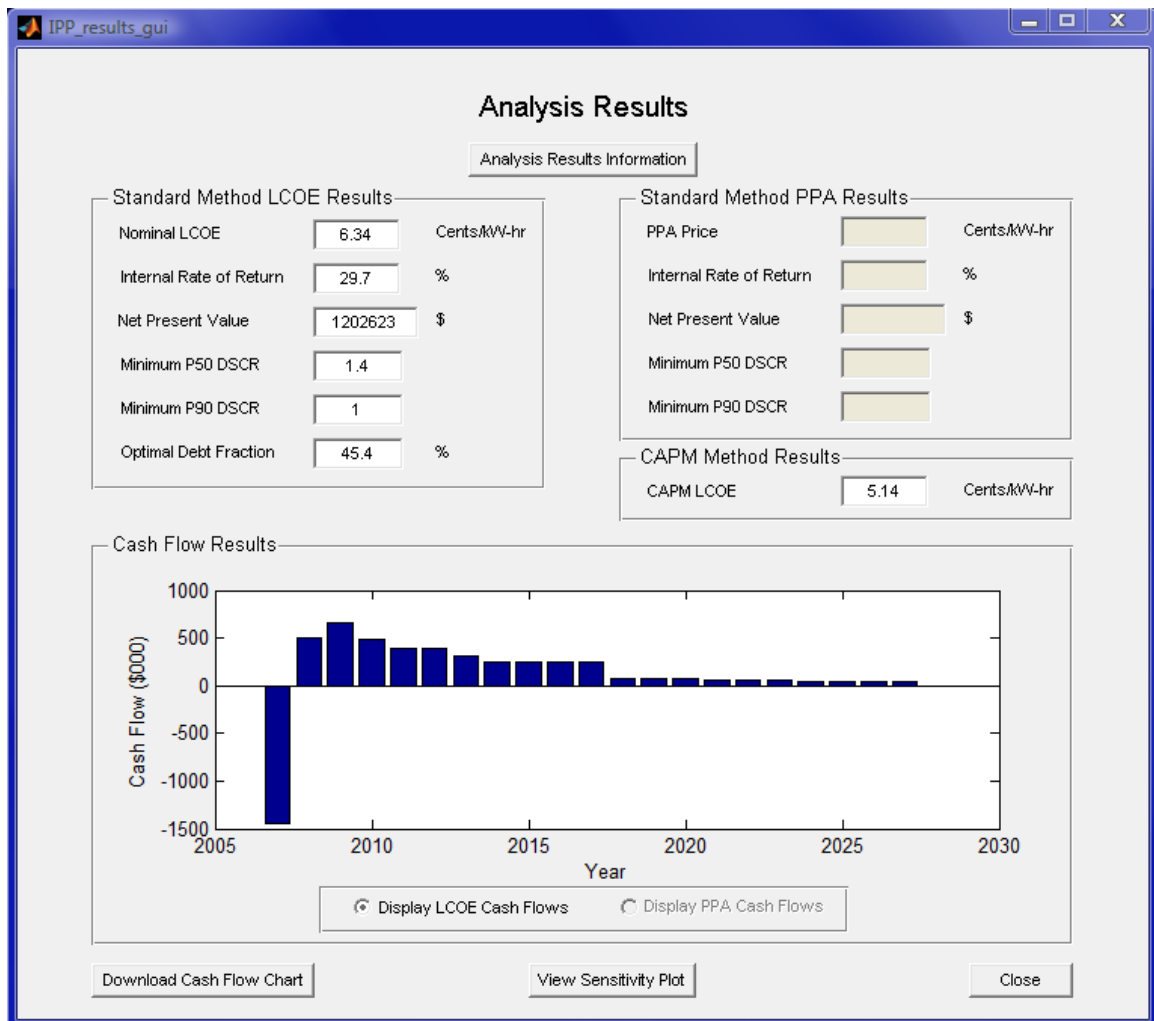


Figure 67 – SSAM Economic Results

2.6 Important SSAM Features

Other notable features of the SSAM software include:

- The ability to save a previous analysis, and then load it at a later point.
- The ability to save the cash flow sheet for the particular economic analysis in a text file, which can be read into a spreadsheet.
- The ability to view sensitivity plots for the primary economic parameters, which demonstrate the effect of changing these parameters on the important economic results.

3.0 SSAM Conclusions

Overall, the SSAM approach provides a new framework for wind energy site assessment, with multiple potential analysis methods and strategic approaches. Many of the new approaches have the potential to significantly improve the site assessment process from an accuracy, uncertainty, and financial perspective.

The SSAM software allows for the SSAM framework to be executed, as all of the various strategic choices are incorporated into the program, presenting the user with a wide variety of approaches to wind energy site assessment. While the program is very flexible and allows for a wide range of inputs and analysis techniques, it also automates many of the difficult and cumbersome processes such as MCP and cash flow analysis, and therefore accelerates the site assessment analysis process. The combination of this new and improved approach to site assessment with a software tool that implements this approach hopefully allows for advancement in the way wind energy site assessment is carried out.

CHAPTER IX

CONCLUSIONS

1.0 Summary

This research explores a new approach to wind energy site assessment. The traditional method of site assessment, while extremely common in its use, is inhibited by the use of a met tower for wind resource measurement, which results in long measurement periods and potentially inaccurate estimates of the wind resource. The streamlined site assessment methodology presented in this research provides a broader, more flexible, and often improved approach to wind energy site assessment. The SSAM framework encompasses a variety of possible approaches, and the particular approach taken can be selected based on the priorities, constraints, and goals of the site assessment. This methodology can drastically alter the way that wind energy site assessment is conducted. The resulting approach provides:

- Better characterization of uncertainty.
- Efficient and more rapid decision making.
- Improved evaluation of multiple sites in a single year.
- Reduced uncertainty and improved accuracy when evaluating a single site.

The following summarizes the important methods and contributions developed in this dissertation.

- Uncertainty Analysis in Wind Energy Site Assessment (Chapter III). This work produces two major contributions. First, a comprehensive survey of the

uncertainty sources that arise in traditional wind energy site assessment is conducted. The survey explores the most common and important uncertainty sources in detail, and provides approximate values for all of the sources when it is appropriate. This research provides a useful and thorough summary of uncertainty sources in traditional wind energy site assessment. Second, a rigorous mathematical method for combining uncertainty sources in the site assessment process is developed. Specifically, this work develops methods for determining the wind resource uncertainty, and then combining all of the major uncertainties to get an overall uncertainty of the energy production. Explicit functions for the Weibull parameter sensitivity functions are derived, and so the sensitivity factors can be calculated exactly instead of assumed. These methods for combining uncertainty sources are general, and can be applied to any type of wind resource measurement approach, not just the traditional method using a met tower. Overall, the research presented in Chapter III contributes an improved method of handling uncertainty analysis in wind energy site assessment, for both traditional and alternative approaches to the process.

- The Objective Decision Making Strategy (Chapter IV). Measuring the wind resource for a full year allows for seasonal variations in the wind resource to be captured, and so more accurately estimates the long-term wind resource at the site. At many sites, however, a decision of whether or not to build a wind farm is possible well before a year of measurement is complete, despite the larger uncertainty. This could be due to either a very good or very bad wind resource. The research in this Chapter develops a decision making approach to wind

resource monitoring, which allows for an objective decision of whether or not to build a wind farm, or to continue measuring the wind resource, at any point in the measurement process. This method is highly effective, with the accuracy of the decisions comparable to that of a full year of measurement. It also results in a substantial monetary savings due to decreased monitoring costs and more rapid development of wind energy.

- The Round Robin Site Assessment Strategy (Chapter V). This technical approach for wind resource measurement entails measuring the wind resource at multiple nearby sites in a single year, by transporting a ground-based device back and forth between the sites over the course of the year. This results in a discontinuous measured data set. The results indicate that this strategy is an effective method of increasing the number of sites that can be measured in a single year, without the significant sacrifice in accuracy and uncertainty that usually accompanies measurement periods less than one year. An added advantage of this approach is that the ground-based device measures the wind resource at hub height, obviating the need for shear extrapolation. The result is that the round robin strategy may produce both more accurate estimates of the wind resource, while also doubling or tripling the number of sites that can be measured in a single year.
- The Short-Term Shear Measurement Strategy (Chapter VI). Shear extrapolation is often the largest source of uncertainty when estimating the wind resource at a site. This strategy aims to improve the accuracy of shear extrapolation by augmenting one year of measured data from a met tower with a short-term period of measured data from a ground-based device. For a variety of reasons, it may be

necessary for a met tower to be installed at a site, or a ground-based device may not be available for an entire year. This strategy helps mitigate the inherent drawbacks of using a met tower. The results of this analysis indicate that this strategy is extremely effective at improving the accuracy and reducing the uncertainty of hub height wind speed estimates, even when only a short-term amount of hub height data are available. Overall, this strategy is easily implemented and should be used uniformly when a met tower is installed at a site as the primary method of wind resource measurement.

- Wind Energy Economic Analysis (Chapter VII). An economic analysis of a wind farm is necessary to determine the economic performance and financial success. This Chapter has two main contributions. First, it describes the development of a Wind Energy Financial Calculator, which is a tool used for analyzing wind energy developments. The WEFC utilizes cash flow methods to perform the economic analysis, and the entire program is created with a graphical user interface. Second, interesting new and alternative methods of evaluating wind energy are presented. Specifically, modern finance theory based on CAPM and MVP techniques, external cost analysis, and energy balance analysis are investigated and described. The unifying theme when using these three approaches is that the relative value of wind energy, and renewable energy in general, is improved relative to traditional sources of energy. It implies that the traditional methods of valuing energy are biased against wind energy, and that new methods should be encouraged so that the true value of wind energy is captured and quantified.

- The Streamlined Site Assessment Methodology (Chapter VIII). The research and tools developed in Chapter III – Chapter VIII are synthesized into an overarching site assessment framework, dubbed the “Streamlined Site Assessment Methodology”. This approach provides a flexible and comprehensive set of strategies and analysis techniques that can be used to improve wind energy site assessment in a variety of ways. This Chapter describes the SSAM framework and how the priorities and constraints of a particular site assessment dictate the particular strategies and techniques that are utilized. A SSAM software tool is also described, which incorporates all of the aspects of SSAM into a software program that can be used for actual applications. This tool is very general and can be applied to a wide variety of situations. Overall, this Chapter summarizes and fuses the previous research into a general strategic approach that can drastically alter and improve wind energy site assessment.

2.0 Recommendations

The methods that constitute the SSAM approach have been tested and validated using a large amount of actual data. The ability of SSAM to improve the wind energy site assessment process appears to be assured. On the other hand, many of these methods entail significant deviations from the traditional approach to wind energy site assessment. They are likely to experience resistance, as they represent a new and unknown approach. The ability to secure a loan for a wind energy development depends strongly on the lender’s confidence in the estimates of the energy production and financial success, and therefore in the estimates of the wind resource at the site. Regardless of the performance

of the methods, they will not be employed if their use results in a rejection from a lender. Furthermore, in many cases the methods utilize a ground-based device, and in order for the methods to achieve acceptable performance, these devices must produce measurements with accuracy and precision comparable to that achieved using the traditional approach to wind speed measurement. The potential hesitancy to adopt this new methodology, while not surprising, would represent a significant missed opportunity to save both time and money in the site assessment process.

In the short-term, the SSAM approach may not be generally adopted. The likely early adopters may be institutions or developers who do not require substantial loans for wind farm developments. For example, government sponsored resource assessment campaigns, which then finance turbine purchases for towns or municipalities, are potential early adopters of the SSAM approach. In these cases, there is no risk-averse lender to satisfy, and the goals of the development may be broader than simply financial profit and instead include energy production diversification, increased use of renewable energy in the region, and rapid development. The SSAM approach is well suited to these situations, as it offers a means of accelerating the site assessment process.

In the long-term, as experience with this approach is gained, a wider variety of potential developers may consider adopting some or all of the SSAM approach. The results presented here show substantial promise, and the motivation to achieve these results in practice is compelling. It is hoped that this research will serve as the basis for an evolution in the way wind energy site assessment is conducted, with the resulting approach providing significant improvement over the traditional site assessment process.

REFERENCES

- [1] Baily, B., "Wind Resource Assessment Handbook," AWS Scientific, Inc. Report, 1997. Available: <http://www.nrel.gov/wind/pdfs/22223.pdf>.
- [2] Elliot, D.L., Holloday, C.G., Barchet, W.R., Foote, H.P, and Sandusky, W.F., "Wind Energy Resource Atlas of the United States," Pacific Northwest Laboratory, Richland, Washington and National Renewable Energy Laboratory, Golden, CO, 1986.
- [3] Gardner, P., Garrad, A., Jamieson, P., Snodin, H., Nicholls, G., and Tindal, A., "Wind Energy - The Facts - Technology (Volume 1)," European Wind Energy Association Report, 2004. Available: http://www.ewea.org/fileadmin/ewea_documents/documents/publications/WETF/Facts_Volume_1.pdf.
- [4] "Know Your Wind," Available: <http://www.windustry.org/basics/04-knowwind.htm>, Accessed on 9/25/2007.
- [5] Andre, D., Grove, J., Grossman, L., Moynihan, S.P., and Raker, J., "Community Wind: An Oregon Guidebook." Northwest Sustainable Energy for Economic Development Report, Oregon, 2005. Available: http://www.energytrust.org/RR/wind/community/oregon_wind_guidebook.pdf.
- [6] McCaa, J., "Understanding the Wind: Its Causes and Variability," *AWEA and CanWEA Resource Assessment Workshop*, Syracuse, NY, 2006.
- [7] Oliver, A., "Translating Data into Results: Analysis and Interpretation of Data," *AWEA and CanWEA Resource Assessment Workshop*, Syracuse, NY, 2006.
- [8] Brower, M., "The Role of Wind Flow Modeling and Mapping," *AWEA and CanWEA Resource Assessment Workshop*, Syracuse, NY, 2006.
- [9] Justus, C.G., Mani, K., and Mikhail, A.S., "Interannual and Month-to-Month Variations of Wind Speed," *Journal of Applied Meteorology*, Vol. 18, No. 7, 1979, pp. 913-920.
- [10] Baker, R.W., Walker, S.N., and Wade, J.E., "Annual and Seasonal Variations in Mean Wind Speed and Wind Turbine Energy Production," *Solar Energy*, Vol. 45, No. 5, 1990, pp. 285-289.
- [11] Klink, K., "Trends and Interannual Variability of Wind Speed Distributions in Minnesota," *Journal of Climate*, Vol. 15, 2002, pp. 3311-3317.
- [12] Livingston, J.T., and Anderson, T., "Wind Shear, Taller Turbines, and the Effects on Wind Farm Development Create a Need for Taller MET Towers," Windtower Composites Report, LLC, Heber City, Utah, 2004. Available: <http://compositetower.com/pdf/windshearpositiondoc.pdf>

[13] Quarton, D., "WIND TURBINES – Part 121: Power Performance Measurements of Grid Connected Wind Turbines," IEC 61400-12 Ed.1, 2004.

[14] Jones, S., "Considerations for Optimizing Deployment of Met Towers During Project Development," *AWEA Windpower '05*, Denver, CO, 2005.

[15] Jesty, D., "Financing Considerations Debt Perspectives," *AWEA and CanWEA Resource Assessment Workshop*, Syracuse, NY, 2006.

[16] Elkinton, M.R., Rogers, A.L., and McGowan, J.G., "An Investigation of Wind-Shear Models and Experimental Data Trends for Different Terrains," *Wind Engineering*, Vol. 30, No. 4, 2006, pp. 341-350.

[17] Feuquay, L.F., Crescenti, G.H., and Celta, D.J., "Validation Study of the Use of Wind Shear Exponents in Extrapolating Wind Speeds for Wind Resource Estimations," *13th Symposium on Meteorological Observations and Instrumentation*, Savannah, GA, 2005.

[18] Manwell, J.F., Rogers, A.L., and McGowan, J.G., "Recommendations for Alternative Monitoring Plan and Long Term Monitoring Sites," Renewable Energy Research Laboratory Report, University of Massachusetts, Amherst, MA, 2005.

[19] "NRG TallTower: Installation Manual and Specifications," NRG Systems, Inc., Hinesberg, Vermont, 2006. Available: <http://www.nrgsystems.com/upload/software/TallTowerManual-7.10.pdf>, Accessed on 9/25/2007.

[20] "NRG Systems Product Catalog," NRG Systems, Inc., Hinesberg, Vermont. Available: <http://www.nrgsystems.com/store/>, Accessed on 9/25/2007.

[21] Manwell, J.F., McGowan, J.G., and Rogers, A.L., *Wind Energy Explained*, John Wiley & Sons LTD, West Sussex, England, 2002.

[22] Pedersen, T.F., and Paulson, U., "Classification of Operational Characteristics of Commercial Cup-Anemometers," *EWEA '99*, Nice, France, 1999.

[23] Pedersen, T.F., "Characterisation and Classification of RISØ P2546 Cup Anemometer," Risø National Laboratory Report, 2004. Available: http://www.risoe.dk/Risoe_dk/Home/Knowledge_base/publications/Reports/ris-r-1364.aspx.

[24] Lockhart, T., and Bailey, B., "The Maximum Type 40 Anemometer Calibration Project," NRG Systems Report, 1998. Available: http://www.nrgsystems.com/store/product_detail.php?cd=11&s=1899&tab=support

[25] Westermann, D., "Investigation and Classification of the Anemometer Thies First Class," Deutsche WindGuard Wind Tunnel Services GmbH Report, 2003. Available: <http://www.thiesclima.com/WindGuard.pdf>.

[26] "Summary of Cup Anemometer Classification According to IEC61400-121 Committee Draft - Make and Type: RISØ P2546," Risø National Laboratory Report, 2004. Available: <http://www.cupanemometer.com/technical/P2546%20Classification%20IEC61400-121CD.pdf>.

[27] Neal, B., "ART SODar Home Page." Available: <http://www.sodar.com/>, Accessed on 9/25/2007.

[28] Walls E., Rogers, A.L., and Manwell, J.F., "Long Island, MA: SODAR-Based Wind Resource Assessment," Renewable Energy Research Laboratory Report, University of Massachusetts, Amherst, MA, 2006.

[29] Bradley, S., Antoniou, I., von Hunerbein, S., de Noord, M., and Jorgensen, H., "SODAR Calibration for Wind Energy Applications," Final Report on WP3, EU Wise Project, The University of Salford, Greater Manchester, UK, 2001. Available: http://www.acoustics.salford.ac.uk/res/vonhunerbein/WISE_WP3_pdf_version.pdf.

[30] Rogers, A.L., Walls, E., Henson, W., and Manwell, J.F., "Addressing Ground Clutter Corruption of Sodar Measurements," *45th AIAA Aerospace Sciences Meeting and Exhibit (ASME Wind Energy Symposium)*, Reno, NV, 2007.

[31] Albers, A., "Evaluation of ZephIR." Deutsche WindGuard Consulting GmbH Report, Germany, 2006. Available: http://www.windguard.de/website_deutsch/veroeffentlichungen/2006/PWG06005_Zephir_First_Report_V2.pdf

[32] "ZephIR Operations and Maintenance Manual," QinetiQ, London, England, 2006. Available: <http://www.qinetiq.com/home/commercial/energy/ZephIR.html>.

[33] Smith, D.A., Harris, M., Coffey, A.S., Mikkelsen, T., Jorgensen, H.E., Mann, J., and Danielian, R., "Wind LIDAR Evaluation at the Danish Wind Test Site in Horsore," *Wind Energy*, Vol. 9, 2006, pp. 87-93.

[34] Jaynes, D., Rogers, A.L, Manwell, J.F., and McGowan, J.G., "A Validation and Uncertainty Analysis of Coherent Laser Radar (Lidar) for Wind Resource Assessment and the Effect of Vertical Turbulence on Lidar and Cup Anemometer Wind Speed Measurements," Master's Thesis, Renewable Energy Research Laboratory, University of Massachusetts, Amherst, MA, 2007.

[35] Pedersen, T.F., "Power Curve Measurements Under Influence of Skew Airflow and Turbulence," Risø National Laboratory Report, 2004. Available: <http://www.mea.com.au/files/skew%20airflow.pdf>.

[36] Pedersen, T.F., Gjerding, S., Ingham, P., Enevoldsen, P., Hansen, J.K., and Jørgensen, H.K., "Wind Turbine Power Performance Verification in Complex Terrain and Wind Farms," Risø National Laboratory Report, 2002. Available: http://www.risoe.dk/Knowledge_base/publications/Reports/ris-r-1330.aspx

[37] Rogers, A.L., Rogers, J.W., and Manwell, J.F., "Comparison of the Performance of Four Measure-Correlate-Predict Algorithms," *Journal of Wind Engineering and Industrial Aerodynamics*, Vol. 93, No. 3, 2005, pp. 243-264.

[38] "National Data Buoy Center," Available: <http://www.ndbc.noaa.gov/>, Accessed on 9/25/2007.

[39] Anderson, M., "A Review of MCP Techniques," Renewable Energy Systems Ltd, Tech. Rep. 01327R00022, 2004.

[40] Riedel, V., Strack, M., and Waldl, H., "Robust Approximation of Functional Relationships Between Meteorological Data: Alternative Measure-Correlate-Predict Algorithms," *EWEC '01*, Copenhagen, Denmark, 2001, pp. 806-809.

[41] Woods, J.C., and Watson, S.J., "New Matrix Method of Predicting Long-Term Wind Roses with MCP," *Journal of Wind Engineering and Industrial Aerodynamics*, Vol. 66, 1997, pp. 85-94.

[42] A. Derrick, "Development of the Measure-Correlate-Predict Strategy for Site Assessment," *14th British Wind Energy Conference*, Nottingham, UK, 1992, pp. 259-265.

[43] Bardsley, W.E., and Manly, B.F.J., "Regression-Based Estimation of Long-Term Mean and Variance of Wind Speed at Potential Aerogenerator Sites," *Journal of Applied Meteorology*, Vol. 22, No. 2, 1983, pp. 323-327.

[44] Mortimer, A.A., "A New Correlation/Prediction Method for Potential Wind Farm Sites," *16th British Wind Energy Conference*, Stirling, UK, 1994, pp. 349-352.

[45] Joensen, A., Landberg, L., and Madsen, H., "A New Measure-Correlate-Predict Approach for Resource Assessment," *EWEC '99*, Nice, France, 1999, pp. 1157-1160.

[46] Addison, J.F., Hunter, A., Bass, J., and Rebbeck, M., "A Neural Network Version of the Measure Correlate Predict Algorithm for Estimating Wind Energy Yield," *COMADEM 2000: Proceedings of 13th International Congress on Condition Monitoring and Diagnostic Engineering*, Houston, TX, 2000, pp. 917-922.

[47] Bechrakis, D.A., Deane, J.P., and McKeogh, E.J., "Wind Resource Assessment of an Area Using Short Term Data Correlated to a Long Term Data Set," *Solar Energy*, Vol. 76, 2004, pp. 725-732.

[48] Nfaoui, H., Essiarab, H., and Sayigh, A.A.M., "A Stochastic Markov Chain Model for Simulating Wind Speed Time Series at Tangiers, Morocco," *Renewable Energy*, Vol. 29, No. 8, 2004, pp. 1407-1418.

[49] Garcia-Rojas, R., "Algorithm for the Estimation of the Long-Term Wind Climate at a Meteorological Mast Using a Joint Probabilistic Approach," *Wind Engineering*, Vol. 28, 2004, pp. 213-224.

- [50] King, C., and Hurley, B., "The SpeedSort, DynaSort and Scatter Wind Correlation Methods," *Wind Engineering*, Vol. 29, 2005, pp. 217-241.
- [51] A. Derrick, "Development of the measure-correlate-predict strategy for site assessment," *EWEC '93*, Lubeck-Travemunde, Germany, 1993, pp. 681-685.
- [52] Rogers, A.L., Rogers, J.W., and Manwell, J.F., "Uncertainties in Results of Measure-Correlate-Predict Analyses," *AWEA Windpower '05*, Denver, CO, 2005.
- [53] Landberg, L., and Mortensen, N.G., "A Comparison of Physical and Statistical Methods for Estimating the Wind Resource at a Site," *15th British Wind Energy Association Conference*, York, UK, 1993, pp. 119-125.
- [54] "Addendum to WindPact Turbine Design Scaling Studies, Technical Area 3 - Self-Erecting Tower and Nacelle Feasibility." Global Energy Concepts, LLC Report, 2001. Available: <http://www.nrel.gov/docs/fy03osti/29493A.pdf>
- [55] Mortensen, N.G., "Wind Measurements for Wind Energy Applications - A Review," *16th British Wind Energy Conference*, Stirling, UK, 1994, pp. 353-360.
- [56] Taylor, J., *An Introduction to Error Analysis*, 2nd ed., University Science Books, Sausalito, CA, 1997.
- [57] Frandsen, S., and Christensen, C. J., "Accuracy of Estimation of Energy Production from Wind Power Plants," *Wind Engineering*, Vol. 16, No. 5, 1992, pp. 257-268.
- [58] Istchenko, R., "Reducing Energy Assessment Uncertainty," *AWEA and CanWEA Resource Assessment Workshop*, Syracuse, NY, 2006.
- [59] Kristensen, L., "Cup Anemometer Behavior in Turbulent Environments," *Journal of Atmospheric and Oceanic Technology*, Vol. 15, No. 1, 1996, pp. 5-17.
- [60] Kristensen, L., "The Perennial Cup Anemometer," *Wind Energy*, Vol. 2, 1999, pp. 59-75.
- [61] Papadopoulos, K.H., Stefanatos, N.C., Paulsen, U.S., and Morfiadakis, E., "Effects of Turbulence and Flow Inclination on the Performance of Cup Anemometers in the Field," *Boundary Layer Meteorology*, Vol. 101, 2001, pp. 77-107.
- [62] Petersen, E., Mortensen, N., Landberg, L., Hojstrup, J., and Frank, H., "Wind Power Meteorology," Risø National Laboratory Report, Roskilde, Denmark, 1997. Available: http://www.wind-energie.de/fileadmin/bilder/Technik/Wind_Power_Meteorology.pdf.
- [63] Albers, A., Klug, H., and Westermann, D., "Outdoor Comparisons of Cup Anemometers," *DEWI Magazine*, Vol. 17, 2000, pp. 5. Available: http://www.dewi.de/dewi_neu/deutsch/themen/magazin/17/02.pdf.

[64] Albers, A., and Klug, H., "Open Field Cup Anemometry," *DEWI Magazine*, Vol. 19, 2001, pp. 276. Available: <http://www.mea.com.au/files/comparison%20report.pdf>.

[65] Albers, A., Klug, H., and Westermann, D., "Cup Anemometry in Wind Engineering, Struggle for Improvement," *DEWI Magazine*, Vol. 18, 2001, pp. 17. Available: http://www.dewi.de/dewi_neu/deutsch/themen/magazin/18/04.pdf.

[66] Curvers, A.P.W.M., and van der Werff, P.A., "Identification of Variables for Site Calibration and Power Curve Assessment in Complex Terrain," Relative Power Curve Measurements in Complex Terrain Task 7, ECN-C--01-102 Report, 2001. Available: <http://www.ecn.nl/docs/library/report/2001/c01102.pdf>

[67] Kline, J., and Young, M., "Wind Speed Measurement and Turbine Performance Projection Variance Between NRG Max40 and Risø P2546A Anemometers," *AWEA Windpower '05*, Denver, CO, 2005.

[68] Kline, J., "Effects of Tubular Anemometer Towers on Wind Speed Measurements," *AWEA Windpower '02*, Portland, OR, 2002.

[69] Rogers A.L., Ellis, A., and Manwell, J.F., "RERL Tower Installation Field Safety Manual," Renewable Energy Research Laboratory Report, University of Massachusetts, Amherst, MA, 2006.

[70] Elkinton, C., Geer, T., Henderson, C., and Rogers, A.L., "Renewable Energy Research Laboratory (RERL) Data Processing Handbook," Renewable Energy Research Laboratory Report, University of Massachusetts, Amherst, MA, 2006.

[71] Maribo Pedersen, B., Hansen, K.S., Oye, S., Brinch, M., and Fabian, O., "Some Experimental Investigations on the Influence of the Mounting Arrangements on the Accuracy of Cup-Anemometer Measurements," *Journal of Wind Engineering and Industrial Aerodynamics*, Vol. 39, 1992, pp. 373-383.

[72] Moon, D., and Miler, R., "Long-Term Reference Analysis - Statistics and Uncertainty from Length of Reference Data," *AWEA Windpower '05*, Denver, CO, 2005.

[73] Breslow, P.B., and Sailor, D.J., "Vulnerability of Wind Power Resources to Climate Change in the Continental United States," *Renewable Energy*, Vol. 27, 2002, pp. 585-598.

[74] Doran, J.C., and Verholek, M.G., "A Note on Vertical Extrapolation Formulas for Weibull Velocity Distribution Parameters," *Journal of Applied Meteorology*, Vol. 17, No. 3, 1977, pp. 410-412.

[75] Wieringa, J., "Shapes of Annual Frequency Distributions of Wind Speed Observed on High Meteorological Masts," *Boundary Layer Meteorology*, Vol. 47, 1989, pp. 85-110.

[76] Taylor, M., Machiewicz, P., Brower, M., and Markus, M., "Quantifying Uncertainty in Wind Resource Estimates," *AWEA Windpower '05*, Denver, CO, 2005.

[77] Landberg, L., Myllerup, L., Rathmann, O., Petersen, E.L., Jorgensen, B.H., Badger, J., and Mortensen, N.G., "Wind Resource Estimation - An Overview," *Wind Energy*, Vol. 6, No. 3, 2003, pp. 261-271.

[78] "Windpower.org," Danish Wind Energy Association. Available: <http://www.windpower.org/en/tour/wres/pwr.htm>, Accessed on 9/25/2007.

[79] Jones, S., "Examining Project Underperformance," *AWEA Windpower '06*, Pittsburgh, PA, USA, 2006.

[80] Homola, M.C., "Impacts and Causes of Icing on Wind Turbines," Navrik University College Report, 2005.

[81] Bailey, B., and Brower, M., "Estimation of the Long-Term Average Wind Speed and Energy Production at the Proposed East Mountain Wind Project Site," AWS True Wind, LLC Report, 2004.

[82] Adams, R., "Update of Sheffield Wind Farm Energy Assessment for the Gamesa G87," Garrad Hassan America, Inc. Report, 2005. Available: <http://www.sheffieldwind.com/PDFs/CRV-6%20-%20GH%20Power%20Rpt-update-10-27-05.pdf>.

[83] Mills, T., "Matching Wind Turbines to the Resource." *AWEA and CanWEA Resource Assessment Workshop*, Syracuse, NY, 2006.

[84] Weisstein, E.W., "Leibniz Integral Rule," From MathWorld--A Wolfram Web Resource. Available: <http://mathworld.wolfram.com/LeibnizIntegralRule.html>.

[85] Lackner, M.A., Rogers, A.L., and Manwell, J.F., "Uncertainty Analysis in Wind Resource Assessment and Wind Energy Production Estimation," *45th AIAA Aerospace Sciences Meeting and Exhibit (ASME Wind Energy Symposium)*, Reno, NV, 2007.

[86] Schwartz, M., and Elliott, D., "Wind Shear Characteristics at Central Plains Tall Towers," *AWEA Windpower '06*, Pittsburgh, PA, USA, 2006.

[87] Kirchhoff, R.H., and Kaminsky, F.C., "Wind Shear Measurements and Synoptic Weather Categories for Siting Large Wind Turbines," *Journal of Wind Engineering and Industrial Aerodynamics*, Vol. 15, 1983, pp. 287-297.

[88] Sumner, J., and Masson, C., "Influence of Atmospheric Stability of Wind Turbine Power Performance Curves," *Journal of Solar Energy Engineering*, Vol. 128, 2006, pp. 531-538.

[89] Rohatgi, J., "An Analysis of the Influence of Atmospheric Stability on Vertical Wind Profiles," *Wind Engineering*, Vol. 128, 1996, pp. 531-538.

- [90] Elliott, D., and Cadogan, J., "Effect of Wind Shear and Turbulence on Wind Turbine Power Curves," *EWECC '90*, Madrid, Spain, 1990, pp. 79-83.
- [91] Irwins, J.S., "A Theoretical Variation of The Wind Profile Power-Law Exponent as a Function of Surface Roughness and Stability," *Atmospheric Environment*, Vol. 13, 1979, pp. 191-194.
- [92] Zoumakis, N.M., and Kelessis, A.G., "Methodology for Bulk Approximation of the Wind Profile Power-Law Exponent Under Stable Stratification," *Boundary Layer Meteorology*, Vol. 55, No. 1-2, 1991, pp. 199-203.
- [93] Elkinton, M.R., Rogers, A.L., and Manwell, J.F., "Accuracy of Wind Shear Models for Estimating the Wind Resource in Massachusetts," Renewable Energy Research Laboratory Report, University of Massachusetts, Amherst, MA, 2005.
- [94] "Energy and Environmental Research Center: Regional Wind Databases," Available: <http://www.undeerc.org/wind/winddb/default.asp>, Accessed on 9/25/2007.
- [95] Wiser, R., and Kahn, E., "Alternative Windpower Ownership Structures: Financing Terms and Project Costs," Energy & Environment Division Report, Lawrence Berkeley National Laboratory, University of California, Berkeley, CA, 1996.
- [96] "IRS Publication 946 (2006) - How to Depreciate Property," 2006. Available: <http://www.irs.gov/publications/p946/index.html>.
- [97] Awerbuch, S., "Investing in Renewables: Risk Accounting and the Value of New Technology," *Energy Policy*, Vol. 28, 2000, pp. 1023-1035.
- [98] Hohmeyer, O., "Social Costs of Energy Generation - How Does Wind Compare," *AWEA Windpower '89*, San Francisco, CA, 1989.
- [99] "ExternE: Externalities of Energy, Methodology 2005 Update," European Commission Report, 2005. Available: http://ec.europa.eu/research/energy/pdf/kina_en.pdf
- [100] Awerbuch, S. "Towards A Finance-Oriented Valuation of Conventional and Renewable Energy Sources in Ireland," *Sustainable Energy Ireland*, Dublin, Ireland, 2004. Available: www.awerbuch.com/shimonpages/shimondocs/Ireland_SEI-Jun-25-04.doc.
- [101] Awerbuch, S., "The True Cost of Fossil-Fired Electricity in the EU: A CAPM-Based Approach," Initial Draft Report, 2003. Available: http://www.london.edu/assets/documents/PDF/2.3.3.7.10_otm_seminar_true_cost_of_fossil_electricity.pdf

[102] Awerbuch, S., "Output Variability as an Issue Surrounding the Integration of Wind in Ireland," SPRU Energy Group Report, University of Sussex, Brighton, UK, 2005. Available: <http://www.dcmnr.gov.ie/NR/rdonlyres/4336304D-1618-4177-99CD-23AF960E902B/0/Airtricityappendix2.pdf>.

[103] Cleveland, C., Kubiszewski, I., and Endres, P., "Energy Return on Investment (EROI) for Wind Energy," *Encyclopedia of Earth*, Washington, D.C., 2007. Available: [http://www.eoearth.org/article/Energy_return_on_investment_\(EROI\)_for_wind_energy](http://www.eoearth.org/article/Energy_return_on_investment_(EROI)_for_wind_energy).

[104] Lenzen, M., and Munksgaard, J., "Energy and CO₂ life-cycle analyses of wind turbines—review and applications," *Renewable Energy*, Vol. 26, No. 3, 2001, pp. 339-362.

[105] "The Energy Balance of Modern Wind Turbines," Danish Wind Turbine Manufacturers Association, *Wind Power Note*, No. 16, 1997. Available: [http://www.windpower.org/media\(444,1033\)/The_energy_balance_of_modern_wind_turbines,_1997.pdf](http://www.windpower.org/media(444,1033)/The_energy_balance_of_modern_wind_turbines,_1997.pdf).

[106] White, S., and Kulcinski, G., "Net Energy Payback and CO₂ Emissions from Wind-Generated Electricity in the Midwest," Fusion Technology Institute Report, University of Wisconsin, Madison, WI, 1998. Available: <http://icf4.neep.wisc.edu/pdf/fdm1092.pdf>.